Thèse de Doctorat

Yinghao LI

Mémoire présenté en vue de l'obtention du
grade de Docteur de l'Ecole Centrale de Nantes
sous le label de L'Université Nantes Angers Le Mans

École doctorale : Sciences Pour l'Ingénieur, Géosciences, Architecture (SPIGA)

Discipline : Terre, enveloppes fluides
Unité de recherche : *CEREMA*

Soutenue le 01/07/2015

Modeling of hydrological processes of an urban catchment

Study of a saturated soil flow module and application to an urban development zone of the future Paris-Saclay University

JURY

Président :	
Rapporteurs :	**Isabelle BRAUD**, Directeur de recherche, IRSTEA, Lyon **Bruno TASSSIN**, Directeur de recherche, LEESU, Marne-La-Vallée
Examinateurs :	**Emmanuel BERTHIER,** Docteur, CEREMA, Trappes **Fabrice RODRIGUEZ**, Directeur de recherche, IFSTTAR, Nantes **Pierre RIBSTEIN**, Professeur, SISYPHE, Paris **Pierre-Yves HICHER**, Professeur, Ecole Centrale Nantes
Invité :	**Antoine DU SOUICH**, Ingénieur, Etablissement Public Paris-Saclay, Orsay
Directeur de Thèse :	**Fabrice RODRIGUEZ**, Directeur de recherche, IFSTTAR, Nantes
Co-directeur de Thèse :	**Emmanuel BERTHIER**, Docteur, CEREMA

École Centrale de Nantes
École Doctorale Sciences Pour l'Ingnieur, Géosciences, Architecture (SPIGA)

MODELING OF HYDROLOGICAL PROCESSES OF AN URBAN CATCHMENT – STUDY OF A SATURATED SOIL FLOW MODULE AND APPLICATION TO AN URBAN DEVELOPMENT ZONE OF THE FUTURE PARIS-SACLAY UNIVERSITY

A Thesis in
Departement of hydrology
by
Yinghao Li

Submitted in Partial Fulfillment
of the Requirements
for the Degree of

Doctor of Hydrology

June 2015

Abstract

In the broad framework of building sustainable and resilient cities, integrated water management in urban areas has come to the top of agenda of city planners and managers. As one of the key elements of this paradigm, stormwater management is developed towards to at-source controls with intensive development of low impact development (LID) practices. Hydrological modeling turns towards to distributed, physically-based, and integrated approaches capable of taking into consideration of all the compartments of the water cycle as a whole. This Ph.D consists of contributing to the development of the distributed model URBS that has been being developed since about fifteen years by IFSTTAR. The scientific contribution focuses on the implementation of the saturated flow module WTI, and the model URBS-WTI is evaluated at an experimental catchment in the city of Nantes in France, where rich hydro-climate data are available. After a sensitivity study, the simulation of both the groundwater levels and the discharge rate at the catchment outlet with the calibrated model is satisfying. The contradictory effect of some processes has been observed, which explains the complexity in estimating the overall water balance and groundwater recharge. The model shows great sensibility to physical parameters: the difficulty in calibrating the model simultaneously for each piezometer may be related to the spatial variability of the soil properties. Once validated, the model URBS-WTI is applied on an urban development area within the territory of the future Paris-Saclay University (south-west of Paris). After the model calibration under pre-development conditions by groundwater data series, continuous simulations ($\sim$ year) are carried out with small time steps ($\sim$ min). The pre-development hydrological regime of the site is estimated, emphasizing the great importance of both the evapotranspiration process and the groundwater drainage by sewer networks in the catchment water balance. Then a scenario study for the post-development hydrology is undertaken at both the catchment and urban block scales, aiming to evaluate the impacts of urban planning on local hydrology and the efficiency of certain LID practices in runoff volume control. This study shows that surface sealing can increase runoff volume and reduce the evapotranspiration loss. The results highlight the seasonal groundwater recharge regimes, related to the different evapotranspiration rates. All the tested LID practices show their capability of reducing peak discharge; some practices are also capable of reducing the recurrence of low flows. On the other hand, overland flow caused by soil saturation may be observed locally. The use of rainfall infiltration devices should thus take into account of the underground settings, especially in the case where shallow groundwater is present. Generally speaking, the WTI module introduction has improved the model robustness of URBS, in particular in the modeling of groundwater flow.

KEY WORDS: urban hydrology, stormwater management, low impact development, distributed model, physically-based, groundwater modeling, water balance, land use change, sewer network

Résumé

Contexte

Les enjeux de l'urbanisation sont à la fois environnementaux, économiques et sociaux, et se situent à une échelle mondiale. Du point de vue de l'hydrologie urbaine, d'importants impacts de l'expansion de l'urbanisation sur les hydrosystèmes sont exercés à travers les changements d'occupation des sols et l'apport d'infrastructures relative à la gestion de l'eau, en surface ou dans le sous-sol. Les défauts des systèmes de drainage centralisé se multiplient: débordements, fuites, mauvais branchements volontaires ou involontaires, infiltration d'eau du sol dans les tuyaux et leurs tranchées de pose, coûts croissants pour la gestion et l'entretien, etc.

Développées depuis les années 1990 dans différents pays, les techniques alternatives (TA) sont conçus pour atténuer les impacts négatifs de l'urbanisation sur les hydrosystèmes et préserver l'hydrologie naturelle (Dietz, 2007). Aujourd'hui, les bénéfices de l'utilisation des TA sont bien connus et acceptés par les scientifiques et praticiens. Néanmoins, les questions se posent souvent liées à l'efficacité et la durabilité de ces systèmes, et au problème de pollution dans les nappes par ces pratiques (Pitt, 1999; Dietz, 2007). Dans la plupart des cas, une TA est basé sur l'infiltration d'eau dans le sol, et sa performance est ainsi conditionnée par la capacité d'infiltration du sol sous-jacent. Néanmoins, les impacts de ces nouvelles pratiques de gestion des eaux pluviales sur les nappes sont rarement étudiés (Göbel et al., 2004).

Le cycle de l'eau urbaine est un système complexe comprenant les compartiments naturels (eau de surface et eau souterraine) et des infrastructures. Comprendre et quantifier les interactions de ces composantes et l'impact résultant sur le bilan hydrologique reste un challenge majeur dans le domaine de l'hydrologie urbaine (Fletcher et al., 2013). L'introduction de pratiques alternatives de gestion des eaux pluviales doit être cohérente avec l'équilibre global du bilan hydrologique. Il est ainsi essentiel de considérer la gestion des eaux pluviales dans des approches intégrées de gestion des eaux urbaines.

L'eau souterraine est à la fois une source vitale d'eau potable et une composante clé du cycle de l'eau urbaine. La gestion quantitative et qualitative des eaux pluviales est un sujet complexe couvrant des échelles spatiales et temporelles variées. La nappe est rechargée principalement par l'infiltration de la pluie dans le sol. Ce processus naturel est altéré par l'imperméabilisation des surfaces. Dans le même temps, l'eau est importée dans le milieu urbain par les réseaux d'eau (potable et assainissement). Ces réseaux enterrés peuvent être le lieu de fuites, ce qui constitue une source supplémentaire pour la recharge de la nappe (Lerner, 2002). Les interactions entre les eaux de surface, les eaux souterraines et les réseaux d'eau sont complexes dans l'espace et dans le temps (Schirmer et al., 2007; Thomas, 2006).

La recherche en hydrologie urbaine poursuit deux objectifs principaux (Andrieu and Chocat, 2004): avancer dans la compréhension des processus hydrologiques en milieux urbanisés et contribuer au développement de méthodes et techniques de gestion pour les eaux urbaines. D'une part, les processus hydrologiques des milieux urbains ne sont pas si différents de ceux des milieux naturels et aucune frontière absolue existe entre la ville et son environnement naturel. D'autre part, l'hydrosystème urbain

a ses particularités liées aux échelles spatiales réduites, aux hétérogénéités en surface et en sous-sol, aux forts impacts anthropiques relatifs à l'évolution permanente de l'occupation des sols, et aux pratiques et stratégies d'utilisation et de gestion... Les modèles hydrologiques sont en général développés en se basant sur la transformation pluie/débit, et dans un objectif de dimensionnement des ouvrages. Les modèles existants décrivent relativement bien les processus en surface, mais rarement les flux dans les sous-sol et leurs interactions avec la surface (Rossman, 2004). La tendance actuelle de modélisation consiste à mettre en œuvre des approches à base physique et distribuées, permettant de représenter les dynamiques spatiales et temporelles des réponses des bassins versant à la pluie.

Dans le cadre du projet national "Grand Paris", le projet du futur campus Paris-Saclay a été lancé en 2010, avec la création de l'Établissement Public Paris-Saclay (EPPS) comme pilote du projet. Le lieu d'accueil du projet est le plateau de Saclay, situé à 20 km au sud-ouest de Paris. Le plateau est délimité au nord par la vallée de la Bièvre et au sud par celle de l'Yvette, toutes les deux étant fortement urbanisées. L'enjeu de la gestion des eaux pluviales du futur campus est ainsi crucial, et s'inscrit dans une démarche globale d'Éco-territoire. La gestion des eaux pluviales sur le plateau suivra une gestion selon différentes échelles: parcelles, quartier, et plateau. L'hydrosystème du plateau est complexe, en raison de la présence d'un réseau de collecteurs et de rigoles datant du 17ème siècle, et d'une nappe discontinue proche de la surface, dont le fonctionnement reste méconnu. En coopération avec le CEREMA, l'EPPS s'est engagé dans cette thèse CIFRE dans l'objectif de progresser dans la compréhension du fonctionnement de l'hydrologie du plateau, et d'établir une estimation préalable de l'impact du projet d'aménagement sur l'hydrologie du site.

Objectifs et méthodologies

La présente thèse suit deux objectifs. D'un point de vue scientifique, le travail souhaite contribuer au développement d'un modèle distribué et à base physique pour de petits bassins versants urbains (jusqu'à quelques centaines d'hectares) , le modèle URBS (Rodriguez et al., 2008) développé à l'IFSTTAR. Il est capable d'effectuer des simulations sur des chroniques (plusieurs années) et à des pas de temps fins (minutes) en tenant compte du cycle intégré des eaux pluviales. Si l'objectif à long terme du développement est de construire un outil d'aide à la décision, la présente thèse se concentre sur l'intégration dans URBS du module WTI (Branger, 2007) pour les flux horizontaux de la zone saturée, sa validation et son application. D'un point de vue opérationnel, l'étude souhaite étudier les impacts d'un projet d'urbanisation sur le fonctionnement hydrologique du milieu urbain. Elle se base sur le site d'un des quartiers du futur campus Paris-Saclay, le quartier du Moulon. Une attention particulière est portée à l'impact sur la nappe, et justifie l'utilisation du modèle URBS avec le module spécifique pour la zone saturée URBS-WTI.

Le travail de thèse s'est déroulé en deux étapes. La première étape consistait à l'introduction du module WTI dans URBS. Une "interface" a été définie entre deux éléments unitaires adjacents. Le flux saturé est calculé sur cette interface avec la loi de Darcy. Pour pallier la difficulté dans la définition du niveau du substratum de la nappe, dont l'information est limitée, la formulation de Darcy a été adaptée à une forme intégrale depuis la surface de l'interface jusqu'à l'infinité en profondeur, ce qui était possible grâce à la représentation du sol dans le modèle, contrôlée par une décroissance exponentielle de la conductivité hydraulique à saturation.

Le modèle URBS-WTI ainsi construit a été évalué sur le Pin Sec (Nantes), un des bassins urbains expérimentaux de l'Observatoire Nantais des EnVironnements Urbains (ONEVU), pour lequel des données hydro-météorologiques et géographiques riches sont disponibles. Partant d'une simulation réalisée avec une première estimation des paramètres physiques du sol (calcul de référence), le modèle a fait l'objet d'une analyse de sensibilité. Cette étape a permis de réaliser une simulation plus performante par un ajustement des paramètres. L'effet de l'homogénéisation des niveaux de nappes simulés, liée à l'introduction du module WTI, a été évalué sur un simple critère: l'écart type des niveaux de nappe simulés entre les éléments unitaires.

La deuxième étape de la thèse a consisté à l'étude hydrologique sur le quartier du Moulon avec le modèle URBS-WTI. L'originalité de ce travail porte sur l'évaluation du modèle avec comme seules observations les données piézométriques. Dans un premier temps, l'analyse du fonctionnement hydrologique actuel du Moulon avant l'aménagement a été réalisée. Une étude de sensibilité du modèle a été réalisée en se basant sur les simulations des niveaux de la nappe afin d'ajuster les paramètres pour ce cas spécifique. Le modèle a été ensuite appliqué sur la période de trois années 2011-2013 en continu et au pas de temps de 6 minutes. Les variations des niveaux piézométriques ont été analysées et comparées aux observation, ainsi que le bilan hydrologique et les débits continus aux exutoires des réseaux d'eaux pluviales, uniquement sur la base des simulations.

Dans un deuxième temps, l'analyse du fonctionnement hydrologique futur du quartier du Moulon aménagé (à l'horizon de 2025) a été faite grâce à une étude de scénarios. Une condition initiale de l'occupation des sols a été établie, avec laquelle une simulation de référence a été menée. À partir de cette simulation de référence, l'étude de scénarios a été conduite à deux échelles : quartier et îlot urbain. À chacune des échelles, deux types de scénarios ont été testés : scénarios de densité d'urbanisation et de techniques alternatives. Pour chaque scénario, trois types de résultats ont été analysés : niveaux piézométriques, bilan hydrologique, et débits aux exutoires. Ces résultats ont été comparés avec les résultats de référence, afin d'évaluer les impacts des aménagements et les effets des techniques alternatives.

Un pré-traitement des données géographiques est nécessaire à la mise en œuvre du modèle, pour les caractéristiques du milieu (occupation des sols) et les réseaux hydrographiques. La mise en place du module WTI introduit un nouveau type de donnée géographique, tel que l'interface entre les éléments unitaires. La construction de ces fichiers de d'entrée a nécessité d'importants pré-traitements géomatiques avec des outils SIG, dont la plupart ont été automatisés.

Principaux résultats

Le module de flux saturé WTI a été correctement intégré dans URBS, ce qui a permis d'améliorer sensiblement la qualité du modèle. Les niveaux piézométriques simulés s'accordent bien avec les observations, exception faite de piézomètres aux comportements atypiques. Dans le cas du bassin versant du Pin Sec où les mesures de débit sont disponibles, le modèle URBS-WTI a permis d'améliorer légèrement la simulation des débits. Sa capacité à simuler le cycle d'eaux pluviales en tenant compte des interactions entre l'atmosphère, la surface et le sol est confirmé.

Les effets antagonistes des processus hydrologiques ont été mis en évidence, comme par exemple la réduction simultané d'infiltration et d'évapotranspiration par l'imperméabilisation des surfaces. Les impacts résultants sur la quantité de ruissellement et la variation du niveau de la nappe se sont avérés complexes et parfois surprenants. L'étude a affirmé l'importance du processus de drainage de l'eau du sol par les réseaux d'assainissement. Pour les deux cas d'études, cette composante représente près de 30% de la précipitation annuelle, même si cela n'a pas pu être validé sur le quartier du Moulon.

Le modèle a montré une sensibilité aux paramètres physiques, qui varie d'un cas d'étude à l'autre et selon la variable étudiée. Ceci montre qu'il est important d'effectuer systématiquement des études de sensibilités dans les futures applications du modèle. L'évaluation de sensibilité sur la simulation des niveaux piézométriques s'est avérée complexe car elle est reliée à la variabilité spatiale des propriétés du sol urbain. L'impact de la discrétisation spatiale du modèle a aussi été mis en évidence.

Le bilan hydrologique du quartier du Moulon a été estimé. Le rôle majeur du processus de l'évapotranspiration a été mis en évidence, ainsi que le drainage de l'eau du sol par les réseaux d'assainissement. Les résultats de niveaux piézométriques ont confirmé la grande variabilité spatiale des grandeurs hydrologiques, ce qui confirme aussi l'intérêt des approches distribuées dans la modélisation hydrologique urbaine.

L'impact de l'expansion de l'urbanisation sur l'hydrologie a été estimé par les études de scénarios pour l'état futur du Moulon après aménagement. L'effet de la réduction d'infiltration et d'évapotranspiration des surfaces imperméabilisées a été observé. Néanmoins, en raison des interactions complexes entre les

processus, le bilan hydrologique final n'est pas toujours évident à prévoir. Les différences saisonnières dans les régimes de recharge de la nappe ont été constatées. L'introduction des techniques alternative a mis en exergue leur capacité à réduire les volumes ruisselés et atténuer les débits de pointe. Mais cet effet positif vis à vis du contrôle du risque d'inondation pour l'aval peut être préjudiciable au régime de recharge de la nappe, et peut conduire localement à une saturation locale du sol en surface. Il est ainsi important de prendre en compte l'impact sur la nappe peu profonde des pratiques d'infiltration. Le potentiel du modèle à tester des scénarios d'aménagement ou de gestion des eaux pluviales a été illustré.

Conclusion et perspective

Cette thèse a contribué au développement du modèle hydrologique distribué URBS, en particulier par l'intégration d'un module d'écoulement horizontal dans la zone saturée. Le modèle URBS-WTI a montré la capacité d'améliorer la simulation des niveaux piézométriques. Une évaluation du modèle originale a été réalisée sur le quartier du Moulon, en s'appuyant sur des données observées de piézométrie et sans donnée de débit. Ce travail a montré le potentiel et les limites d'un modèle distribué et à base physique dans le cadre de l'application à des projets réels d'aménagement urbain, en particulier sur l'impact de techniques alternatives de gestion des eaux pluviales. Le modèle URBS-WTI est désormais fonctionnel et est prêt à être appliqué sur d'autres sites. Des interrogations persistent toutefois sur la capacité du modèle à bien prendre en comte la variabilité spatiale des propriétés du sol, dans un cadre urbain où peu d'informations sont disponibles pour qualifier rigoureusement cette variabilité. Ce sujet devrait être approfondi pour améliorer la robustesse du modèle.

Table of Contents

List of Figures

List of Tables

List of Symbols

All values of elevations are in the NGF (General leveling of France) system.

Symbol	Units	Description
i	-	superscirpt for land use type. *nat* for natural land, *str* for street and *hou* for house
A^i	m^2	area of the land use i
A^{tot}	m^2	total area of catchment
$a^{orifice}$	$mm^{0.5}/s$	coefficient of orifice drainage flow for a flat roof or a green roof
b	-	parameter for the shape of the water retention curve in Brooks-Corey law
d	m	saturation deficit
E^{surf}	m/s	surface evaporation flux
F	m/s	flux between the vadose zone and the saturated zone
H	m	hydraulic head
I	m/s	surface infiltration
I_{drain}	m/s	groundwater drainage by by sewer networks
int	-	subscript for interface
j	-	superscript for segment of the drainage network
K	m/s	hydraulic conductivity
K_{int}	m/s	hydraulic conductivity assigned on an interface
K_s	m/s	saturated hydraulic conductivity at ground surface level
K_{sat}	m/s	saturated hydraulic conductivity at soil depth
K_v	m/s	hydraulic conductivity applied between the saturated zone and the vadose zone
M	-	scaling parameter of hydraulic conductivity
p	-	superscript for parcel
P	m	rainfall
Q	m	runoff
R	m	surface runoff
S_S	m	surface storage
S_{Smax}	m	storage capacity of the surface reservoir
$S_{drain}^{f.r.}$	m	threshold for drainage of a flat roof
$S_{drain}^{g.r.}$	m	maximum storage in the drainage layer of a green roof

S_{vad}	m	storage in the vadose zone
t	-	superscript for time step
TR	m/s	transpiration
u	-	superscript for UHE
z_{int}	m	elevation of an interface
z_g^A, z_g^B	m	elevation of the center of gravity of $\mathrm{UHE_A}$ ($\mathrm{UHE_B}$)
z_{root}	m	penetration depth of tree roots
z_s	m	saturation depth
θ	-	volumetric water content in the vadose zone
θ_{root}	-	volumetric water content within the tree roots zone
θ_s	-	saturated water content
θ_{wp}	-	wilting point water content
Ψ	m	suction
Ψ_e	-	air entry suction
σGWL	-	standard deviation of groundwater levels among the UHEs of the catchment

Acknowledgments

First and foremost I would like to thank Dr. Fabrice Rodriguez, thesis director, and Dr. Emmanuel Berthier, supervisor of my daily work, for all their ideas, thorough editing, support and friendly guidance all along the way, which make my Ph.D. experience productive and stimulating. You have been tremendous mentors for me. I would like to thank you for encouraging my work and for allowing me to grow as a research scientist in urban hydrology.

A great thanks to Antoine du Souich, co-supervisor of my thesis CIFRE, for guilding me through my first professional experience in the EPPS. It has been a great pleasure to work with you, your professonalism as an engineer and team leader has set for me an excellent example.

The members of the EPPS and CEREMA have contributed immensely to my personal and professional time. They have been a source of friendships as well as good advice and collaboration. A special thanks to Dr. David Ramier who has taught me a lot. The joy and enthusiasm he has for his research was contagious and motivational for me. Thanks to Laurent Bonnifait who has been an exceptional colleauge. Thank you for all your support, both scientific and personnal. I am greatful to Didier Gallis, who has given me much knowledge about urban drainage and skills in computer science. Thank you for your time and patience. During my work, I have had the pleasure to communicate with Clément Bertinatti, Emmanuel Dumont, Ghislain Mercier. My work has been able to be progressed thanks to your collaboration and help.

I would also like to thank Dr. Flora Branger and Dr. Sonja Jankowfsky, who had developed the initial code of the module that I worked on, as well as certain GIS processing programs that have been used during my thesis. Thank you for your time and consideration.

Thanks to Qingxiao Zhou and Khalil Farias, past master's students that I have had the pleasure to work with. I appreciate your special contribution to this thesis.

I gratefully acknowledge the funding sources that made my Ph.D. work possible. I was funded by the EPPS and the ANRT for my first 3 years and was honored to be a fellow of CEREMA for the year 4. Thanks to Mr. Pierre Veltz, Mr. Guillaume Pasquier, Mrs. Lise Mesliand of the EPPS and Mr. Emmanuel Neuville of CEREMA for having accepted me as a fellow. The research projet was also supported by the region of Île-de-France.

Lastely, I would like to thank my parents for all their love, support and encouragement. They have raised me, sent me abroad, and made great sacrificies alongside of my whole study here in France. My little achievement today is specially indebted to them. I would like to express my great gratitude toward Patricia Le Calvez, Pascal Guillaume and their children, my dear French family who have been providing me help and love during all these years. Thank you.

Part I

Introduction

Low impact development for urban stormwater management

Urbanization is an emerging issue with ecological, economic and social implications. Today over half (54%) of the world's and 73% of Europe's population is living in urban areas. According to the United Nations (2014), by 2050 these numbers are going to rise to 66% and 84%, respectively, with 2.5 billion people projected to be added in urban area.

Urbanization has led to great land use change, and brought dramatical impacts on the natural regime of urban storm runoff. Stormwater management in cities during the 20th century was marked by the development of urban sewer systems with the rapid urban expansions after the Second World War (at least in developed countries). Today, the shortcuts of this centralized urban drainage system are more and more recognized: overflows, water main leak, illegal discharges (connections), groundwater infiltration, increased capital costs, etc.

Low impact development (LID) practices are being developed all over the world since the 1990s as a way to mitigate the negative effects of urbanization and preserve the pre-development hydrology of a site (Dietz, 2007). Today, beneficial uses of LID practices have been well documented. However, questions are frequently raised concerning the efficiency, suitability, risk of groundwater contamination, etc. (Pitt et al., 1999; Dietz, 2007). The performance and efficiency of a LID practice is firstly to be addressed prior to setting up. In most cases the LID practices are infiltration-based therefore conditioned by the absorbing capacity of the soil, but mutual impacts with soil water of a general application of such practices are rarely studied (Göbel et al., 2004).

Urban water system is a complex aggregation of natural water compartments (surface water and groundwater) and man-made infrastructures, in particular water supply and sewer systems that modify the natural water cycle. Understanding and quantifying the interactions of these components and the overall assessment on urban water balance have been the objective of intense studies, but remains one major challenge in urban hydrology (Fletcher et al., 2013). Any innovative practice for stormwater runoff mitigation can not be really efficient only if it does not in conflict with the equilibrium of the global water balance nor with the interests in urban landscape, economic development and water users. It is therefore essential to consider the urban stormwater management in an integrated approach.

"Integrated" approach can refer to a multiple of things depending on the level of integrity: (i) integrated stormwater cycle referring to the track of rainfall from where it falls to catchment outlet, (ii) integrated urban water cycle involving water supply, sewage, stormwater and groundwater, (iii) integrated consideration for stormwater in the broad framework of ecological prevention and preservation in urban and suburban areas, (iv) a even broader paradigm of sustainable development of future cities with integrated reflection on social, political and economic factors. Stormwater management in cities, as well as urban hydrology in general, towards today to more and more integrated approaches in the interest of finding solutions for specific problems in the highly complex urban system. Still, a regard on the integrated stormwater cycle remains fundamental and can provide direct solutions to stormwater stresses under a specific urban setting.

Water balance and groundwater recharge in urban areas

Groundwater has critical value as a source of both potable and non-potable water. Over history, settlements often relied on groundwater from springs and shallow wells as a reliable source of clean potable water. In many cities, the underlying groundwater systems represent both the last reserve in terms of water resource and also the ultimate sink for persistent urban pollutants. Even if groundwater is not used for water production, urban aquifers are a potential storage location for stormwater and constitute a key part for stormwater management (Göbel et al., 2004).

On the other hand, groundwater can present insidious and persistent problems for urban development, especially in central districts as water tables rebound rather than continuing to fall, due to abandon of heavy industries, conversion of high-density residential areas to commercial, or new water supplies and imports (Foster and Vairavamoorthy, 2013). Water table rise in shallow groundwater systems, as a result of increased urban groundwater recharge, can cause flooding problems that affect the sewer pipes and septic tanks (Foster et al., 2010).

Maintaining the quality and quantity of urban water resources is recognized as a very complex task including different spatial and temporal scales. The key to understand the deterioration of urban water resources is the knowledge of the tremendous impact of urbanization on the entire water household (Schirmer et al., 2013). Despite its importance, groundwater is often not sufficiently considered in urban water management (Shepherd et al., 2006; Wolf et al., 2006). Nowadays, new urban projects acknowledge generally (at least in developed countries) the need for an understanding of water and land management techniques to improve the resilience and sustainability of the water system. The recharge to (shallow) groundwater should be taken account into to achieve sound management for water resources.

From a hydrological point of view, groundwater are mainly recharged by infiltrated rainfall into the soil. Urbanisation modifies greatly this natural recharge process related to surface sealing. Meanwhile, water is imported into the urban areas by water supply and sewer systems. Water can leak from these infrastructures and become artificial source of groundwater recharge (Lerner, 2002). In general the manifold interactions of surface-, ground-, and artificial water compartments are complex in time and space and still leaves many questions open (Schirmer et al., 2007; Thomas, 2006).

Hydrological modeling for urban area

Urban hydrology has initially developed as an engineering science. From a scientific point of view, urban hydrology pursues two objectives: improving the knowledge of hydrological processes in urbanized areas and contributing to the development of new methods and technologies for the management of urban waters (Andrieu and Chocat, 2004). Urban hydro-system has its particularities that distinguish it from natural hydrology, such as reduced scales, high spatial heterogeneities on surface and subsurface, severe impact by human activities, regular evolutions in land use and water-use practices and management policies. On the other hand, hydrological processes are not really different in cities and rural areas, and no borderline

exists between the urban area and its natural environment (Andrieu and Chocat, 2004).

Hydrological models have been generally developed based on rainfall-runoff modeling. In urban settings, the trend is to develop physically-based, spatially distributed, continuous models that are able to represent the spatial and temporal dynamics of the rainfall-runoff response (Fletcher et al., 2013). Surface water – groundwater interactions are important processes controlling catchment hydrology, thus should be considered in holistic manners. Existing softwares in the sector of urban hydrological modeling describe well the processes on surface, but rarely represent subsurface flows and their interactions with surface, or represent them in very simplified ways (Rossman, 2004). Several authors have proposed initiatives on distributed modeling in integrating the compartments from soil to the interface soil/atmosphere (Jia et al., 2001; Rodriguez et al., 2008) but need to be further developed.

Urban development project Paris-Saclay

The campus project Paris-Saclay was launched in 2010 within the broader framework of Grand Paris, with the foundation of Établissement Public Paris-Saclay as project pilot and manager. The future urban-campus Paris-Saclay locates on the Saclay plateau (20 km south-west of Paris), delimited by two densely-urbanized valleys at north and south. Face to challenges of flooding risk control, the EPPS is engaged in a sustainable and integrated approach for the water management on the plateau, key element within a ambitious plan of eco-territory for Paris-Saclay.

On the other hand, the hydro-system on the plateau is complex, being composed of a network of collectors and channels dating back to the 17th century and a shallow aquifer system, of which the functioning is nowadays unknown. In order to get an overall knowledge of the hydrological regime of the territory and to have a quantitative estimation on the possible impacts of the urban development they lead, the EPPS has been being engaged in this Ph.D program, in cooperation with the public research institution CEREMA.

Objectives of the Ph.D work

The Ph.D work pursues thus a double objectives. From a scientific point of view, the research is devoted to the development of a physically-based, spatially distributed hydrological model for urban catchments, which simulates the urban stormwater cycle in an integrated way. If the long-term aim of the model development is to build it an integrated decision-support tool for urban and suburban environment, the present study make an emphasis on the implementation, validation and application of a groundwater module.

From a practical point of view, the study takes the urban development site of Paris-Saclay as a model application case. Focus is paid on the quantitative evaluation of the effect of land use change on the catchment water household, with a special attention on the dynamics of the shallow groundwater.

In accordance with the two objectives, the Ph.D work has been organized in two phases. The first phase was for scientific development of the model, in addressing the following issues:

- Introduce the saturated module and calibrated the integrated model with field data of an experimental urban catchment in Nantes, France, of which a variety of hydro-climate datasets are available, as well as a a complete geographical database labeled "UrbanDataBank" (UDB).
- Improve the groundwater modeling performance of the model with the introduced module.

To meet these objectives, two supplementary work have proved to be necessary and valuable during the Ph.D thesis:

- Ameliorate the model in terms of coding rigour and of functionalities including mass-balance assessment, numerical-error-checking module, etc.
- Establish a prototype for geodata pre-processing of the model with ready-to-use GIS processing programs, as well as robust geodata-error-checking procedure.

The second phase was for the case study at Paris-Saclay urban development. One district of the future campus, the Moulon district, has been chosen for the model application. The following issues have been addressed:

- Estimate changes in catchment water balance as a result of urban development.
- Investigate the sensitivity of these changes to scenarios of urbanization density and of water management.
- Evaluate the efficiency of sustainable water management facilities with a combined consideration on surface water and groundwater.
- Provide sound informative modeling results to support urban designers in their decisions of campus planning.

Thesis outline

Following these objectives, the present thesis is structured in three parts. The first part contains uniquely Chapter 1 and describes the scientific context of this research work: advance in our knowledge of hydrological processes under urban settings, improvement in sustainable stormwater management, and state of art in urban hydrological modeling. The utility of Geographic Information System in urban hydrological modeling is also discussed.

The second part represents the scientific development of the thesis. Chapter 2 sketches our model URBS with an emphasis on the description of its soil parameterization and on the modules of LID devices that have been integrated in the model. Chapter 3 details the integration and implementation

of the saturated flow module Water Transfer Interface in URBS, followed by a report of the necessary modifications in the initial model scripts. Chapter 4 depicts the geodata pre-processing by means of GIS for the preparation of geometrical input files. The integrated model URBS-WTI is evaluated and validated at an experimental urban catchment in the Nantes city. This case study is represented in Chapter 5.

The third part represents the model application on the real urban development case Paris-Saclay, which is composed of two phases of study: hydrological modeling of Moulon under pre-development settings, described in Chapter 7; and scenarios study for the area under presumed post-development settings, described in Chapter 8. The impacts of the urban development on local hydrology are estimated by means of the comparison between the modeling results under pre-development and post-development conditions (Chapter 8).

Part II

Context of study

Chapter 1

Stormwater management in urban area and urban hydrological modeling

Contents

Introduction

With increased impervious surfaces, compaction of soils and drainage infrastructures, urban sprawl causes "dramatic" changes in hydrology (Fletcher et al., 2013). As illustrated in Figure 1.1, this encompass increase in runoff rates and volumes, decrease in infiltration and baseflow, faster runoff response to rainfall,

shorter times of concentration and recession, higher recurrence of small floods, altered water balance and groundwater recharge, all well documented dating back to the 1960s (Harris and Rantz, 1964; Leopold, 1968; Simmons and Reynolds, 1982; Ku et al., 1992; Booth et al., 2002; Shuster et al., 2005; Dietz and Clausen, 2007; Huang et al., 2008; Kauffman et al., 2009; Hawley and Bledsoe, 2011; Braud et al., 2013). If the mechanism of an individual process is well understood, the overall effect on urban stream flow and groundwater recharge remain subject to continuous research, as they can be further complicated highly variable from case to case (Lerner, 2002; Meyer, 2002; Brandes et al., 2005; Konrad and Booth, 2005; Lee et al., 2005; Haase, 2009; Kauffman et al., 2009; Salavati et al., 2014).

Emerged since the 1990's and largely accepted today by scientists and practitioners in urban hydrology, low impact development (LID) (Prince George's County, 1999) favors near-natural management for urban stormwater through retention and infiltration devices. Their benefits have been shown in a large number of studies, but remain active study topics. Understanding the interactions of LID devices with other compartments of the water cycle and their roles in groundwater recharge is of key importance in urban planning and drainage design.

Hydrological modeling offers a suitable tool for understanding hydrological processes and for hydrological prediction. Traditionally focused on stormwater runoff models, the development of urban hydrological modeling has been going towards to process-based, spatially distributed approaches which are capable of representing complex interactions among physical processes. With rising concern on urban water quality and development of LID practices, more and more models are designed to be able to integrate assessment for urban water quality and simulate the process and efficiency of LID devices.

Geographical Information Systems (GIS) have become a powerful tool in (urban) hydrological modeling by providing tool sets for data collection, analysis, description, and map-based visualization for spatial information as well as for modeling outputs. Hydrology modules are being actively developed in GIS softwares, and vice versa, promoting versatile and multi-purpose couplings between GIS and urban hydrological models.

This first chapter is dedicated to a brief description of the general context in urban hydrology. Main hydrological processes under urban conditions are first discussed with a focus laid on the impacts of urbanization on surface and subsurface water compartments. As alternative solutions to centralized drainage systems, the LID practices are described in the second section. Hydrological modeling tools are addressed in the third section. Application and coupling of GIS tools in hydrological modeling are presented in the last section.

1.1 Impacts of urban development on hydrology

1.1.1 Infiltration and surface runoff

Surface sealing in cities prevents water from infiltrating and strengthens surface flows, which constitutes the main resource of the discharge at the outlets of an urban catchment via stormwater drainage systems.

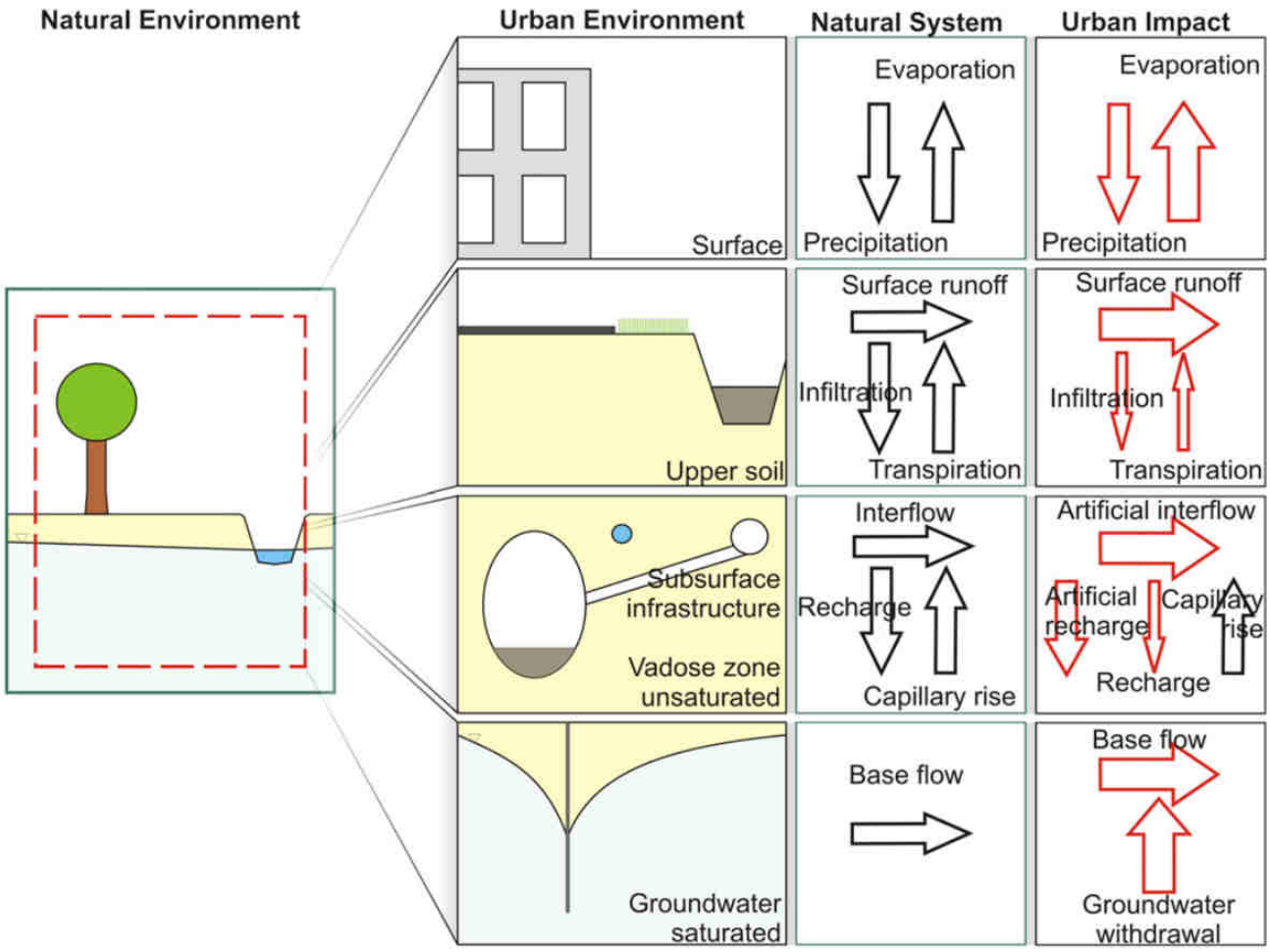

Figure 1.1 – Simplified urban impact on the water balance by Schirmer et al. (2013). The red arrows represent water flow which has been modified or newly introduced by urbanization.

Before encountering a sewer inlet, surface flows are either diffused or canalized. The transfer times of the two regimes are normally different, which forms a first difficulty for understanding urban runoff (Berthier, 1999).

Conventionally considered to be totally impervious in simplified approaches, sealed surfaces have been demonstrated to undergo unexpected infiltration. The infiltration rate is highly variable depending on surface material and rainfall feature, making it difficult to clearly assess the roles of these "impervious" pavements in the generation of urban runoff. This observation was firstly mentioned in the 1980s by Davies (1981) and Hollis and Ovenden (1988), who found significant differences in runoff-rainfall ratio between a roof and a street. Ramier et al. (2011) studied two street segments over a 38-month period in the oceanic climate of Nantes (France), concluding that even runoff was the dominant process on the impervious surfaces, runoff losses through infiltration and evapotranspiration were not negligible. Streets, roofs, parkings can be connected to drainage systems. A great part of rainfall on these surfaces are transformed to direct discharge. Some impervious surfaces such as pavements around a construction can

be disconnected from drainage systems. In this case, the hydrological signal of the impervious surface is likely to be attenuated (Alley and Veenhuis, 1983; Walsh and Kunapo, 2009), or even reversed due to locally enforced infiltration (Göbel et al., 2004). For an urban catchment in the city of Leipzig, Germany, Musolff et al. (2010) found that only 11% of the precipitation discharges to the combined sewer systems, in spite of the 25% of overall surface sealing, due to most likely low connection ratio to the sewer systems.

Runoff regime of natural (non-sealed) urban surfaces attracts the attention of numerous researchers. While some of them state that these surfaces have little contribution to runoff (Ando et al., 1984; Boyd et al., 1994), others find that it can not be ignored (Booth and Jackson, 1997; Berthier, 1999; Price et al., 2010). As a matter of fact, antecedent moisture condition underlying a permeable surface controls directly its infiltration capacity, and subsequently the quantity of land runoff. Depending on the features of the soil and of the rainfall, the subsurface moisture condition is heterogeneous in space and time. Consequently, the contribution to runoff of natural surfaces is variable with respect to surface, site and storm event (Berthier et al., 2004).

1.1.2 Subsurface flow and sewer leak/infiltration

Impact of urbanization on subsurface flow is complex, resulting from characteristics of the catchment (geology, topography, vegetation, etc.) and the urbanization itself (spatial arrangement of impervious surfaces, nature of the sewer systems, etc.). Man-made underground infrastructure is multiple in urban areas and disturbs the natural regime of underground water flow: rise of piezometric level at upstream and drop at downstream, change of groundwater flow direction and distribution, hydraulic gradient between the infrastructure and groundwater outlet (Gilli et al., 2004; Garcia-Fresca and Sharp, 2005).

The trenches of sewer pipes are often composed of sand and gravel that are more permeable than surrounding soil, and drain consequently the soil by supplying preferred water pathways (Garcia-Fresca and Sharp, 2005). Conversely, water and pollutant leaking out of sewers can flow laterally to find a convenient route to penetrate deeper into the aquifer or to infiltrate in downstream sewer pipes. The processes of sewer leak and infiltration are observed/modeled in numerous studies. Gustafsson (2000) observed and simulated groundwater incursion to a combined sewer systems of the Köpinge village in Sweden. The foul flow was found to be only 15% - 30% of the total drainage volume, and the rest was due to groundwater infiltration. Prigiobbe and Giulianelli (2009) reported 50% of infiltration in sewer networks of an historical area in Rome and 14% for a recent area.

Among French cases, Breil (1990) showed 40-70% of the wastewater sewage networks of Paris was concerned by groundwater infiltration problem. Dupasquier (1999) analyzed flow volumes in sewer networks for four urban catchments in France and showed that groundwater infiltration could represent 1/3 of the total drainage volume during summer and up to 3/4 during winter. In the context of the Rezé (Nantes) experimental catchment (Berthier, 1999), groundwater infiltration appeared in winter with rapid dynamics responding to precipitation. Rodriguez et al. (2008) modeled this catchment with the URBS model (cf. Chapter 2) and estimated 11% and 18% of the total annual rainfall infiltrated in the storm-

and wastewater sewer network, respectively. Braud et al. (2013) decomposed the annual discharge in a combined sewer system of a suburban catchment near Lyon, and found that groundwater incursion accounted for 30-40% of the total annual combined discharge in the sewer system.

Groundwater infiltration reduces the efficiency of the sewer systems and results in higher treatment costs. Meanwhile, sewers serve as drains for groundwater during wet-weather periods and storm events and mitigates the problem of increasing groundwater levels (Karpf and Krebs, 2011b). Accurately quantifying the groundwater infiltration is thus essential to the understanding of the water cycle under urban settings and benefit to integrated water management.

1.1.3 Evapotranspiration

Evapotranspiration (ET) is a major part of the water balance, by making up around 60-95% of mean annual rainfall in forested catchments (Zhang et al., 2001). In urban areas, ET was firstly studied by climatologists with their interest in urban energy budget (Grimmond et al., 2010). From an hydrological point of view, it has been often neglected, mainly because hydrologists focus on the hydraulic design of drainage systems and consequently on the simulation of catchment response to intense rainfall. More recent studies showed that ET remains a significant component of the water balance in urban areas. For example, the city of Vancouver (Canada) returns, under temperate climate, 38% of total annual rainfall to the atmosphere by ET flux. This percentage rises up to 81% during summer (Grimmond and Oke, 1991).

With the development of LID, interactions between ET and the other processes become an important research issue, with the motivation of knowing how urban design and low-impact stormwater drainage systems influence urban water balance. SVAT (Soil Vegetation Atmosphere Transfer) models are for this purpose adapted to the urban context (Berthier et al., 2006; Dupont et al., 2006; Lemonsu et al., 2007). Wang et al. (2008) developed a model UFORE-Hydro (for Urban Forest Effects Hydrology), which simulated water balance at catchment scale in order to study the influence of trees. Mitchell et al. (2008) assessed the influence of urban design on water balance, confirming the importance of ET in evaluating the efficiency of sustainable systems in water management. Fletcher et al. (2013) states that there is an emerging interest in the use of techniques for restoring ET as part of a more integrated approach to stormwater management, but knowledge of such practices at this stage is quite primitive.

Related to the heterogeneous land use, urban ET has high spatial and temporal variabilities. Berthier et al. (2006) simulated ET flux on the small suburban site Rezé and found that dominating contribution to annual ET (90%) was from natural surfaces with seasonal contrast (more than 50% from summer), while paved surfaces accounted for less than 10% of annual ET but with relatively constant flux through the year.

1.1.4 Urban streamflow

The influence of urbanization on streamflow through the combined effect of spatial arrangement of surface development and drainage networks are studied by both empirical data and modeling approaches. Burns et al. (2005) compared three small headwater catchments representative of suburban development levels. Peak magnitudes were found to increase and recession time decrease with increasing urbanization; higher baseflow occurred in dry periods in the high-density residential catchment. Braud et al. (2013) proposed indicators of impact of sewer overflow devices for a suburban catchment in France. Decrease of specific discharge was found from upstream to downstream with increased urbanization. Sheeder et al. (2002) examined five hydrographs from three catchments of various levels of urban development. The catchments displayed different peaks for a single rain event, thus separated urban from rural signals. The multiple-peak feature of urban hydrographs was confirmed by Braud et al. (2013) and Furusho et al. (2014).

1.1.5 Groundwater recharge

Groundwater are mainly recharged by infiltrated rainfall into the soil. Urban land use comprises highly heterogeneous patterns of land cover and vegetation density which affects natural groundwater recharge process. There exists evidence that surface sealing can lead to a reduction in infiltration (Rose and Peters, 2001; Deal and Daniel, 2004; Brett et al., 2005; Schoonover et al., 2006). At the same time, evapotranspiration is reduced both by surface sealing and groundwater drains (for water level control) and is susceptible to counter-balance the infiltration lost (Rose and Peters, 2001; Endreny, 2005; Vázquez-Suñé et al., 2010; Barron et al., 2013). The resultant effect of this offset on groundwater recharge is variable. In Haase's (2009) investigation of the effects of long-term (130 years) urbanization on water balance, evapotranspiration dropped by 25%, runoff increased by 182%, but recharge exhibited a reduction of only 4%. On the other hand, infiltration can occur locally through, e.g. gaps between kerbstones and cracks in the gutter (Hollis and Ovenden, 1988). Runoff retention basins, infiltration basins, recharge boreholes and permeable pavements are used in may cities, providing local recharge routes (Ku et al., 1992).

As illustrated in Figure 1.2, leak from and infiltration into water mains and sewer networks constitute a non-neglected part in the groundwater balance of a catchment both at annual scale (Yang et al., 1999; Lerner, 2002; Rodriguez et al., 2008) and event scale (Berthier et al., 2004). In the case where wastewater are re-infiltrated after treatment, this quantity of water can also represent an important component in groundwater recharge (Burns et al., 2005). Vázquez-Suñé et al. (2010) identified urban recharge sources for the city of Barcelona, Spain, and showed that 50% of the water in the aquifer originated from water supply and sewer networks. Yang et al. (1999) estimated 70% of the urban recharge in Nottingham, UK, was from main leak and sewer leak.

The overall effect of urbanization on the volume and distribution of catchment-wide groundwater recharge are difficult to quantify and must differ from case to case (Ku et al., 1992; Lerner et al., 1994; Misstear et al., 1995; Thomas, 2006; Schirmer et al., 2007). Furthermore, they can not be easily isolated from other urban stresses such as pumping. Based on a long-term spatially distributed groundwater

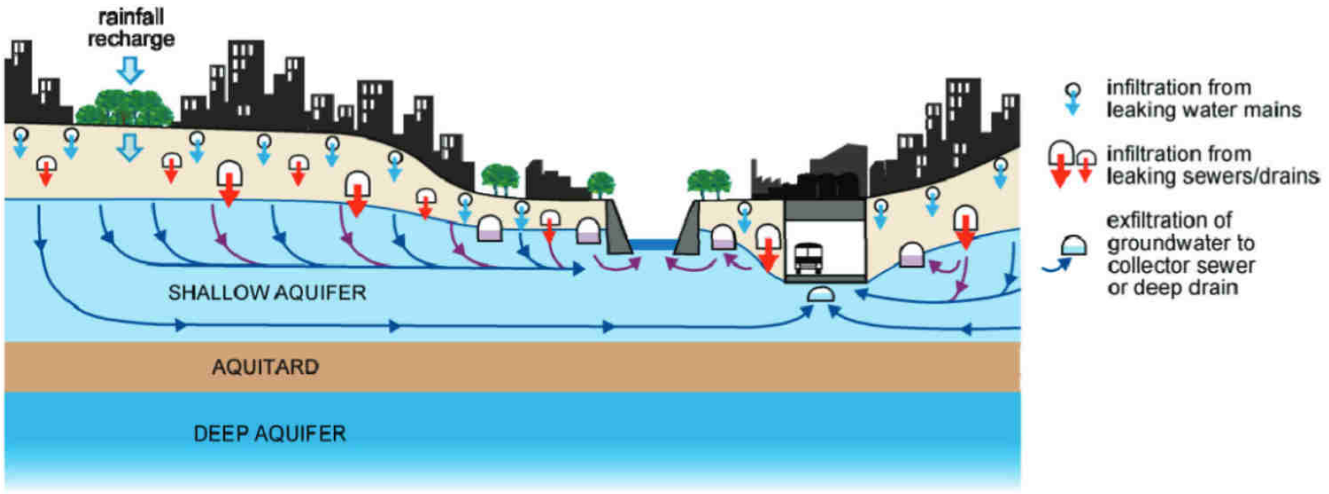

Figure 1.2 – Typical modifications by sewer systems of the urban groundwater regime (Foster and Vairavamoorthy, 2013)

monitoring in the city of Seoul, Lee et al. (2005) observed an increase of groundwater table at some places and a decrease at the others. Similar statement has been established by Jeppesen et al. (2011). Some studies found even increased recharge of groundwater along with urban development (Lerner, 2002; Brandes et al., 2005). The authors explained this by over-irrigation for gardens and parks, and by concentrated infiltration that was more efficient in terms of recharge.

1.2 Low impact development (LID) for stormwater management

Management in cities for stormwater of the last century was marked by the development of buried piping systems. Focused on the reduction of peak discharge rate, these pipe-based systems were conceived to transport storm- and wastewater out of the city and to downstream water courses as quickly as possible (Prince George's County, 1999). Initial combined sewer systems for storm- and wastewater were progressively replaced by separate sewers. Today, this centralized conveying and treatment through pipe sewers is recognized as far from being satisfactory and suffers from overloading by urban expansions. Consequently, challenges of city flooding has returned under the spotlight, with the costs for traditional collection and conveyance systems rising sharply.

Pollution from stormwater runoff is also a major concern. Rainwater washing across streets and sidewalks can pick up spilled oil, detergents, solvents, pesticides, fertilizer, and bacteria. Stormwater drains do not typically channel water to treatment facilities, but carry runoff directly into streams, rivers and lakes. Carried untreated into streams and waterways, these pollutants increase algae content, reduce aquatic life, and require additional costly treatment to make the water potable for downstream water systems. Although some conventional techniques may incorporate conservation design to minimize flooding and improve water quality with detention facilities, they do not promote infiltration, groundwater recharge,

and water quality improvement (USEPA, 2000).

Emerged in the 1990's, the idea of low impact development (LID) approach is to try to mitigate the effect of urbanization and emulate natural hydrological systems that use cost-effective solutions through a large variety of green infrastructures favoring at-source retention and infiltration: permeable pavements, infiltration trenches, swales, rain gardens, green roofs, ponds, lakes, detention basins... These devices can be applied at multiple scales, from parcel backyard to district, in both urban and rural environments. They can be designed into new developments or retrofit into existing community open spaces, parks, rear areas of homes and buildings, rooftops, below parking lots and in other settings (Hunt et al., 2010), which reduce the need for a centralized stormwater drainage system. Being developed simultaneously at different institutions and driven by local perspectives and context, the concept of LID has been described by different terminology, such as Water Sensitive Urban Design (WSUD) (Fletcher et al., 2004a), Best Management Practices (BMPs), or Sustainable Urban Drainage Systems (SUDS) (CIRIA, 2013). With slightly different points of focus, they describe broadly the same approaches (a detailed review on this terminology can be found in Fletcher et al. (2014)) and adhere to the following principles among others:

- Integrate stormwater management strategies in the early stage of site planning and design.
- Mitigate storm discharge rate and volume to water treatment plants and receiving water bodies.
- Maintain or return the flow regime as close as possible to the natural (pre-development) level.
- Limit rising expenditure for water conveyance and treatment.
- Enhance groundwater recharge for water resource conservation and protection.
- Fight against the deterioration of water quality and protect flora and fauna.
- Enhance the urban landscape and amenity by incorporating stormwater management measures which offer multiple benefits into the landscape.
- Make water a major component of urban environment and life quality: restoration of streams, water parks.

Beneficial uses of LID practices have been demonstrated at the catchment scale (Hood et al., 2007; Selbig and Bannerman, 2008; Wang et al., 2010) and micro-scales such as lot level (Hunt and Lord, 2006; Gregoire and Clausen, 2011). Today, although the need for at-source runoff and pollution control are generally well accepted both by scientists and practitioners, debates surround many of these practices and aspects pertaining to their benefits, indicating that knowledge gaps exist in regard to the effectiveness and application of LID practices (Ahiablame et al., 2012). Understanding the hydrological cycle is an integral component in planning for the sustainability of our water resources. It is recognized that interactions between the components of the urban water cycle are as important as the individual components themselves (Fletcher et al., 2013). The technical, environmental, sanitary, social and economic benefits of LID

practices depend on both the technologies themselves including the installation quality and the quality of governance (policy, planning, conception, construction, maintenance, etc.). A practice is really efficient only if it does not in conflict with other interests (urban development, landscape, users, ...). In order to reach high degree of sustainability, it is necessary to consider urban storm runoff in a broader urban water management framework and take into account of the urban water cycle by integrated approaches. In such an approach, the act of managing rain water and water resources is connected, compartments of the water balance (atmosphere, canopy, land surface, underground...) and their connections are considered in an integrate way. Man-made infrastructures, such as water supply and sewer systems, are also seen as parts of the integrated physical system (Mitchell et al., 2007).

1.3 Hydrological modeling for urban area

1.3.1 Stormwater model and integrated hydrological model

Urban hydrological modeling has been historically developed centering on stormwater models, which concentrate on catchment response to storm events as a function of time and spatial arrangement. Attention is usually paid on runoff on impervious surfaces and transport of the runoff in drainage systems. A stormwater model can be divided, in terms of structure, in two basic components: (i) rainfall-runoff modeling (ii) transient modeling, as illustrated in Figure 1.3.

Rainfall-runoff modeling is the transformation of observed rainfall series to runoff quantity at a catchment or sub-catchment scale. Depending on the model complexity, hydrological processes covered in this stage can include canopy interception, evapotranspiration, infiltration, percolation, groundwater flow and sewer leak/infiltration. Besides climate forcings such as rainfall intensities and potential evapotranspiration rates, major factors affecting the runoff generation include topography, surface sealing extent, other land uses and their spatial arrangement, as well as antecedent moisture conditions. All the processes can not be systematically detailed. Linear or non-linear reservoir approaches are the approximations often used in simplified models. In the Wallingford Model (Bettess et al., 1978), the rainfall-runoff model uses a modified rational method, with the inclusion of a routing coefficient. It incorporates the proportion of impervious area, soil type, evapotranspiration and antecedent conditions. The runoff is estimated by distributing rainfall onto roofs, sealed and pervious areas. Rodriguez et al. (2003) proposed a more detailed parameterization for runoff formation and concentration at upstream of sewer system hydraulics. Streets were incorporated in the routing map and flow transfer at the parcel scale were explicitly modeled (cf. Chapter 2).

Transient modeling simulates the routing process from where runoff is produced to catchment's outlet. The type of routing employed can be classified, according to the model complexity, to simple storage, hydrological and hydraulic routing. Hydraulic modeling is used for hydraulic processes in sewer systems. Shallow water wave equations and its approximations, kinematic and diffusion wave equations, are often used for this purpose. For example, the well-known Muskingum–Cunge method (Cunge, 1969) is an

implicit finite difference approximation of the kinematic wave equation. STORM (Hydrologic Engineering Center, 1977) calculates hourly runoff based on three methods without computing hydraulic routing: coefficient method, soil-complex-cover method and unit hydrograph method. SWMM (Huber and Dickinson, 1988; Rossman, 2004) or MOUSE (Danish Hydraulic Institute, 1998) combines an hydrological stage which simulates hydrographs at small urban catchments with the propagation of these hydrographs in pipe networks based on St-Venant equations. More sophisticated models can refine the transient process and simulate surface flow upstream of sewer drainage. In case where drainage data is not available, conceptual lumped approaches can be used as an alternative (Desbordes, 1987). Water flow paths at the surface can be identified from high-resolution digital elevation models (Smith and Brilly, 1992), and sewer pipes can be conceptualized as open thalwegs (Zech et al., 1994; Rodriguez et al., 2000).

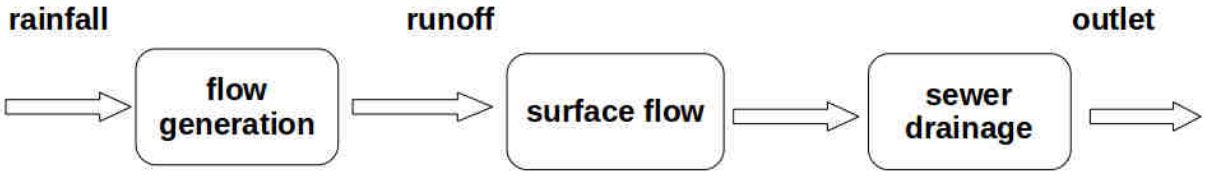

Figure 1.3 – Conventional structure of an urban stormwater model.

Based on modeling scale, stormwater models can be described as event-based and continuous models. Large design storms have been traditionally and successfully used for urban drainage design over the past century, safeguarding urban areas from flooding and associated damages. However, it is well accepted today that different drainage design objectives require the examination of different types of rains (Pitt, 1999). The use of simple design storms is no longer adequate, especially when the issue of receiving water quality are addressed. Long-term continuous simulations should be used in order to promote the integration of quantity and quality objectives. Many models are capable of performing both event-based and continuous modeling. For example, the DR_3M-QUAL Model (Alley and Smith, 1982a,b) of the USGS can be executed using any time step over any time. STORM is a continuous model using hourly time steps and it can be used for single events. The Wallingford model can be applied to stormwater or wastewater systems or to combined systems using 15-minute time steps. SWMM is also both a continuous and single-event model.

The development of policies for integrated water management in cities encourages researchers to work on more sophisticated, physically-based modeling tools that can consider the urban hydrological processes and their interactions in integrated ways, moving beyond a management of urban runoff in isolation from other components of the urban water cycle. Besides the classical assessment on impervious

runoff production and hydraulic sewer routings, these models are also conceived to examine miscellaneous flow and storage components in the water cycle, pollutant transient, drainage and treatment installations.

Stormwater quality aspects can be incorporated in models, including pollutant production (Zoppou, 2001), transport (Fatta et al., 2002) and treatment (Elliott and Trowsdale, 2007). Pollutant concentrations and loads can not be estimated without an examination on water flows, and mitigations of quantity and quality degradation are complementary (Zoppou, 2001). For example, LID devices such as retention basins reduce flood peaks as well as trap sediments.

As LID practices develop, evaluating the efficiency and impacts of these techniques is also a function that more and more models incorporate (Ackerman and Stein, 2008; Wild and Davis, 2009; Golroo and Tighe, 2011). In his literature review, Ahiablame et al. (2012) divided the modeling of LID practices as practice-presented and process-presented. In the first class of modeling, effects on runoff and water quality of a practice are measured as a whole and presented in one parameter (e.g. representing the effects of green roof, bioretention and permeable pavement). This approach is usually utilized to compare development scenarios, prior to more detailed studies for practical implementation. In the second class of modeling, processes (infiltration, sedimentation, adsorption, evapotranspiration, settling, transformation of pollutants) occurring in a LID practice are represented in a more detailed manner, in order to allow suitable modeling for design, construction and optimization of development scenarios. But this type of modeling involves extensive computational and data requirements. Some models include or couple with "optimization" techniques, which allow to determine optimum values for a given set of decision variables that will maximize or minimize an objective function, usually cost (Chu and Bowers, 1977; Allen and Bridgeman, 1986; Behera et al., 1999). MUSIC, for example, can be used to model water treatment and flow for a multiple of systems: wetlands, ponds and sediment basins, swales and buffer strips, bio-retention and infiltration systems as well as stormwater harvesting systems (eWater CRC, 2009; Fletcher et al., 2004b). The URBS model incorporates several LID devices modules based on the process-represented approach. Processes within the devices such as infiltration, percolation, evapotranspiration are simulated with physically-based methods. These modules are described in Chapter 2, Section 2.7.

After all, most of the models consider one or several of these components/aspects, and rarely a model could integrate the urban water cycle and LID devices in a throughout way (Fletcher et al., 2004b). Highly complex models are difficult to calibrate and incorporate parameter and structural uncertainty as well as non-deterministic behaviour (Rauch et al., 2002).

Parcel is a basic structural element for urban analysis, planning and property governance (Lynch, 1960). Working at parcel scale allows for the understanding of stormwater management options from local to district scale, in taking advantage of the development of urban database. Mitchell et al. (2007) proposed a model called "Aquacycle" which simulated hydrological processes with a daily time step and at a spatial resolution of an urban block. Hardy et al. (2005) introduced their integrated model, UrbanCycle, which simulated water supply, stormwater and wastewater using allotments as the basic building block. The same approach has been adopted in the Urban Developer (eWater CRC, 2014) and the SWITCH

program (Last and Mackay, 2010). The URBS model (Rodriguez et al., 2008) belongs to this category of model.

1.3.2 Model coupling

Coupling existing models for new modeling objectives is a commonly used practice. This can help to benefit the advantages of each of the models, value the fruitful of other research work, and promote communication among researchers. There exist a great number of coupled models for research and/or operational purposes. Below are several examples which are deemed to be close to the model coupling realized in the present work (see Chapter 3).

In the TEB-ISBA model developed by Lemonsu et al. (2007), the town energy balance (TEB) scheme (Masson et al., 2002) was coupled with a soil-biosphere-atmosphere (ISBA) scheme (Noilhan and Planton, 1989) to simulates water energy balances for urban covers, with the TEB for paved surface simulating and ISBA for natural surface and subsurface simulating.. With an objective of describing geo-hydrological processes and interactions with sewer networks, Gustafsson (2000) realized a dynamic coupling between MOUSE (for sewer hydraulics) and MIKE SHE (for catchment hydrology and groundwater). The coupled package was applied in two urban cases in Sweden and showed high performance for groundwater infiltration modeling. Giangola-Murzyn et al. (2012) developed a multi-process platform Multi-Hydro by coupling different modules relying on existing models for runoff processes, sewer discharge and subsurface processes. The model has been implemented on a case study in Paris. Gires et al. (2014) reported a second version of Multi-Hydro which coupled a 2D model for surface runoff and infiltration and the hydraulic part of SWMM for flow in sewer pipes. (Jankowfsky et al., 2014) constructed the PUMMA model for suburban settings. The models BEREFT (Branger et al., 2008) and URBS (Rodriguez et al., 2008) have been coupled on the LIQUID platform for modeling the processes of rural and urban area respectively. The integrated PUMMA model has been proved to be robust.

1.4 Geographical Information System (GIS) in hydrological modeling

Tremendous geospatial information handling capacities of Geographical Information System has promoted the development of spatial distributed hydrological modeling, which, in return, value GIS's functionalities in hydrological modeling field (Maidment, 1991; Feldman and DeVantier, 1993; Ogden et al., 2001; Carrera-Hernández and Gaskin, 2006). In urban areas, constructions, land sealing and various man-made structures modify both morphological features of the catchments and natural water flow paths, making morphological characteristics a central factor in urban water management and modeling. By offering a possibility to simplify the pre- and pro-processing of morphological urban data, GIS is of considerable use in almost all aspects of urban development (Sui and Maggio, 1999; Laurini, 2001; Ogden et al., 2001). This section gives an insight in GIS's utilities in urban hydrological modeling.

1.4.1 How can GIS help (urban) hydrological modeling

Modeling spatial variables is a data-intensive task to which GIS have become powerful tools. They offer efficient techniques for terrain description (soils, cities, land use, land cover, streets, vegetation properties, snow covers, underground pipes, etc) and convert these spatial information to digital datasets. GIS can extrapolate locally measured data to areas. For example, the GIS software GRASS can extrapolate point data through the r.surf.rst module (Mistasova and Mitas, 1993). The great capabilities of GIS for site description and analysis make it a versatile tool for delineating basins and sub-basins, deriving stream networks and determining model parameters related to the direction of movement or to the mode of transmission.

The Digital Elevation Models (DEM) are widely used in hydrological modeling. Flow velocities can be derived from geomorphological characteristics, such as slopes and upstream areas (Moniod, 1983). Surface flow paths can also be easily derived from DEM (Maidment, 1993; Lhomme et al., 2004). In urban settings, flow paths could be derived from DEM if buildings and artificial networks are correctly considered. Rodriguez et al. (2003) derived urban unit hydrographs directly from geospatial data analysis for three urban basins and found that the unit hydrographs such derived were similar in shape and scale to that from rainfall-runoff measurements.

Additional data collection is important for enhanced terrain description in urban hydrological modeling. Global Positioning System allows accurate location of hydraulic control points such as curbs and valves, and can greatly improve the ability of the GIS and hydrological model in prediction of flow paths in an urban setting (Feldman and DeVantier, 1993). Development of aerial photography and satellite remote sensing opens up new avenues for GIS to extend its potentialities and benefits in the field of urban modeling.

GIS offers a comfortable platform for visualizing and analyzing modeling output in the form of maps, thus makes it possible to analyze changes over an area as well as over time (Goodchild et al., 1996). The analysis of distributed modeling output by GIS techniques is described as post-processing (Jankowfsky, 2011).

Parameter estimation is probably the most active area in the GIS field related to hydrology (Ogden et al., 2001). In this case, the objective is to assign relevant parameter values through the manipulation and analysis of various terrain data sets. Information on land slope, channel slope, soil characteristics and land cover can be derived from digital raster and vector data layers. The use of GIS helps to automate the parameterization process and improves model performance (Evans et al., 1992; Bian et al., 1996). Preparation of spatially distributed hydrological modeling data is described as pre-processing (Jankowfsky, 2011).

In urban settings, buildings, streets and other man-made infrastructures make the morphological features and land uses more complex than natural settings. Natural topology is locally altered by urbanization, which modifies consequently surface flow paths. Stormwater systems collect and convey water, reform subsequently deeply the hydrographic network. Detailed information on these infrastructures is

needed for correctly delineating catchments and sub-catchments, deriving drainage network and defining geographical parameters. GIS offers a suitable and inevitable tool to these work.

The widespread development of multi-purpose Urban DataBanks (UDB) is a good example of utility of GIS for urban spatial databases (Rodriguez et al., 2003). Urban cadastre records are modernized through GIS, and UDB includes a greater number of layers superimposed on the parcels. Private buildings and gardens are detailed within parcels with sometimes precise information such as the height and type of building. Street networks is treated both as two-dimensional polygons and line objects in relation to underground installations: energy, telephone, Internet, water supply and sewer networks. Green surfaces and hydrographic networks are also included in UDB as specific layers. Information on hydrographic networks is however usually partial, embedding only large water bodies such as rivers and lakes (Rodriguez et al., 2003). In our modeling work on urban catchments in Nantes city (cf. Chapter 4), geospatial information on parcels is provided by Urban DataBanks of Nantes Métropole.

1.4.2 Links between GIS and hydrological models

Maidment (1991) identified four distinct hydrologic applications of GIS: hydrological assessment, hydrological parameter determination, hydrological model set up using GIS and hydrologic modeling inside GIS. The first two types of application refer to pre- and post-processing of geospatial input or of modeling output, without necessarily narrow embedding within the hydrological model. The last two stages refer to more sophisticated interactions between the GIS tool and the hydrological model where GIS provides the user interface, both programs share a common database and the hydrological model can even make use of GIS libraries. Sui and Maggio (1999) classified the links between GIS and hydrological modeling: embedding GIS in the hydrological modeling, or vice versa, tight coupling and loose coupling. Examples for embedding GIS in hydrological model are the widely used MODFLOW (Mcdonald and Harbaugh, 1988), HEC-RAS (Brunner, 2010) and CANOE (Sogreah and Insavalor, 2005). Examples for embedding hydrological models in GIS interfaces are TOPMODEL (Beven and Kirkby, 1979), SWAT (Srinivasan and Arnold, 1994), ANSWERS (Beasley et al., 1980) and AGNPS (Young et al., 1989), which are embedded into GRASS (GRASS GIS, 2014). An example for tight coupling is Bhatt et al. (2008) who incorporated PIHM model into QGIS and created the open source GIS software PIHMgis. Thomas (2006) proposed a sophisticated GIS based model of urban recharge and non-point source pollution and applied it to the city of Birmingham, UK. The model is able to quantify spatially distributed runoff, interception and evapotranspiration.

The loose coupling defined by Sui and Maggio (1999) corresponds somehow to the hydrological assessment and parameter determination defined by Maidment (1991). In this kind of coupling, hydrological modeling and GIS exchange data using either ASCII or binary data format, among several different software packages without a common user interface. Contrary to other types of links, this approach has the advantage of being flexible, since several GIS softwares could be used at the same time. Urban geospatial data is organized and treated with GIS pre-processing, than converted to text input files of the model.

An example is the physically-based model MIKE SHE (Abbott et al., 1986), which can be coupled to ArcView/Geoeditor where 3D geological models can be built based on geological field data. MIKE SHE has also a built-in mini GIS system. Another example is MHYDAS (Lagacherie et al., 2010) of which geodata pre-processing is conducted in GRASS. The PUMMA model (Jankowfsky, 2011) was loosely coupled with GRASS and PostgreSQL for the preparation of the model mesh as well as calculation of geometrical parameters. A series of Python program has also been developed to automate this pro-processing. Because computer programming is minimal, this approach may be the most realistic method for most GIS users and hydrological/hydraulic engineers to conduct modeling work (Sui and Maggio, 1999). In the present study, our hydrological model belongs to this type of coupling with GIS applications.

1.4.3 GIS softwares

Many GIS softwares are existing or under development. The most commonly used GIS is probably ArcGIS® of ESRI (ESRI, 2014), which has the largest set of functions. People are contributing continuously to develop open source GIS softwares. In addition to the economic advantage, open source GIS provide access to their source codes, thus allow user to explore totally their capabilities and develop new plugins for their own purposes. Another advantage of open source GIS is that they provide mailing lists for user supports and tutorials. The most widely used open source GIS softwares include QGIS, GRASS, OpenJump, SAGA, PostgreSQL/PostGIS. Some others are being actively developed, amongst which we can cite the French OrbisGIS (Bocher et al., 2014) in which the GDMS library is integrated with a convenient SQL shell. OrbisGIS is one of the main GIS softwares used during the present work (Chapter 4).

Most of the GIS applications are based on JTS Topological Suite libraries (JTS, 2013) and GEOS (GEOS, nd), as well as other libraries such as GDAL (GDAL, 2013) for the import of raster data. Instead of developing new GIS softwares, the tendency is integrated GIS platforms. The incorporation of GRASS in QGIS is a good example which allows for benefiting the advantages of both. A more detailed description of the two softwares is given in Chapter 4.

Part III

Development of the saturated flow module WTI in the distributed hydrological model URBS

Chapter 2

Description of the URBS model

Contents

Introduction

URBS, for Urban Runoff Branching Structure, is a physically-based distributed hydrological model developed at IFSTTAR[1], research institution in urban science and engineering located in Nantes, France. URBS is designed for catchment-scale modeling (up till to several hundreds of hectares). It is capable of simulating continuously for periods of the order of years, and at small time steps of minutes. Highly based on Urban DataBanks (UDBs), URBS is the fruit of a series of Ph.D thesis (Rodriguez (1999), Morena (2004)) and articles (Rodriguez et al. (2003, 2008)). Detailed description of the original model can be

[1] Institut français des sciences et technologies des transports, de l'aménagement et des réseaux

found in these publications. Here we only make a sketch for several key elements that concern the present doctoral work. The modeling of subsurface fluxes, which is the main focus here, is described in greater details.

2.1 Spatial discretization of URBS by Urban Hydrological Element (UHE)

URBS describes an urban catchment as a set of Urban Hydrological Elements connected to the flow routing network. This two-dimensional representation of an urban catchment is considered to be suitable for hydrological modeling purposes.

An UHE is composed of a parcel and its adjacent street segments, as illustrated in Figure 2.1. Within an UHE, the surfaces are divided into three types of land use: house (^{hou}), street (^{str}) and natural surface (^{nat}). Both streets and natural surfaces can be partially or totally covered by trees. Geographical parameters of one UHE include:

- surface areas of the three land uses and of tree-covers
- geomorphological features: elevation, slope, length
- coordinates of the connection point to flow routing network

The "street" land use includes both streets and pavements within the parcels (pavements surround buildings such as pathways and parks).

2.2 Modeling at the UHE scale - description of the "production" function

URBS models hydrological components of the water cycle at UHE scale. Each of the three land uses of an UHE is modeled by a vertical profile, as illustrated in Figure 2.2a. Each profile is composed of four reservoirs. From top to bottom, these reservoirs represent the tree-cover, ground surface, the vadose zone and the saturated zone.

The transformation of rainfall-runoff, labeled as "production", is computed at each vertical profile by a set of equations governing the hydrological processes (Figure 2.2b):

- canopy interception and surface depression
- surface runoff
- surface infiltration
- surface evaporation

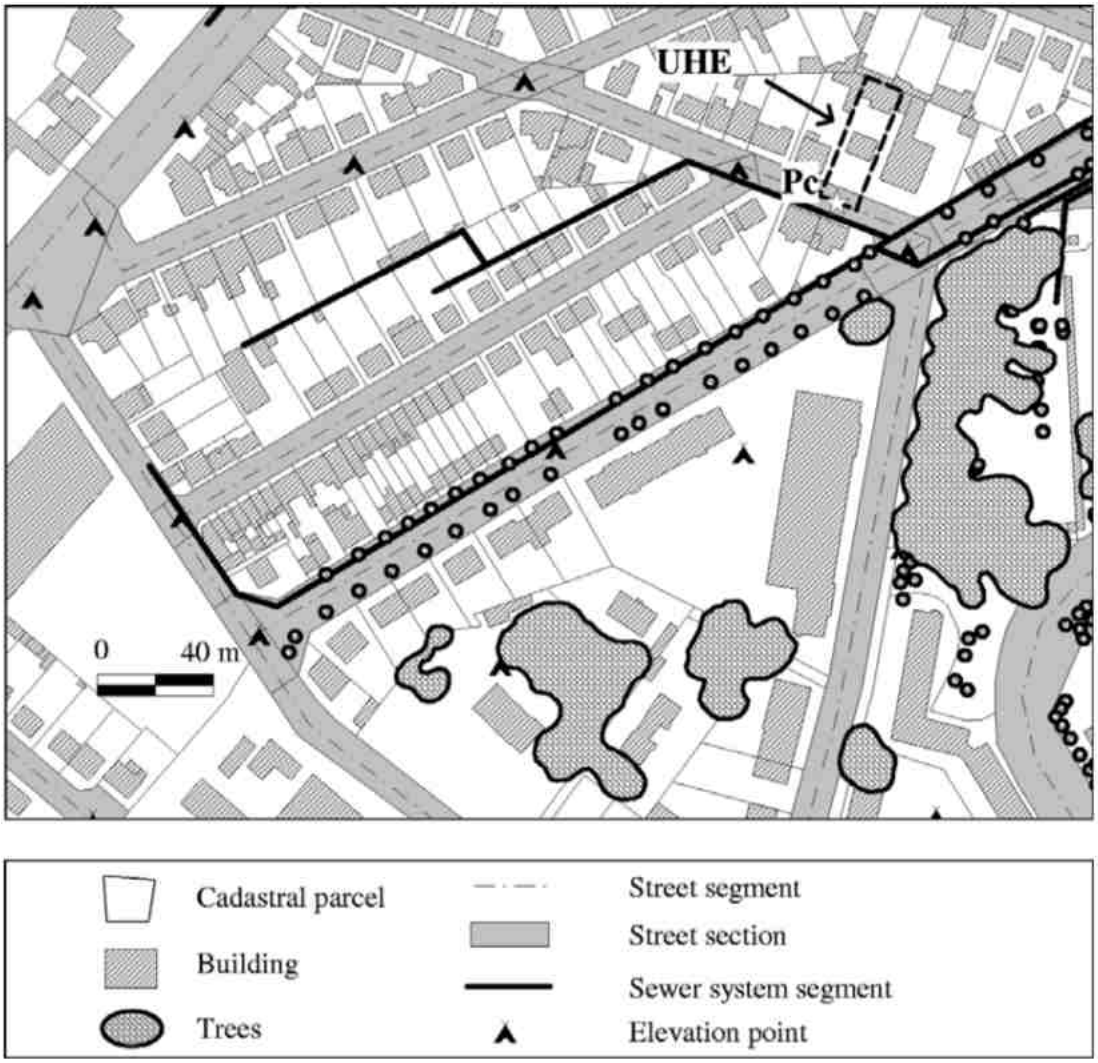

Figure 2.1 – Schematic of the definition of an UHE based on urban parcel map (Rodriguez et al., 2008).

- evapotranspiration of trees
- percolation from the vadose zone to the saturated zone
- capillarity rise
- infiltration flow of groundwater to sewer networks

Flow computation is based on physical laws adopted from the literature. The whole set of equations can be found in Rodriguez et al. (2008). The model assumes uniformity in the hydrological characteristics within each of the land use types, i.e. physical parameter values are uniformly assigned at a land use.

Flows of the UHE are the area-weighted sum of the flows at the profiles. Storage in the reservoirs is updated individually at each profile. Groundwater level is expressed by saturation depth, which is updated at the end of a time step at each UHE.

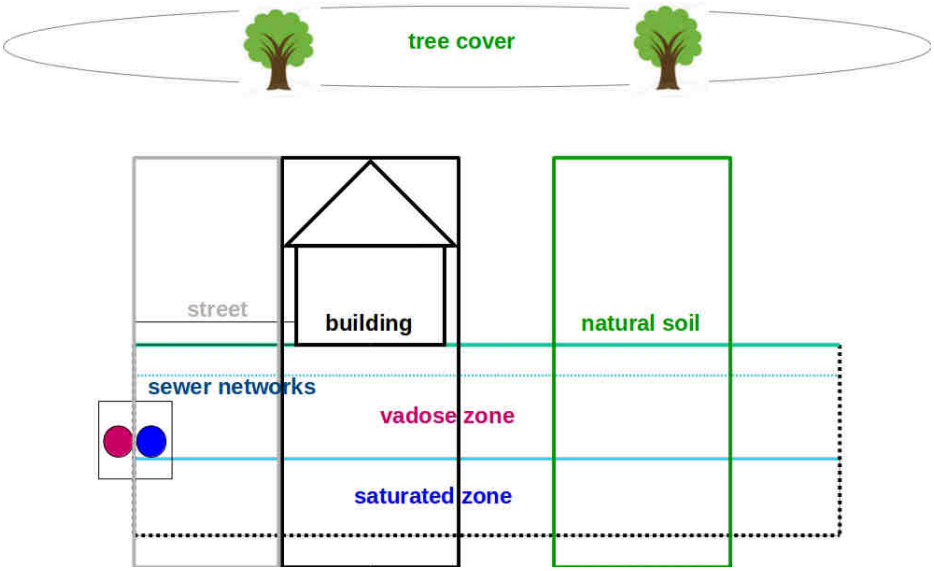

(a)

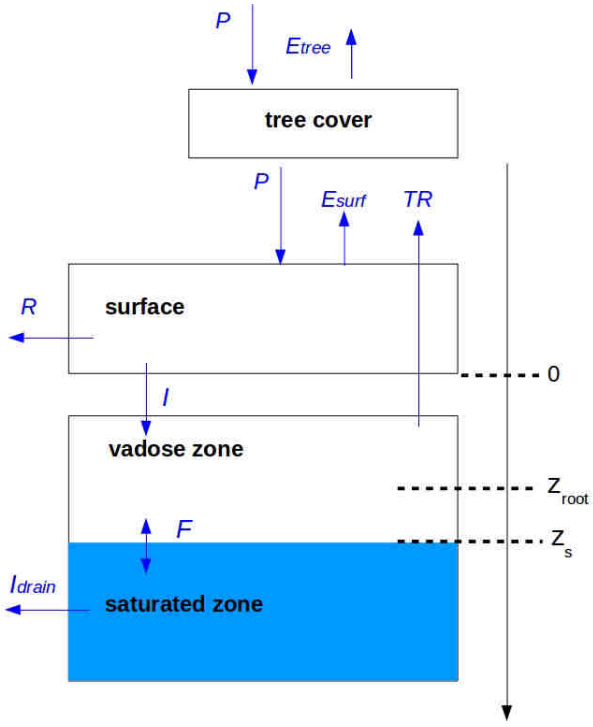

(b)

Figure 2.2 – Two-dimensional schematic of (a) an UHE and (b) vertical profile adopted for each land use, where P – precipitation, E_{tree} – tree evaporation, E_{surf} – surface evaporation, TR – transpiration, R – surface runoff, I – infiltration, F – percolation or capillarity rise, I_{drain} – groundwater drainage by sewer networks.

Saturated horizontal transfer within an UHE is realized by averaging the saturated depths of the profiles at each time step. However, inter-UHE transfer in the saturated zone is not represented in the model, despite a previous attempt of coupling URBS and MODFLOW by Le Delliou (2009) (cf. Chapter 3, Section 3.1). Groundwater level varies independently at each UHE, with the possibility to be averaged for giving the mean groundwater level at catchment scale.

2.3 Flow routing - description of the "transfer" function

Rodriguez et al. (2003) have shown that the geometrical information available in Urban Databanks allowed to construct detailed vector map for water flow paths along UHEs, street gutters and inside the stormwater network, hereinafter referred as Runoff Branching Structure (RBS). The "transfer" function of urban catchments could be derived from the RBS. The flow routing in URBS is an extension of the routing scheme outlined in Rodriguez et al. (2003), as containing two modeling stages:

- Routing of surface runoff from UHEs up to sewer inlets, represented by the travel time. The detailed procedure is described in URBS-UH (Rodriguez et al., 2003).
- Hydraulic routing inside the sewer networks, represented by the Muskingum-Cunge scheme, which offers an approximate solution to the diffusive wave equation (Cunge, 1969).

With this configuration, the runoff routing function gives runoff rate at every node of the flow routing network. This local-scale knowledge can be of utility in various water management applications.

2.4 Temporal discretization of URBS

The two functions "production" and "transfer" are executed within each time step t, as illustrated in Figure 2.3. For any UHE u, under climate forcings, fluxes are computed in each reservoir of each profile from top to bottom based on physical formulations (see Section 2.5) and with the reservoir storage of the previous time step $t-1$. The storages of the canopy, surface and vadose zone reservoirs are updated by the calculated flows at the end of t, and ready to be utilized for the calculation of the next time step $t+1$. The saturation depths of the profiles are area-weighted to give the saturation depth $z_s^{u,t}$ of u, which is equivalent to the groundwater level of u. The groundwater is then drained by the sewer network associated with u, if it is deeper than the saturation depth of u (see Equation 2.12). Then $z_s^{u,t}$ is updated. At the beginning of $t+1$, the saturation depth of each profile $z_s^{u,i,t+1}$ is re-initialized by $z_s^{u,t}$ for the computation within $t+1$. The surface runoff and groundwater drainage produced at u at t is routed into the flow routing network by the "transfer" function at the end of t, and the flow rate at each segment is updated. The time step can be of the order of minutes, depending on the size or response time of the catchment. This is coherent with the rapidly varying transients in urban settings (Rodriguez et al., 2008).

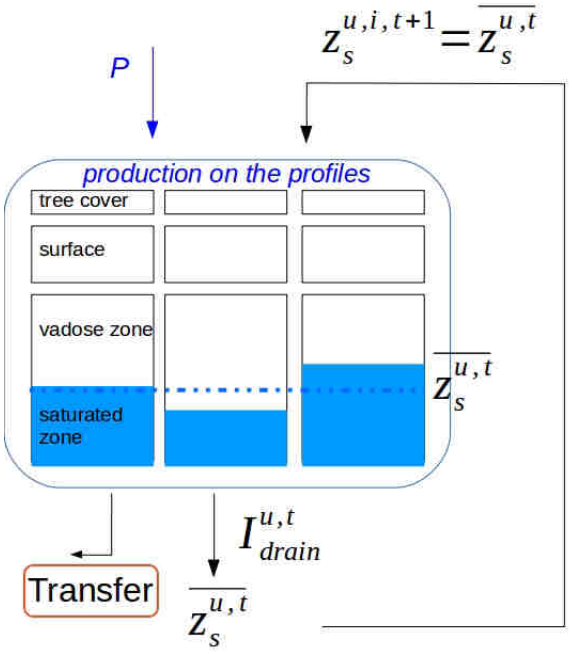

Figure 2.3 – Diagram of the algorithm on a given UHE in URBS. See Section 2.5 for the significations of the variables.

2.5 Computing in subsurface layers

In this work, a special attention has been paid on the saturated zone simulation. Due to this, it is necessary to give preliminarily a description of the parameterization for soil in the model URBS. The presentation below is validated for any of the three vertical profiles within any time step, thus the profile indicator i and time indicator t are omitted in the formulae, except for storage terms in continuity equations where t is necessary.

The soil in URBS is represented by the vadose zone and the saturated zone reservoirs, as illustrated in Figure 2.2 and Figure 2.4. "Reservoir" is actually an abusive use of term for the saturated zone, as it does not have any proper storage capacity, but parameterized by the saturation deficit d (m), defined as the water depth needed to saturate the vadose zone, as inspired by Beven and Kirkby (1979). d is linked to the saturation depth z_s (m) by the moisture content at saturation θ_s (-), which is a model parameter, by:

$$d = z_s \theta_s \tag{2.1}$$

The influence of soil structure, which tends to be more compact in depth, is taken into account by means of an exponential decrease in hydraulic conductivity at saturation K_{sat} with depth z, as inspired by the Top Model (Beven and Kirkby, 1979):

$$K_{sat}(z) = K_s exp(-z/M) \tag{2.2}$$

where $K_{sat}(z)$ (m/s) is the saturated hydraulic conductivity at the depth z (m), K_s (m/s) the hydraulic conductivity at ground level saturation, M a scaling parameter (-). Storage in the reservoir of the vadose

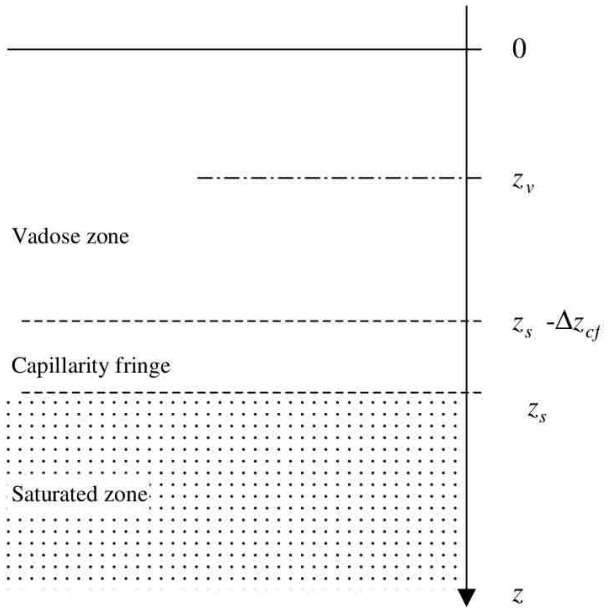

Figure 2.4 – Schematic of the vadose zone in URBS (Rodriguez et al., 2008). See the texts for the significations of the variables.

zone can be written as:

$$S_{vad} = \theta . z_s \tag{2.3}$$

where z_s (m) is the saturation depth at time t and θ (-) the average moisture content in the vadose zone, whose temporal evolution is required herein. The vadose zone receives surface infiltration, exchanges water with the saturated zone and provides the transpiration needs for trees. The continuity equation for the vadose zone is written as:

$$S_{vad}^{t} = S_{vad}^{t-1} + (I^t - F^t - TR^t)\Delta t \tag{2.4}$$

where I (m/s) is infiltration flux from the surface, F (m/s) exchange flux between the vadose zone and the saturated zone that can be either positive or negative, TR (m/s) transpiration flux by the roots of trees.

Infiltration flux I is conditioned both by available water in surface reservoir and moisture condition in the soil:

$$I\Delta t = \min[K_{sat}\Delta t,\ Ss,\ d - S_{vad}] \tag{2.5}$$

where Ss (m) is surface storage, $d - S_{vad}$ (m) the capacity of reception for water in the vadose zone.

The vadose zone is parameterized by its average moisture content θ, assumed to be uniform in the vadose zone, and a capillarity fringe of thickness Δz_{cf} (m) located above the saturation surface, as illustrated in Figure 2.4. This capillarity fringe is supposed to be saturated and its thickness is set equal

to the air entry suction Ψ_e (m), a model parameter.

Flux between the vadose zone and the saturated zone F is calculated by Darcy's law that is applied between the saturation depth and a representative point V of the vadose zone. The depth of the representative point is proportional to the saturation depth:

$$z_v = \alpha_v[z_s - \Delta z_{cf}] \tag{2.6}$$

where z_v (m) is the depth of the point V and α_v the proportion coefficient acting as a model parameter. Darcy's equation is thus written as:

$$F = -K_v \left(\frac{H_s - H_v}{z_s - z_v} \right) \tag{2.7}$$

where K_v (m/s) is hydraulic conductivity, H_s (m) and H_v (m) hydraulic head at the saturation depth and at point V, respectively:

$$H_s = -z_s, \;\; H_v = -z_v - \Psi(\theta) \tag{2.8}$$

where Ψ (m) is the suction, function of θ adhering to the Brooks-Corey law (cf. Equation 2.10), and K_v (m) is the smaller one between the hydraulic conductivity at saturation at the depth of groundwater head $K_{sat}(z_s)$ (m) and the hydraulic conductivity at point V, $K(\theta, z_v)$ (m):

$$K_v = \min[K_{sat}(z_s), K(\theta, z_v)] \tag{2.9}$$

$K_{sat}(z_s)$ is calculated by Equation 2.2, and $K(\theta, z_v)$ is derived from $K_{sat}(z_v)$ (m), hydraulic conductivity at saturation at the depth z_v, by the Brooks - Corey law:

$$\Psi(\theta) = \Psi_e(\theta/\theta_s)^{-b} \quad \text{and} \quad K(\theta, z_v) = K_{sat}(z_v)(\theta/\theta_s)^{3+2b} \tag{2.10}$$

where b is a dimensionless parameter that defines the shape of the water retention curve. In substituting H_s and H_v in Equation 2.7 by 2.8, F is expressed as:

$$F = K_v \left(1 - \frac{\Psi(\theta)}{z_s - z_v} \right) \tag{2.11}$$

Transpiration TR is determined by both the moisture content within the root zone θ_{root} and the wilting point moisture content θ_{wp} (Feddes et al., 2001). θ_{root} depends on the root depth z_{root}, a model parameter. For detailed transpiration equations, please refer to (Rodriguez et al., 2008).

As mentioned above, the saturated zone is characterized by the saturation depth z_s. It is updated by the exchange flow with the vadose zone. z_s is calculated at each soil profile for a given UHE and the saturation depth of the UHE $\overline{z_s}$ is obtained by the area-weighted z_s. Hence, the saturated zone is the only "reservoir" that allows horizontal water exchanges between the profiles within a UHE.

Moreover, the saturated zone is the reservoir where groundwater drainage by pipes takes place. If the

groundwater level in a given UHE is higher than the contiguous drainage pipe, the infiltration process is activated. The drainage pipes are supposed to behave as an ideal drain (Cassan, 1986; Gustafsson et al., 1996):

$$I^u_{drain} = K^{nat}_s e^{\overline{-z_s}/M} \frac{\lambda}{L} (z_{soil} - z_{net} - \overline{z_s})^{\mu} \tag{2.12}$$

where I^u_{drain} (m/s) is the infiltration flux, K^{nat}_s (m/s) the hydraulic conductivity at saturation of the natural profile at ground surface, z_{soil} (m) the elevation of the UHE, z_{net} (m) the elevation of the invert of drainage pipe, L (m) a geometrical feature of the UHE, λ and μ two parameters describing the type and health state of the drainage pipe and its trench. The saturation depth $\overline{z_s}$ of the UHE is then re-estimated by I_{drain}:

$$\overline{z_s{}^{u,t}} = \overline{z^{u,t-1}_s} + \frac{I^u_{drain}\Delta t}{\theta_s} \tag{2.13}$$

At current stage, for reducing the data requirements of the model, only information of stormwater network is queried for calculating I_{drain}. The fraction to the stormwater and wastewater networks of the drainage flux is approximately estimated by the linear ratio of the two networks. For the Pin Sec catchment for example (Chapter 5), the wastewater networks linear are about two times as long as that of the stormwater networks, the total groundwater drainage flux is thus assumed to be devided in 2/3 to the wastewater networks and 1/3 to the stormwater networks.

2.6 Recapitulation of model input data

In summary, URBS needs two types of entry data: hydro-climatic data and geographic data (hereinafter referred to as "geodata"). Hydro-climatic data includes observation series of rainfall and potential evapotranspiration. These data can be obtained from the nearest weather stations. Depending on specific need, distributed data can be generated. For our studied catchments in France, hydro-climatic data is provided by weather stations of Météo France.

Geodata includes two groups of datasets, each being arranged in a text file:

- an UHEs file recapitulating geometrical parameters of each UHE, and adjacent relationships between the UHEs and the street segments

- a flow routing file showing the paths for stormwater runoff: upward-downward connections between street segments and stormwater sewer segments

Once the program executed, it reads the two data files and registers the data before any simulation process. Table 2.1 shows the geometrical parameters of an UHE needed by URBS, and Table 2.2 that of a segment in the flow routing network (street or sewer pipe).

Table 2.1 – Geometrical parameters of an UHE. All elevation values are expressed in the NGF (General leveling of France) system.

abbreviation	signification	unit
A^{nat}	area of natural soil	m^2
A^{hou}	area of building roof	m^2
A^{str}	area of adjacent streets	m^2
A^{nat}_{tree}	tree-covered area on natural soil	m^2
A^{str}_{tree}	tree-covered area on streets	m^2
(x_g, y_g)	coordinates of the gravity center C_g of the parcel	m
z_g	elevation of C_g	m
(x_p, y_p)	coordinates of the connexion point to the flow routing network C_p	m
z_p	elevation of C_p	m
d_f	distance between C_p and the most distant point in the parcel C_f	m

Table 2.2 – Geometrical parameters of a flow routing segment in URBS.

abbreviation	signification	unit
l_{seg}	length	m
$diam_{seg}$	diameter	m
z_{up}, z_{down}	elevation of the upstream (downstream) nodes	m
(x_{down}, y_{down})	coordinates of the downstream node	-
id_{down}	identity of the downstream segment	-

2.7 Modeling of LID devices in URBS

One of the perspectives for future development of URBS is to integrate modules for modeling LID devices. Some modules are already in the model, several others are being developed. This section gives a short description of the existing modules.

2.7.1 Flat roof

Flat roofs stock water temporarily during storms and release it slowly in regulated flow rates. Roof downspouts can either be connected to stormwater drainage system, or disconnected from it and directed onto lawn, garden or other receptors. A flat roof is usually composed of a waterproof substrate, a flow control system combined and an overflow device.

In URBS, a flat roof is parameterized by its maximum storage capacity $S^{f.r.}_{max}$ (mm, $f.r.$ for *flat roof*) and a minimum threshold $S^{f.r.}_{min}$ (mm) for the activation of regulated downspout flow. The regulated

downspout flow $D^{f.r.,t}$ (mm/s) is calculated with orifice law:

$$D^{f.r.,t} = a^{f.r.}\sqrt{S^{f.r.,t-1} - S^{f.r.}_{min}} \tag{2.14}$$

where $a^{f.r.}$ (with a unit of $\sqrt{\text{mm}}$) is the coefficient of the orifice flow and $S^{f.r.,t}$ (mm) is the water depth on the roof at time t. Rooftop overflow is permitted and calculated as $R^{f.r.,t} = S^{f.r.,t} - S^{f.r.}_{max}$.

$D^{f.r.,t}$ or/and $R^{f.r.,t}$ can be optionally conducted to stormwater sewer systems or onto the natural land. The mass balance equation for a flat roof is then given by:

$$S^{f.r.,t} = S^{f.r.,t-1} + (P^{f.r.,t} - E^{f.r.,t} - R^{f.r.,t} - D^{f.r.,t}) \times \Delta t \tag{2.15}$$

where $P^{f.r.,t}$ is the rainfall intensity (mm/s) and $E^{f.r.,t}$ the evaporation rate (mm/s).

2.7.2 Green roof

A green roof is a building rooftop partially or completely covered with a system of vegetation over high quality waterproof membranes (Rowe, 2011). Research related to the performance of green roofs as a means to manage stormwater quantity and quality have been reported for a variety of climate conditions (Hutchinson et al., 2003; Carter and Rasmussen, 2005; Dietz, 2007; Rowe, 2011; Carpenter and Kaluvakolanu, 2011; Stovin et al., 2012; Gromaire et al., 2013). A green roof typically consists of multiple layers, as illustrated in Figure 2.5a: a water proof membrane or material that prevents water from entering the building; drainage material such as geotextile webbing that allows water to flow to the drains when the substrate is saturated, and soil or substrate (growing medium).

In URBS, a green roof is modeled by three compartments: surface, a vadose zone (the substrate) and drainage layer, as illustrated in Figure 2.5b. This structural description is analogous with the soil description in URBS. The surface reservoir is parameterized by a storage capacity $S^{g.r.}_{max}$ (mm). It receives the precipitation and infiltrates water to the substrate layer. The substrate layer is parameterized by its height, $z^{g.r.}$ (mm), and its moisture content at saturation $\theta^{g.r.}_s$ (-). It receive water from surface infiltration and loses water by (i) vegetation transpiration; (ii) percolation to the drainage layer. The drainage layer is parameterized by its storage capacity $S^{g.r.}_{drain}$. It receives water by percolation from the substrate and discharges by drainage. The orifice drainage flow is calculated by orifice law as for a flat roof (Equation 2.16). The drainage can be conducted either to stormwater systems or onto natural land.

2.7.3 Permeable pavement with storage structure

Permeable/porous pavements are commonly made up of a matrix of concrete blocks or a plastic structure with voids filled with sand, gravel, or soil. They are designed to temporarily store surface runoff by allowing slow infiltration into subsoil, and traps suspended solids and filters pollutants (USEPA, 1999). The percolated water is stored in a subsurface structure, favoring evaporation and infiltration and mitigating

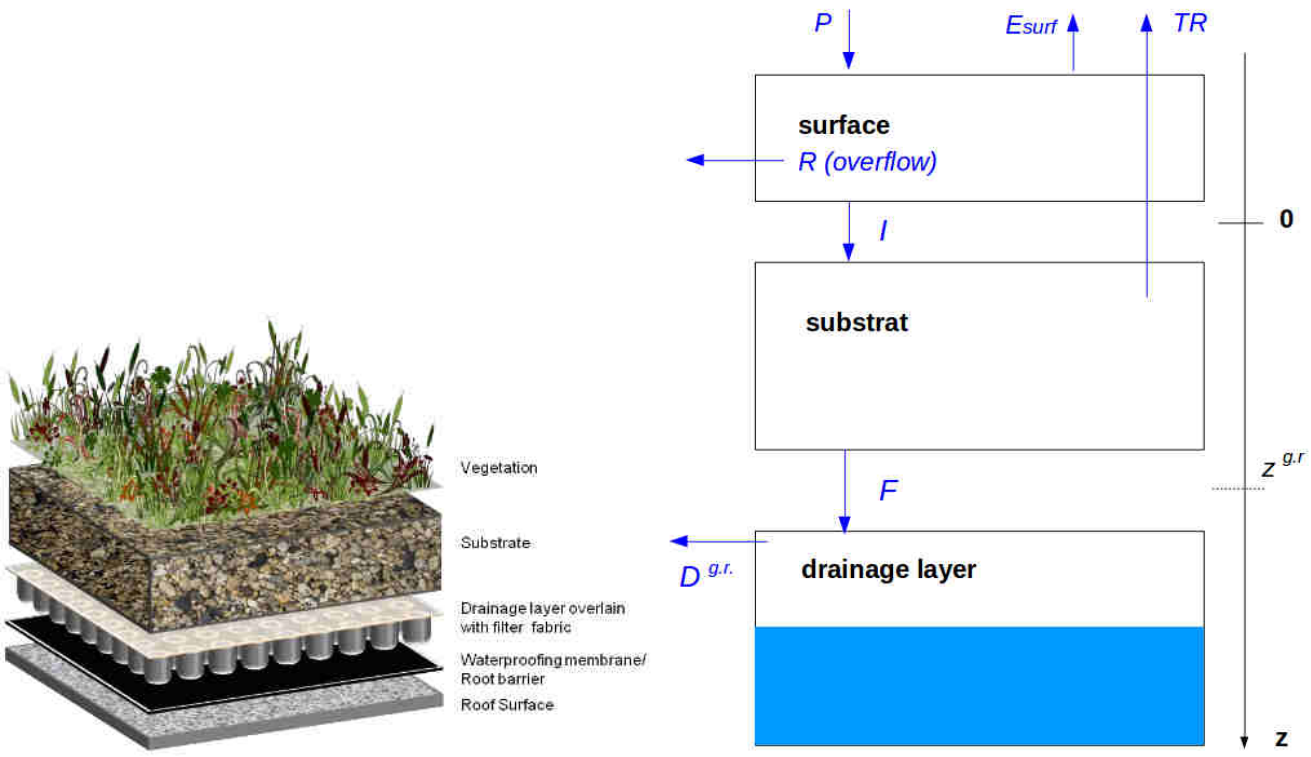

Figure 2.5 – Typical green roof composition (a) (Fassman-Beck and Simcock, 2013) and schematization in URBS (b).

the impacts of stormwater runoff caused by urban development. Regulated drainage is connected to sewer systems. Research on permeable pavements have shown reduced runoff and associated pollutant loads in a variety of locations (Dietz, 2007; Collins et al., 2008; Fassman and Blackbourn, 2010; Beecham et al., 2012).

In URBS, permeable pavements are applied on the street land use. The device is modeled by (i) raising the hydraulic conductivity at saturation of the street land use K_{sat}^{str}; (ii) adding a storage reservoir under the surface and above the vadose zone, as illustrated in Figure 2.6. This reservoir receives water across surface (Equation 2.5) and releases it to the underlying vadose zone. It is parameterized by its hydraulic conductivity $K_{sat}^{p.p.}$ (*p.p.* for *permeable pavement*) (m/s), its retention capacity $S_{max}^{p.p.}$ (mm) and a minimum threshold $S_{min}^{p.p.}$ (mm) for the drainage flow out of the reservoir and into sewer systems. When the storage in the reservoir $S^{p.p.,t}$ (mm) arrives at $S_{max}^{p.p.}$, the infiltration flux is stopped. The drainage flow $D^{p.p.,t}$ (mm/s) is computed by orifice law:

$$D^{p.p.,t} = a^{p.p.} \sqrt{S^{p.p.,t} - S_{min}^{p.p.}} \tag{2.16}$$

where $a^{p.p.}$ is the coefficient of the orifice flow ($\sqrt{\text{mm}}$).

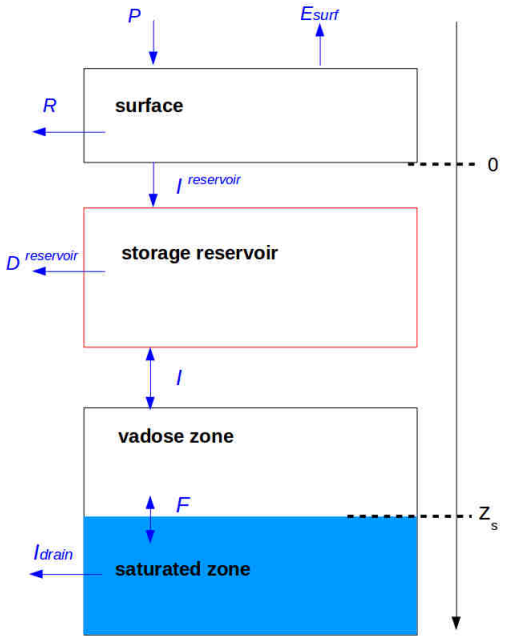

Figure 2.6 – Representation in URBS of a permeable pavement with storage structure.

The mass balance of the reservoir is given by:

$$S^{p.p.,t} = S^{p.p.,t-1} + (I^{p.p.,t} - I^t - D^{p.p.,t}) \times \Delta t \tag{2.17}$$

where $S^{p.p.,t}$ (mm) is the storage at time t, $I^{p.p,t}$ (mm/s) the infiltration flux from surface to the storage structure (=0 if $S^{p.p.,t} = S^{p.p.}_{max}$), I^t (mm/s) the infiltration flux from the storage structure to the vadose zone.

2.7.4 Swale

A grassed swale is a graded and engineered landscape feature appearing as a linear, shallow open channel with gentle side slopes, filled with erosion and flood resistant vegetation. Swales are designed to promote the conveyance of storm water at a slower, controlled rate and acts as a filter medium removing pollutants and allowing stormwater infiltration (Kirby et al., 2005). Due to its linearity, a swale can not only have a storage role for water but also a convey role, which makes it a substitution of classical underground pipe network for stormwater drainage in new urban development projects. Swale can efficiently operate under a variety of seasonal conditions (Fach et al., 2011).

Based on this idea, a swale is incorporated in URBS as a segment of the flow routing network: it collects surface runoff of adjacent UHEs and the flow from upstream segment, and conveys it downstream, which is either a swale or a sewer pipe. The information on each swale, including its geometrical characteristics and its upstream/downstream connexion with a swale or a drainage pipe, is arranged in the flow routing

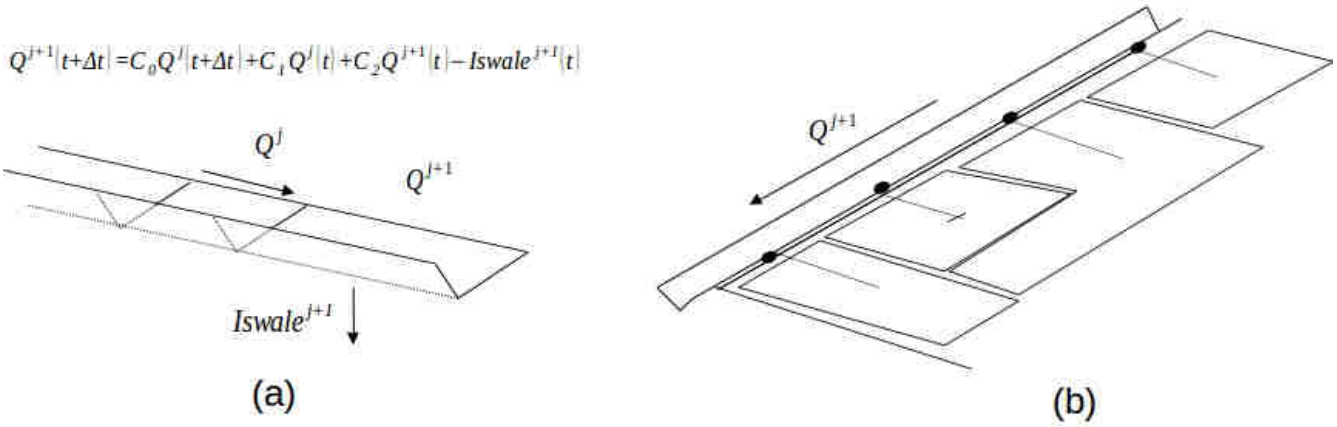

Figure 2.7 – Modeling of a swale in URBS by modification of Muskingum routing scheme: (a) Introduction of a swale infiltration function in the Muskingum equation, (b) re-distribution of the swale infiltration in the vadose zone of the adjacent UHEs.

data file. The infiltration through a swale is modeled by a water re-distribution procedure (Figure 2.7): at each time step, a certain quantity of water ex-filtrates of the swale and is injected into the vadose zone of surrounding UHEs. The ex-filtration flow I_{swale} (m/s) is calculated as the hydraulic conductivity of the swale K_{sat}^{swale} (mm/s) multiplied by a fictive "width" of the swale (m), both of which are model parameters. The volume of ex-filtrated water are re-distributed to each adjacent UHE proportionally to its natural land area.

Conclusion

In this chapter, we have outlined the modeling principles of URBS. It is adapt to urban settings as it can carry continuous simulations at small time steps at the urban parcel scale. Modules of LID devices are in active development, which will strengthen the model adaptability to more integrated urban water management strategies.

As mentioned previously, one shortcoming of URBS is that saturated horizontal flow is not represented. Consequently, the simulated groundwater levels of adjacent UHEs can be abruptly contrastive, which is not physically realistic. The present thesis tends to fill this "gap" by implementing a saturated flow module. This work is described in the next chapter.

Chapter 3

Integration of the WTI module into URBS

Contents

Introduction

This chapter is dedicated to the implementation of a saturated flow module into URBS, the main contribution to the development of URBS that has been fulfilled during the present thesis.

In the first place, we make a short review on current saturation modeling in integrated hydrological models, by which our work has been inspired. Then the module implementation work is presented, with a detailed description of the module and how it is introduced in URBS. In the last section, a complementary explanation is given on modifications in initial model scripts of URBS during the module implementation.

3.1 Review of groundwater modeling

Groundwater flow modeling is obviously not a specificity in urban hydrology. Flow regimes in aquifers as well as their modeling have always been an active research topic in water science, naturally with more advances in natural hydrology than in urban hydrology. Studies in groundwater flow and modeling in urban areas are based on progresses achieved in natural hydrology, and groundwater modeling implementation in urban hydrological models are generally undertaken in the same way as in rural studies (Musolff et al., 2010; Yang et al., 1999; Jeppesen et al., 2011). This section gives firstly an insight in the state of the art of the groundwater hydrology and groundwater modeling, then makes a zoom at recent research effort in urban groundwater modeling.

3.1.1 Historical development and state of the art of groundwater hydrology

Groundwater has been used since early times and hypotheses explaining the occurrence of groundwater were given early by Greek and Roman philosophers (Kashef, 1986; Dogan, 1999). Understanding of the origin of groundwater as related to the hydrologic cycle was established in the later part of the seventeenth century (Cap, 1961; De Wiest, 1965).

Groundwater hydrology was shifted from a descriptive subject to a more rigorous analytical science in the late 19th / early 20th centuries by works of Darcy (1856), Dupuit (1863), Thiem (1906), and Forchheimer (1898), pioneers in the field. During the whole twentieth century, groundwater hydrology, or hydrogeology, recognized the most great progress ever since (Dogan, 1999).

Numerical models appeared in the 1960s with the era of digital computers, which provided the possibility of solving transient flow problems in complex geological systems. By the early 1970s, computer simulation of aquifers was widely used in water resource evaluations. In the late 1970s, research emphasis was shifted from resource development issues to environmental issues pertaining to chemical contamination. Soil scientists and agricultural engineers began to investigate unsaturated soil characteristics and flow processes in the vadose zone. Brandt et al. (1971), Neuman (1973) and Haverkamp et al. (1977) are among those researchers.

In the 1980s, interest steadily grew in characterizing flow processes in the vadose zone. Advancements in computer technology eased researchers' job and motivated them to search for better numerical techniques to solve governing nonlinear partial differential equations (Dogan, 1999). Many sophisticated groundwater models were developed. The most well-known, MODFLOW, was created by Mcdonald and Harbaugh (1988) and widely used by hydrogeologists since.

In the 1990s, attempts were made to couple variably saturated flow models, root water uptake models and groundwater models to simulate the complete hydrological process and express groundwater - surface water interactions, and dynamics between the vadose zone and the saturated zone. Fully three-dimensional physically based numerical approaches were often used (Yeh et al., 1996; VanderKwaak, 1999; Sudicky et al., 2000; Weng et al., 2003). A full three-dimensional numerical solution of saturated zone - vadose zone

processes encounters limitations for mesoscale (10–10^3 km^2) applications because of its high demands in computation effort, problems with subsurface boundary conditions and insufficient knowledge of hydraulic properties and soil parameters (Krause et al., 2007). The three-dimensional numerical formulations are given in Appendix B. Approximations and simplifications of the three-dimensional numerical approaches exist in different levels, with conceptual modeling for the for the vadose zone (Lasserre et al., 1999), or the saturated zone (Spieksma and Schouwenaars, 1997).

3.1.2 Groundwater modeling in urban area

Urban groundwater is a huge receiver as well as a source for water and solutes in urban areas acting on much longer time scales. Long term trend of rising water tables in urban areas, resulting from deterioration of vegetation covers in favor of farmland (Favreau and Leduc, 1998) or reduced industrial abstraction (Tait et al., 2004), has led to well documented basement and tunnel flooding and geotechnical problems (Greswell et al., 1993; Lerner and Tellam, 1997).

Efficient integrated urban water management need to consider the role of urban groundwater in relation to the other and more visible urban water compartments (Schirmer et al., 2013). In urban hydrogeology, modeling is also a valuable tool to represent and predict the process driving the groundwater movement.

The urban groundwater compartment interacts closely with the unsaturated zone, sewer systems and surface water. Depending on the task, groundwater models often have to be coupled to the other compartments. This can be done by loose coupling, where output of one model, e.g. a model of sewer flow and ex-filtration, is taken as input for the groundwater model (Schirmer et al., 2013).

There seems to be a recent trend to incorporate groundwater in fully coupled surface water - sewer network - groundwater models systems. DeKeyser et al. (2010) incorporated groundwater into a multi-media model of micro-pollutant flux in water, air and soil. Sommer et al. (2009) and Karpf et al. (2011) showed the interaction of groundwater, surface water and sewer systems during a flood event in the city of Dresden, Germany, by fully coupled water flow models. Karpf and Krebs (2011a) introduced an improved model of sewer ex-filtration based on Darcy's law. Dynamic sealing of the leaks with changing hydraulic conductivity over time are taken into account. Advantages of these models are the identification of the likely changes in individual components of the water balance and overall discharge from a catchment with groundwater (Barron et al., 2013).

Despite the studies cited above, the incorporation of groundwater into urban water system modeling remains rare (Schirmer et al., 2013). Elliott and Trowsdale (2007) reviewed the 10 most commonly used urban hydrological models, indicating most of them do not include groundwater fluxes into the analysis. A few (SWMM, MOUSE, MUSIC) have limited capability for analyzing surface water and groundwater interactions and factors influencing baseflow or groundwater interception by urban drains.

3.2 Integration of the WTI module into URBS

As mentioned initially in Chapter 2, horizontal flow of shallow groundwater between the UHEs were not modeled in URBS. The saturation depth, and subsequently the shallow groundwater level, is computed individually for every UHE and could be abruptly variable from one UHE to another. As part of the doctoral work of Le Delliou (2009), an attempt to couple MODFLOW and URBS was made aiming to simulate horizontal flow exchanges between UHEs. But the coupling was proved difficult to be operated, due to the differences in soil configuration of the two models.

The difficulties encountered during the coupling MODFLOW/URBS implies that a suitable modeling for the saturated flow should keep the soil configuration of URBS, as well as its spatial discretization. On the modeling platform LIQUID, Branger (2007) developed a module to represent lateral saturated flows between irregular model units, branded Water Transfer Interface (WTI). A "model unit" refers to a land use type that is hydrological meaningful, such as an agricultural field or a ditch in rural area, or a parcel in urban area. Hydrological processes within each model unit is modeled by a specific module. URBS has been implemented in LIQUID for the modeling within urban parcels (Jankowfsky, 2011). Horizontal saturated flow between two URBS units are modeled by WTI. The module has proved to be adequate and robust (Branger, 2007; Jankowfsky, 2011). Inspired by these work, we propose to implement WTI as a specific module of the URBS model. The future integrated model will be labeled as URBS-WTI.

In this section, the module principle is firstly outlined. Then the development of the URBS-WTI model is described in a detailed manner. Supplementary geographical data required by the module implementation is summarized in the third part.

3.2.1 Description of the WTI module

Figure 3.1 illustrates the concept of the WTI module. Shallow groundwater flow between two hydrologic elements (HE)[1] A and B is assessed by Darcy's equation. The geometrical support for the Darcy's equation is an object called *interface*, defined as the surface of contact of two HEs. Each interface has and only has two adjacent HEs. Reciprocally, two adjacent HEs have systematically an interface.

Darcy's equation applied on Interface 3 between A and B is expressed as:

$$Q_{A\to B} = K_{int} A_{int} \overrightarrow{\nabla} H \tag{3.1}$$

where $Q_{A\to B}$ (m^3/s) is the water flow between A and B, K_{int} (m/s) the hydraulic conductivity applied on the interface, A_{int} (m^2) the surface area of the interface and $\overrightarrow{\nabla} H$ (-) the hydraulic gradient between

[1] An hydrologic element is equivalent to a "model unit" described above. The two terms were alternatively used in the module development (Branger, 2007; Jankowfsky, 2011) depending on context.

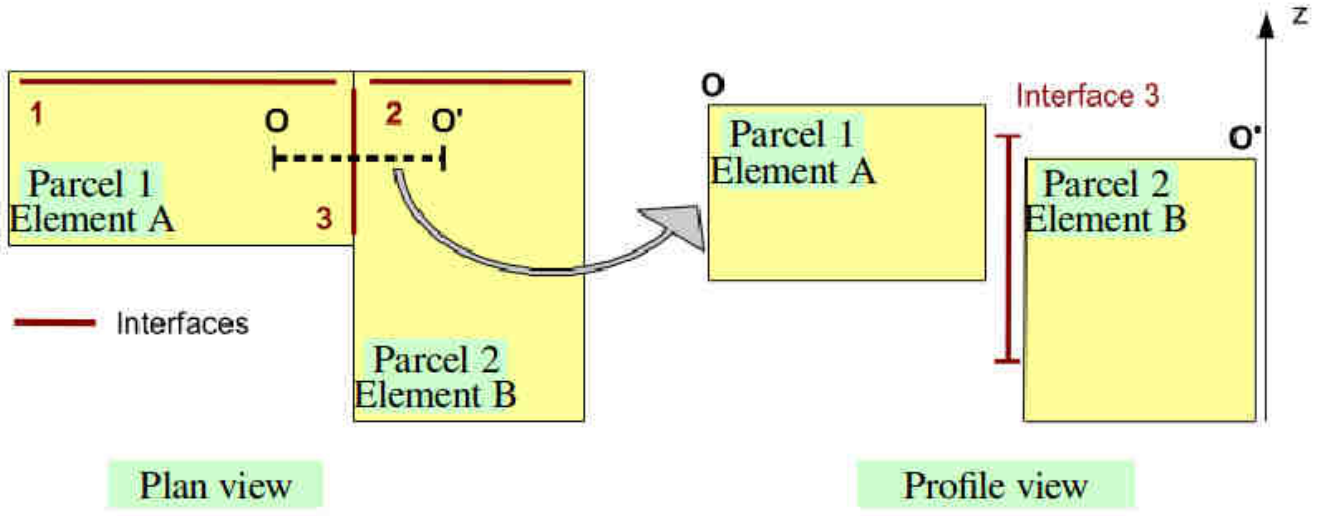

Figure 3.1 – Illustration of two adjacent Hydrologic Elements and their interfaces (Branger, 2007).

A and B, calculated as:

$$\vec{\nabla} H = \frac{H_A - H_B}{d_{AB}} \quad \text{with} \quad d_{AB} = d_A + d_B \tag{3.2}$$

where H_A and H_B are the hydraulic heads in A and B, and flow path length is approximated by the distance between the geometrical centers of A and B d_{AB}. d_{AB} is approximated by the sum of the distances between the geometrical center of the interface and that of the HEs. The groundwater level within an HE is assumed to be uniform and represented by the groundwater level at its geometrical center. A_{int} is calculated by $l_{int} \times (H_{int} - H_{bottom})$, where l_{int} is the length of the interface, H_{int} the groundwater level at the interface, and H_{bottom} the elevation of the substrate of the interface. H_{int} is variable and calculated at each time step by a linear interpolation of the hydraulic gradient between A and B:

$$H_{int} = \frac{H_B - H_A}{d_A + d_B} \times d_A + H_A \tag{3.3}$$

Branger (2007) carried out multiple tests in the LIQUID framework and showed that the module WTI was robust in the computation of water flows. The implementation of WTI within a distributed model for peri-urban catchments labeled as PUMMA (Jankowfsky et al., 2014), through the LIQUID platform as well, proved to be satisfying. The landscape of a suburban catchment was discretized into parcels for urban areas and irregular hydrological response units for rural areas.

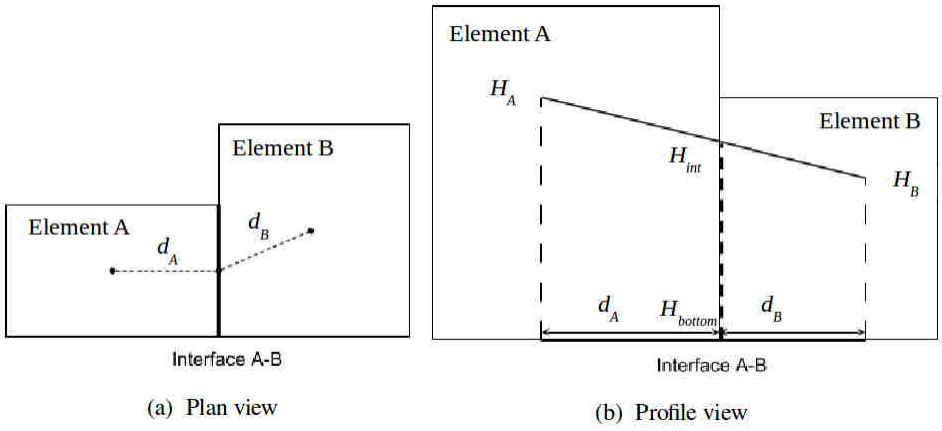

Figure 3.2 – Estimation of parameters of the WTI flow: (a) distance between the interface and the centers of the hydrological elements (b) water depth on the interface (Branger, 2007).

3.2.2 Methodology for the module integration in URBS

The integration of the WTI module into URBS during the present thesis is inspired by the works of Branger (2007) and Jankowfsky et al. (2014) presented in the last section.

The main idea is to introduce, between every adjacent UHEs, an *interface* (cf. Section 3.2.1), through which horizontal groundwater flow between the UHEs is calculated by Darcy's equation. In terms of geometry, the interface is a delimited line viewing from the top (Figure 3.3 (a)), and a surface in the soil column (in the plan (x,y), not shown in the figure).

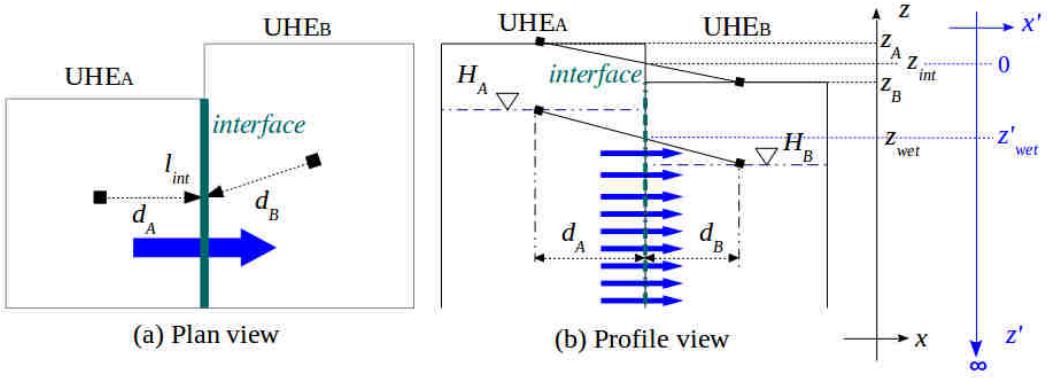

Figure 3.3 – Plan view and profile view of the principle of WTI in URBS. Axes in black represent the NGF system in which all elevation variables are expressed. Axes in blue is the initial system of URBS in which *saturation deficit* is expressed. The calculation of WTI is based on this system, but the analysis of modeling results will base on the NGF system.

At every time step, water flow between the UHE_A and UHE_B is computed by Equation 3.1 and 3.2. In URBS, the hydraulic conductivity at saturation is subjected to an exponential decrease from ground surface to the soil depth (cf. Chapter 2, Section 2.5). From a compatibility point of view, it makes sens

to keep this feature in WTI. On the other hand, as explained in Chapter 2, Section 2.5, the soil in URBS is not limited at bottom, i.e. there is not a substrate of the subsurface layers. The groundwater level is represented be means of the concept of *saturation deficit* of which the reference is the ground surface. As a consequence, the interfaces of the UHEs do not have the bottom neither, and it is delicate to estimate a mean value for the hydraulic conductivity to be assigned on the interface K_{int}.

This was one of the major difficulties during the implementation of WTI. To solve the problem, a method has been worked out which consists of writing Equation 3.1 in an integrated form. The "elemental volume" for the integration is the flow volume through an elemental surface area of the interface, as illustrated in Figure 3.3. The upper border of the integration is the groundwater level at the interface, and the lower level is infinity.

Here a tough problem is related to the direction of the z axis. As a matter of fact, during previous development of URBS, z was oriented downwardly, in a context where it was the saturation depth that was handling through the variable *saturation deficit*, not the groundwater level in the NGF system. And each UHE had in fact its own 0 level, which was the ground surface of the UHE. However, a saturated module (in this case WTI) models the horizontal water flow between the UHEs driven by the hydraulic gradient, it seems more convenient to work with the NGF system with a uniform reference 0 level. Meanwhile, if we work with the NGF system, the exponential decrease equation (2.2) will be no longer validate. And there is no way (to the author's knowledge) to transform this formulation from one coordinate system to another.

Consequently, we face a dilemma: either we keep the downward z for the WTI flows, but shift to the NGF system while analyzing simulation results; or we abandon the z-downward system and do everything in the NGF system. In the first case, the 0 level will be at ground surface, thus defined individually for each interface. In the second case, we have to find a proper way to express Equation 2.2 in the new system. Further more, the second option may cause unexpected problems to other processes that has been till now simulated in the z-downward system.

Ultimately, we have chosen the first solution. As illustrated in Figure 3.3, for WTI calculations, we are placed in a z-downward system (axes in blue and noted with "$'$") where the 0 level of each interface is at its ground surface. This level is calculated by the distance-weighted elevation (thus in the NGF system) of $\mathrm{UHE_A}$ and $\mathrm{UHE_B}$. The groundwater level at the interface z_{wet} is calculated by the distance-weighted groundwater level of the two UHEs, but will be expressed in the z-downward system (z'_{wet}).

The integration is written in the z-downward system and from z'_{wet} to infinity:

$$\begin{aligned} Q_{A\to B} &= K_{int} A_{int} \overrightarrow{\nabla} H \\ &= \int_{z'_{wet}}^{\infty} K_s^{nat}.exp(-z'/M).\frac{H_A - H_B}{d_A + d_B}.dA_{int} \\ &= \int_{z'_{wet}}^{\infty} K_s^{nat}.l_{int}.\frac{H_A - H_B}{d_A + d_B}.exp(-z'/M).dz' \end{aligned} \tag{3.4}$$

where l_{int} (m) is the length of the interface and M is the scaling parameter of the hydraulic conductivity.

If we write the antiderivative of Equation 3.4 in doing the approximation that the hydraulic gradient between the two UHEs is a constant in depth, we have:

$$\begin{aligned} Q_{A\to B} &= \int_{z'_{wet}}^{\infty} K_s^{nat}.l_{int}.\frac{H_A - H_B}{d_A + d_B}.exp(-z'/M).dz' \\ &= K_s^{nat}.l_{int}.\frac{H_A - H_B}{d_A + d_B}.\int_{z'_{wet}}^{\infty} exp(-z'/M)dz' \\ &= -K_s^{nat}.l_{int}.M.[exp(-z'/M)]_{z'_{wet}}^{\infty} \end{aligned} \tag{3.5}$$

Since $exp(-z'_{wet})/M$ towards 0 when z'_{wet} approaches infinity, the antiderivative is ultimately given by:

$$Q_{A\to B} = K_s^{nat}.exp(-z'_{wet}/M).l.M.\frac{H_A - H_B}{d_A + d_B} \tag{3.6}$$

Equation 3.6 is the final equation by which water flow between two adjacent UHEs is computed at their interface. Hereinafter, "saturation depth" is referred to land surface and is actually a direct modeling output, related to the concept of "saturation deficit" in URBS. "groundwater level" is in the NGF system.

The WTI module is activated, in each time step, after the groundwater drainage flux (thus after the "production" computation for the profiles, Figure 3.4).

The computation of WTI flow is applied with a loop on the interfaces. As illustrated in Figure 3.5, for any interface int of a given UHE u, Equation 3.6 is applied to compute the exchanged water volume $Q_{A\to B}^{int}\Delta t$ (m^3) on this interface, always preceded by a sign (+ for receiving water or − for giving water). Once the loop is done, the exchanged water volumes of all the interfaces of u is summed to assess the total gain (+) or lost (-) of water V_{WTI}^u (m^3) of the UHE:

$$V_{WTI}^u = \sum_{int=1}^{n_u} (Q_{A\to B}^{int}\Delta t) \tag{3.7}$$

where n_u is the number of the interfaces of u. Then the saturation depth of u is updated by V_{WTI}^u:

$$\overline{z_s^{u,t}} = \overline{z_s^{u,t}} + \frac{V_{WTI}^u}{A^u.\theta_s} \tag{3.8}$$

where A^u (m^2) is the surface area of the UHE and θ_s is the moisture content at saturation (see Equation 2.1).

The approach described above for computing horizontal water flows between the model units (UHEs) based on Darcy's equation and volume conservation laws is not, strictly speaking, a coupling of a groundwater model with URBS. But it makes the modeling of water transfer between the units of URBS to be possible, and has several advantages:

1. It keeps the spatial discretization of URBS based on parcels (UHEs).

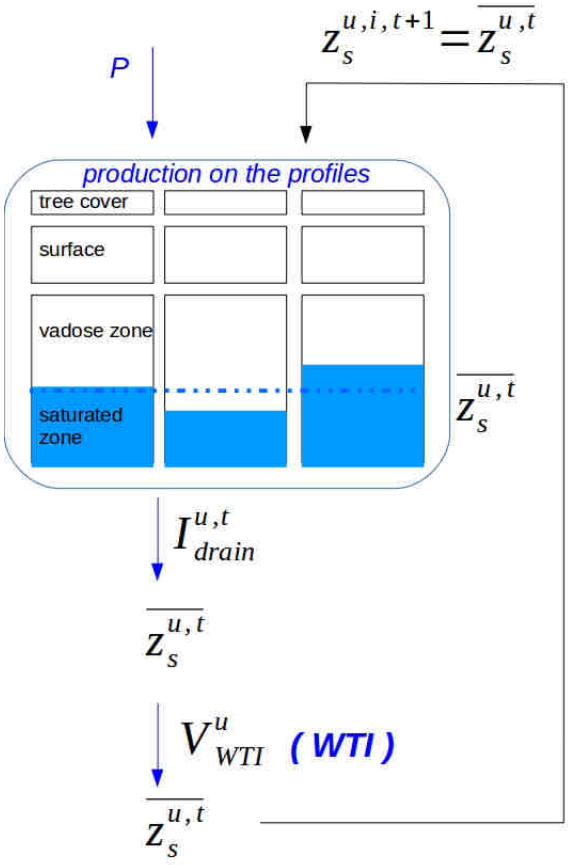

Figure 3.4 – Diagram of the WTI module within the temporal discretization of URBS.

2. It keeps the soil representation in URBS, thus assures maximally the compatibility with URBS.

3. It is an simple approach based on Darcy's law, without introducing supplementary model parameters.

4. It does not bring major structural problem.

The "new" model of URBS with the WTI module integrated in will be described by "URBS-WTI" hereinafter.

3.3 Modifications to the initial model of URBS during the WTI module integration

3.3.1 Purpose of the modifications

During the introduction the WTI module, numerous modifications have been brought to the initial code. These modifications are for various purposes. Some are necessary for the functioning of the introduced

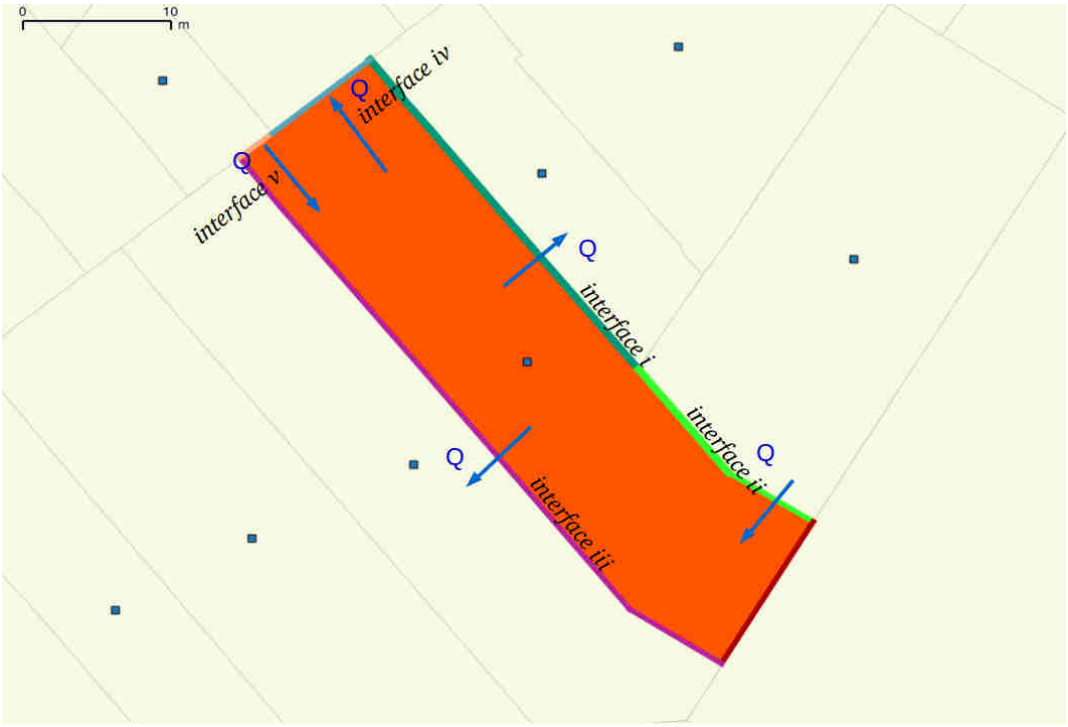

Figure 3.5 – Groundwater flow between an UHE and its five adjacent UHEs through the interfaces.

module. Some are to make the routines more rigour. Others are more "essential" which are for detecting and correcting errors.

The first type of modifications are fore the correct functioning of the WTI module. If the module has been introduced as a "plugin", i.e. it does not request any change in the other parts of the program, some small modifications of the initial script are inevitable. For example, the name or dimension of some variables or parameters need to be adjusted in such a way that they can be used within and outside the WTI module. These modifications are classified as for the functioning of the introduced module and are detailed in Appendix C.1.

The second type of modifications concern the "capillarity fringe" defined in the soil. As shown in Chapter 2, Section 2.5, the capillarity fringe is a particular layer separating the vadose zone and the saturated zone. In URBS, the capillarity fringe is modeled by a uniform layer that has saturated moisture content, but the layer "behaves like an unsaturated medium" (Rodriguez et al., 2008). The thickness of the capillarity fringe Δz_{cf} is set to be constant equaling to the air entry suction Ψ_e, and the moisture content is $\Psi_e \times \theta_s$.

The formulations of the subsurface flux imply that the layer of the vadose zone must exist, i.e. the storage in the vadose zone S_{zns} can not be zero, otherwise there will be numeric problems. Meanwhile, the water table is free to vary and updated by percolation from the vadose zone and infiltration to sewer networks. It can happen that the water table rise to a critical level where the capillarity fringe at the ground surface, i.e. no space left for the vadose zone. Although this configuration is totally possible in

the real-life (surface soil saturation), it is not mathematically accepted by the program. As a matter of fact, this situation has never occurred during previous model development, for some unknowing reasons (which worth further examination but is out of the scope of the present work). With the introduction of the WTI module, the surface soil saturation appeared, involving numerical problems.

To solve this problem, the technique that we take consists of limiting the rise of the saturated zone by the thickness of the capillarity fringe Δz_{cf}: the soil is considered to be saturated once the surface of the saturated zone is raised to Δz_{cf} below the ground surface, and all supplementary recharge is to be discharged as surface runoff. With this consideration, the capillarity fringe does not exceed the ground surface level, and the vadose zone always exists and its minimum height is Δz_{cf} : when the soil is saturated, the storage in this vadose zone is equivalent to the saturated moisture content.

This pragmatic approach allows to avoid numerical problems caused by the excess of the capillarity fringe to ground surface and by the vadose zone removal. The quantity conservation law is also maintained, which guaranties the coherence of water balance. The modifications according to this configuration are detailed in Appendix C.2.

The third type of modification is for the purpose of verifying water balance. Making sure that no water quantity is added or lost by the model routines is believed to be essential. As a new module has been introduced, some configurations have been changed, and the computing of the flux has very high spatial and temporal complexities, checking the quantity conservation is a fundamental methods to avoid errors while we brought change to the model.

This work, seeming easy, requires actually great programming effort, due to the complexity of the soil representation and the large number of variables which are heterogeneous in dimension and unity. But this contribution makes the computation of water balance to be possible in future model development. The major model modifications related to this issue is given in Appendix C.3.

Another type of modifications is for the purpose of programming rigour, and is given in Appendix C.4. Some errors existing in the program have also been found during the present thesis and were corrected. These modifications are given in Appendix C.5.

For evaluating the behavior of the introduced WTI module (Chapter 5), the anisotropy of hydraulic conductivity, which did not exist in the model, has been introduced. A new parameter K_s^{lat} has been introduced to represent the lateral hydraulic conductivity (Appendix C.6).

3.3.2 Methodology

A large number of modifications are thus needed to be brought into the initial code, in addition to the introduction of the new module. A suitable work method is needed to be predefined in order that the modifications are brought in conveniently, e.g. no new error is created while eliminating old errors.

The work method that we defined was: For any modification in the code, we take a new model run and examine the entire modeling outputs, in order to see if the change in the results is consistent with what we expected with the modification. If it is not the case, we must find out why. Every time a significant

modification is taken, we create a new model version, in such a way that the final program is established stage by stage from the initial one with a clear track. 12 versions have been created and enumerated by v1 - v12. Future model developers can review easily the modifications during the present work.

Conclusion

In this chapter, we detailed the development of the modeling of the saturated layer in the model URBS. The Water Transfer Interface is integrated as a module that computes horizontal groundwater flow between the model units UHE. This Darcy's law based approach allows the computing of groundwater flow in a simple but physically meaningful manner, without disturbing the spatial discretization and soil configuration of the URBS model.

The functioning of the WTI module is based on a particular geographical feature, interface, and needs a new series of geodata related to it. The construction of the interface input file will be presented in the next chapter.

In addition to the module introduction, numerous additional modifications were brought into the initial program script because of their necessity. Either serve as back-up of the new module, or aim to make the program to be more rigour in computing water balance and checking computation errors, these modifications are believed to be an important contribution to the development of URBS. Although all the modifications are not easily valued from a scientific point of view, great effort was exerted in order to assure the reliability of this work.

Chapter 4

Geodata pre-processing for the URBS-WTI model

Contents

Introduction

The Water Transfer Interface module, integrated into the URBS model, simulates saturated soil water flow between the modeling units UHEs. If the newly integrated module does not require new physical parameters, it needs a new geodata input file for the interfaces, which serve as the geometric support to WTI. Meanwhile, the interfaces is not an urban landscape object included in Urban DataBanks. A geodata pre-processing is therefore necessary to create the interfaces and the associated geodata input file.

The interfaces are limitrophe surfaces of adjacent UHEs and which appear as lines on a two-dimensional map. The drawing of interfaces should base on vector objects (polygons) of the UHEs. Up till now however, if the conception of an UHE is easily understood and accepted, the polygons of the UHEs has not yet been created. Consequently, the drawing of interfaces makes it necessary to implement the drawing of UHE polygons.

The GIS layer construction of both Interfaces and UHEs require manipulations of existing datasets such as spatial analysis, geometric editing and table queries. Errors existing in the datasets can preclude the processing. This is the reason for which a pre-treatment of initial datasets *parcels* and *streets* is compulsory for correcting all errors .

This chapter describes the geodata pre-processing for the Pin Sec catchment (Nantes, France), which is the application site of the model URBS-WTI (cf. Chapter 5). GIS softwares that are used during this work are firstly described. After a brief recall on the required geodata in the URBS-WTI model, the error-correction work is presented, following by the construction of the vector maps of UHE and Interface, and of the geometrical parameters.

4.1 GIS softwares used in the geodata pre-processing

During our work three open-source GIS softwares have been mainly used: QGIS, GRASS and OrbisGIS. QGIS was initialized in early 2002 (by Gary Sherman), who became an incubator project of Open Source Geospatial Foundation (OSGEO, 2014). QGIS is a cross-platform free and open source desktop GIS that provides data viewing, editing and analysis applications. GIS deals with both raster and vector layers and allows users to create maps assembled in different formats and using different projections. QGIS runs on a multiple of operation systems including Linux and MS Windows. One of the advantages of QGIS is the user-friendly graphic interface and its efficient node-correction tool, as illustrated in Figure 4.1. Another feature of QGIS is that it allows integrations of plugins developed by people around the world, which contributes to a rapid evolution of the software.

GRASS was initially developed by the Environmental Division of the U.S. Army Construction Engineering Research Laboratory as a general-purpose spatial modeling and analysis package. GRASS development and management is now being directed by the GRASS Project Steering Committee, a multinational team consisting of developers at numerous locations (PSC, 2014), which had released GRASS 6.4 on 3rd September 2010. As QGIS, GRASS is an official project of the Open Source Geospatial Foundation. GRASS is highly interactive and graphically oriented, providing tools for developing, analyzing and displaying spatial information. Under the UNIX/Linux environment, GRASS can run both through a command line window or a graphic user interface. GRASS has multiple capabilities for raster and vector data manipulations: reclassification of vector labels, superimposition of layers, geometry options, vector/raster conversion, attribute management, vector queries, etc. GRASS offers also correction tools of topology errors. GRASS integrates a Python shell which allows users to run python command directly

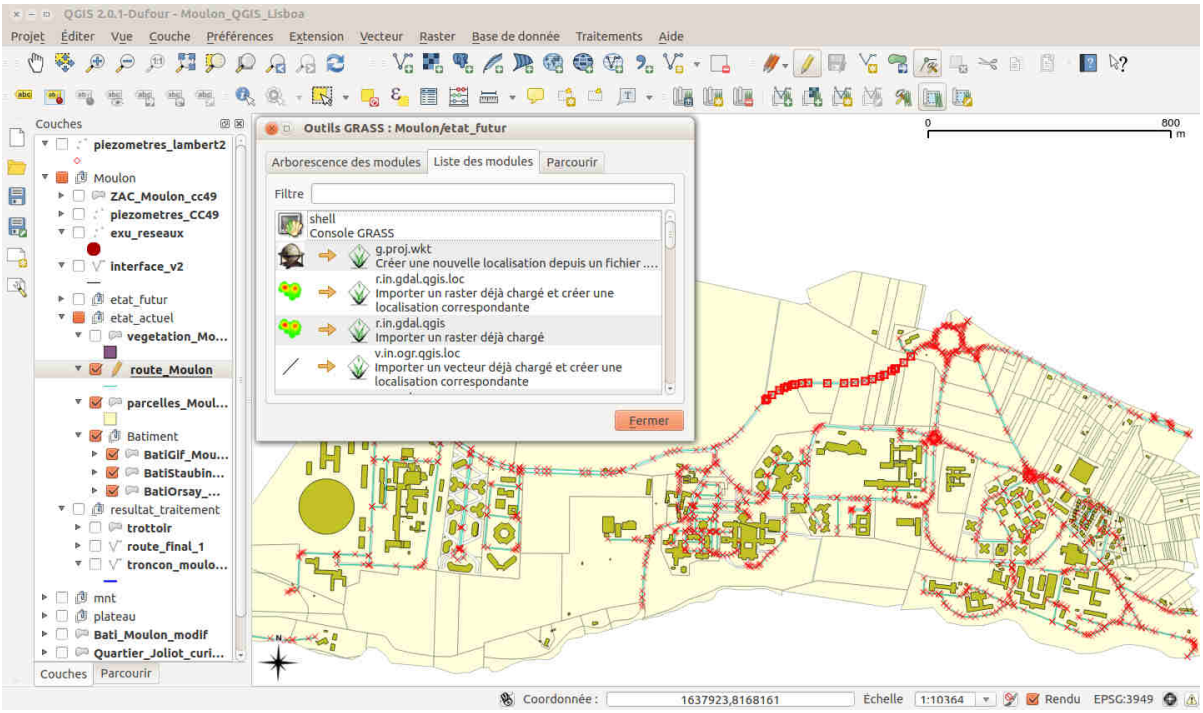

Figure 4.1 – Graphic interface of QGIS desktop.

in the GRASS environment, as illustrated in Figure 4.2. GRASS is incorporated into QGIS desktop as a plugin, which makes it possible to access the functionalities of both on a common platform (Figure 4.1).

OrbisGIS (Bocher et al., 2014) is a French open-source GIS desktop being developed by the IRSTV[1] institution of the CNRS. One leading feature of OrbisGIS is an integrated powerful and user-friendly SQL shell, as illustrated in Figure 4.3.

These softwares work with both raster and vector data and have many common functions. But each of them has its own features and advantages. For example, while GRASS deals well with topological error detection and correction, QGIS offers a more user-friendly graphic interface and vector correction tools. OrbisGIS provides a handy console to support efficient treatment. In the present study, pre-processing of geodata files were conducted in combining tools provided by the three GIS softwares.

[1]IRSTV: Institut de Recherche en Sciences et Techniques de la Ville, Nantes, France

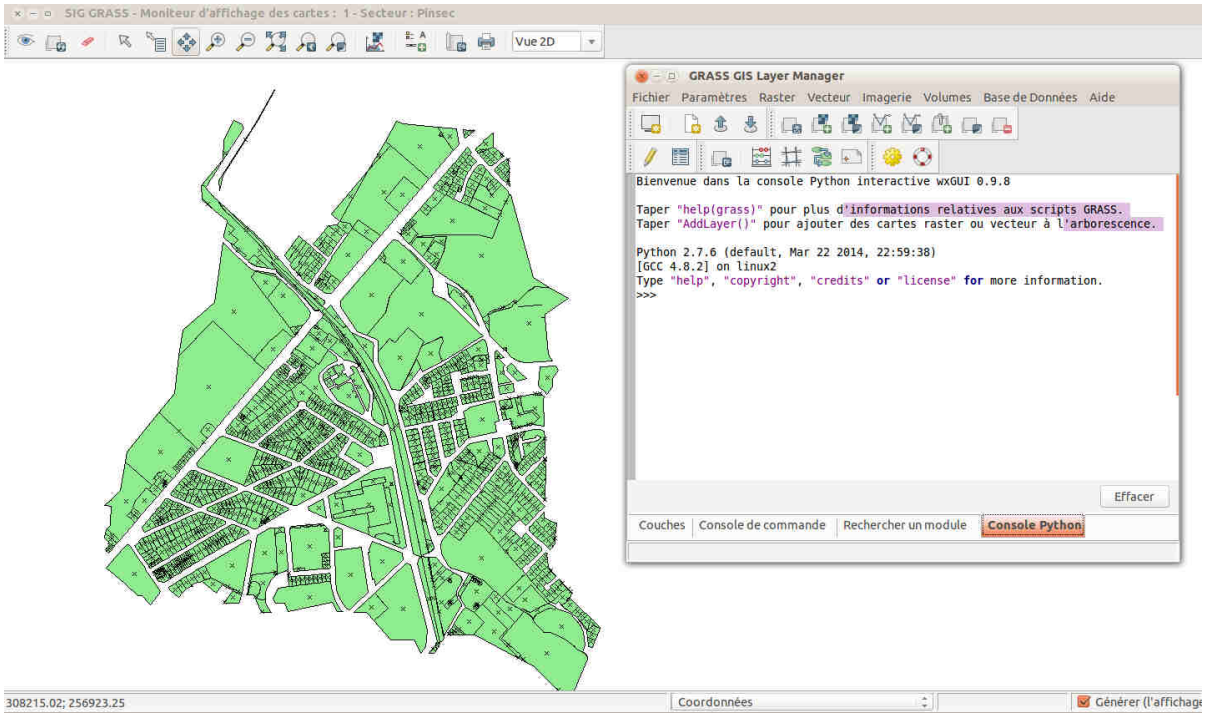

Figure 4.2 – Graphic interface of GRASS desktop.

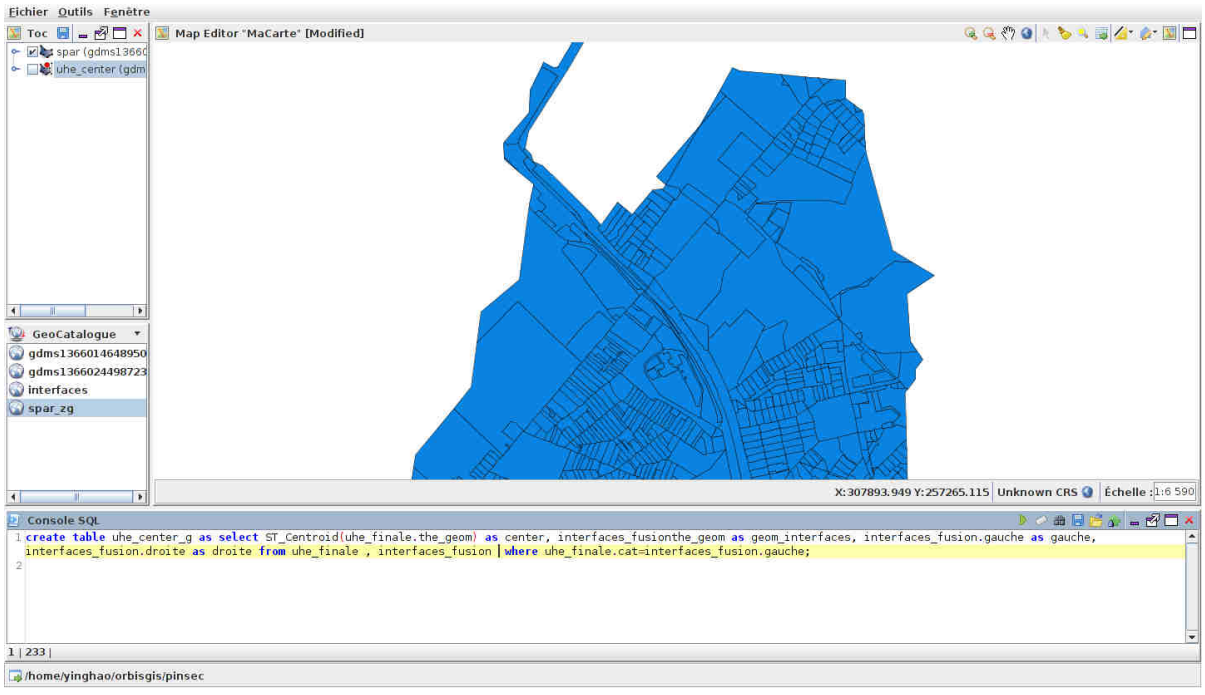

Figure 4.3 – Graphic interface of OrbisGIS desktop.

4.2 Geodata required by URBS-WTI

Geometrical features of an interface are listed in Table 4.1. This information will be summarized the attribute table of the layer Interfaces. Adjacent relationship among UHEs and interfaces are also to be assessed: which are the two UHEs adjacent to an interface.

Table 4.1 – Geometrical parameters of an interface. Elevation values are in the NGF system.

abbreviation	signification	unit
id_{int}	interface identity	-
id_u^A, id_u^B	identity of the adjacent UHE_A and UHE_B	-
l_{int}	length of the interface	m
z_{int}	elevation of the ground surface of the interface	m
d_A, d_B	distance between the gravity centers of the UHEs and that of the interface	m
z_g^A, z_g^B	elevation of the gravity centers of the UHEs	m

4.3 Collection and correction of existing data

Purpose

Urban DataBanks of Nantes Métropole provides all geodata that have been used in URBS, including vector maps (parcels, streets, trees, stormwater systems), MNT and aerial photographs. Geodata input files of URBS, which are in .txt format, are derived from attribute tables of these vector layers. Although URBS is based on GIS, the latter acts as a pre-treatment procedure of the model, and does not require modelers to investigate in geometrics processing, or only at a relatively superficial level.

On the other hand, the Urban DataBanks has been established for administrative or engineering purposes, and rarely at the intention of scientific research (at least to the author's knowledge). If the attribute values are more or less credible, errors in the vector maps is not something rare. A typical example is the *spatial errors*[1] that are recurrent. Detection and correction of these errors has already become a specific study subject (Yao et al., 2012).

In the geodata sets used in URBS, spatial errors exist with a non ignorable quantity. These errors had not been detected during prominent model development (or maybe detected but did not prevent the model from functioning, thus ignored by the developers). They were, however, detected at the very beginning of the work for constructing the UHE vector map, which were based on an automatic procedure of fusion (presented in Section 4.4) of parcels and street surfaces. If the parcel layer was relatively reliable, this was not the case of the street surface layer, as it was derived from the information of street line.

[1] *Spatial error* is a specific notion in GIS science related to the *topology rules*. For more information, please refer to <http://help.arcgis.com/en/arcgisdesktop/10.0/help/index.html>

An option consisted in doing everything by hand in looking at the aerial photographs and without using the automatic procedure. Considering the number of UHEs that we dealt with (more than 800 in the case of Pin Sec, cf. Chapter 5), this seemed to be impossible. On the other hand, high-quality datasets with no error can certainly be benefit for people working on the same catchment, and maybe afford relevant information to urban database constructors in terms of data quality. Moreover, if the automatic procedure program proved to work well, it could afford a great potential utility for modeler successors. Based upon the reasons above, a error-correction campaign was undertaken during the present study.

Work method

Errors detected in the vector maps that we have are numerous. Making an exhaustive list of all the errors with an suitable classification requires high-level knowledge of GIS science and goes beyond the scope of the present thesis. Here we only refer some typical topology errors that we found in the data:

- Overlap: area belonged to two or more polygons (Figure 4.4a).
- Gap: void between adjacent polygons (Figure 4.4b).
- Overlap with: polygons in one feature class overlapped with polygons in another class (Figure 4.4c). For example, a polygon of *building* class overlapped with a polygon in *parcel* class.
- Dangle: endpoint of a line not touched any another line (Figure 4.4d).
- Self-intersect: feature that cross or intercept itself (Figure 4.4e).
- Duplicate feature: feature that is replicated two or more times.

The names of error defined above are based on the guideline on the geodatabase topology rules compiled by ArcGIS® (ESRI, 2014). What has been mentioned in the list does not cover all the errors that we met in the datasets.

Ultimately, the great part of errors is lied to the problem in vertices, i.e. vertices that are wrongly drawn who damage lines and polygons. The GIS softwares integrate tools for the detection or/and correction of topology errors in automatic ways. QGIS's *Geometry Validity* function and *Topology Checker Plugin* look over vector files and check the topology with several topology rules (QGIS, 2014). GRASS's toolset *v.clean* is designed to correct topological errors in an automatic way. This tool should be used in combination with other command lines.

After several tests on these tools, we found:

- Neither QGIS nor GRASS were capable of detecting all errors.
- There was not tool in QGIS for automatic error correction.

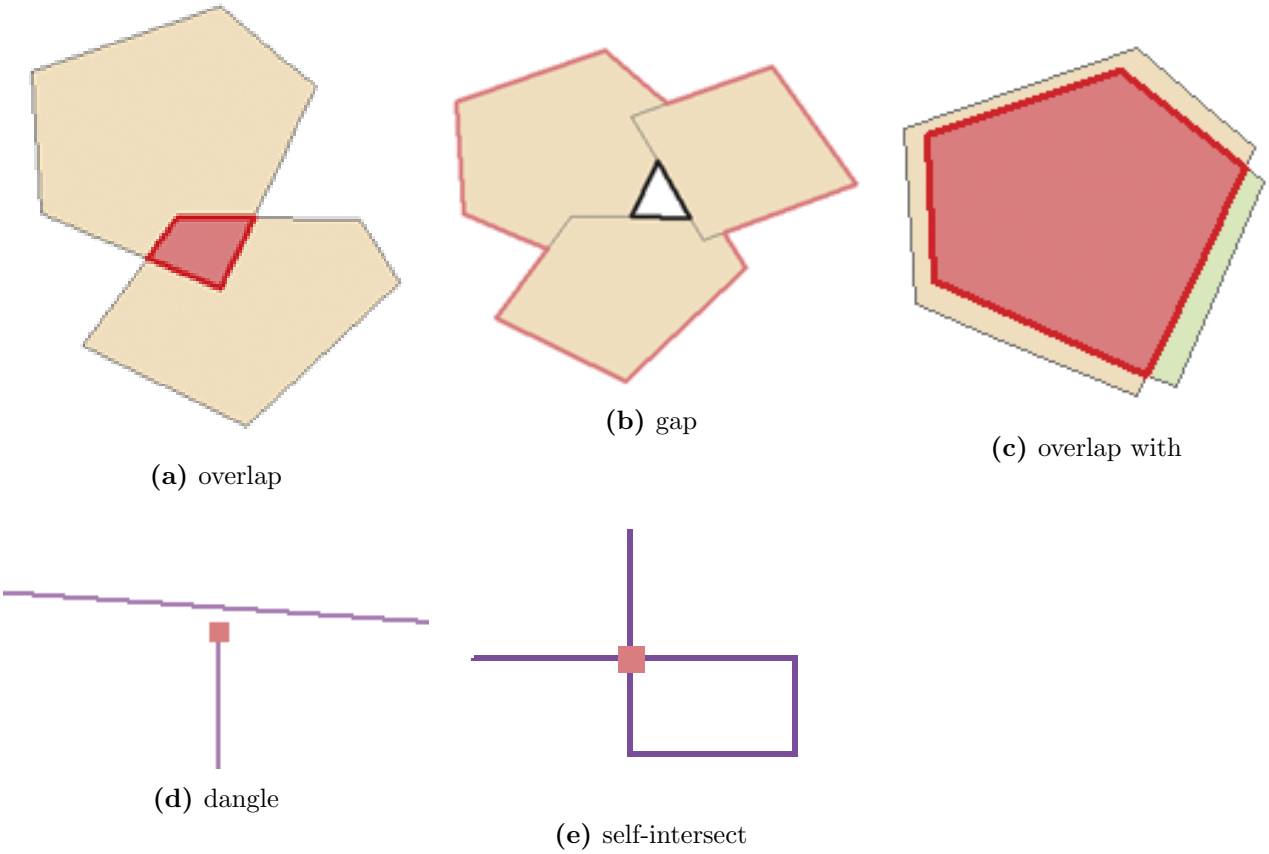

(a) overlap **(b)** gap **(c)** overlap with **(d)** dangle **(e)** self-intersect

Figure 4.4 – Illustration of typical topological errors in GIS data.

- OrbisGIS did not have topology tools.
- GRASS's tools, if powerful, required high-level understanding of GIS philosophy in order to well define the options and parameters in the command lines. And wrongly defined option or parameter value, which was normal for a no-expert level user, could lead to drastic results.

Following the statements above, we defined double-filter procedure:

- A vector map is firstly checked by QGIS (*Geometry validity*), which renders the number and locations of the detected errors. These errors are then corrected manually, before a new check by QGIS and so on, until no more error is detected.
- The QGIS-corrected vector map is imported in GRASS, which can render new errors that have not been detected during the first stage. A second round of manual correction is then taken out.

This double-filter procedure has always been completed by visual inspection. Due to the complexity of the errors and the limited software capacities, this procedure is highly time-consuming. But it is the only way to make sure to hunt down all errors and get everything clear.

Results

By this error-correction work, the initial GIS datasets have been "cleared" in such a way that no more topological error existed in the vector maps. These clean vector maps permit to create new maps of UHEs and Interfaces.

4.4 Construction of UHEs

The pre-processing for the creation of UHEs is based on an automation program written by Paille (2010), during his master's thesis. The program was initially developed in the purpose of generating a geodatabase for hydrological modeling for suburban catchments on the LIQUID® platform (Jankowfsky, 2011). During the present thesis, the program was modified and adapted to meet the requirements of URBS. Based on tools of GRASS, the program is designed to run in Python (Python, 2014) environment. The advantage of coupling Python is that it offers the possibility to execute automatically an entire program of GRASS scripts, instead of executing the command lines one by one in GRASS interface.

The entire procedure covers two stages, each of which is based on a script. The first stage, based on the program *adjacent.py*, consists of segmenting street surfaces in such a way the adjacent street surfaces of any parcel is identified. The second stage, based on the program *UHE.py*, consists of making the fusion of the parcels with their adjacent street surfaces. The two programs are outlined briefly below. For detailed scripts, please refer to Appendix A.2.

adjacent.py

This program splits up the street surfaces in order that they can be attributed later to adjacent parcels, according to the spatial description of urban catchment by UHEs introduced in Rodriguez et al. (2008). Two vectors are required: *street line* (line) and *parcel* (polygon). The process can be resumed in four steps (Figure 4.5):

1. identify the borders between parcels and street surfaces;
2. locate the intersection points of the parcels on the borders;
3. make an orthogonal projections on the street line for the intersection points;
4. construct polygons for the areas surrounded by the border, the projection lines and the street line and make it a vector layer labeled as *adjacent*.

UHE.py

This program finalizes the UHE construction by making the fusion of the parcels and their adjacent street surfaces defined above. Figure 4.6 shows the principles of the fusion of parcels and street surfaces. The whole code is in Appendix A.2.

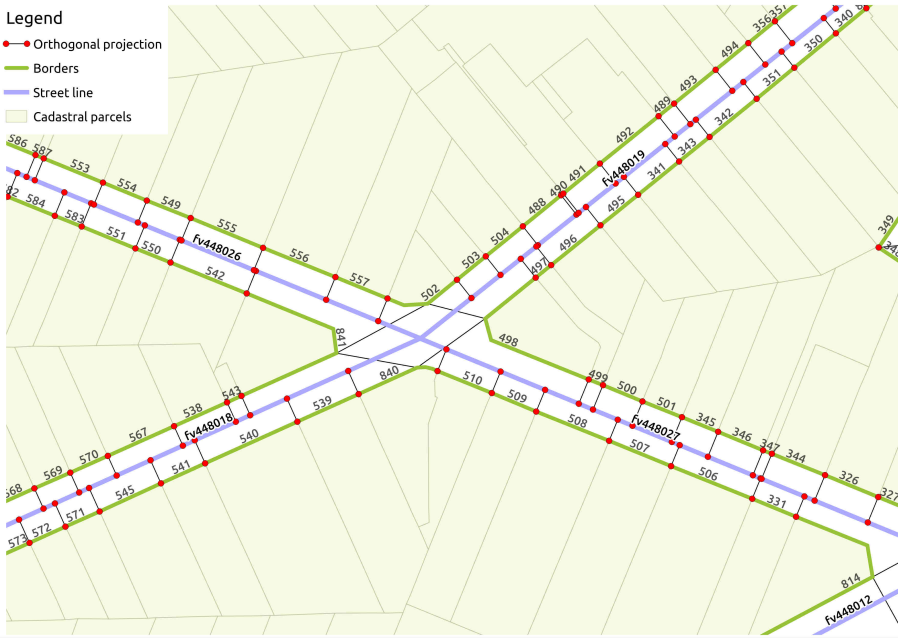

Figure 4.5 – Definition of adjacent relationship between parcels and street surfaces by the program *adjacent.py*.

4.5 Construction of Interfaces

Once the UHEs are created with polygons properly identified by their id number, their interfaces are drawn by the category adding function of GRASS (*v.category*). This function extracts border lines of the UHE polygons and convert them to a separate vector map, termed *interface*. The association of the UHEs with their interfaces are established based on their identity numbers. The constructed Interfaces are illustrated in Figure 4.7. The detailed code is in Appendix A.3.

4.6 Geometrical features

4.6.1 UHEs

The attribute table of the parcels has already been constructed during prior development of URBS (for Pin Sec catchment, cf. Chapter 5). The same table was used for the UHEs (cf. Table 2.1), as the UHEs and the parcels match one-to-one.

4.6.2 Interfaces

During his master's thesis, Zhou (2013) developed a program for creating automatically the attribute table for parcels (for URBS model as well) with the SQL tool in OrbisGIS. The program for the construction of Interfaces attribute table presented here is inspired by the work of Zhou (2013). Here we only outline briefly the process. Detailed SQL commands can be found in Appendix A.4.

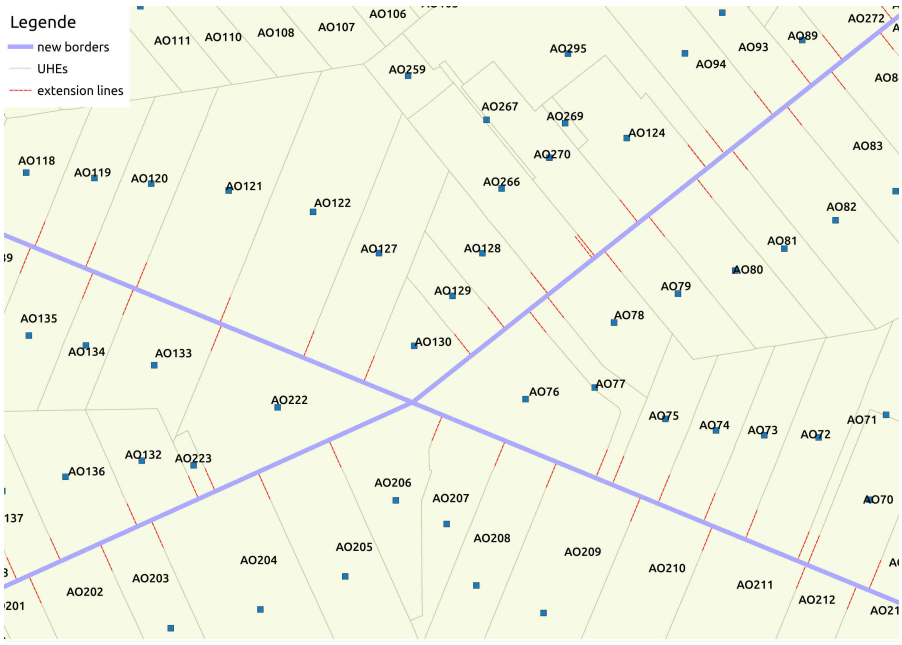

Figure 4.6 – Construction of UHEs polygons by fusion of the parcels with their adjacent street surfaces. The red-dashed lines show the extension of initial parcels by merging with adjacent street surfaces. The blue line shows the newly generated border lines of the UHEs.

id_{int}

The identity numbers id_{int} of the interfaces have been generated automatically during their creations by GRASS (cf. Section 4.5).

d_A and d_B

The computation of the distances d_A and d_B includes two steps:

1. Add the centroids of the parcels.
2. Compute the distance between each parcel centroid and the geometry center of each interface, by the spatial SQL function *ST_Distance*.

z_{int} z_g^A and z_g^B

The elevation of a UHE z_g is represented by that of the centroid of the UHE. These elevations are computed with the Digital Elevation Model (DEM) of the Pin Sec catchment. The vector-based primary DEM dataset is at a 20-meter resolution. The function *ST_interpolate* build a raster DEM by interpolating the primary DEM dataset based on Delaunay triangulation. Then the geometric function *ST_Z* returns the elevation Z of the defined point.

The elevation of an interface z_{int} is represented by that of the centroid of the interface. This elevation is computed by the the distance-averaged elevation of the adjacent UHEs.

l_{int}

The geometry function *ST_Length* allows to return the length of a geometry, i.e. of an interface in this case.

4.7 Flow routing map

The flow routing of the URBS model is composed of two stages: i) flow from each UHE to the inlet of stormwater sewer systems; ii) flow inside sewer pipes (Section. 2.3). The *flow routing* file contains thus information on i) geometrical parameters of each segment of streets and of the sewer networks; ii) upstream/downstream relationships of the segments. This map has been constructed during previous model development (Le Delliou, 2009).

Finally, 875 UHEs, 2481 Interfaces and 392 segments of flow routing segment are obtained for the Pin Sec catchment. They are illustrated in Figure 4.7.

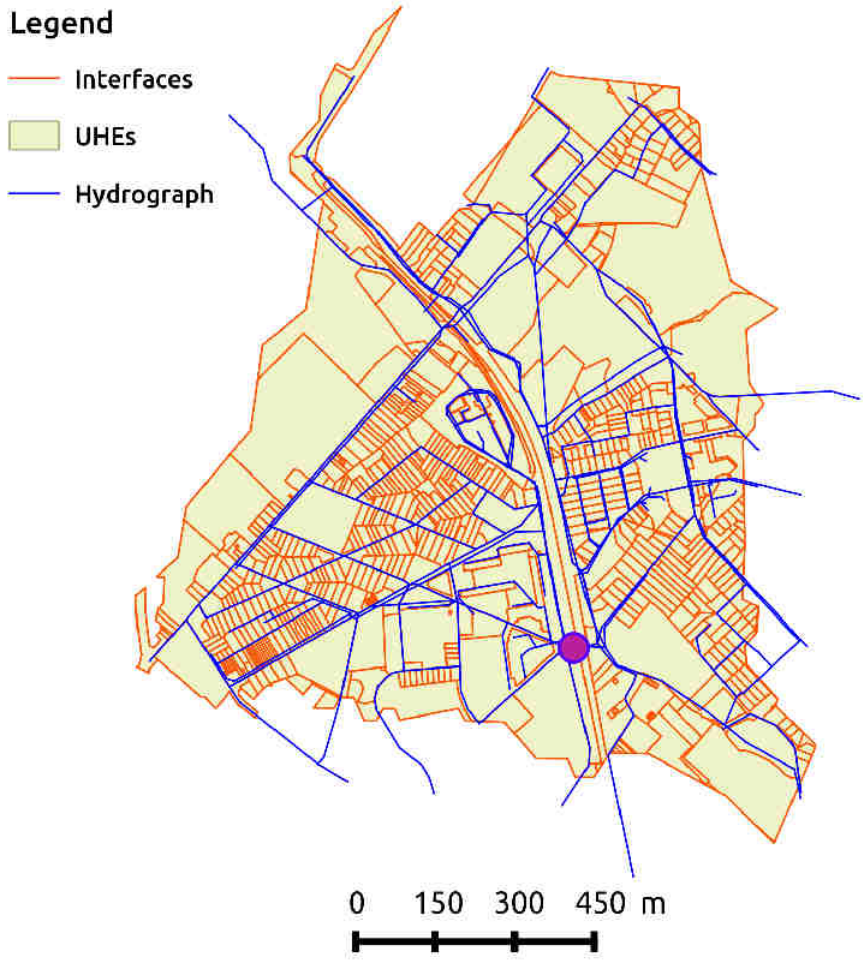

Figure 4.7 – UHEs, interfaces and the flow routing map of Pin Sec by geodata pre-processing.

Summary and conclusion

This chapter has described the geodata pre-processing for the Pin Sec catchment, of which the purpose is to construct three geodata input files for the model URBS-WTI: *UHEs*, *Interfaces* and *flow routing*.

The vector map of the UHEs is created by a series of two Python programs embedding command lines of GRASS. The vector map of the Interfaces is created by an extraction of border lines of the UHEs, always in GRASS environment. Geographical parameters of the Interfaces are generated with tools in OrbisGIS. Due to numerous errors existed in the vector maps or in their attribute tables, great effort has been exerted to correct the errors. This work is inevitable for the application of the newly developed module WTI in URBS. The fruit of this time-consuming geodata pre-processing can be however useful: clear GIS layer of parcels, street lines and surfaces; correct attribute values; and the newly constructed UHEs and Interfaces.

Chapter 5

Case study on Pin Sec catchment and module evaluation

Contents

Introduction

The work of integrating the saturated module WTI in the model URBS was presented in Chapter 3. For evaluating this integration and the behaviour of the module, the integrated model URBS-WTI was applied and evaluated on the small urban catchment (31 ha) of Pin Sec within the city of Nantes in the west of France. With a separated sewer networks, Pin Sec is an experimental catchment monitored by the IFSTTAR and IRSTV. It has various hydrological observation data: rainfall, discharge rate and groundwater level, which serve as input of the model and underpinning for the result evaluation.... In this chapter we give a detailed presentation of this case study.

Section 5.1 outlines the climatic and hydrogeological characteristics of the Pin Sec catchment. The available hydrological datasets are presented in Section 5.2. Data of land use is provided by Nantes Métropole[1] and prepared for the use of the URBS-WTI model by GIS pre-processing. Given the importance of this work, it has been presented separately in Chapter 4, and recalled in Section 5.3. Section 5.4 outlines the principles of a model base-run on Pin Sec. The results of the base-run is given in Section 5.5. Section 5.6 details the processes by which we calibrated manually the model based on a parameter sensitivity analysis. For each parameter, both URBS and URBS-WTI are studied and their results are compared. Section 5.7 shows the results of the calibrated modeling. In the last section (5.8), we discuss a test of artificial forcing of the WTI module by introducing a parameter.

5.1 Urban catchment and hydrogeological catchment of Pin Sec

5.1.1 Geography

The urban catchment of Pin Sec (31ha, dotted line in Figure 5.1) is located in the east of Nantes city in France, between the rivers Loire and Erdre. It is delimited by a separated sewer networks for storm- and wastewater. Within the catchment, land cover is shared by small collective and individual dwelling areas. The current impervious ratio is about 45%. Mean slope is 1.1% from north-west to south-east. The highest and lowest elevation is 28 m and 17 m NGF respectively (Ruban et al., 2007; Mestayer et al., 2011).

[1]Nantes Métropole: The Urban Community of Nantes, inter-communal structure gathering the city of Nantes and some of its suburbs.

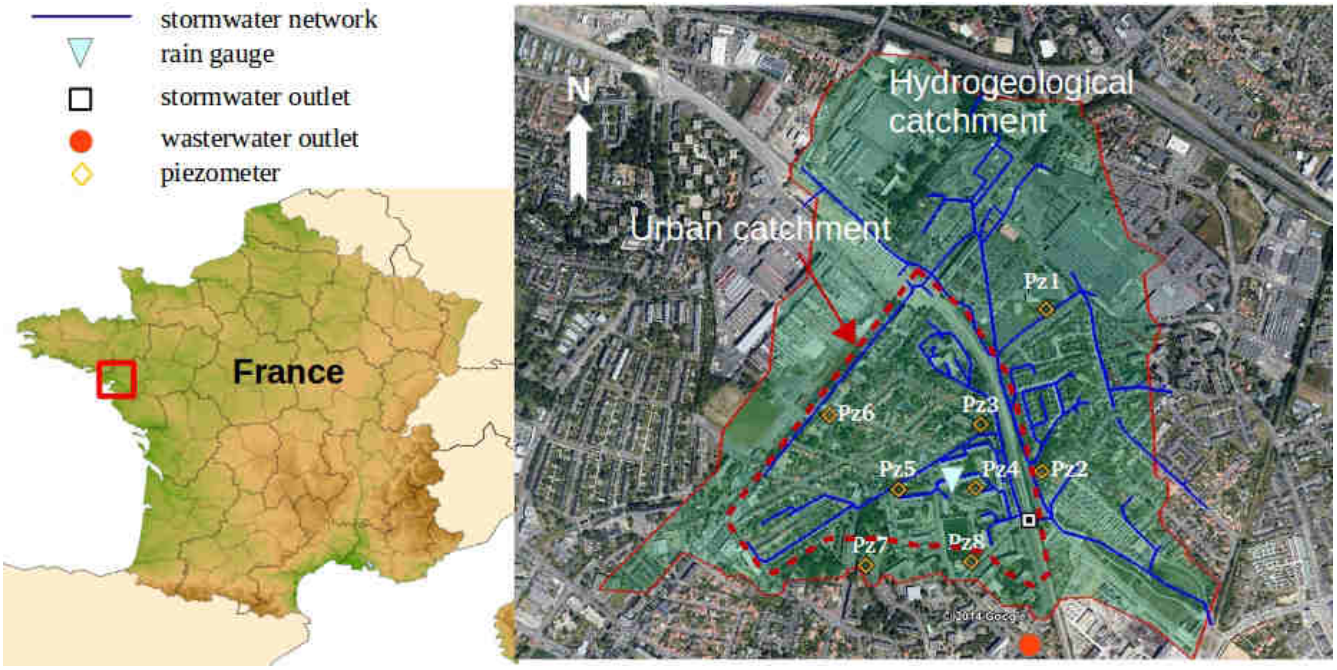

Figure 5.1 – Location of the urban catchment of Pin Sec (dotted line) and the larger hydrogeological catchment (solid line). Stormwater network, rain gauge and the network of eight piezometers are shown over an aerial photograph. The unique outlet of the stormwater sewer networks is located in the south-east of the urban catchment.

The outlets of the storm- and wastewater sewer networks are situated to the south-east of the catchment with a distance of 300 m (Figure 5.1). Total length of the stormwater sewerage network is 4 km, and that of the wastewater is 7.3 km. The outlet of the stormwater network is an underground pipe that drains into the Les Gohards stream. The wastewater network is connected to the WWTP of Tougas 10 km to the west.

The urban catchment is contained within a hydrogeological catchment, defined by a ridge line. With an area of 133 ha (zone delimited by red solid line in Figure 5.1), the hydrogeological catchment of Pin Sec is located between 13 m and 29 m NGF, with a weak mean slope of 0.9%.

5.1.2 Climate

The city of Nantes is located at 47°13'N, 01°33'W, 80 km from the Atlantic coast. Dominant climate type is oceanic featured by dispersed low-intensity annual rainfall. According to Météo France (French national meteorological service), the long term average annual rainfall for the period of 1971-2000 is 797 mm, with 10 rainy days per month in average. The average annual temperature for the same period is 12.2℃, with a relatively narrow range of variation. The lowest daily mean temperature is 5.8℃ in January, and the highest is 19.4℃ in July and August. The prevalent wind comes from the south-west and north-west (Le Delliou, 2009).

5.1.3 Hydrogeology

Pin Sec is underlain by the *Massif Armoricain* formation which has complex geological conditions. Three layers can be distinguished: silt, alluvium and mica schist. A detailed description of these formations can be found in Le Delliou (2009).

An unconfined aquifer *nappe de socle* lies in deeper ground. In this type of formation, water is mainly stored in altered rocks, moving through rock cracks and fissures, according to Wyns et al. (2004) and Mougin and Conil (2005). These authors studied the aquifer within the city of Nantes and observed that the groundwater table fluctuated between -2.5 m and -5.7 m during winter. Within Pin Sec, the groundwater table is lower, fluctuating between -3 m and -4 m. Mougin and Conil (2005) indicates that the aquifer is naturally drained by the rivers Loire and Erdre.

5.2 Hydro-climatic data

With a separated sewer network for storm- and wastewater, the urban area of Pin Sec is an observation catchment of ONEVU (Observatoire Nantais des EnVironnements Urbains), in-situ environmental observatory in hydrology, micro-meteorology, climatology, air, water and soil quality. With OPUR[2] and OTHU[3], ONEVU is one of the three main national environmental observatories in France and benefits financial support from European Regional Development Fund and INSU[4].

Hydrological measurements on Pin Sec include rainfall, flow rates at the storm- and wastewater outlets, and groundwater monitoring by a network of piezometers. Observational data series used in the present study include:

- rainfall intensity for the 5-year period of 01/01/2006 - 31/12/2010 at 5-min time step
- daily average potential evapotranspiration (PET) rate for the same period provided by Météo France (calculated by the Penman-Monteith equation (Monteith, 1981))
- discharge measured at the outlet of the stormwater sewer network for the same period at 5-min time step
- piezometric records for the period 01/06/2006 - 31/12/2010 at 20-min time step

The hourly PET rate is estimated from daily average PET using an approximated diurnal cycle. Instantaneous PET is assumed to be zero before sunrise and after sunset. Beginning at sunrise, the PET rate is assumed to follow a sinusoidal form that peaks at solar noon.

The piezometers are installed at the depth of altered mica schist (Rodriguez et al., 2013). There is no impermeable layer between ground surface and the measured depth. The measured level is thus the

[2]OPUR: Observatoire des Polluants Urbains en Île-de-France
[3]OTHU: Observatoire de Terrain en Hydrologie Urbaine
[4]INSU: Institut National des Sciences de l'Univers.

shallow free water table. As shown in Figure 5.2 and 5.3, groundwater table varies between -4.5 m and -0.5 m, with high level in winter and low level in summer.

The hydro-climatic data series have been subjected to a pre-treatment for eliminating some “obvious” errors, such as abrupt increasing and decreasing limbs or long-time flat in the curves.

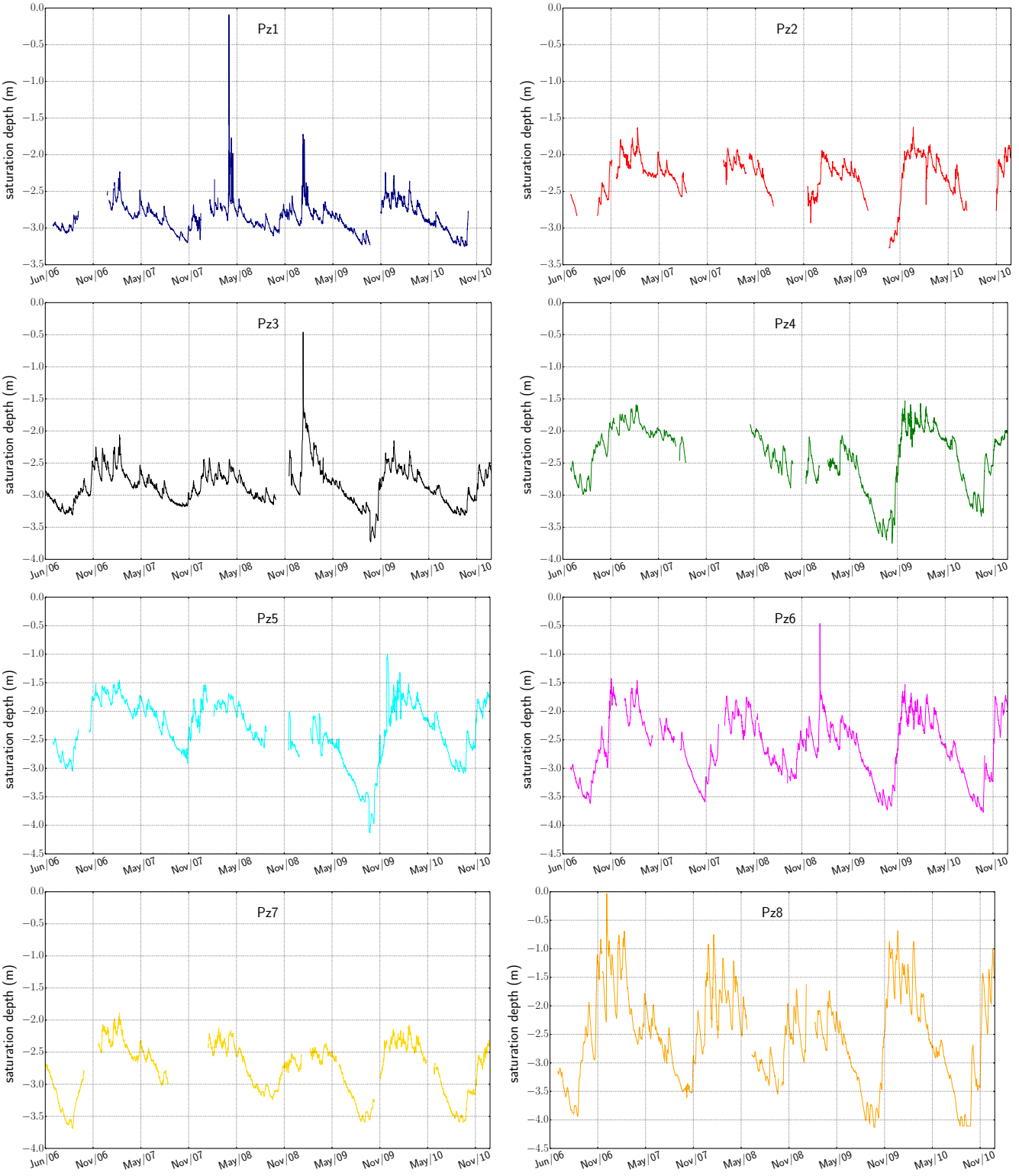

Figure 5.2 – Recorded time series of groundwater level of Pin Sec for the period of 01/06/2006 - 31/12/2010 at 20-min time step.

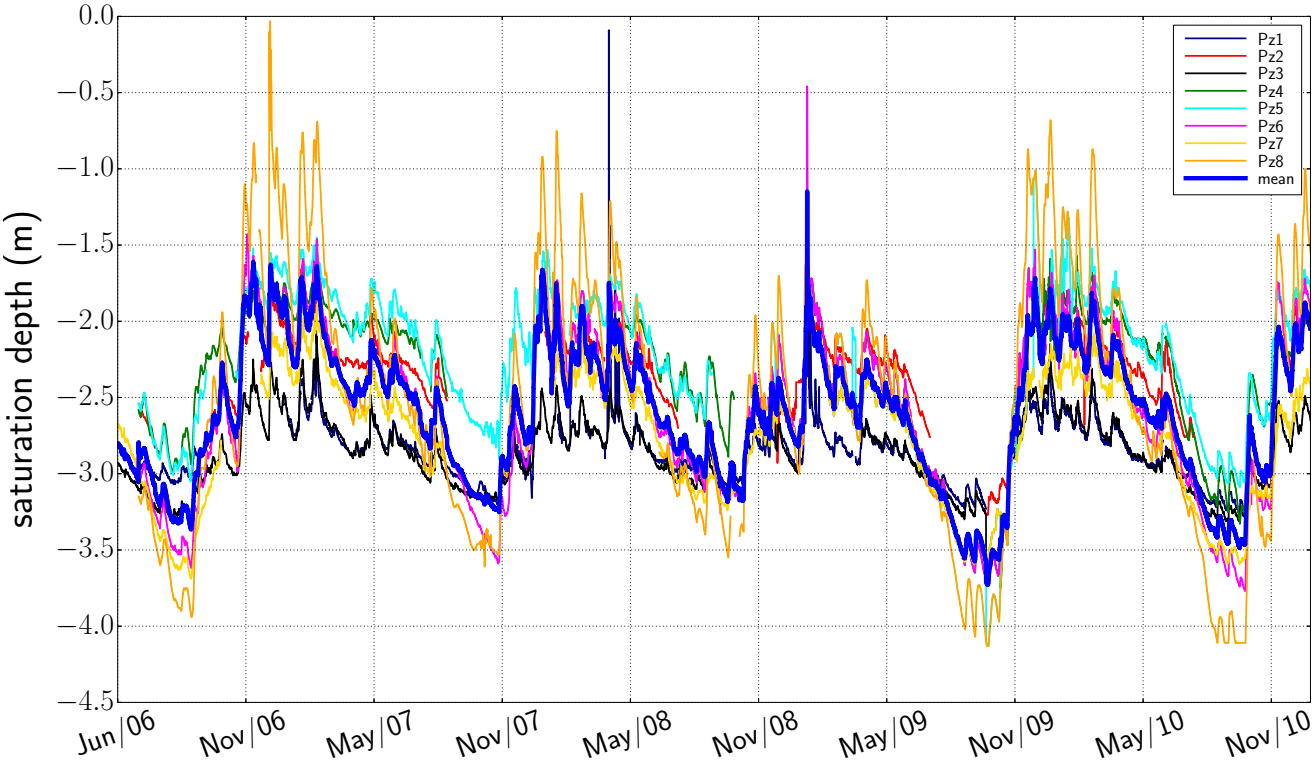

Figure 5.3 – Mean groundwater level of Pin Sec for 01/01/2006 - 31/12/2010.

5.3 Land use and geodata

The hydrogeological catchment of Pin Sec, with a total area of about 133 ha, is composed of 875 parcels ranging from 1.54 m^2 to 117 724 m^2. The total surface area of the parcels is 114 ha. The last 20 ha are street surfaces, as illustrated in Figure 5.4. Within the parcels, buildings occupy a total area of 25 ha (A^{hou}), a little less than 1/5 of the total area. Pavements occupy about 16 ha. Their areas are accounted in the *street* land use (A^{str}), assumed by the model. Natural surface occupies about 72 ha (A^{nat}). 1/3 of the natural surface, about 21 ha, are covered by trees (A^{nat}_{tree}). This percentage is much weaker on streets (A^{imp}_{tree}), only 5777 m^2, about 1.6% of A^{imp}. The roofs and streets are totally connected to sewer networks, while the natural surfaces have a coefficient of connection of 0.2 to the sewer networks.

The geodata is provided by the Urban Databanks of Nantes Métropole. Based on these data, the input geodata files were prepared (cf. Chapter 4, Section 4.3).

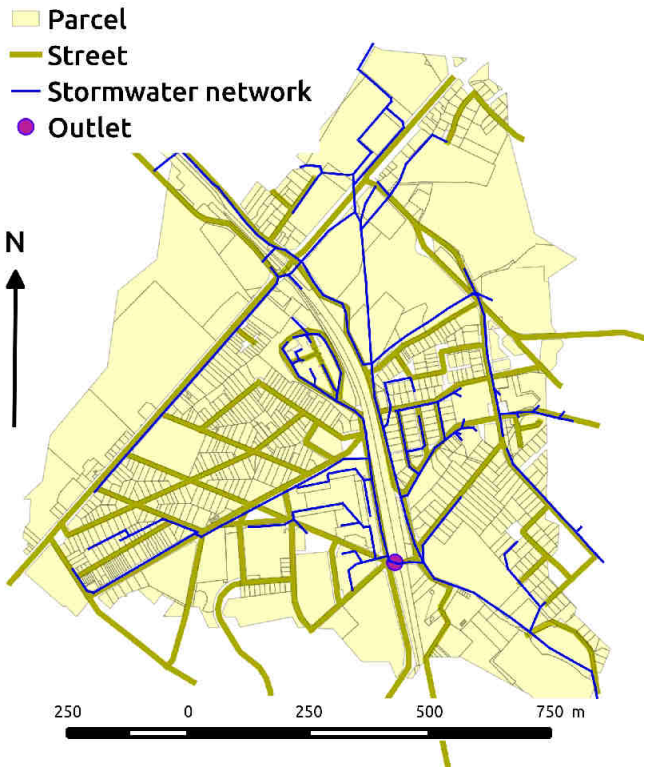

Type	Description	(ha)
A^{nat}	natural surface	72
A^{hou}	building surface	25
A^{str}	streets & pavements	36
A^{imp}	impervious surface	61
A^{nat}_{tree}	tree-cover on natural surface	21
A^{imp}_{tree}	tree-cover on impervious surface	0.57
A^{tot}_{tree}	total area of tree-cover	21
		$A^{tot} = 133$ ha

Figure 5.4 – Vector map of Pin Sec and land cover classification assessed by the geo-data pre-processing. The catchment encompasses 875 parcels and 9.6 km of stormwater drainage linear.

5.4 Methodology for the module evaluation through a model base-run

The behaviour and performance of the WTI module are examined through a model base-run of URBS-WTI on Pin Sec catchment. The base-run is conducted continuously on the 5-year period of 01/01/2006 - 31/12/2010 at 5-min time step.

The measured series of rainfall intensity and potential evapotranspiration (PET) rate are uniformly applied on the catchment. The hourly PET rate has been referred to each time step of 5 minutes under an assumption that the daily PET profile is sinusoidal.

In order to overcome the difficulty in defining boundary conditions of groundwater flow for the urban catchment, of which we had little information, the model is applied at the whole hydrogeological catchment, with a zero-flow subsurface boundary condition. (Rodriguez et al., 2013) has estimated that the average soil flow out of the catchment of Pin Sec is only 0.023 mm/day, which is non-significant in front of the other fluxes in the water balance.

Two urban catchments in the neighborhood of Pin Sec, the Rezé and les Gohards, have been subjected to model application of URBS by Morena (2004) and Rodriguez et al. (2008). Physical model parameters have been calibrated on these catchments. Since the geology conditions of Pin Sec are the same as Rezé and les Gohards, the same parameter values are used for the model base-run. However, since the geology in URBS-WTI is parametrized in a simple way (cf. Chapter 2), reasonable parameter values can be different

from one catchment to another. Thus, the parameters for soil, especially the ones operating directly on the WTI flux (Equation 3.4) is subjected to a sensitivity analysis, which is presented in Section 5.6. The concerned parameters are listed in Table 5.1. For the description of the whole set of model parameters, please refer to Morena (2004) or Rodriguez et al. (2008).

Saturation depth is uniformly initialized (z_s^0) through the catchment. There is no information on groundwater level on the beginning of the simulation period (01/01/2006). In a prominent model application of URBS on the same catchment for the period 2009 - 2010 (not published), the average groundwater level of the catchment on 01/01/2010 has been estimated at -0.65 m. This value has been chosen for the initial condition of saturation depth z_s^0, which is also subjected to the sensitivity analysis.

Modeling outputs at every time step include:

- flux (infiltration, evaporation, transpiration, surface runoff, etc.) at catchment scale and for each type of land use, expressed in water depth (meter or millimeter)
- storage in the reservoirs at catchment scale: tree, surface, vadose zone and saturated zone, expressed in water depth (meter or millimeter)
- continuous discharge rate at the catchment's outlet and in every pipe of the stormwater sewer network, expressed in volume (m^3) or water depth (meter or millimeter)
- groundwater level of every UHE, expressed as a saturation depth (cf. Chapter 2)

For evaluating the model performance, these outputs will be analyzed in a throughout way. Three comparison criteria will be used:

- Bias error C_b, which indicates the general deviation of the simulated series as regard to the observed series, calculated as (where D is a hydrological variable):

$$C_b = \frac{\sum_{t=1}^{n}(D_{sim}^t - D_{obs}^t)}{\sum_{t=1}^{n} D_{obs}^t} \qquad \in \quad [-\infty, +\infty] \tag{5.1}$$

Table 5.1 – Values and variation ranges of the parameters that can influence the WTI module. The variation ranges are drawn from Rodriguez et al. (2008).

	Unit	Description	Value	Range
K_s^{nat} (K_s^{lat})	m/s	Hydraulic conductivity at saturation at ground surface level	1.3×10^{-5}	[1.3×10^{-8}, 1.3×10^{-4}]
M	-	Scaling parameter of the hydraulic conductivity	0.2	[0.1, 3]
λ	-	Coefficient of groundwater infiltration to sewer networks	4	[0, 100]
z_s^0	m	Initial saturation depth of the catchment	-0.65	[-0.05, -10]

- Coefficient of determination R^2, defined as the squared value of the coefficient of correlation, calculated as:

$$R^2 = \frac{[\sum_{t=1}^{n}(D_{sim}^t - \overline{D_{sim}})(D_{obs}^t - \overline{D_{obs}})]^2}{\sum_{t=1}^{n}(D_{sim}^t - \overline{D_{sim}})^2 \sum_{t=1}^{n}(D_{obs}^t - \overline{D_{obs}})^2} \qquad \in \quad [0,1] \tag{5.2}$$

  It estimates the combined dispersion against the single dispersion of the observed and simulated series. The range of R^2 lies between 0 and 1 which describes how much of the observed dispersion is explained by the simulation.

- Nash-Sutcliffe efficiency C_{nash} (Nash and Sutcliffe, 1970), hereinafter referred to as "Nash criterion", defined as one minus the sum of the absolute squared differences between the simulated and observed values normalized by the variance of the observed values during the simulation period, calculated as:

$$C_{nash} = 1 - \frac{\sum_{t=1}^{n}(D_{sim}^t - D_{obs}^t)^2}{\sum_{t=1}^{n}(D_{obs}^t - \overline{D_{obs}})^2} \qquad \in \quad [-\infty, 1] \tag{5.3}$$

  The normalization of the variance of the observation series results in relatively higher values of C_{nash} in catchments with greater dynamics and lower values in catchments with lower dynamics. The range of C_{nash} lies between 1 and -∞.

where D_{sim}^t is the simulated value of the output D at time t, D_{obs}^t the observed value of the same variable at time t, $\overline{D_{sim}}$ the mean of D_{sim}^t and $\overline{D_{obs}}$ the mean of D_{obs}^t. The modeling quality is as better as C_b is close to 0, R^2 and C_{nash} are close to 1.

The so-called model "base-run" includes in fact two modeling series: one by the initial URBS model without the WTI module, and one with URBS-WTI. Comparison between the modeling results of URBS and URBS-WTI can indicate the impacts of the WTI module on the model behaviour. For the sake of clarity and simplicity, hereinafter the term "URBS-WTI" will be used referring to the model with WTI, and the term "URBS" without WTI.

In order to evaluate the impacts of the WTI, especially in smoothing groundwater levels between adjacent UHEs, a simple criterion is the temporal variation of the standard deviation σ of the simulated groundwater levels of the UHEs, calculated for each time step t as:

$$\sigma GWL^t = \sqrt{\frac{\sum_{u=1}^{U}(GWL^{u,t} - \overline{GWL^t})^2}{U}} \tag{5.4}$$

where σGWL^t is the standard deviation of the groundwater levels, $GWL^{u,t}$ (m) the groundwater level of UHE u in the NGF system, $\overline{GWL^t}$ the mean groundwater level of all the UHEs and U the number of UHEs. A lower value of σGWL^t indicates a more homogeneous groundwater table through the catchment.

To compare the simulation with the observation, groundwater level simulated at each piezometer is represented by the area-averaged groundwater level of the UHEs in the vicinity of the piezometer, with a 50m distance threshold. Since the geometry of the UHEs are irregular, the numbers of UHEs concerned may vary along the piezometers.

5.5 Results of the base-run

5.5.1 Water balance

Table 5.2 shows the simulated water balance at the catchment scale by the base-run of URBS and URBS-WTI, with each component as being the quantity of:

- Q^{hou}, Q^{str}, Q^{nat}: runoff of the three land use types (house, street, natural land)
- Q^{drain}: groundwater infiltration to sewer networks
- E: surface evaporation
- TR: transpiration
- Δstorage: storage variation in the soil between the end and the beginning of the simulation period
- P: rainfall

The catchment water balance equation is written as:

$$P = Q^{hou} + Q^{str} + Q^{nat} + Q^{drain} + E + TR + \Delta\text{storage} \tag{5.5}$$

The first observation is that URBS-WTI estimates the same water balance as URBS. The WTI module simulates flow in the saturated zone and the results indicate that it does not change the global water balance of the catchment.

Table 5.2 – Simulated water balance of Pin Sec both by URBS and URBS-WTI for the period of 01/01/2006 - 31/12/2010. All the flow and storage components are expressed in percentage of total rainfall.

	Q^{hou}	Q^{str}	Q^{nat}	Q^{drain}	E	TR	Δstorage	P
URBS	16.6	13.9	13.6	9.9	11.5	33.4	0.8	100
URBS-WTI	16.6	13.9	13.6	9.9	11.6	33.2	0.8	100

More than 40% of total rainfall P returns to the atmosphere by evapotranspiration (E+TR). About 30% of P is transformed into impervious surface runoff, with half from roofs (Q^{hou}) and half from streets (Q^{str}), despite the larger surface area of streets. This can be explained by the different hydraulic conductivities assigned to these two surfaces: while roofs does not permit any infiltration to the soil ($K_s^{hou} = 0$), streets have a weak infiltration capacity ($K_s^{str} = 7.5 \times 10^{-8}$ m/s). A suprising component is the natural surface runoff (Q^{nat}), which accounts for 13.6% of P. This is caused by saturation overland flow (see Section 5.5.3). This great natural surface runoff is questionable, even if it is in similar with the results of the Rezé catchment (Morena, 2004), where natural surface runoff represents 10% of the total rainfall. Groundwater drainage by sewer networks Q^{drain} represents 9.9% of P, as divided into 6.6% to

wastewater and 3.3% to stormwater networks (for the explication of this fraction, see Chapter 2, Section 2.5). Rodriguez et al. (2013) estimated that the groundwater drainage by the storm- and wastewater sewer networks of the Pin Sec accounted for 24% and 8% of the total annual rainfall. Compared to these reported values, the estimated values by the model seem to be too weak. Considering the high surface runoff produced by natural surface, and the low groundwater drainage by sewer networks, it seems that the value of the coefficient of groundwater drainage $\lambda = 4$ is not optimal. A calibration on this parameter seems necessary.

5.5.2 Discharge

Table 5.3 shows the comparison criteria values calculated on the simulated and observed continuous discharge rates at the outlet of the stormwater sewer network. The total discharge volume is well predicted by the models with a low bias error $C_b = 0.20\%$. But the dynamics in the discharge rates is not as well simulated, with relatively weak values $C_{nash} = 0.50$ and $R^2 = 0.59$. But these low criteria values are partially related to the small time step (5 min) of the data series. Besides, the results on discharge confirm the fact that the WTI module does not affect the global water balance of the catchment.

Table 5.3 – Comparison criteria values for simulations of continuous discharge rates at the outlet of Pin Sec by model base-run. The criteria are computed for the period of 01/01/2006 - 31/12/2010.

	C_b (%)	C_{nash}	R^2
URBS	0.20	0.502	0.589
URBS-WTI	0.21	0.502	0.592

5.5.3 Saturation depth

Figure 5.5 plots the simulated saturation depth at each of the piezometers by the model base-run. Table 5.4 gives the values of comparison criteria. Both the models URBS and URBS-WTI overestimate the groundwater levels. While the observed average saturation depth for the studied period is -2.55 m, the simulated one is about -0.60 m. For some of the piezometers (Pz3, Pz4, Pz7 and Pz8), the simulated series contain numerous periods where the soil is saturated (Figure 5.5). This uniform overestimation supposes that the initial condition for saturation depth z_s^0 = -0.65 m needs to be re-examined. The seasonal variations are relatively well reproduced: the simulated rising and descending limbs of groundwater level are in line with the observation. The criteria R^2 is however quite weak (around 0.3).

Related the great difference in the simulated and observed saturation depths, C_{nash} are very poor. More importantly, great dispersions are observed in C_{nash} of the piezometers, confirming the spatial heterogeneity of the groundwater level.

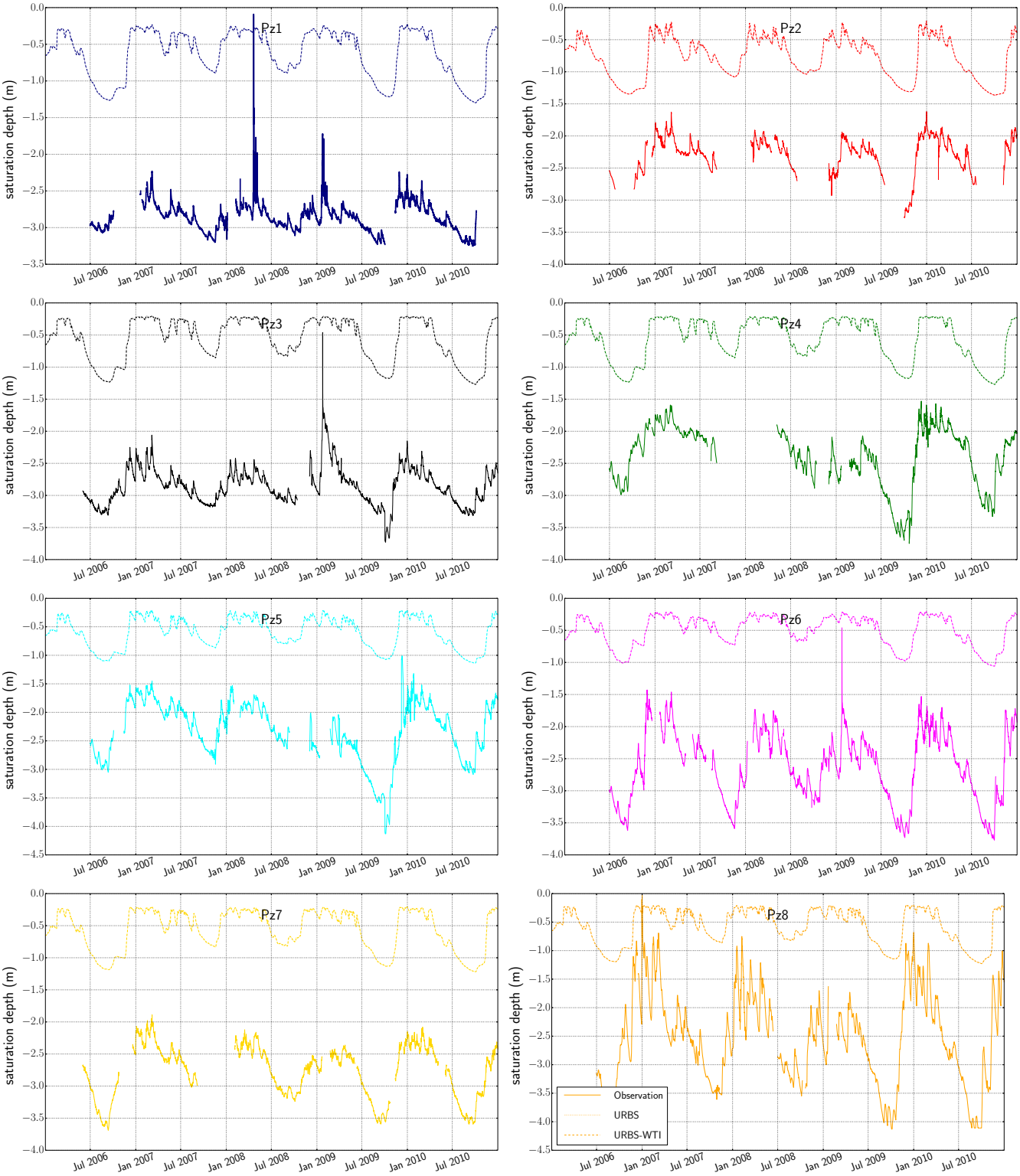

Figure 5.5 – Time series of simulated groundwater level of Pin Sec (dotted line) by model base-run, compared with measured series (solid line). Due to the similarity of the results by URBS and URBS-WTI, their curves are superimposed.

Table 5.4 – Modeling results on saturation depth of Pin Sec by model base-run, for the period of 01/01/2006 - 31/12/2010 at a 20-min time step.

(a) mean annual saturation depth (m)

	Pz1	Pz2	Pz3	Pz4	Pz5	Pz6	Pz7	Pz8	mean	error
Obs.	-2.86	-2.28	-2.86	-2.40	-2.33	-2.63	-2.36	-2.78	-2.55	
URBS	-0.56	-0.82	-0.62	-0.54	-0.58	-0.48	-0.55	-0.55	-0.59	-77%
URBS-WTI	-0.56	-0.82	-0.49	-0.54	-0.58	-0.48	-0.55	-0.55	-0.57	-78%

(b) C_{nash}

	Pz1	Pz2	Pz3	Pz4	Pz5	Pz6	Pz7	Pz8	mean
URBS	-136.5	-30.9	-61.6	-17.1	-12.0	-16.2	-30.6	-6.6	-38.9
URBS-WTI	-136.6	-30.9	-66.9	-17.0	-12.0	-16.1	-30.6	-6.6	-39.6

(c) R^2

	Pz1	Pz2	Pz3	Pz4	Pz5	Pz6	Pz7	Pz8	mean
URBS	0.308	0.277	0.348	0.292	0.282	0.339	0.362	0.378	0.323
URBS-WTI	0.308	0.277	0.279	0.292	0.282	0.338	0.361	0.378	0.314

5.5.4 Smoothing effect of the WTI module on simulated groundwater levels

Figure 5.6 shows the standard deviation σ of the simulated groundwater levels GWL of the UHEs by URBS and URBS-WTI. Generally speaking, high values are observed in wet season and low values in dry season. In winter, the higher groundwater level is more influenced by land use types and their spatial heterogeneity. The spatial variation of the groundwater level is thus more pronounced than in summer.

If the WTI module can not change the season trends of σGWL, dominated by climate forcings, it reduces its magnitude. But the reduction is light with regard to the seasonal variability.

5.5.5 Summary of the model base-run

The model base-run of URBS-WTI (as well as URBS) on the Pin Sec catchment has not shown satisfying model performance: water balance is not convincing with great runoff generated on natural surface and weak groundwater drainage; piezometric levels are overestimated. Only the simulated discharge series shows a relatively good fit with measured data.

The integrated module WTI has not shown significant effect on groundwater level – the simulated groundwater level series by URBS and URBS-WTI are almost identical. If the reduced σGWL signifies slighter dispersions of the groundwater levels among the UHEs, it seems that the effects of lateral saturated flow are obscured by vertical flux under climate forcings. On the other hand, the (almost) same results

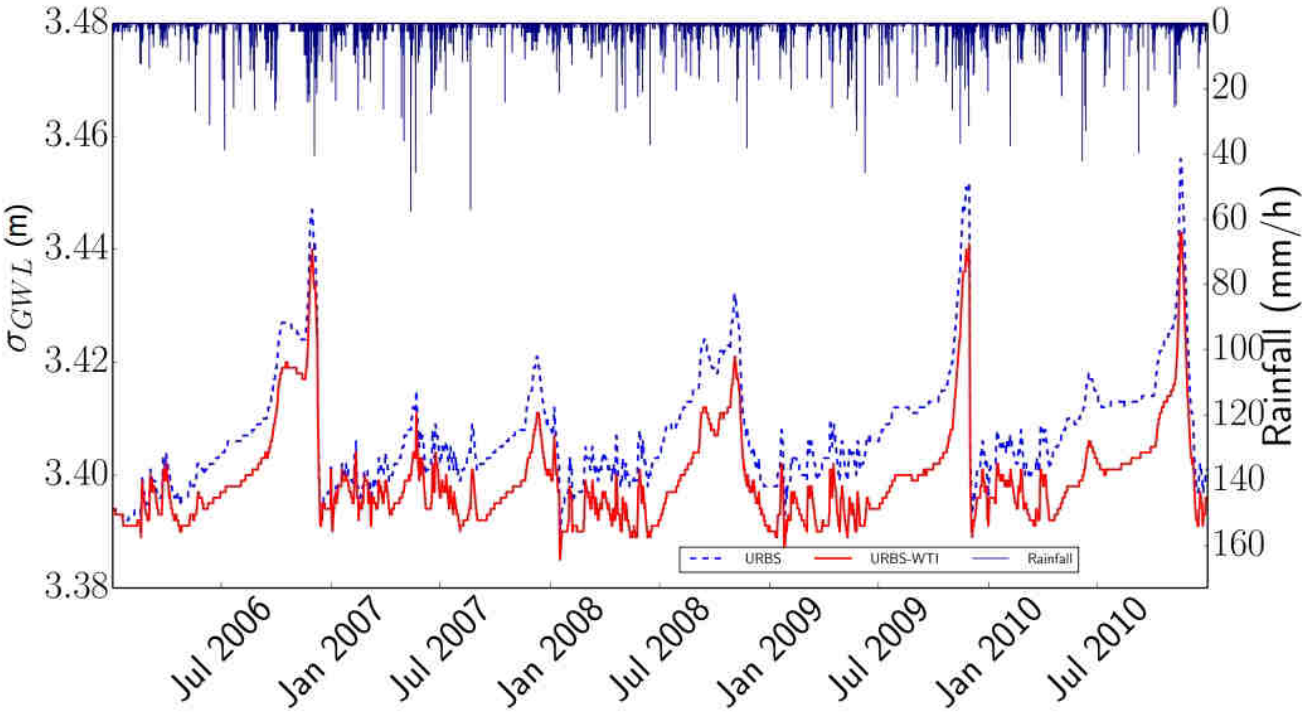

Figure 5.6 – Standard deviation of the simulated average groundwater level series (elevation in the NGF system) of Pin Sec by model base-run for the period of 01/01/2006 - 31/12/2010.

in water balance and discharge given by URBS and URBS-WTI signify that the new module does not change the global model behaviour, nor deteriorate its performance in flow simulating. From a modeling point of view, this is relatively assuring: the low model performance is not caused by the integration of the WTI module, but a priori linked to the parameters, which have been validated on other sites and applied on Pin Sec.

Thus, a sensitivity analysis on the parameters is necessary, which can show:

1. how the model URBS-WTI is sensitive to the parameters and if this sensitivity is different from URBS
2. if an optimal set of parameter values can be found for Pin Sec, for both URBS and URBS-WTI
3. if URBS-WTI has better performance than URBS in groundwater level simulation

This study is described in the next section.

5.6 Sensitivity analysis and model calibration

5.6.1 Methodology of the sensitivity analysis

Morena (2004) studied the model sensitivity for the whole set of physical parameters of URBS on the Rezé catchment. In the present study, it is thus not compulsory to re-examine all the physical parameters,

but the several ones that influence the WTI module: i) saturated hydraulic conductivity at the natural soil surface K_s^{nat}, ii) scaling parameter M of the exponential decrease of K_s^{nat}, and iii) coefficient of groundwater infiltration to sewer networks λ. K_s^{nat} and M operate directly on the WTI flow (Equation 3.6). λ does not operate directly on the WTI equation, but it impacts the storage in the saturated zone by regulating the sewer infiltration flux, thus has indirect impact on the lateral saturated flow.

The initial condition for saturation depth z_s^0 should not alter saturation patterns after a model "warm-up" period. And this stability should not be deteriorated by the WTI module. However, the overestimation of groundwater levels made it necessary to take a test on z_s^0. The tested parameters and their values are listed in Table 5.1.

We introduced anisotropy to the model (Chapter 3, Section 3.3), which allowed us to examine exclusively the sensitivity of the lateral component of K. The simulations have proved to be quite time and memory consuming. The sensitivity analysis was based only on one-year simulation of 2010.

The entire modeling outputs were studied in order to have a precise idea on how URBS-WTI reacted to changes in parameters: i) flow components in the water cycle, ii) discharge and iii) saturation depths.

For the results of i), the reference was the model base-run of initial URBS (without WTI). No observation data was available for evaluating the simulated water balance. For the results of ii) and iii), results of URBS and URBS-WTI were compared between them, and both to observation series. We also compare the model sensitivity assessed here with the study by Morena (2004), which is the only study on model sensitivity for URBS until now. But the comparison needs to be carried out with caution, as the model outputs examined in the two studies are not exactly the same. As an example, in the present study, we analyse the discharge rate in the stormwater network and compare them to observation, while Morena (2004) compared the generated total runoff (before routing in the sewer network) in different model run.

The one-factor-at-time method (Morris, 1991) was used to evaluate the influence of the parameters. This method consists of computing the model outputs by varying an input parameter individually from other parameters. The evaluation of the outputs were based on the three criteria C_b, R^2 and C_{nash}.

During the analysis, we referred to the assessment in the work of Morena (2004), which is the only study on model sensitivity for URBS until now. But this comparison was taken with caution, since the outputs examined in the present study were not exactly the same as in Morena (2004). For example, we analyzed the discharge rates in stormwater network and compared them to observation series, while Morena (2004) takes the total produced runoff and compared it with a reference modeling.

5.6.2 Sensitivity on flow components of the water balance

Figure 5.7 shows the sensitivity to each of the tested parameters of the main flow components: surface runoff Q^{nat}, Q^{str}, Q^{nat}, surface evaporation E^{surf}, transpiration TR and infiltration to sewer pipe Q^{drain}.

As seen in Figure 5.7a, the lateral saturated hydraulic conductivity K_s^{lat} influences significantly the flow components: C_b varies between -100% and more than 100% for K_s^{lat} between 1.3×10^{-8} and 1.3×10^{-4} m/s. The high sensitivity of Q^{drain} is expected, as K_s^{lat} operates directly on this flux. As for the surface runoff

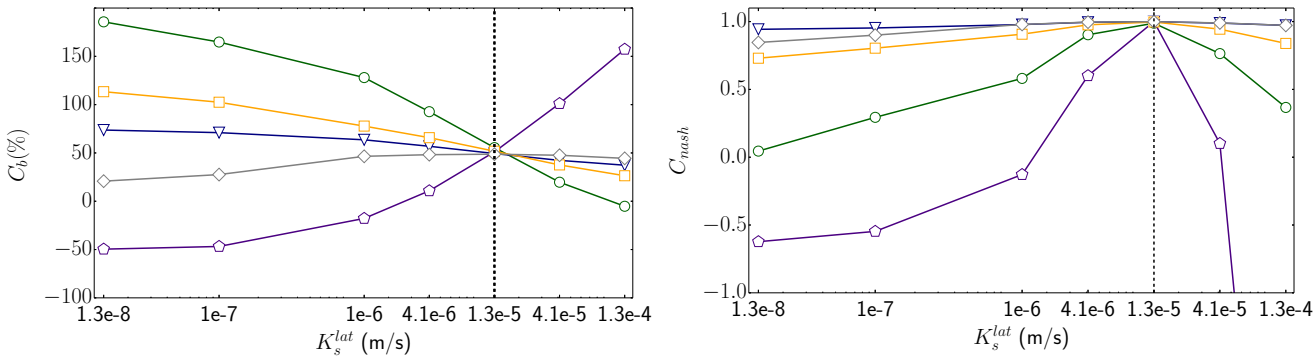

(a) Lateral hydraulic conductivity at saturation K_s^{lat}

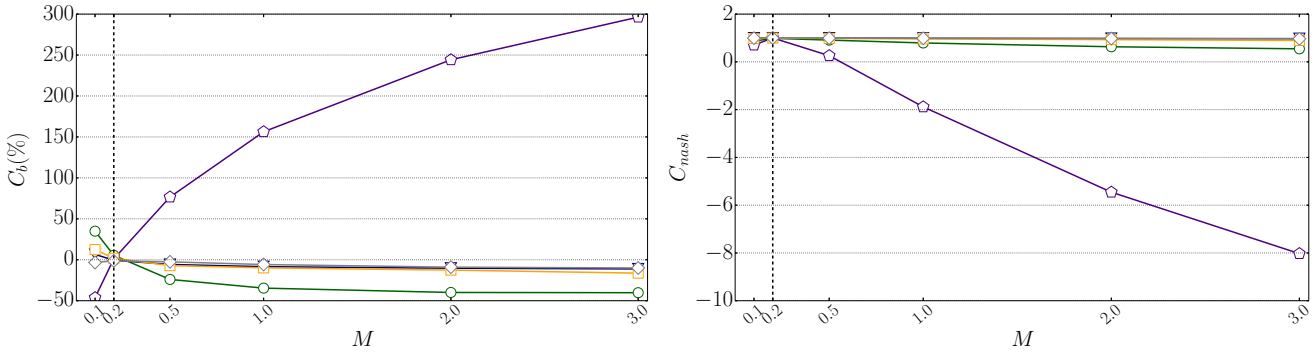

(b) Scaling parameter M

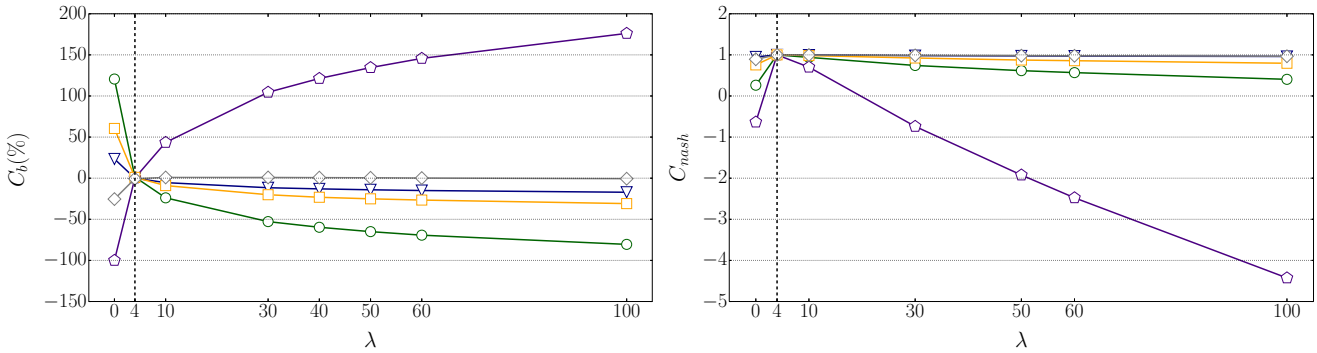

(c) Coefficient of groundwater drainage λ

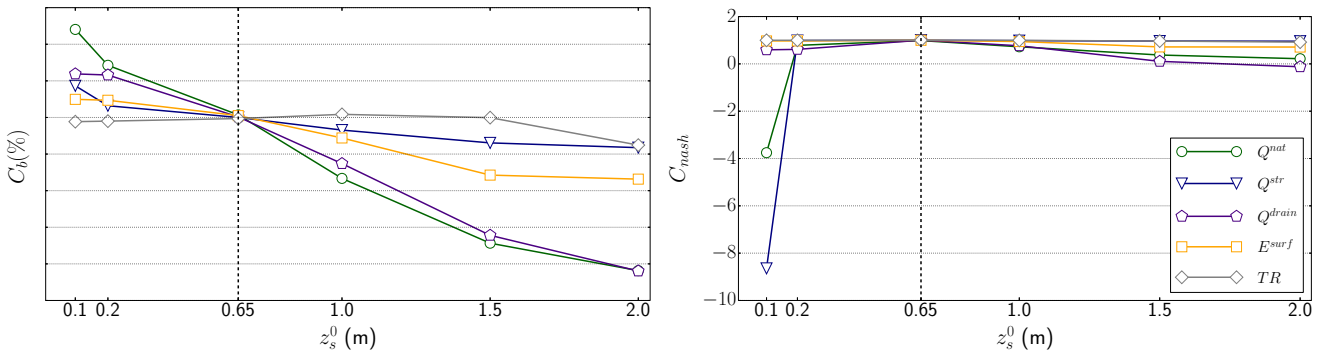

(d) Initial saturation depth z_s^0

Figure 5.7 – Sensitivity on flow components of the water balance. The reference is the simulation of URBS (without WTI) with base-run parameters. The reference value of each parameter is marked by a vertical dotted line.

and evapotranspiration, although they are not regulated directly by K_s^{lat}, they are closely interactive with lateral flux such as Q^{drain} and the WTI flux through the updating of saturation depth. For example, if storage in the vadose zone is increased and groundwater table raised due to weaker Q^{drain} (smaller K_s^{lat}), then surface infiltration will be constrained because of reduced receiving capacity of the soil, and there will be more runoff produced on land surface and more surface evaporation. At the mean time, transpiration of trees will be hold by excess storage on surface. Note that assumed by URBS, the transpiration process is activated only if land surface is dry. Q^{nat} is extremely sensitive to variation of K_s^{lat}. This could be explained by the more active interaction of natural land surface with subsoil layers compared to covered land (streets and houses).

The criteria C_{nash} is rapidly deteriorated when K_s^{lat} increases or decreases, especially for Q^{nat} and Q^{drain}. This signifies a modified K_s^{lat} is susceptible to alter greatly the original dynamics in the model, thus should be avoided or used with caution.

The parameter M has high influence on Q^{drain}: C_b varies between -50% and 300%, C_{nash} between 1 and -8 (Figure 5.7b). M is the scaling parameter of the exponential decrease of K_s with soil depth: the stronger the M, the less rapidly K_s decreases with depth. Strong values for M lead to higher average hydraulic conductivities, and vice versa. That is why Q^{drain} has a similar trend with M as with K_s^{lat}. The other fluxes do not seem very sensitive to M, except Q^{nat}, of which C_b can increase or decrease up to 40%. Morena (2004) showed that URBS was not sensible to M, in basing on simulated total produced runoff. Our results here confirm what has been found by Morena (2004), and provides a couple of further information:

- The infiltration to sewer network flux is extremely sensitive to M, compared to other fluxes.
- The apparent no-sensitivity based on total produced runoff can be caused by the balance effect of certain flows, e.g. Q^{nat} and Q^{drain}.

As with M, the coefficient of groundwater drainage λ shows less influence to the flow components, except Q^{drain} and Q^{nat} (Figure 5.7c). Here again, the two fluxes reveal an opposite trends: while Q^{drain} is enhanced by stronger λ, Q^{nat} plots a decreasing limb that counter-balances Q^{drain}. On the other hand, from a point of view of the dynamics, Q^{drain} is much more disturbed by the variation of λ compared with Q^{nat}: C_{nash} of Q^{drain} is altered much more rapidly and heavily (Figure 5.7c).

The initial condition of saturation depth z_s^0 has also substantial impacts on the flow components (Figure 5.7d). All the fluxes have a decreasing trend with increasing z_s^0, especially Q^{nat} and Q^{drain}, of which C_b vary between 40% and -80%. C_{nash} also degrades rapidly with varying z_s^0, especially for small values. Figure 5.8 plots the simulated average saturation depth of Pin Sec in 2010 against z_s^0. For z_s^0 weaker than the reference value -0.65 m, the model needs a "warm-up" period about 3 months. Beyond 3 months, the model assessed the same saturation depth. But for $z_s^0 > 1$ m, the effect of z_s^0 is not only seen at the beginning of the simulation period, but the whole time series, which confirms the great impact of z_s^0 on the simulation results. Especially when $z_s^0 > 2$ m, the model needs almost one year to "warm-up".

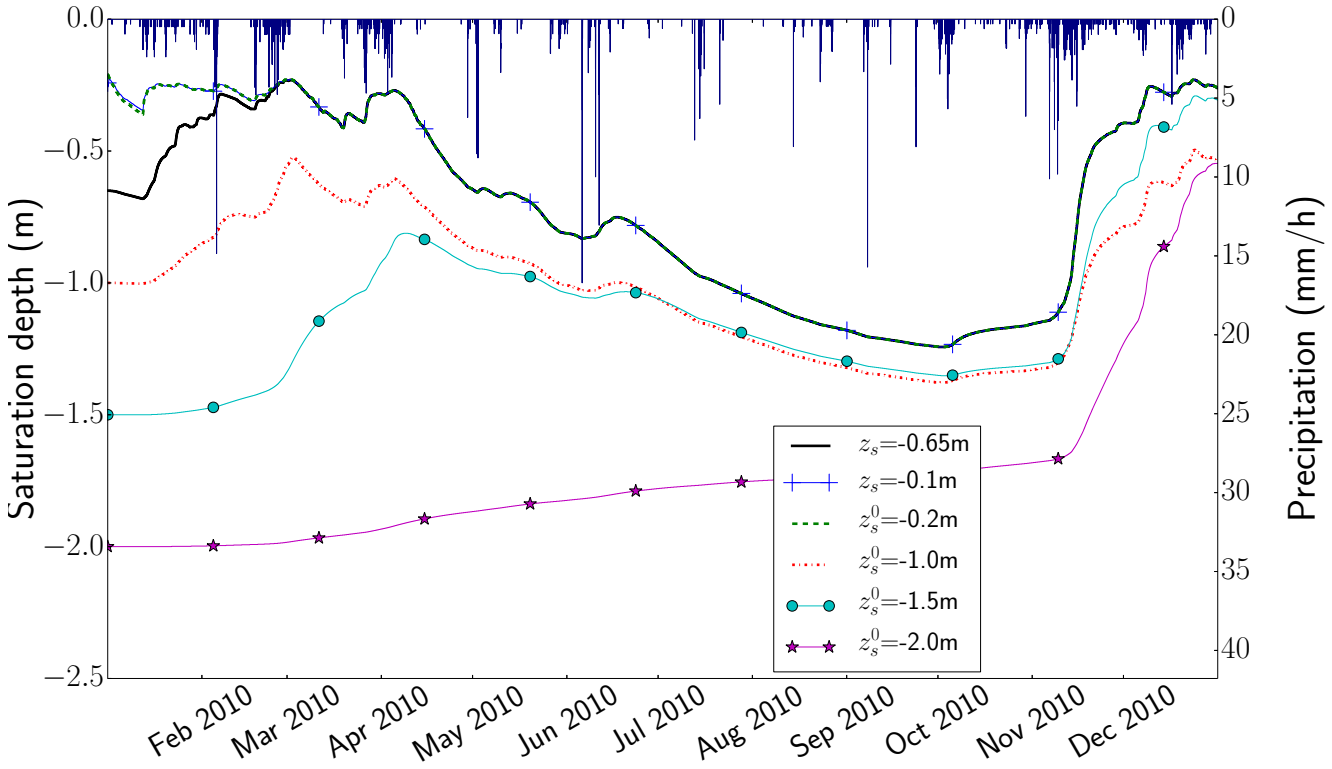

Figure 5.8 – Simulated average saturation depth of Pin Sec under different initial conditions.

A suitable value for z_s^0 for one-year simulation should be inferior to 1 m.

5.6.3 Sensitivity on discharge

Figure 5.9 plots the evolution with changing parameters of the comparison criteria between simulated and observed stormwater discharge rates. Results of both URBS and URBS-WTI are compared with observation data at the outlet of the stormwater sewer network.

The parameters by default (K_s^{lat}=1.3 × 10^{-5} m/s, M=0.2, λ=4, z_s^0=-0.65 m) can reproduce very well the total discharge volume at annual scale, with very weak bias (C_b = -2% and -0.8% for URBS and URBS-WTI respectively). R^2 and C_{nash} are less good, around 0.5 and varies in small ranges.

The discharge shows an overall non-sensitivity to K_s^{lat} (Figure 5.9a): C_b varies between -10% and 10%, R^2 and C_{nash} also vary in small ranges. This result can be in conflicting with what is shown in Morena (2004): the model is found sensitive to K_s^{nat} with a C_b varying between -15% and 70%. The curve of C_b is interesting: higher K_s^{lat} are expected to increase groundwater drainage by sewer networks Q^{drain}, but C_b shows a decreasing trend. This implies that the enhanced Q^{drain} is offset by the reduced surface runoff, which must be related to enforced infiltration and percolation (between the vadose zone and the saturated zone), signifying that the model dynamics has been increased, despite the fact that K_s^{lat} does not operate directly on vertical fluxes.

The sensitivity of discharge to M is not very high (Figure 5.9b), generally in agreement with Morena

(2004). C_b varies between -4% and 19% for M between 0.1 and 3, R^2 and C_{nash} remain constant almost. While strong M degrade the overall bias C_b, they tend to improve C_{nash}, at least for M inferior to 1. But C_{nash} is limited around 0.5, whatever the value of M. If the simulated discharge rates by URBS-WTI are slightly more sensitive to that by URBS, seen on the curve of C_b, their R^2 and C_{nash} are better than that of URBS.

C_b for the coefficient of groundwater drainage λ varies between -10% and 25%, with a monotonic decreasing limb (Figure 5.9c). But the decrease is not significant for $\lambda > 10$, which is consistent with what was found by Morena (2004). This result affirms again the counter-balance effect of Q^{drain} and Q^{nat}, as seen previously: the stronger the λ, the higher the Q^{drain}, but the weaker the Q^{nat}. R^2 and C_{nash} have the same patterns as for M, and are constrained in a narrow range of variation.

The curve patterns of the criteria for z_s^0 (Figure 5.9d) are quite similar to that of λ. C_b decreases linearly from 15% to -25% when z_s^0 increases from 0.1 m to 2 m. Deeper initial groundwater table reduces both infiltration to sewer network and runoff produced on natural surface. The overall effect of these two mechanisms is the shrinking of discharge at the stormwater outlet. R^2 and C_{nash} are not sensible to the changes of λ, with always very small variation ranges around 0.50.

5.6.4 Sensitivity on saturation depth

Figure 5.10 plots the variations to parameter changing of the comparison criteria between simulated and observed saturation depths at the piezometers. The criteria computed at the piezometers are averaged, which gives an overall performance of the model to fit the observed groundwater level. This series of modeling results serves not only to evaluate the model sensitivity, but also to calibrate the parameter values.

The saturation depths are sensible to K_s^{lat} (Figure 5.10a) and matches what was found by Morena (2004). URBS-WTI has nearly the same performance as URBS: the curves of the both are superimposed. The groundwater level are always overestimated with overall negative C_b and poor C_{nash}. The overestimation tends to be corrected by large K_s^{lat}: C_b is shifted from -78% to -65% when K_s^{lat} rises from 1.3×10^{-8} m/s to 1.3×10^{-4} m/s, R^2 from 0.67 to 0.79, and C_{nash} between -40 to -27. This implies the necessity to strengthen the WTI flow for improving the simulation quality. We limited the rise of K_s^{lat} to 1.3×10^{-4} m/s in considering the physical sense of the parameter.

The parameter M also has strong impacts on saturation depths (Figure 5.10b): C_b varies between -80% and -40%, R^2 between 0.65 and 0.90, C_{nash} between -40 and -15. The evolutions of C_b and C_{nash} are monotonic, with improved values for large M. The trend of R^2 is actually also increasing, if we ignore the weak fluctuations for $M > 1$. Note that Morena (2004) showed that M had little impact on the simulation of saturation depths at the UHE scale.

As mentioned before, strong M lead to strong mean hydraulic conductivity and subsequently enhance the simulated fluxes. Looking at the curves of the criteria for K_s^{lat} and M, it assumes that the fluxes computed need to be strengthened to improve the model performance in modeling groundwater levels.

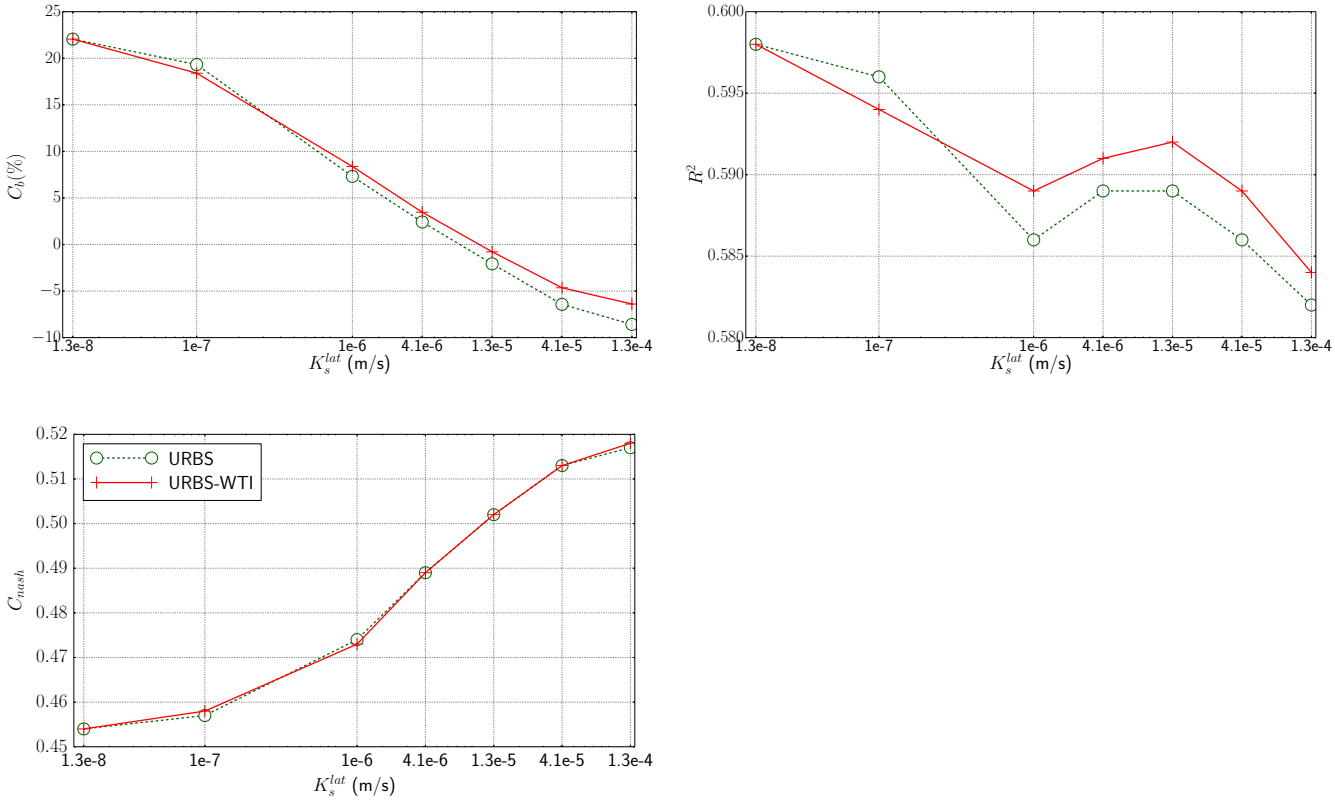

(a) Lateral hydraulic conductivity at saturation K_s^{lat}

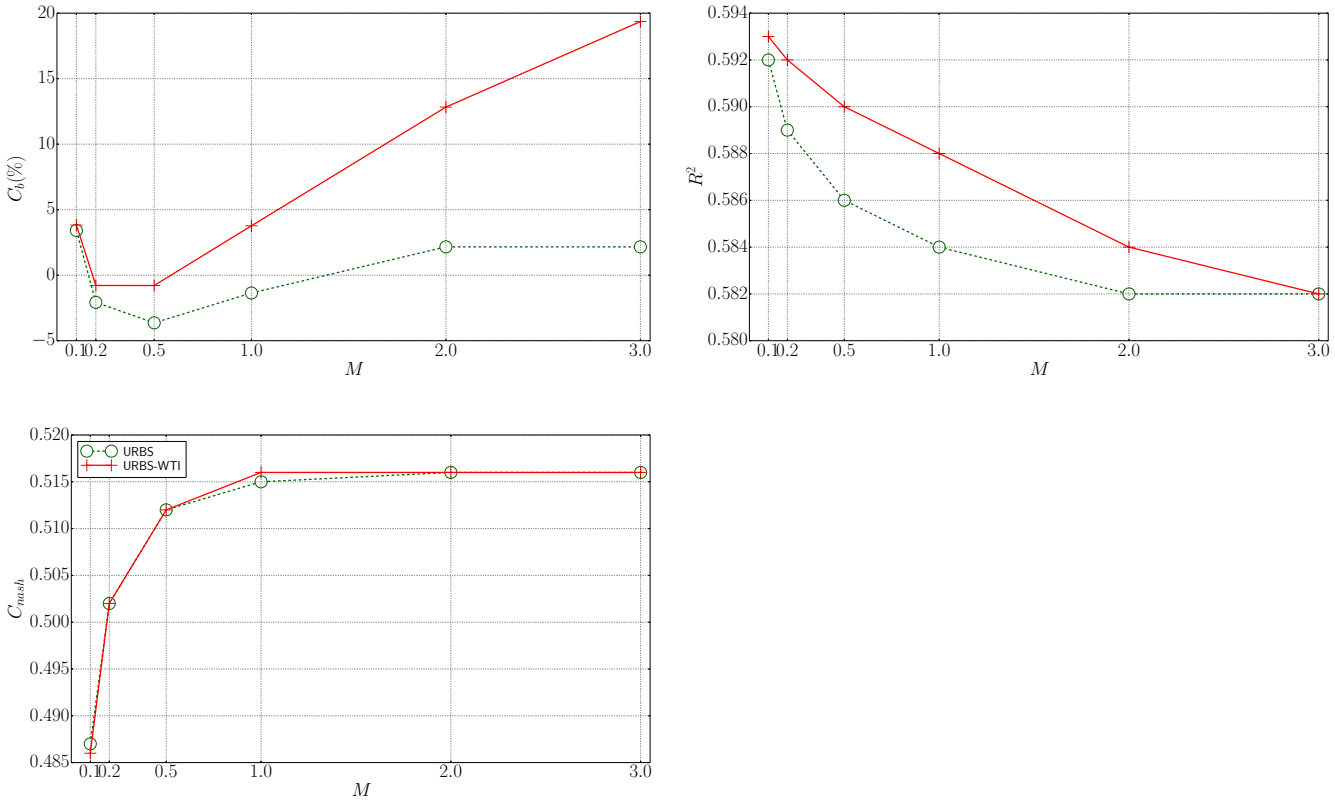

(b) Scaling parameter M

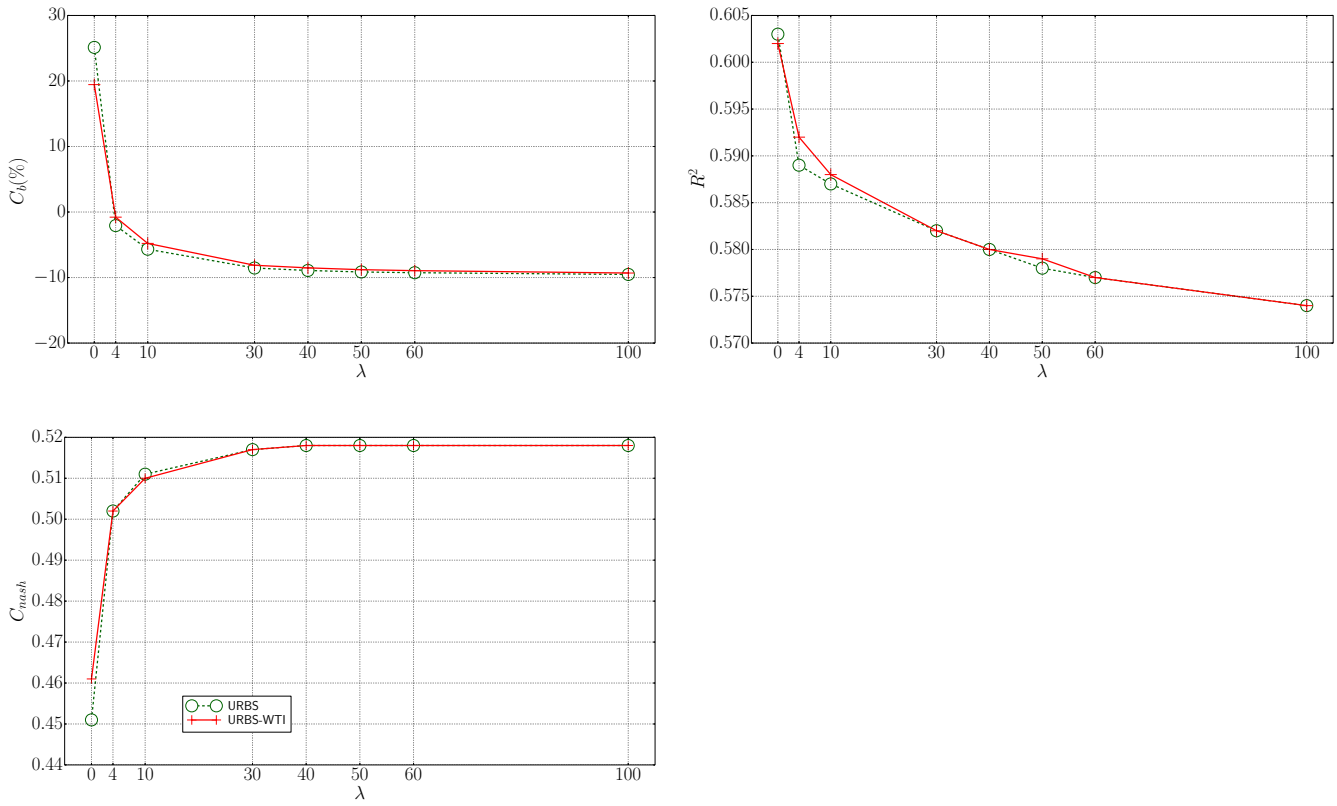

(c) Coefficient of groundwater drainage λ

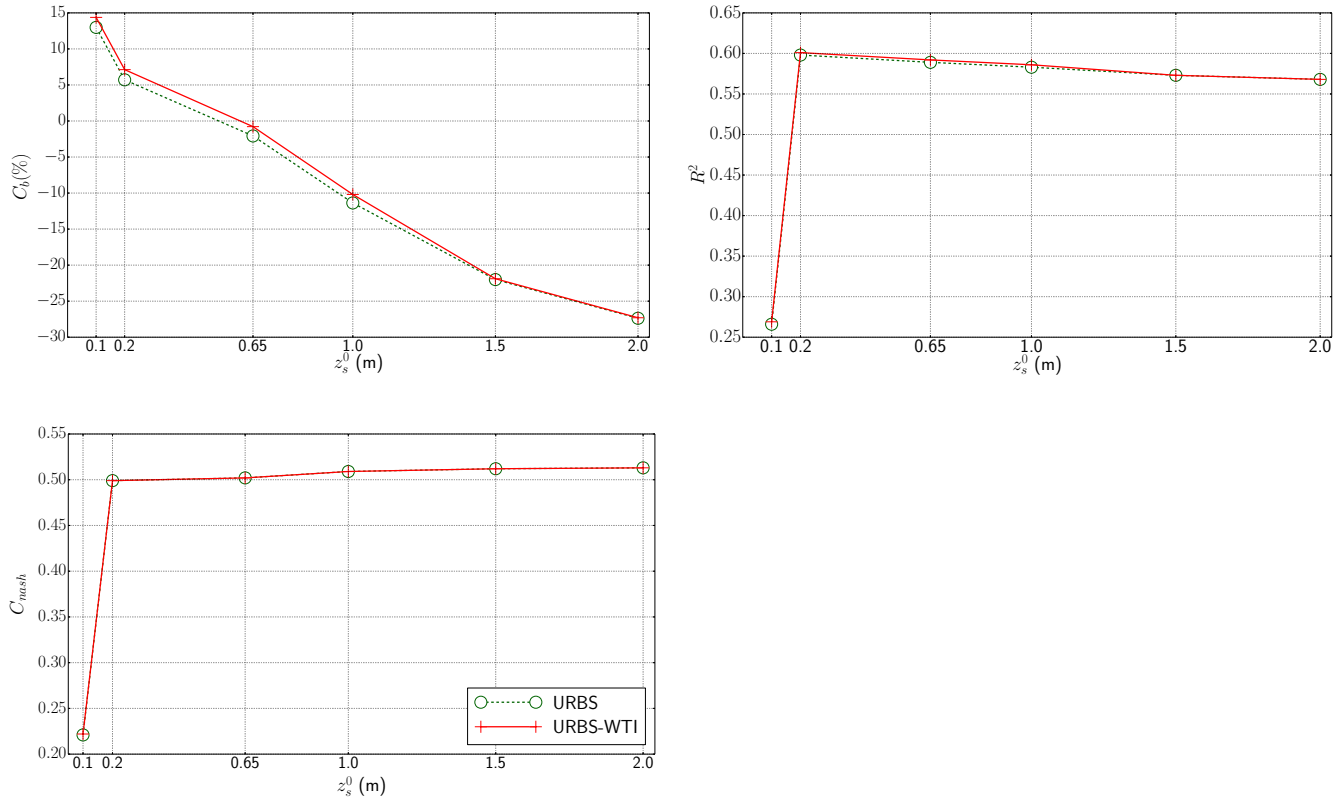

(d) Initial saturation depth z_s^0

Figure 5.9 – Sensitivity on discharge. The reference is observation series of stormwater drainage network.

The curves of λ (Figure 5.10c) confirms this hypothesis: simulation quality gets better when λ rises, enforcing the infiltration flux to sewer Q^{drain}. It confirms also the importance of the drainage process, declared by Morena (2004) and Rodriguez et al. (2008).

Deeper initial conditions z_s^0 lead to better C_b and C_{nash} (Figure 5.10d), but degrade drastically R^2. As a matter of fact, with $z_s^0 > 1.5$ m, the simulated saturation depths lose their temporal variations and remain constant during the simulation period (curves not shown here).

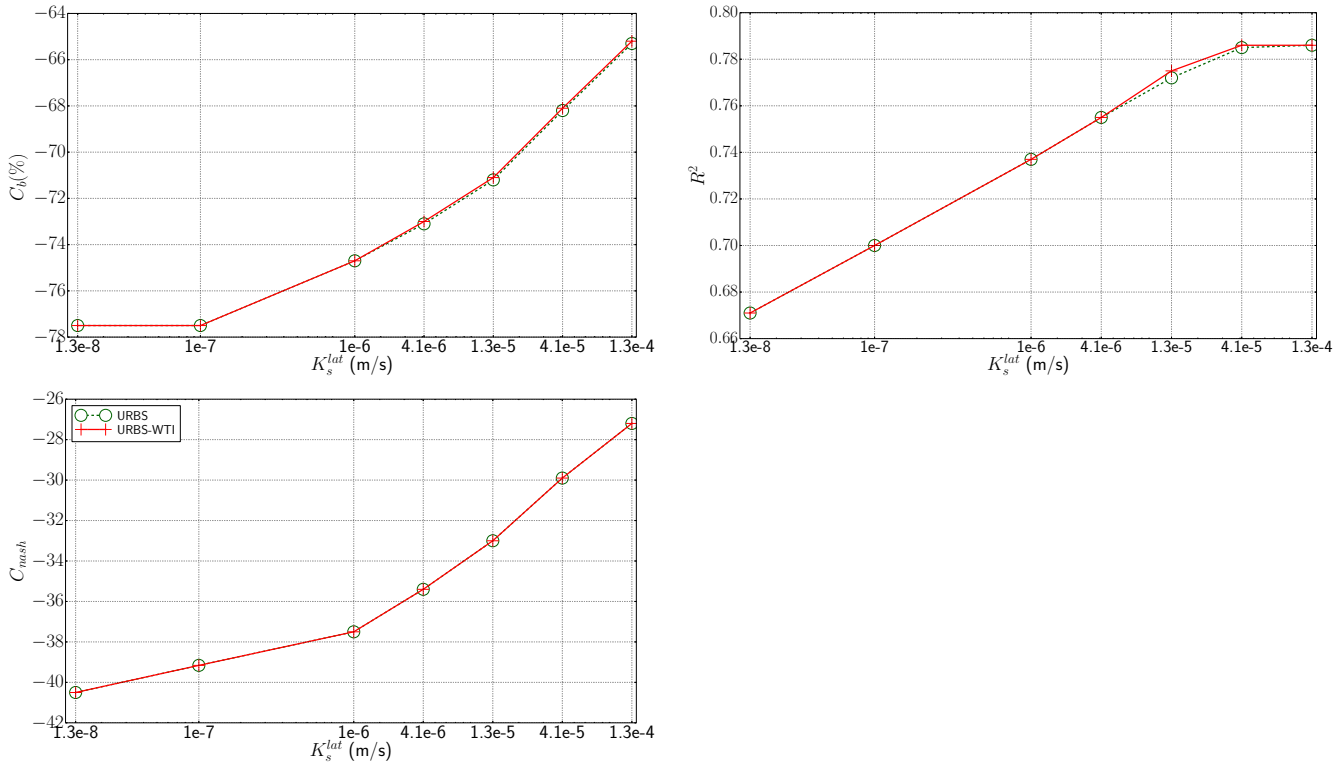

(a) Lateral hydraulic conductivity at saturation K_s^{lat}

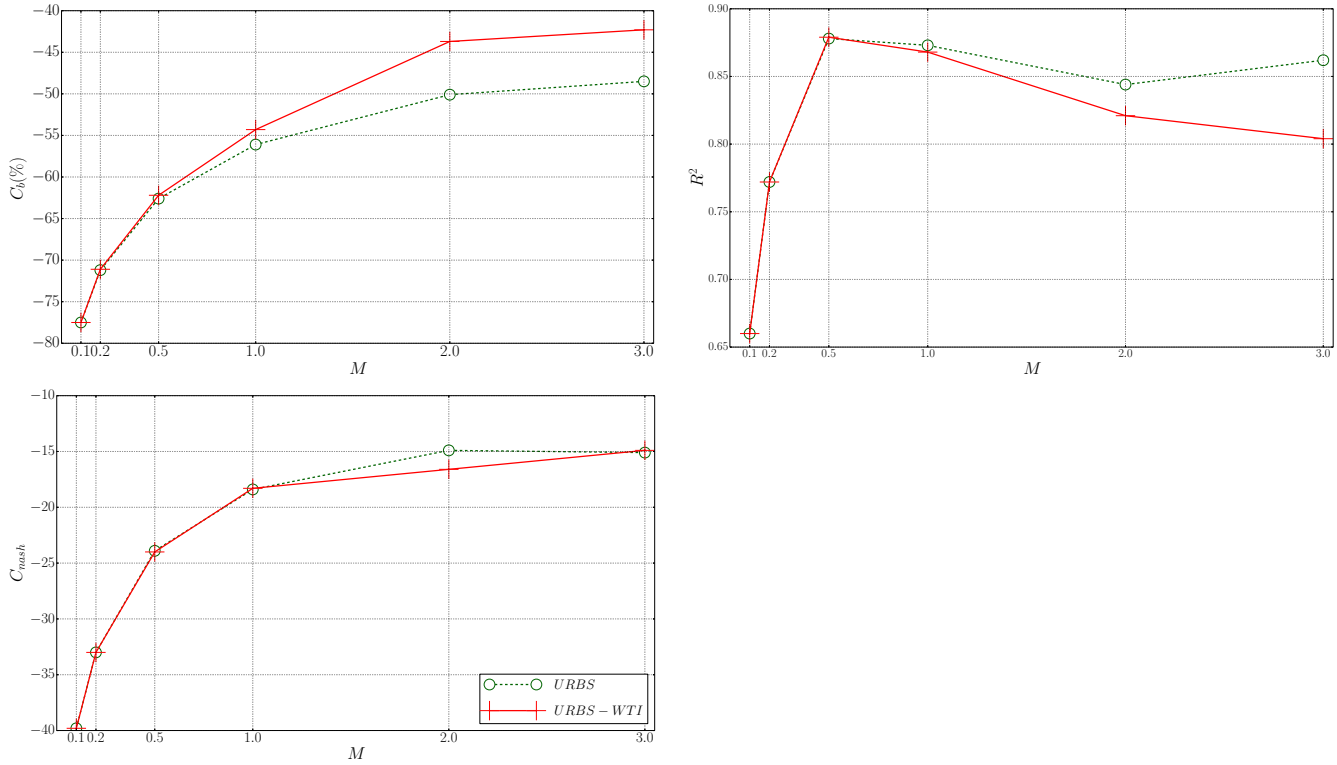

(b) Scaling parameter M

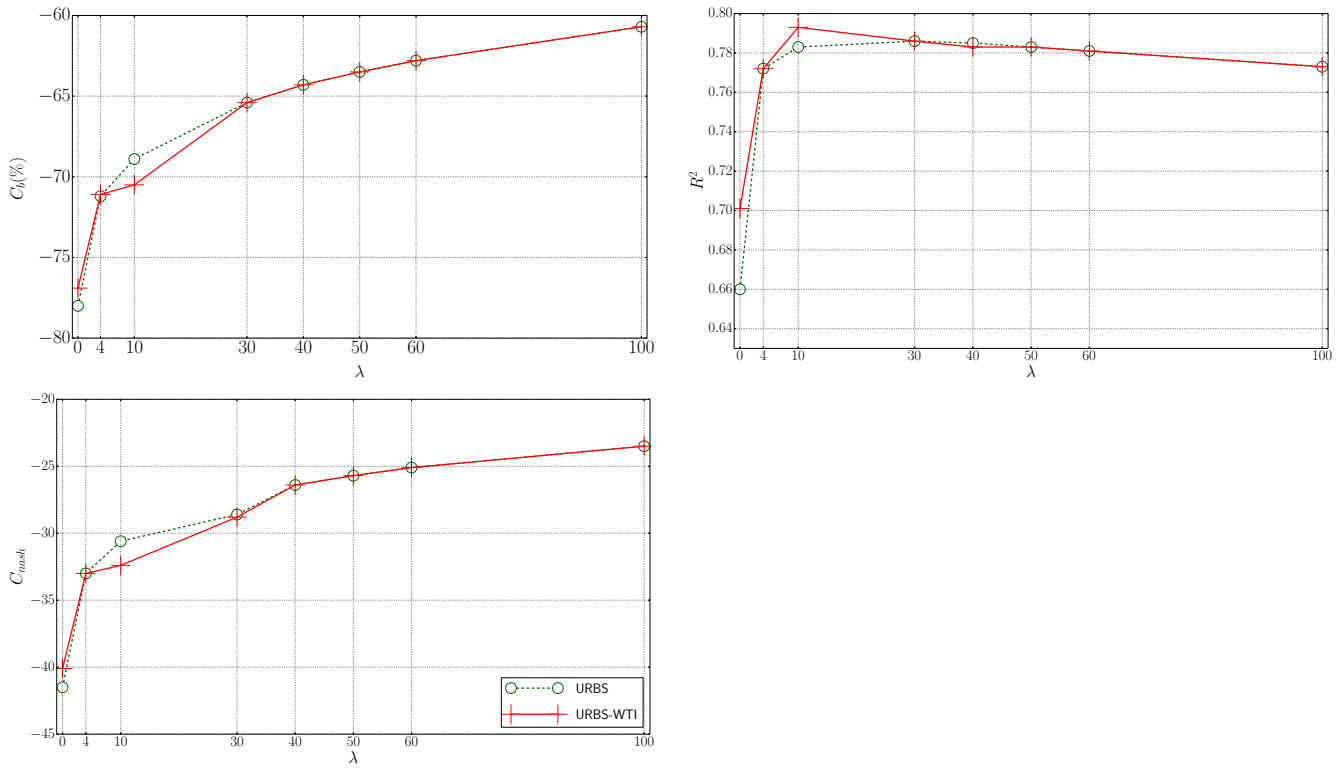

(c) Coefficient of groundwater drainage λ

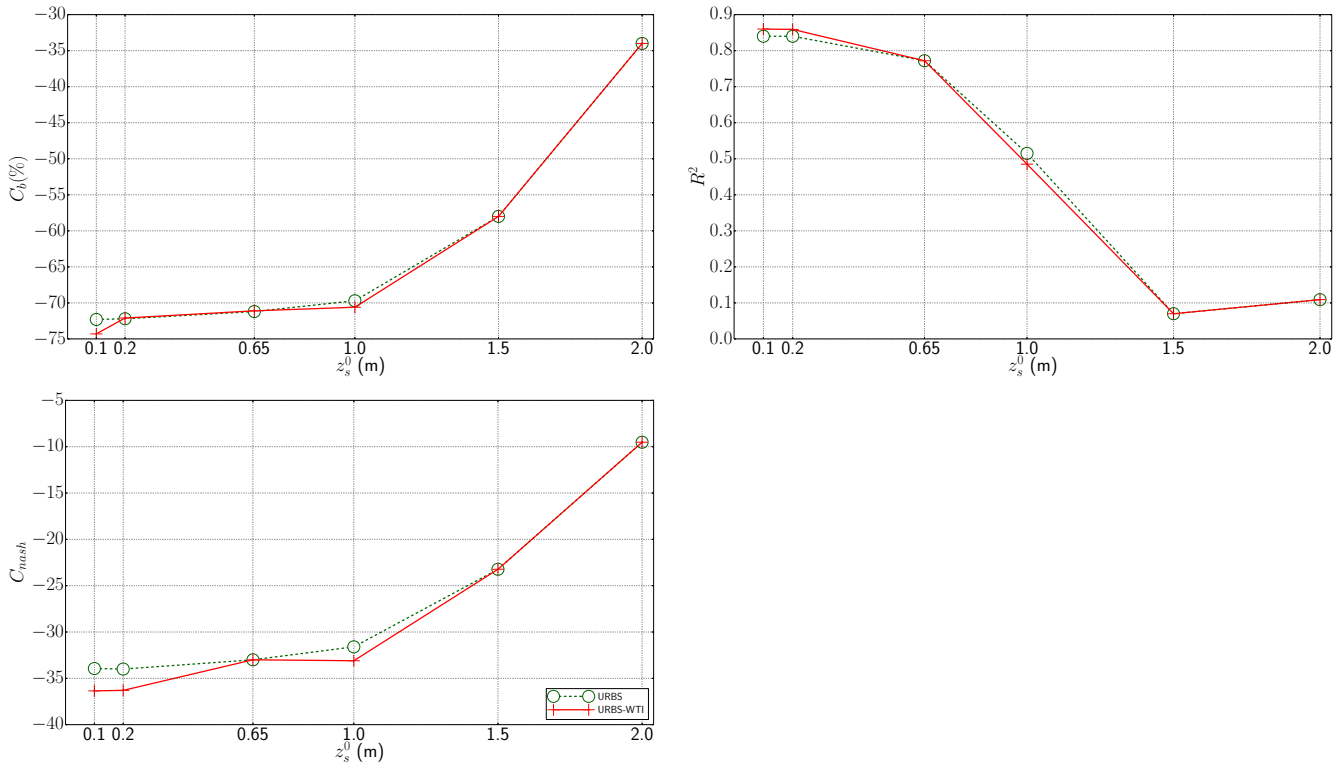

(d) Initial saturation depth z_s^0

Figure 5.10 – Sensitivity on saturation depth. The reference is the observation series at the piezometers.

5.6.5 Summary and discussion

During the sensitivity analysis for the integrated model URBS-WTI, physical parameters that operates directly on the WTI module, K_s^{lat}, M and λ, were tested, as well as the initial saturation depth of the catchment z_s^0. This study had three main objectives, as being to:

1. evaluate the model sensitivity to these parameters and if it was changed by the WTI module.
2. calibrate manually the parameter values.
3. see the extent to which the WTI module can improve the model performance, in particular to the simulation of groundwater levels.

For evaluating the sensibility of URBS-WTI (Objective 1), a series of modeling outputs were explored including flow components in the water balance, discharge at the catchment outlet and groundwater levels. The results of both URBS and URBS-WTI were examined and compared. For calibrating the model (Objective 2) and estimating the role of WTI on model performance (Objective 3), three comparison criteria, C_b, R^2 and C_{nash}, were computed between simulated and observed series for each model run.

Looking at the overall results, the model sensitivity is not impacted by the WTI module. This assures us that the WTI module does not affect the general model behaviour. Water balance was systematically examined, which afforded an insight into what was really happening in the model with each parameter change. This is crucial for understanding the behaviour of the model (module), especially when groundwater is dealt as an integrated compartment. The water balance established in this study could serve as a reference for future study of URBS. All the tested parameters proved to have great impact on the water balance, especially on the runoff on natural surface Q^{nat} and groundwater drainage by sewer networks Q^{drain}. These two fluxes have, in most of the case, an opposite trend with the varying parameter (except for z_s^0), thus can neutralize the overall change in the flow balance. Examining solely the total runoff over the catchment would easily lead to the conclusion that the water balance is not much impacted by parameter change, although it is just one part of the story. Other flow components (Q^{str}, E^{surf} and TR) are less reactive to the parameter values, and it seems that the model dynamics is dominated by Q^{nat} and Q^{drain} on the study case of Pin Sec.

In terms of discharge, continuous simulated flow rates at the outlet of stormwater network were compared with measured data. The most sensible parameters were K_s^{lat}, M and z_s^0; λ impacted the discharge simulation in a less extent. The modeled discharge volume fits well the observation with weak overall bias C_b. R^2 and C_{nash} were weak. Note that the Nash coefficient is very sensitive to the time step. The 6-min time step assigned here is not favorable.

Previous study on model sensitivity made by Morena (2004) was referred to during the study. Since the examined outputs were not exactly the same in the two studies, it was not always possible to realize meaningful comparisons. In confirming certain points claimed in Morena (2004) and questioning some others, the present study offers supplementary information about the model behavior.

Even the main objective was to evaluate WTI, studying the module in an isolated way was not only technically arduous (linked to model structure) but also inadequate: we believed that supervising the entire modeling outputs was essential during the module implementation in order to assure that it did not bring much side-effect to other processes.

The study on saturation depths served both for analysing model sensitivity and for calibrating the parameter set. The simulated saturation depths showed high sensitivity to K_s^{lat}, M and λ, not to z_s^0 when this is inferior to 1 m. When z_s^0 was set deeper than 1 m, the model was no longer able to replicate the temporal variation of the groundwater levels.

Since the modeling of discharge rates is not impacted greatly by the parameters, the model calibration was based mainly on the saturation observation. But it is not always easy to observe clear trends of the simulation quality. For example, while strong values for M and λ improve C_b and C_{nash}, R^2 shows an opposite trend. There seems to be a balance effect between "magnitude" and "dynamics": if a change in parameter tends to get closer the simulated level to observed level, it may erase the dynamics and give flat curves.

On the other hand, since the analysis on parameters was conducted with a one-factor-at-time method, saying that the best parameter set is the combination of the best value of every parameter in a logic of "1 + 1 = 2" can be rash: if two parameter changes can both improve the simulation quality by impacting the modeled fluxes in a similar way or in an opposite way, their coupling can possibly lead to an over-correction or an offset. For example, high values of K_s^{lat} and z_s^0 correct both the overestimation of groundwater levels, but the combination of a large K_s^{lat} and a large z_s^0 will lead to an underestimation.

Another difficulty lays in the heterogeneity in the piezometric observations, linked probably to the complexity of urban land. During our test, amelioration of simulation on certain piezometers was always at the detriment of the others: the most suitable parameter is not the same for all the observed series. Distributing spatially the parameter values into the UHEs could be a valuable subject for future development of the model.

For the reasons above, the tricky work of defining the "best" parameter set obliged us to make a choice. Basically, we based on the criteria on groundwater levels in considering the physical sense of the parameters and without ignoring the water balance and discharge. The calibrated values are shown in Table 5.5.

A regrettable result is that the WTI module did not show much effect, despite the numerous tests that have been undertaken. The overall impression that we have is that the WTI flux is not intense enough facing other fluxes, especially vertical fluxes by climate forcings. At the mean time, the plots are the average of the piezometers, and are maybe not the most suitable criteria for evaluating the WTI module. Thus, it makes sense to do a calibrated model run with the selected parameter sets and see what happens.

Table 5.5 – Calibrated parameter values for Pin Sec by sensitivity study.

Parameter	Unit	Initial	Calibrated
K_s^{lat}	m/s	1.3×10^{-5}	1.3×10^{-5}
M	-	0.2	2
λ	-	4	30
z_s^0	m	-0.65	-2.0

5.7 Calibrated modeling on the Pin Sec catchment

A calibrated modeling for the Pin Sec catchment was conducted with the calibrated parameter (Table 5.5). Since the parameters were calibrated on 2010, the calibrated modeling was carried on the unique year of 2010, considering the quality of the data sets beyond this period. This one-year period might be too short to show long-term trends of the hydrological variables, but it allowed to make comparisons between the model base-run and the calibrated modeling.

5.7.1 Saturation depth

Given the fact that the parameter calibration has been based on the simulation of groundwater levels, this result is firstly examined for the calibrated run. Figure 5.11 plots the simulated saturation depths both by URBS and URBS-WTI against observation data. The assessed criteria values are given in Table 5.6.

Compared to the base-run, the quality of groundwater level simulation is remarkably improved: if the simulated series still do not fit completely the observed ones, the previous over-estimation has been reasonably corrected.

In looking more closely, we can distinguish several cases:

- For Pz3 and Pz5, the simulation curves suite quite well the observation curve, both in magnitude and temporal evolution. While the WTI module (dotted line, triangle marker) tends to raise the groundwater level at Pz3 (discontinued line, circle marker), it shows an inverse tendency at Pz5.

- Variations at Pz8 is also relatively well reproduced by the models, if we ignore the abrupt limbs in the curve, which can be seen as an “atypical” piezometric behaviour. The simulated curves fit well the observed level during the wet half of the year (November - May), but are less good during the dry season, where the model can not predict the lowering of the groundwater table. The curve of URBS-WTI seems to slightly better fit the observation curve than that of URBS.

- Pz1, Pz4, Pz6 and Pz7 remain to be overestimated by the models. But the WTI module is able to slightly correct this problem: compared the curves of URBS, that of URBS-WTI are closer to observation. Pz1 is over initiated, and this over-initiation has not been corrected during the

simulation period. The initial levels of Pz4, Pz6 and Pz7 are approximately equal to, or lower than the measured levels, but their decreasing limbs during dry season are not reproduced by the model.

The comparison criteria confirm the better performance of the calibrated model: C_b is reduced from -71% to -14% and -8% for URBS and URBS-WTI respectively, C_{nash} are also much better than the base-run, though remain negative. But R^2 are reduced, implying that the model dynamics are less predicted by the calibrated run than the base-run. The module WTI seems to, however, be able to mitigate this deterioration.

Generally speaking, the dynamics simulated by the model are weaker than the observation: the magnitudes of variation seen in the observation curves are not all predicted by the model. Certain piezometers show relatively abrupt variations. This could be due to local soil characteristics (compactness, materials, ...), which are highly variable in urban settings, and to possible preferential flow paths in the soil, which are not represented in the model.

Compared to the sensitivity analysis, the WTI module shows much more significant impacts. Except Pz2 for which URBS-WTI and URBS give exactly the same results, the simulated series by URBS-WTI are, to a greater or lesser degree, different to that by URBS. The comparison criteria of URBS-WTI are also better than that of URBS.

Table 5.6 – Comparison criteria (mean) between simulated and observed groundwater levels at the piezometers for the period of 01/01/2010 - 31/12/2010, by the calibrated model of URBS and URBS-WTI.

		C_b (%)	C_{nash}	R^2
base-run	URBS	-71	-33	0.77
base-run	URBS-WTI	-71	-33	0.77
calibrated	URBS	-14	-4.5	0.64
calibrated	URBS-WTI	-8	-2.9	0.72

We plotted the standard deviation of the simulated groundwater level σGWL for the calibrated modeling. Compared to the base-run (Figure 5.6), groundwater levels seem less influenced by climate forcings, with smoother trend, explained perhaps by deeper groundwater level. URBS-WTI shows different behaviors from URBS: if there remain some peaks in the curve of URBS as reply to rainfall, these curves are not observed at all in the curve of URBS-WTI.

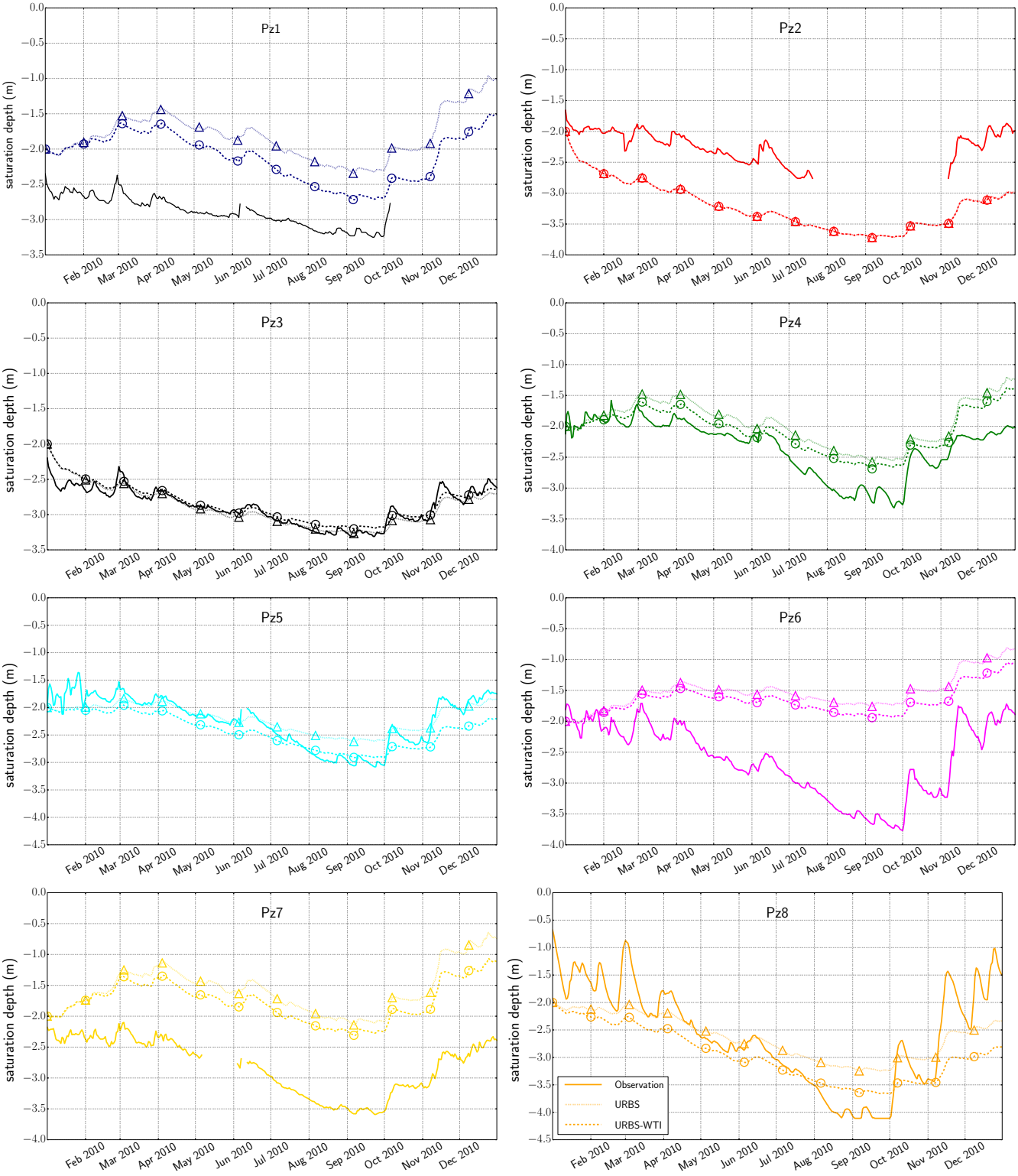

Figure 5.11 – Simulated groundwater level series by model calibrated-run for the year 2010. Both the results of URBS (triangle) and of URBS-WTI (circle) are depicted and compared with observed series.

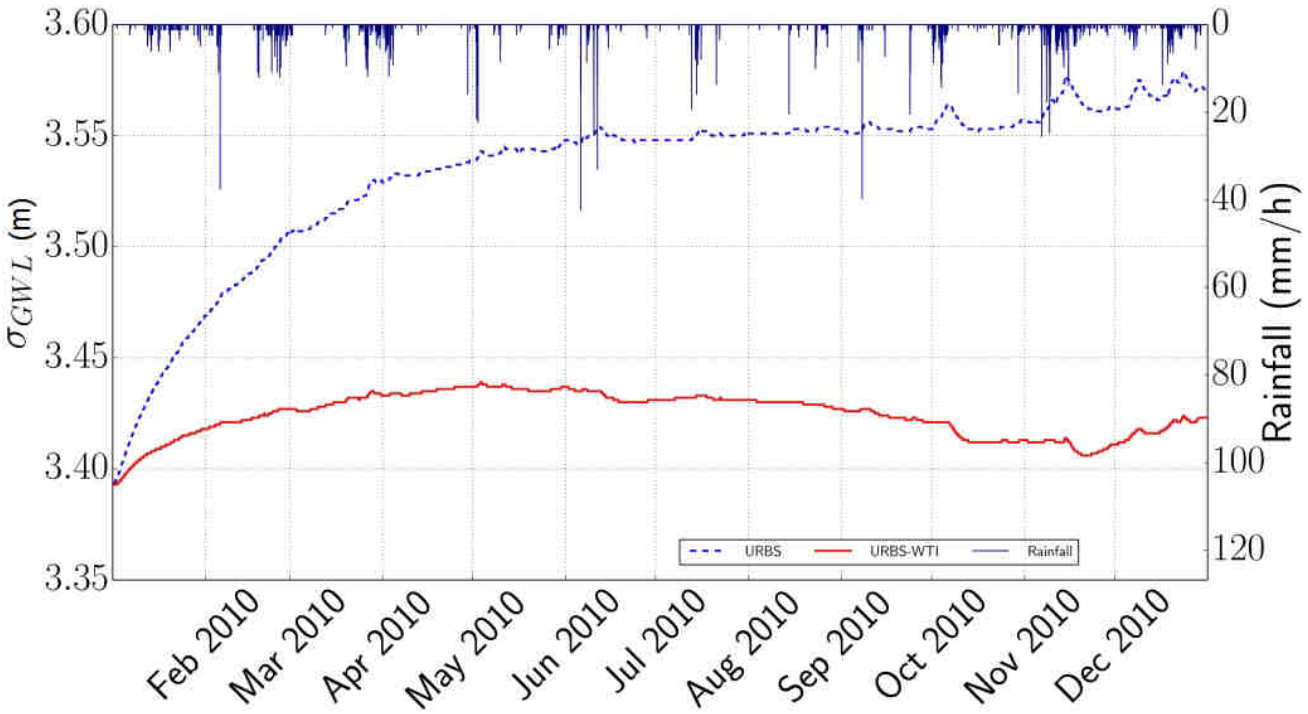

Figure 5.12 – Standard deviation of the simulated groundwater level series of Pin Sec by model calibrated-run for the year 2010.

5.7.2 Water balance

We then examined the water balance and discharge assessed by calibrated modeling of URBS and URBS-WTI (Table 5.7 and 5.8). The two major fluxes, Q^{nat} and Q^{drain} have been largely modified compared to the base-run: Q^{nat} is reduced from 8.0% to 0.4% of the total rainfall, Q^{drain} is raised from 8.4% to 30.9%. The percentage of groundwater drainage by sewer networks is consistent with the results obtained in an observation study on the Pin Sec catchment (Rodriguez et al., 2013). Linked to the deeper groundwater table, the evapotranspiration ($E + TR$) is also reduced.

Table 5.7 – Simulated water balance of Pin Sec by model base-run and calibrated run of URBS and URBS-WTI for the period of 01/01/2010 - 31/12/2010. All the flow and storage components are expressed in percentage of total rainfall.

		Q^{hou}	Q^{str}	Q^{nat}	Q^{drain}	E	TR	Δstorage	P
base-run		16.7	12.8	8.0	8.4	8.9	40.5	4.4	100
calibrated	URBS	16.7	10.3	0.1	27.9	5.7	31.9	6.8	100
calibrated	URBS-WTI	16.7	10.3	0.4	30.9	5.9	31.3	4.1	100

5.7.3 Discharge

Table 5.8 shows the comparison criteria on continuous flow rates at the stormwater network's outlet given by calibrated modeling of both URBS and URBS-WTI, compared to that of the model base-run. C_{nash} are improved compared to base-run, while R^2 are degraded. But both the improvements and the deteriorations are slight. The remarkable difference locates in the values of C_b. Compared to base-run, the models gave less better simulation on the continuous flow rates with higher values of C_b. The deterioration by URBS, -7.58%, is however remarkable.

Table 5.8 – Comparison criteria between simulation and observation on continuous discharge rates at the stormwater network outlet of Pin Sec for the period of 01/01/2010 - 31/12/2010, by the calibrated model of URBS and URBS-WTI.

		C_b (%)	C_{nash}	R^2
base-run	URBS	0.20	0.502	0.589
base-run	URBS-WTI	0.21	0.502	0.592
calibrated	URBS	-7.58	0.562	0.515
calibrated	URBS-WTI	-0.93	0.567	0.516

5.8 Forcing of the WTI module

In looking at the results of the sensitivity analysis and of the calibrated model, we had a feeling that the horizontal saturated flow modeled by the WTI module was too weak to allow the module to show its impacts. However, the results of the calibrated modeling gave us some promising signs of the possibility for WTI to improve modeling qualities. For this reason, we made a test of forcing manually the WTI flow, by introducing a coefficient C_{WTI} into the equation of the WTI flow (Equation 3.4).

We started with C_{WTI}=100. The saturation depths were better simulated: for some of the piezometers, the simulated curves were brought closer to observed ones compared to the calibrated modeling. Then we tried a range of values from 30 to 700 for the coefficient, and found that this could greatly influence the simulated saturation depths.

The "best" C_{WTI} is different along with the piezometers. Figure 5.13 plots the simulated curves by the best set of values for C_{WTI} (see the legend of the figure).

Table 5.9 – Comparison criteria (mean) between simulated and observed groundwater levels at the piezometers for the period of 01/01/2010 - 31/12/2010, by the manually forced WTI module.

		C_b (%)	C_{nash}	R^2
calibrated	URBS	-14	-4.5	0.64
WTI forcing	URBS-WTI	-3	-0.26	0.75

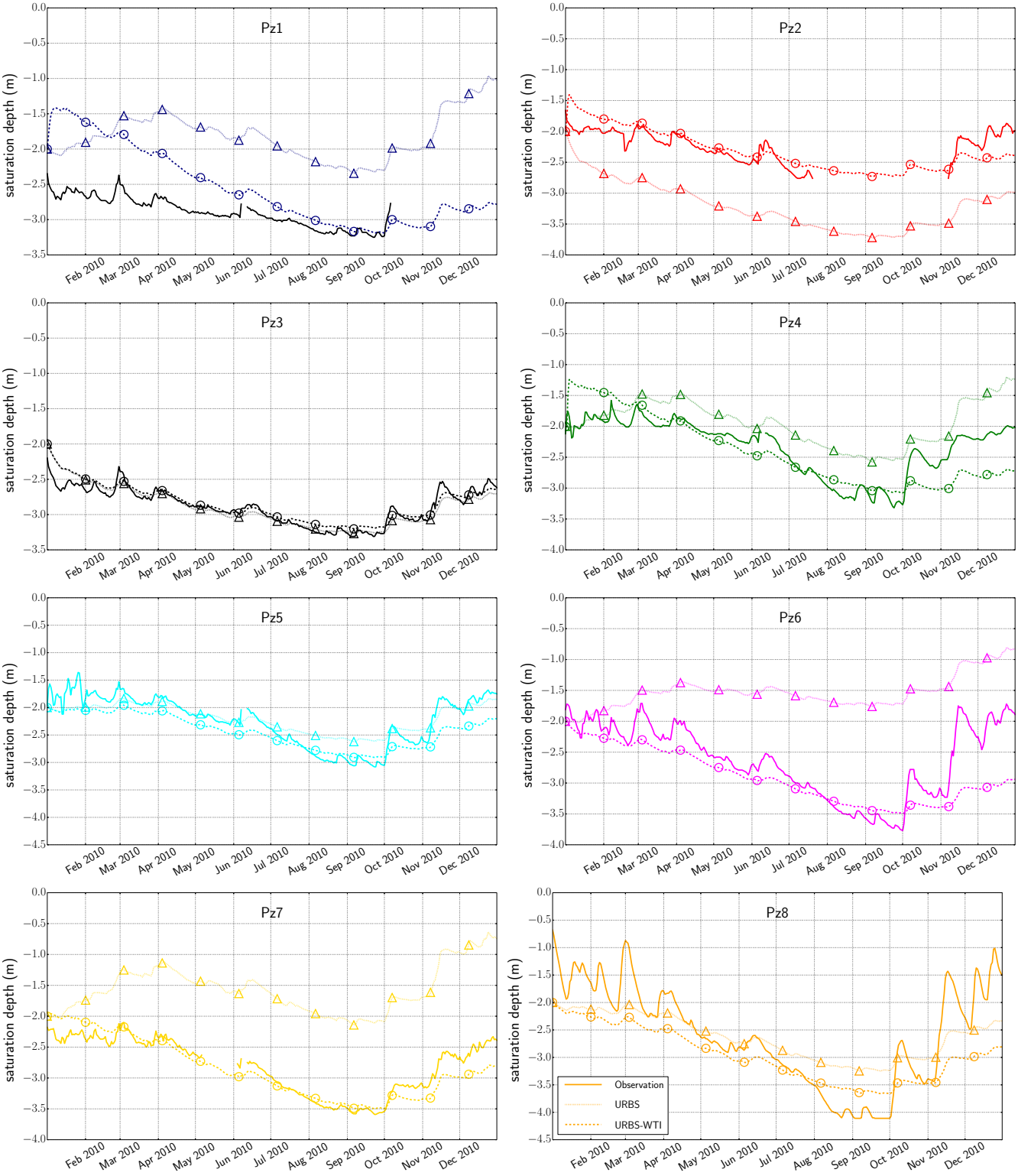

Figure 5.13 – Groundwater level simulated during the supplementary test with a coefficient for the flux WTI. The "best" value of the coefficient is variable according to piezometer: 500 for Pz4; 300 for Pz2, 200 for Pz1, 30 for Pz6 and Pz7; 1 (calibrated run) for Pz3, Pz5 and Pz8.

For Pz1, even if the simulated groundwater level remains higher than the observation during several months at the beginning of the simulation period, it lands finally at a level that is very closer to the observation. For Pz2, Pz6 and Pz7, the results are much better than the calibrated modeling. For Pz4, of which the results of the calibrated modeling were already relatively good, we observed still an improvement. For Pz3, Pz5 and Pz8 where the calibrated run gave already relative good results, there is no need enforce the WTI flow. This reflects the highly variable soil characteristics in space, which is a specificity of urban areas. Table 5.9 shows the average criteria values assessed with the best coefficient values of each piezometer, compared with the calibrated run by URBS. All of the three criteria have been improved.

The value of C_{WTI} which gave a general best performance is 500. Figure 5.14 shows the evolution with time of the standard deviation of simulated groundwater levels σGWL with the C_{WTI} equal to 500. Compared to URBS, URBS-WTI reduces significantly σGWL with the strengthened WTI flow, starting from a certain moment after a period of model warm-up.

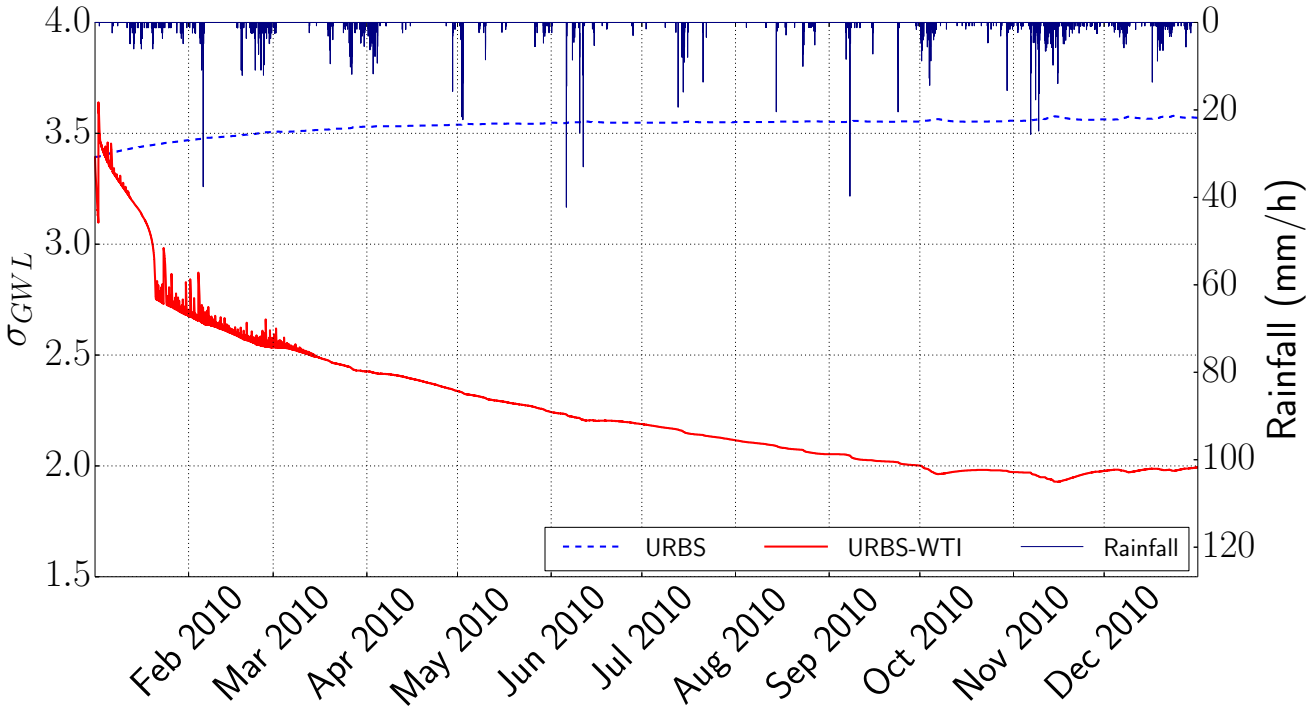

Figure 5.14 – Standard deviation of simulated groundwater level (elevation in the NGF system) of the Pin Sec catchment by for the period of 01/01/2010 - 31/12/2010, by the test with a coefficient of 500 on the WTI flow.

We examined the simulated discharge rates and water balance with C_{WTI}=500 (Table 5.10). As seen from Table 5.10a, the modeling of discharge is not much changed with C_{WTI} compared to that of the calibrated URBS-WTI. But the water balance is more different (Table 5.10b). Both surface runoff on natural surface Q^{nat} and groundwater drainage by sewer networks Q^{drain} are greatly increased, equaling

to 10.7% and 54% of the total rainfall respectively. Groundwater table is much lowered with Δstorage = -32% of P. As a result of the groundwater table lowering, TR is notably reduced.

Apparently, the model needs to release a large quantity of water out of the modeling domain (catchment) in order to correctly predict the observed groundwater levels. Without C_{WTI}, this has not been able to be realized. With C_{WTI}, the WTI flux have been strengthened, which has led to a general increase in the model dynamics. Thanks to this increased model dynamics, the model has successfully released the quantity of water, by Q^{nat} and Q^{drain}, that was necessary for lowering the groundwater level in order to approach the observations. This questions about the zero-flow boundary conditions for groundwater flow that we have assigned to the catchment, especially for the downstream border (south-east): The quantity of groundwater flowing out of the modeling domain is maybe not negligible, as we presumed. The fact that we restrain the groundwater flow between the modeling domain and its outside leads to a cumulation of groundwater at the south-eastern border of the catchment, reason for which groundwater levels have always been overestimated. This statement can be confirmed by the curves of Pz7 that locates at the vicinity of the south-eastern border. However, estimating the groundwater flow out of (or into) the catchment is complicated due to insufficient available information. Rodriguez et al. (2013) have given an estimation of 0.023 mm/day, which should be non-significant in front of vertical fluxes.

Table 5.10 – Modeling of flow rates (a) and water balance (b) with the coefficient of 500 on the WTI flow.

(a) comparison criteria on continuous flow rates at the stormwater network's outlet.

		C_b (%)	C_{nash}	R^2
calibrated	URBS	-7.58	0.562	0.515
calibrated	URBS-WTI	-0.93	0.567	0.516
	$500 \times Q^{wti}$	-4.45	0.538	0.495

(b) water balance

	Q^{hou}	Q^{str}	Q^{nat}	Q^{drain}	E	TR	Δstorage	P
URBS	16.7	10.3	0.1	27.9	5.7	31.9	6.8	100
URBS-WTI	16.7	10.3	0.4	30.9	5.9	31.3	4.1	100
$500 \times Q^{wti}$	17.1	15.4	10.7	54	6.8	27.3	-32	100

Another error origin may be related to the leak of water main. The quantity of leak is estimated to be 10% of total annual rainfall for the year 2010 Rodriguez et al. (2013). This process is not simulated in the model. There may also be other unknown sources of groundwater recharge, such as irrigation of gardens and parks, of which the information is not available.

This test confirms our hypothesis that the module performance of WTI can be improved by the introduction of parameters. Although the results are delightful, the question of the physical signification of C_{WTI} needs to be addressed. It is supposed that the spatial heterogeneity of soil properties has a link

with this. The boundary condition for soil flow also needs to be further studied.

Summary and conclusion

In this chapter, the model URBS with the saturated WTI module integrated has been applied on the experimental urban catchment of Pin Sec. The modeling was carried out continuously for the 5-year period of 01/01/2006-31/12/2010 at 5-min time step. The entire work contained three stages: (i) model base-run, (ii) sensitivity analysis and model calibration; and (iii) model calibrated run. All analysis of modeling outputs was based on comparative approaches, including comparison between simulation series and observation series, comparison between new simulations and the referential one, and comparison between URBS and URBS-WTI. For assuring the model stability after the implementation of the WTI module, a variety of modeling outputs were examined including water balance, discharge and saturation depth.

An accent has been put on the sensitivity study, work through which we have obtained detailed information on the module (model) behaviour. Some results obtained in the present analysis confirmed what have been found in earlier studies, others contradicted them. The disagreements can be linked, among others, to studied areas, examined variables, and in a less extent, to data errors. The parameter calibration has been mainly based on groundwater level simulation through a curve-fitting approach between simulated series and observed series. The such calibrated parameter set is not the one which permits the best simulation/observation fitting for every piezometer, but the one which allows an average good fitting, giving the heterogeneity in the piezometric observation series and the current limited model capability to deal with this heterogeneity.

If the models could reasonably well estimate the water balance and discharge rates, the groundwater levels have been overestimated by all the simulations, whatever the tested parameter values. Besides, the WTI module was incapable to show significant effect. We believe that these two phenomena are linked and infer the supremacy of climate forcings on the simulated hydrological processes. This issue is worth rigorous studies.

The last test of forcing the WTI flows provided some hopeful signs. If the physical meaning of the WTI coefficient deserves further reflections, it shows the possibility to improve the quality of the integrated model URBS-WTI.

Part IV

Application of URBS-WTI on the future urban campus of Moulon & Evaluation of impacts of urban development on catchment hydrology

Chapter 6

Urban development project Paris-Saclay and Moulon sub-project

Contents

6.1 Context

The future development of Paris metropolitan beyond its present political and physical limits is a national priority. The project "Opération Campus", launched by the French government in 2008, aims to raise the competitive power of Paris' university system. Home to 23 French universities and Grandes Écoles, the Saclay plateau is one of the twelve campus selected by the Opération Campus. In 2010, the Établissement

Public Paris-Saclay, EPPS, was founded by Law of Grand Paris[1], with the objective to build an international scientific and technological cluster on the Saclay plateau that can compete with other high-tech business districts around the world, such as Silicon Valley or Cambridge, and enhance the attractiveness and influence of universities in France.

An area of 7700 ha, including the entire Saclay plateau and its surrounding business areas, was defined by the Decree N°2009-248 on 3rd March 2009 for the operation OIN[2] Paris-Saclay, led by the EPPS. In order to involve regional development in the project, the action perimeter of the EPPS is enlarged to an area of 17 km × 14 km. This broaden area covers the departments of Essonnes and Yvelines with 49 French communes grouped in 6 Communautés de communes, 657 000 inhabitants and 350 000 employees.

Within this vast area, the vocation of the EPPS is to led all actions in favor of economic, industrial, educative and innovative development and create the scientific and technological cluster Paris-Saclay. The project consists in the relocation of several Grandes Écoles onto the plateau and the restructuring of the University Paris-Sud 11, to form a unique University Paris-Saclay, which will be the largest university in France and one of the most multidisciplinary universities in Europe.

In this chapter we give a succinct description of some key components of the project. Most of the figures and maps shown below are produced by the EPPS, thus not referred to specifically.

6.2 The Saclay plateau - Historical development and today

Located approximately 20 km in the south-west of Paris (Figure 6.1), the Saclay plateau is a large territory 3.5 times of Paris Intramuros. It is a raised belvedere, with broad visual perspectives, and subjected to high winds. Its edges have wooded steep slopes that shape the development of towns and rail lines (commuter train RER B and C) in the low perimeter around the plateau.

Before the end of the 17th century, the plateau was a vast swampy area. When Louis XIV occupied the Château of Versailles in 1670, his engineer Thomas Gobert constructed a series of hydraulic systems to bring water to the fountains and parks. The result was a system of channels, viaducts, water towers and reservoirs, many exist today, which drained the swamps and created a rich agriculture area.

In the 1950's, the plateau itself began to develop firstly for defense industries (CNRS, CEA, ONERA), and later universities and research institutions (the University Paris-Sud 11, HEC, École Supérieure d'Optique). In the 1970's, École polytechnique and Supélec settled on the plateau. The Moulon farm, which houses currently genetics and plant breeding, was restored in 1978. At this time, institutions on the plateau began to join together.

At the beginning of the 21th century, research centers of private companies settled on the campus. In 2000, Danone firstly chose to establish a R&D center in Palaiseau, joined in 2006 by Thales laboratories, and in 2009 by Kraft Foods. Two thematic advanced research fields are present on the plateau with the

[1]Loi N° 2010-597 du 3 juin 2010
[2]OIN: Opération d'Intérêt National

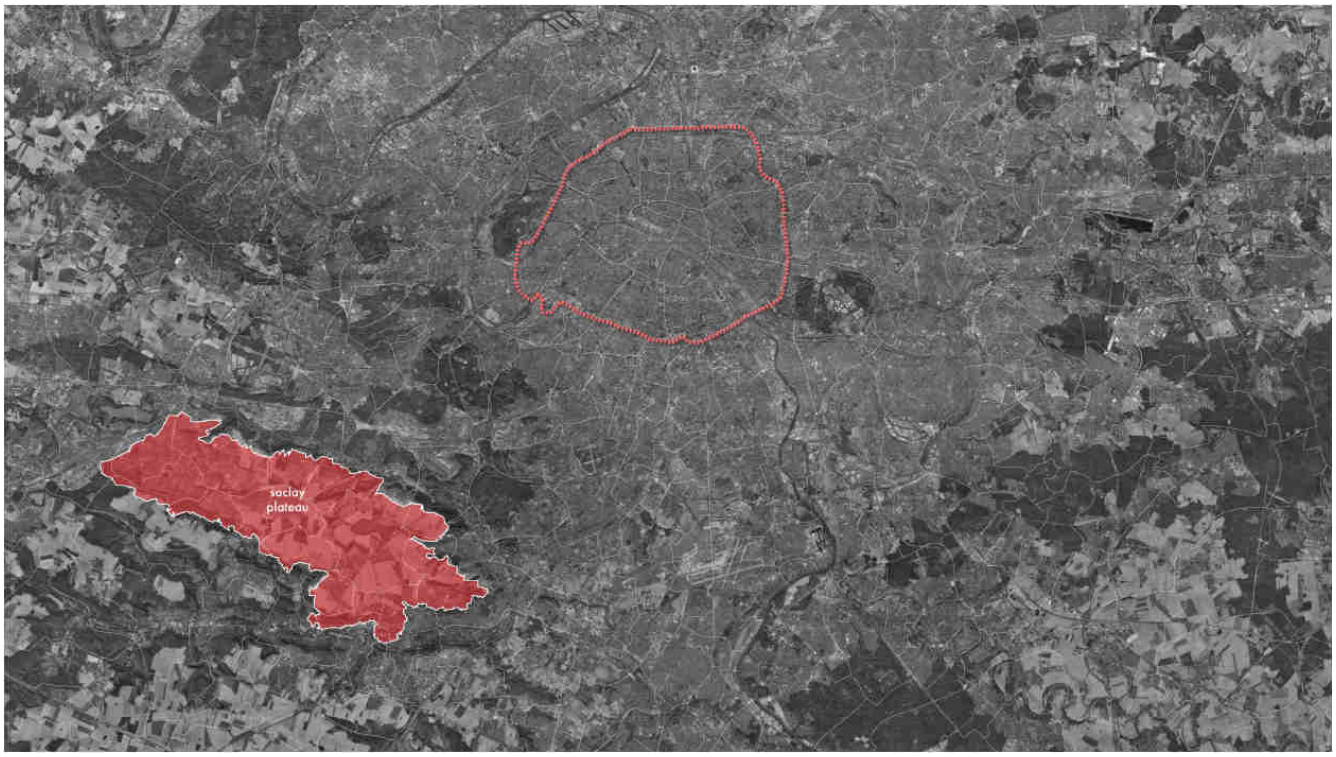

Figure 6.1 – Location of the Saclay plateau (red zone), in comparison with the limit of Paris (red line).

creation of Digiteo and Triangle (de la physique) in 2006. Synchrotron Soleil was inaugurated the same year. The neuroimaging center NeuroSpin was also launched in 2006.

Today, with some 350 000 employees, both public and private, the Saclay plateau focuses 13% of national workforce in R&D, as being the second largest high-tech cluster in France, following Paris Intramuros. The University Paris-Sud 11, the largest university in France, has six of its schools located in the valley and on the plateau. The existing Grandes Écoles and research institutions are widely scattered across the plateau and function as isolated "islands" without holistic planning. With the implantation of a new campus, the intention of the project is to create a dense R&D cluster together backed up on a real community, in order to "break through the traditional institutional boundaries and create new synergies" (Mr. Pierre Veltz, CEO of the EPPS).

As a part of the Seine catchment which was formed during the Lutetian and later during the Pliocene Epoch, the Saclay plateau is one of the most fertile territories in Île-de-France. Intensive agricultural exploitation dates back to the 17th century, with the accomplishment of Louis XIV's hydraulic channel system, which turned the plateau to a drained area. At the beginning of the 20th century, while other suburbans of Paris experienced intensive industrial transformation and urban expansion, the Saclay plateau was kept out of the industrialization and conserved its agricultural identity. Today the plateau is primarily used for wheat farming.

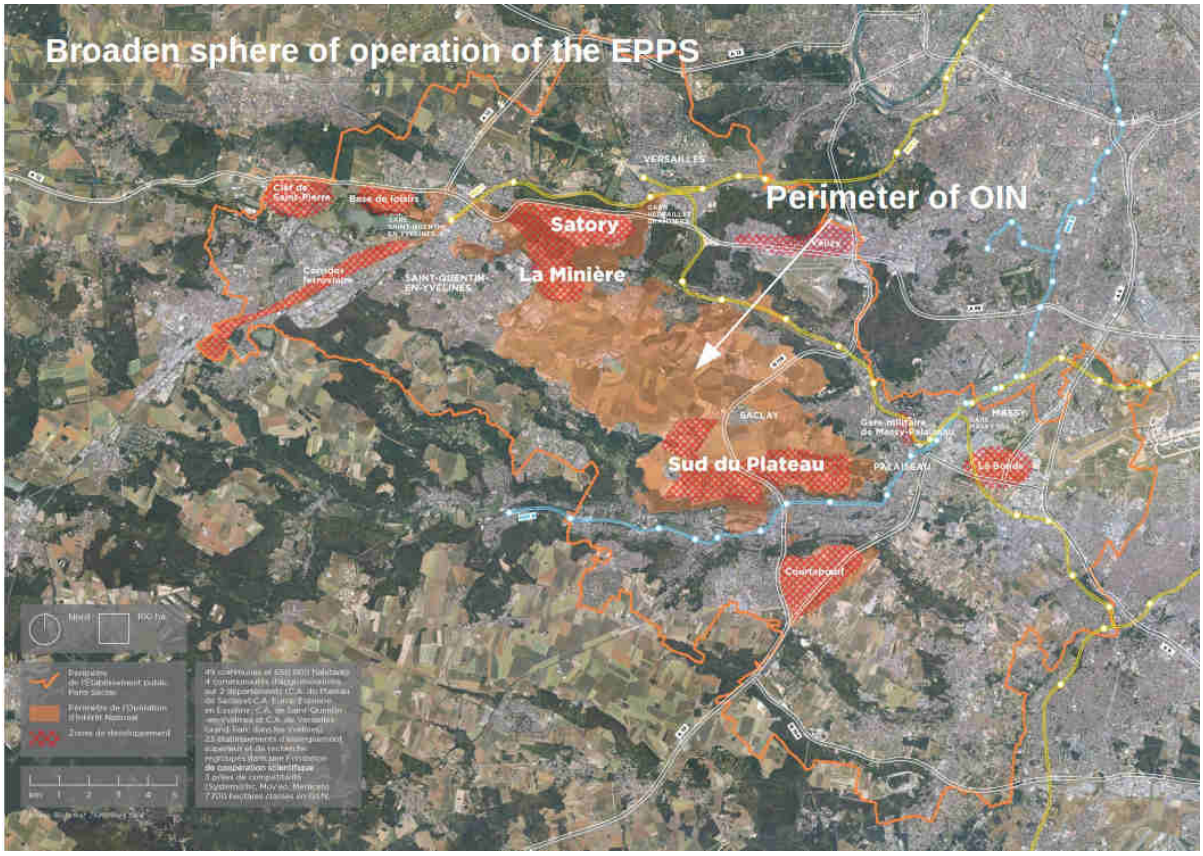

Figure 6.2 – Perimeter of the OIN and the enlarged operation area of the EPPS.

6.3 Urban campus project at Sud du Plateau

6.3.1 University program

Within the operation zone of EPPS, two geographical entities have been identified:

- the southern edge of the plateau, between École Polytechnique in the east and CEA in the west (7 km), labeled "Sud du Plateau" (south of plateau)
- the urban chain Versailles – Satory – Saint-Quentin-en-Yvelines – La Minière

The Sud du Plateau is home to the future Paris-Saclay University. In 2025, this campus will have 20 000 students and 15 000 researchers. The list of participants to the Paris-Saclay University is given in Annexe E. In order to increase the reception capability and enhance the attractiveness of the campus, the project focuses on a compact urban development composed of inter-connected core parts, termed:

- ZAC[3] of École Polytechnique to the east (Palaiseau town) (Figure 6.3)
- ZAC of Moulon in the center (Figure 6.3)

[3]ZAC: Zone d'aménagement concerté, signifies a defined zone dedicated to urban development.

- Orme area of CEA to the west

Existing facilities at the Moulon area include an education center for the police, Supélec and the IUT school of the University Paris-Sud 11, with 1160 persons including 860 students. École Centrale Paris and École Normale Supérieure de Cachan will be newly settled at the campus in a near future. Existing facilities at the Polytechnique area include École Polytechnique, ENSTA ParisTech, ONERA and École Supérieure d'Optique. Coming institutions include Agro ParisTech, ENSAE ParisTech and Télécom ParisTech. These programs are illustrated in Figure 6.4. Together with the University Paris-Sud 11, these Grandes Écoles and institutions will form the future Paris-Saclay University.

The zone of Sud du Plateau includes not only the two ZAC. Four other districts located at the southern edge of the plateau (Corbeville area, CEA area and Camille Claudel area) are also considered in the development planning of Sud du Plateau, but the programs are not presented in the present document.

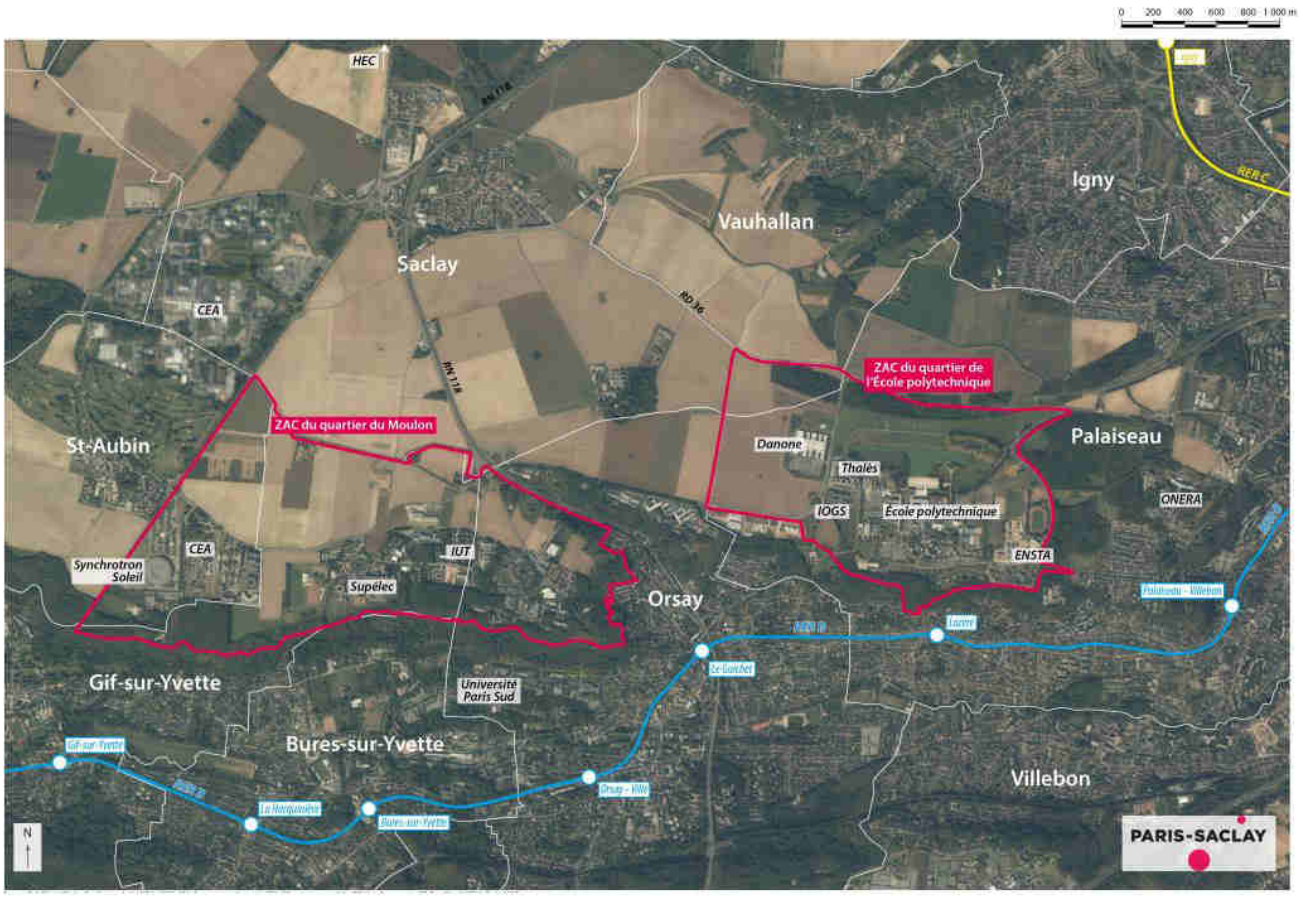

Figure 6.3 – Aerial view of the "Sud du Plateau". (Sources: ESRI, DigitalGlobe, GeoEye, i-cubed, USDA, USGS, AEX, Getmapping, Aerogrid, IGN, IGP, swisstopo, and the GIS User Community, BD TopoPays®/IGN©-Paris-2007)

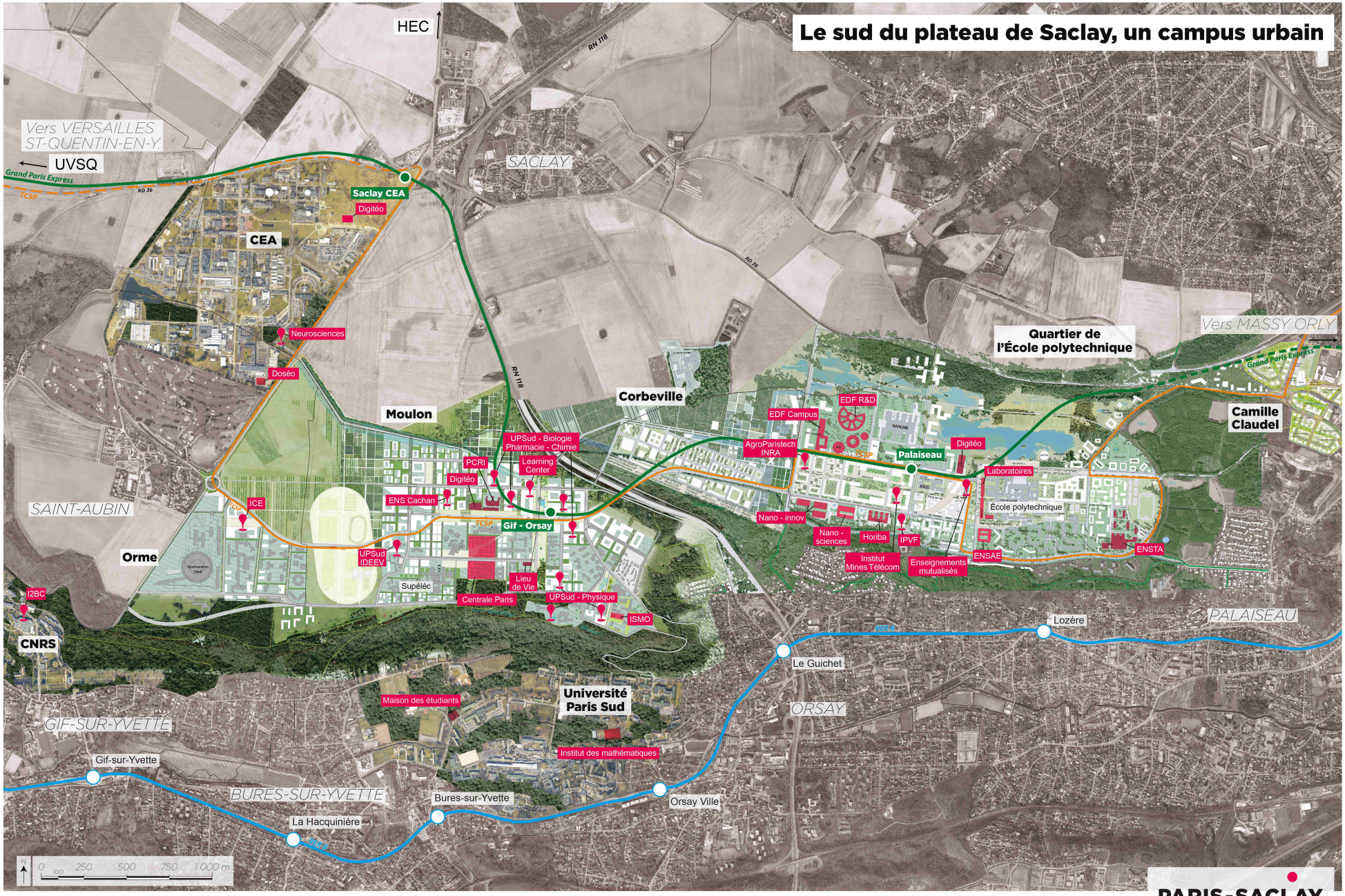

Projet urbain du Moulon, groupement MSTKA :
Saison-Menu architectes-urbanistes, Taktyk paysagiste

Projet urbain du Quartier de l'École polytechnique, groupement MDP :
Michel Desvigne Paysagiste, XDGA / FAA architectes-urbanistes

Réalisation : EPPS / Février 2013 Réf. : 0228-2012-11-16-TD-V3
Source : Groupement CASSY-CAPS-CAEE Orthophoto Aéroscan - Mars 2010, MSTKA, MDP, CAPS

Figure 6.4 – Schematic of the campus Paris-Saclay in 2025.

6.3.2 Project stakes and strategies of the EPPS

The University Paris-Sud 11 and other existing institutions have historically come and settled on the plateau (and in the valley area) one after another without any implementation of common planning. Consequently each entity has only thought of its own needs and functions still today in isolating with the exterior. The suggestion of the EPPS is to break this historical enclosing culture by creating an open educational and economical aggregation. The new campus will be constructed fur the purpose of:

- Proximity. Schools and departments are to be organized in such a way that real scientific synergy can be created.
- Unity. The spatial scattering of institutions must be avoided.
- Collectivity. Contact and exchange are promoted and facilitated in the campus environment.
- Compactness and mixture.

Beyond the objective of setting up a world-class cluster, Paris-Saclay is also of economic, political, environmental and societal importance. Cooperation between university and industry is to be cemented to propel job creation. The campus design itself must inspire this dynamics and increase economic productivity. The agricultural singularity and the natural feature of the territory must not be scarified for urban development, but preserved. This is the reason why the EPPS and its partners have adopted a principle of density and compactness for the construction of the future campus. At least 2300 ha of farmland will be conserved on the plateau center. Innovative technology is to be explored making the campus an exemplar of eco-friendly urban development. In addition to university installation, a large variety of facilities are projected ranging from student and family housing, business hub, sportive compound, to public plaza. The aim is to construct a real urban campus where work and life exist in good mixture.

Connecting the plateau and the valleys as well as other parts of Île-de-France is also one of the priorities of Paris-Saclay. With the underpinning of the enlarged regional railway network Grand Paris (cf. Appendix E.2), the automatic express line 18 in particular, the public transport grid on the plateau will be radically modified towards to greater capacity and improved convenience.

6.4 Landscape and Eco-territory

A group of designers have been selected for the planning of the new campus, represented by landscape architect Mr. Michel Desvigne, associated with three architects - urban designers XDGA (Belgium), FAA (Germany) and AREP (France) and four thematic consultancies ALTO - SETP (environment), TRITEL (transport), SOGREAH (hydraulic) and SETEC (infrastructure).

One of the ambitions of Paris-Saclay is to contribute to urban ecology. Resting on the urban mesh, the campus' landscape develops an urban nature that is accordance with the need of connecting the different spaces. The palette of open spaces defined by the city mesh are the main spaces for the mobility. In this term, the landscape of the campus constitutes a space of daily life for the people on the plateau. By various development program of public spaces, the objective of EPPS and its partners is to enforce the legibility of the campus structure in terms of landscape.

Another value of the landscape design is sustainable and resilient management for water, in a dimension beyond flood risk. Rain water are to be soaked in where possible, flows are to be slowed down, and storage facilities are designed for extreme events. The landscape of the campus, with the meshed opened spaces, is an efficient indicator for natural dynamics in the city. The water management strategies are detailed in Section 6.6.3.

Facing the multiple challenges in the cluster constructing and territorial development, the EPPS and its partners plot their operation strategy around the building of a "park-campus" on the plateau.

The park system stretches out from Moulon to École Polytechnique, an area of about 500 ha over ten kilometers, between the wooded edge and the agricultural landscape. The park serves as links for the plateau and the valley, as well as for different sectors of the campus.

As an integrated part of the campus on the Sud du Plateau, the Moulon area aims at balancing and harmonizing the campus and the plateau, in terms of geography, landscape, activity, transport, and development. Backed on the park system, the urbanization of Moulon pursues creating a real urban ecosystem with equilibriums among its inhabitants, environment and natural resources.

In 2012, EPPS launched a strategical deliberation to make the environment issue the core element in the campus project. The reflection was conducted in cooperation with the CAPS[4] and materialized in the form of Eco-territory. A workshop was organized between November 2012 and April 2013 during which priority issues were investigated: energy, nature - agriculture - biodiversity, material and waste, mobility. Below outlines the strategies defined for the thematics Energy, Water and Waste.

Energy

Paris-Saclay is an opportunity to realize, in a local scale, the energy transition. Three clues are identified:

- Energy sobriety. Global consumption of energy in future campus will be limited to meet the HQE™ standard.
- A part of energy needed in the campus is expected to be produced locally, in favoring renewable energy and energy recycling.

[4]CAPS: Communauté d'Agglomération du Plateau de Saclay, is an agglomeration community composed by 11 communes on the Saclay plateau.

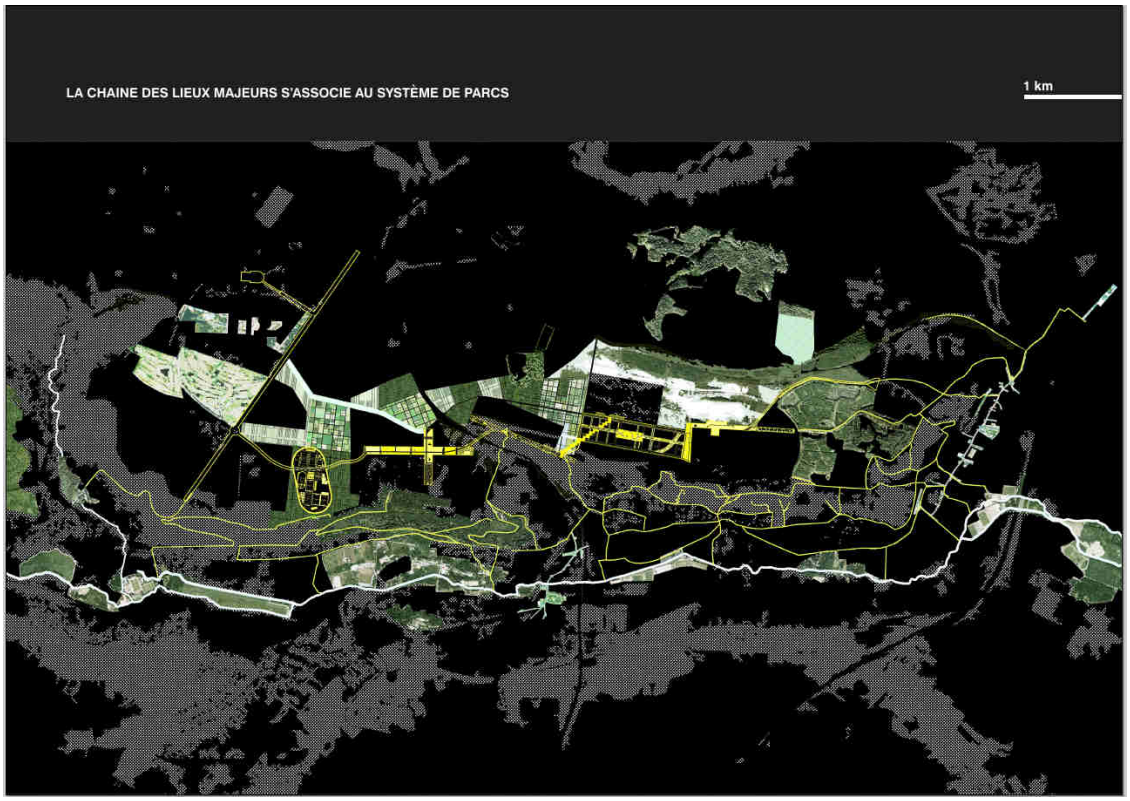

Figure 6.5 – Illustration of the park system with key places in the campus (Michel Devisgne Paysagiste, 2013).

- Smart energy distribution systems by pioneer technology for a better production/consumption balance. The scientific and technological communities on the plateau will be mobilized.

The EPPS works on the planning of innovative energy infrastructures which promote renewable energy, both for electricity and heat supply. Solar panels are to be widely adopted in the campus. A low-temperature heating system will be settled in order to value locally produced geothermal and recycled heat. Buildings will also be equipped by a communication system to optimize consumption and production.

Water management

Located at the junction of several catchments, the Saclay plateau is a complex territory in terms of water management. From 2010 to 2012, a thorough study on the hydrological system of the plateau was led by the EPPS, which has defined the strategy of integrated water management on the plateau: storm, sewage, supplying and aquatic bodies.

Material and waste

For any construction, the environmental and energy impacts in its whole life cycle of the material utilized must be evaluated preliminarily. Waste recycling and reuse are encouraged. The waste recycling will be structured, and a resource center for waste reuse will be built. The possibility of a biological treatment plant by Anaerobic digestion is being studied. Detailed studies on transport, collection, sorting, recycling and reuse are also in progress.

6.5 Other programs

Paris-Saclay is a large campus and urban development project which will have long-term impacts in numerous sectors, including education, research, industry, business, society, agriculture, landscape, environment, etc. The overall programs led by the EPPS include also transportation (creation of new roads and restructuring of the transport grid, construction of future stations of Grand Paris Express and of the TCSP lane[5], creation of pedways and cycling pistes...), installation of public and security equipments, reconciliation of large infrastructures: electricity, gas, heat, telecom..., etc. These programs are as important as the campus installation and the water management, and constitutes key elements for the success of the future urban campus. But giving a exhaustive description of all the programs in the present document goes beyond the objective of the Ph.D present dissertation. In the annexe, some other main programs of Paris-Saclay are described.

6.6 Urban development of the Moulon area

As an extension of the CEA, located on the edge of the plateau, the ZAC of Moulon covers the current area of Moulon and Orme. It is one of the main fields to be developed on the Sud du Plateau. With an area of about 300 ha, Moulon is today mainly occupied by the University Paris-Sud 11 (the IUT school), Supélec, SOLEIL, which present one third of the total surface area. The rest is cereal farming, most of which for experimental use.

6.6.1 Natural conditions of the site

Geography and topography

The Saclay plateau is one part of a larger plateau series belonging to the Région Naturelle de France (Fénié and Benie, 2000) of Hurepoix, to the south-west of Paris. It is delimited in the north by the Bièvre River and in the south by the Yvette River (and its affluent La Mérantaise), each of both rivers shaping a densely-urbanized valley. The Saclay plateau has an overall inclination from west to east.

[5]TCSP: Transport en Commun en Site Propre, is a bus-only lane that will be settled on the plateau and go through the campus

The Moulon area is located on the southern edge and delimited by a small slope in the east, the channel Rigole de Corbeville in the north and Saint-Aubin town in the west. The abrupt and wooded hillside forms a transition between the plateau and the valley of Yvette. From the plateau at an altitude of about 150 m NGF to the valley at about 60 m NGF, the hillside is constituted by two parts: a first abrupt drop of 60 m at 15° inclination, and a second descent much more gentle through a height of 40 - 50 m.

The slope on the plateau is very weak, generally smaller than 3‰. A great part of Moulon dips slightly to the Rigole de Corbeville in the north. A fringe in the south-eastern part inclines towards to the valley, as shown in Figure 6.6.

Figure 6.6 – Topographic map of Moulon.

Climatic condition

A great part of North and Center France is under oceanic climate progressively moderated by continental conditions to the east. Located in the center of this region, Île-de-France features warm summer, cool winter, with a narrow annual range of temperature of about 15℃ and high humidity throughout the year.

Generally controlled by this climate, the Saclay plateau has a specific micro-climate linked to its elevation. According to the records of two weather stations (Toussus-le-Noble and Trappes) of Météo France on the plateau, annual average temperature varies between 6.5℃ and 14.8℃, lower than that of Paris which is between 8.5℃ and 15.5℃. This difference is caused by the dense urbanization in Paris as well as by the altitude of the Saclay plateau. For the period of 1971 - 2000, monthly average temperature in July is between 13℃ and 24℃, and between 1℃ and 6℃ in

January.

Annual rainfall in Paris region is about 650 mm, lower than the national average which is 850 mm. But precipitation is averagely distributed throughout the year, with 111 rainy days (> 1 mm) recorded during the period 1971 - 2000. The Saclay plateau is slightly more humid than regional average, with 700 mm of rainfall and about 118 rainy days per year.

Dominant wind direction is north-east during summer and south-west the rest of the year. But the strongest wind (> 20 km/h) in winter is from the north-east. The speed of wind on the plateau is not very high, 12 km/h in winter and 8.3 km/h in summer. Annual probability of a gust more than 100 km/h is 0.3 day/year.

A particular character of the Saclay plateau is the frequent fog. An average of 41 foggy days were recorded for the period 1991 - 2001, concentrated in autumn and winter, while the regional average is 20 - 30 days. The prevalent fog is narrowly linked with the impermeable soil of the plateau and a layer of shallow ground water (cf. Section 6.6.1).

Hydrology

Paris and the Saclay plateau are both located within the Seine catchment. The Seine and its tributaries drain an area of 78 910 km^2 of North France. They are monitored and governed by the Agence de l'eau Seine-Normandie, a public institution of the Ministry of Ecology, Sustainable Development and Energy. The Saclay plateau is located between the Bièvre River and the Yvette River, with a majority of its site draining into the Bièvre River and a small portion drained into the Yvette River. The Bièvre River flows from Guyancourt up till to Seine in Paris where it is connected to the stormwater network of the city. The Yvette River is a left tributary of the Orge, which is a tributary of the Seine. It flows for 39.3 km and has a catchment of 286 km^2. Annual average flow speed is 1.34 m/s (measured at Villebon-sur-Yvette), but with high seasonal variations.

The Saclay plateau inherits a historical network of collectors for surface water, as shown in Figure 6.7. As time goes on, it has obtained, in addition to its hydraulic function, a patrimonial, natural and landscape value. Initially designed for supplying water for Château of Versailles, this network is composed of:

- a network of channel collectors
- ponds for storage
- aqueducts for water convey to the castle

This hydraulic system had been being operational until the middle of 20th century before being altered due to lack of maintenance and highway constructions. But the supply function for Château of Versailles of the channels has been kept till today. A channel rehabilitation program is being conducted by SYB[6], with the purpose of restoring and improving their hydraulic function. The

[6]SYB: Syndicat Mixte de l'Yvette et de la Bièvre

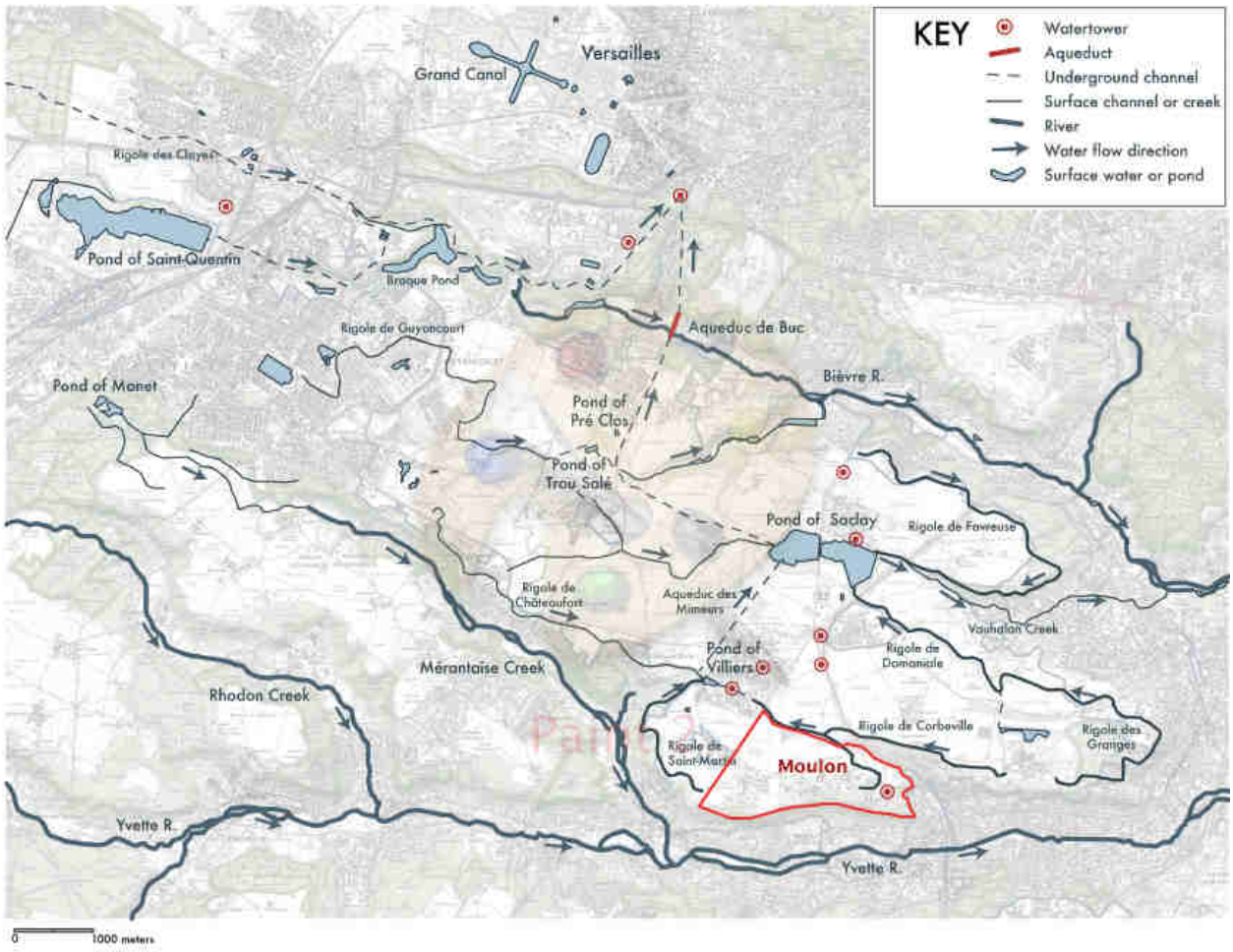

Figure 6.7 – Hydrographic network of the Saclay plateau.

Moulon area is concerned mainly by the Rigole de Corbeville. The interruption at the highway N118 will be reconnected.

In the Rigole de Corbeville, water flows from east to west, in taking resource near the École Polytechnique. Since the construction of N118, the eastern upstream section has been connected to stormwater system of the road. The western downstream section goes alongside Moulon until the storage pond of the CEA (nuclear institution). Overflow of the pond is directed to the Étang vieux de Saclay by the aqueduct of Mineurs.

Current surface runoff of Moulon is organized as in Figure 6.8:

- The green part, about 200 ha, discharges into the Rigole de Corbeville. The Orme area in purple discharges also ultimately into the channel.
- The yellow part discharges ultimately to the stormwater system of N118.
- The orange part is, via existing underground collectors, connected to the stormwater system

of Orsay town.

The final destination of the water from the yellow and orange catchments is the Yvette River, the rest of the catchment is drained into the Bièvre River.

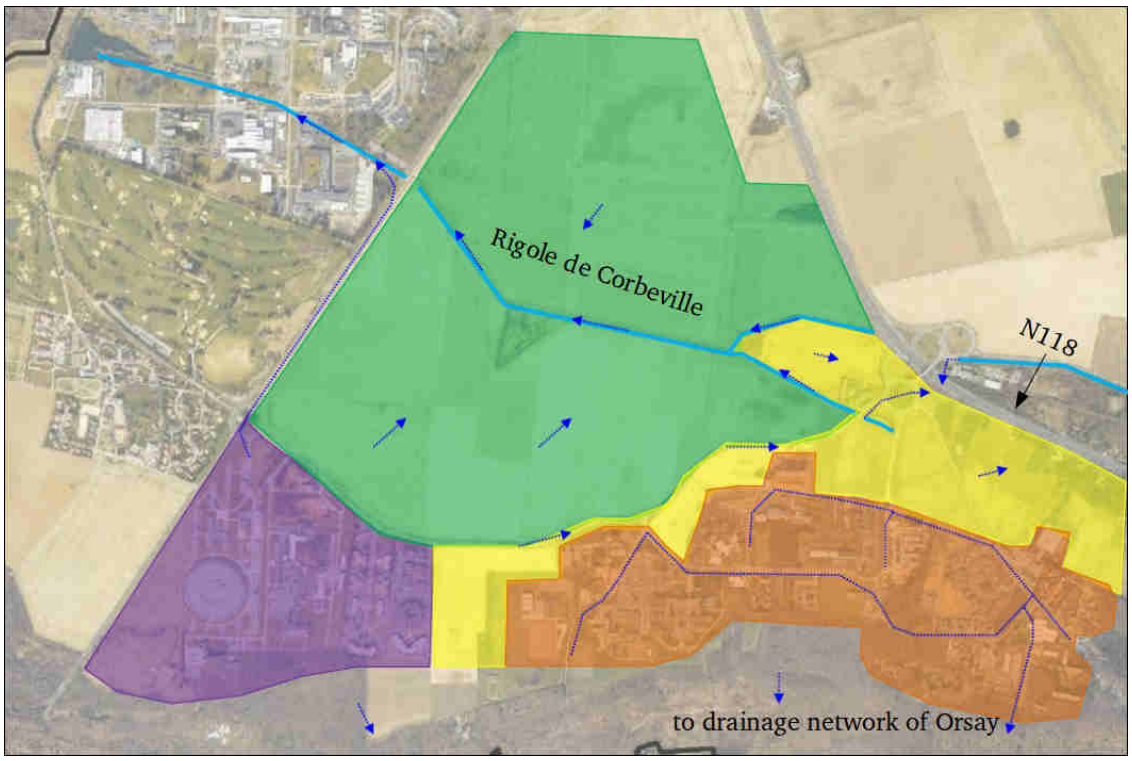

Figure 6.8 – Current catchments of the Moulon area.

Hydrogeology

The Saclay plateau is located in the central part of Paris Basin, the largest sedimentary basin of Western Europe. The landscape of Paris Basin was shaped during the Quaternary Period by the last glaciation. Superficial formations were also formed in this period by erosion. The Saclay plateau is located at the border of two geological entities Brie Française and Hurepoix, which constitute the substratum of the plateau. Superficial geologic formations covering the Saclay plateau are identified as (BRGM, 1999; Dumont et al., 2013):

- Limons (silt) des plateaux: thin clayey sandy sedimentary deposition formed during the Quaternary (1.8 myr), ocher and reddish, at a thickness of 0.5 - 3 m, locally reaching 9 m.

- Sables (sand) de Lozère: complex mixture of sand and clay, fluvial deposits formed in the Mio - Pliocene (20 - 5.3 myr), in the form of quartz and feldspar observed only at the left bank of the Seine, 2 - 5 m in thickness.

- Argiles (clay) à meulière de Beauce: ball clay of Miocene and Pliocene, grey or reddish, ferruginous and dominated by kaolin montmorillonite, forming compact and cavernous gritstones, 1 - 6 m in thickness.

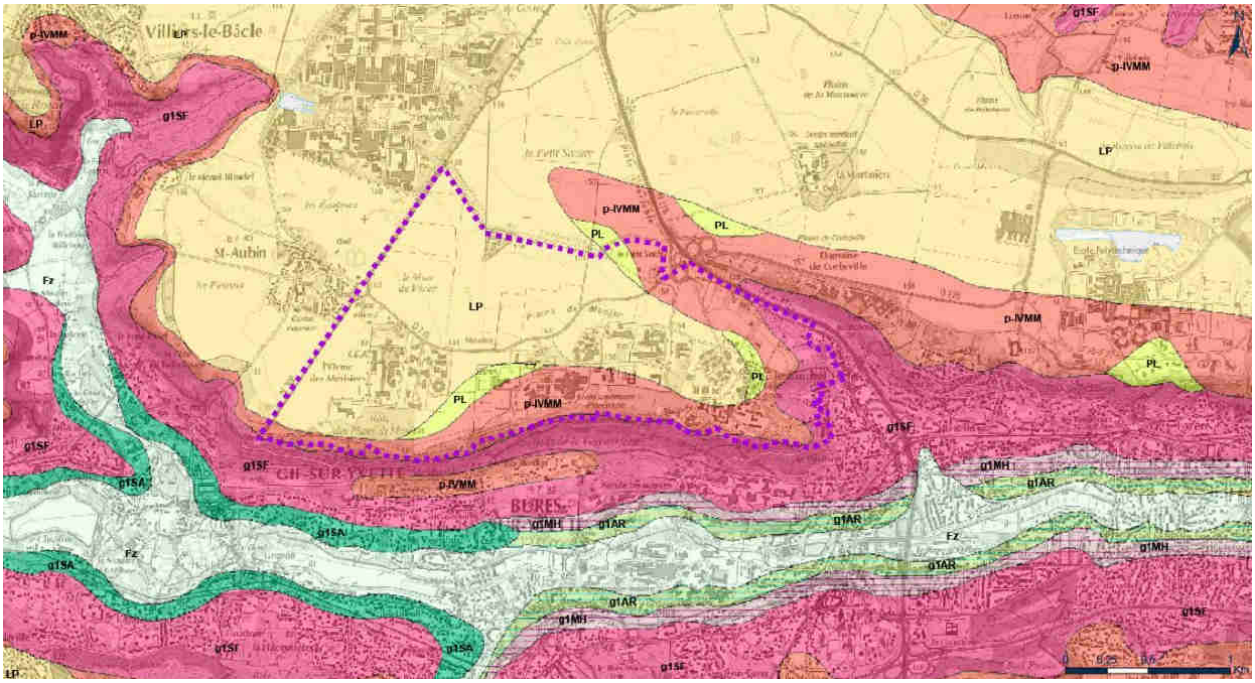

Figure 6.9 – Geologic map of Moulon.

These formations cover the entire Saclay plateau with a thickness between 1 and 18 m. Under the Moulon area, this superficial layer is relatively thick, between 10 and 18 m. Below these superficial formations is the layer Sables (sand) de Fontainebleau, composed by siliceous sands (97% to 99% of quartz). This layer has a thickness of 44 - 73 m and contains a large aquifer. It is separated from deeper aquifers by an impermeable layer of clay, varying between 2 - 18 m. For the sake of clarity, we will keep using the original appellations (in French) of these geological formations.

In summary, the perimeter of the Saclay plateau defines an aquifer system, constituted of two superposing reservoirs:

- Fontainebleau sands aquifer, beard in the Sables de Fontainebleau formation
- superficial aquifer, composed by the Limons des plateaux and the Sables de Lozère and based by the Argiles à meulière de Beauce

The Bièvre River and the Yvette River break the Saclay plateau from other plateaus at the north and south. The only communication is observed at the upstream of the Bièvre, where the Sables de Fontainebleau is in contact with the alluvium aquifer of the river. The Fontainebleau sands aquifer lays throughout the Saclay plateau, flowing mainly from north-west to south-east, and

discharges at the Yvette valley where the aquifer is exposed. The aquifer is recharged mainly by its outcrop parts. It is also supposed to be recharged subordinately by infiltration through the superficial layers, especially below the ponds (Cojean, 1975). But the recharge locations are till nowadays unidentified, and the recharge quantity undefined (BRGM, 1999; Dumont et al., 2013). The Fontainebleau sands aquifer is not supposed to be impacted by the development of Paris-Saclay, thus beyond the scope of the present study.

The matrix constituted by superficial layers is not a real aquifer strictly speaking, but an ensemble of water lenses with great spatial variations in extension and thickness, and of which the hydraulic continuity is not clearly known (BRGM, 1999). The great geological heterogeneity creates contrastive hydraulic conductivity of these water lenses in which water movement is mainly vertical. Channels existing in the Sables de Lozère constitute preferential places for water stay and flow paths. Due to the great heterogeneity, it is difficult to define the hydraulic conductivity of this superficial aquifer (BRGM, 1999; Dumont et al., 2013). According to divers technical reports (GEOTHER, 2014; SAGA, 2014b,a), locally measured permeability varies between 1×10^{-7} m/s to 1×10^{-5} m/s.

This discontinued shallow aquifer is of high interest of our study because it is supposed to be impacted by the campus development. A groundwater monitoring has been conducted by the CEREMA since June 2012. This work is presented in Chapter 7, Section 7.1.2.

6.6.2 Programs at Moulon

As mentioned above, the main programs within the Moulon area include École Centrale de Paris, ENS Cachan, new installations for the University Paris-Sud 11 (departments biology, medicine, chemistry, IDEEV, physics). The Learning center, a multimedia library and auditorium, will be constructed which will serve as a documentation&information center with a variety of facilities such as hotels, restaurants and conference halls. Other installations include office plazas, sport compound, student housings, restaurants and shopping centers. Figure 6.10 shows the location of the main installations.

In terms of building, the program in the Moulon area is fixed at 870 000 m^2, with a floating possibility of 10%. The program is composed of:

- 40.2% of university buildings, around 350 000 m^2
- 23.0% of company buildings, around 200 000 m^2
- 2.9% of public equipment, around 25 000 m^2
- 2.9% of service and stores, around 25 000 m^2
- 31.0% of housing, around 270 000 m^2, with 160 000 m^2 for families and 80 000 m^2 for students

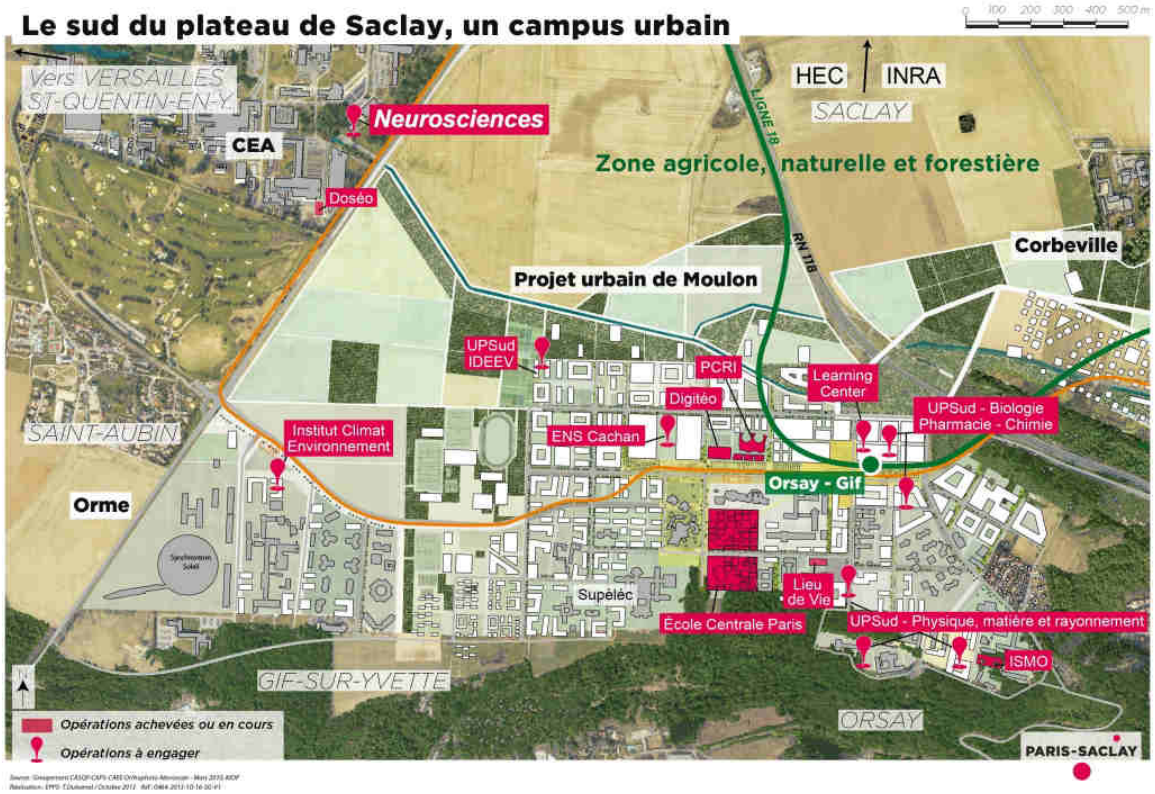

Figure 6.10 – Construction programs in Moulon.

An indicative spatialization of the different programs is shown in Figure E.4 in the appendix.

Two campus poles are defined. The first one, labeled "Métropolitain", is located in the east surrounding the future station of Grand Paris Express. This pole is home to the department of Pharmacy-Bio-Chemistry of the University Paris-Sud 11, the Learning Center, business installations and residences. This area is also an important district for stormwater management. A hydraulic system is to be installed which conveys water towards the Rigole de Corbeville.

The second one, labeled "Joliot-Curie", is located in the west, surrounding a future stop of the TCSP. École Centrale de Paris will site here and coexist with existing Supélec and IDEEV[7]. A mixture of housings and tertiary installations are also planned. Natural landscape dominates this pole, which articulates the wooded plateau edge to the south and farmland to the north.

Relationships of people is a core element in the conception of the campus. Spaces among the block of programs play a crucial part and need to be clearly identified and organized with hierarchy. They are the places where people meet and share their campus life. The concept of public space chain is translated, at Moulon, into three large emblematic places (Figure 6.11):

- A generous public square, oriented east - west, around the pole Métropolitain and along

[7]Institut Diversité Ecologie et Evolution du Vivant

with the future TCSP lane, labeled "Deck". Featured by its large size of 70 m × 80 m and metropolitan landscape, it is designed for the future station of Grand Paris Express and Learning Center.

- Around the pole of Joliot-Curie, with Supélec, École Centrale de Paris and ENS Cachan, a public space labeled "Carré des sciences". Incorporated in the park system, this place is featured by a green landscape: a rain garden in the north, a park in the middle, a gravel square and a meadowland in the south.

- A large sport plain to the west of Joliot-Curie dedicated to sport and leisure activities.

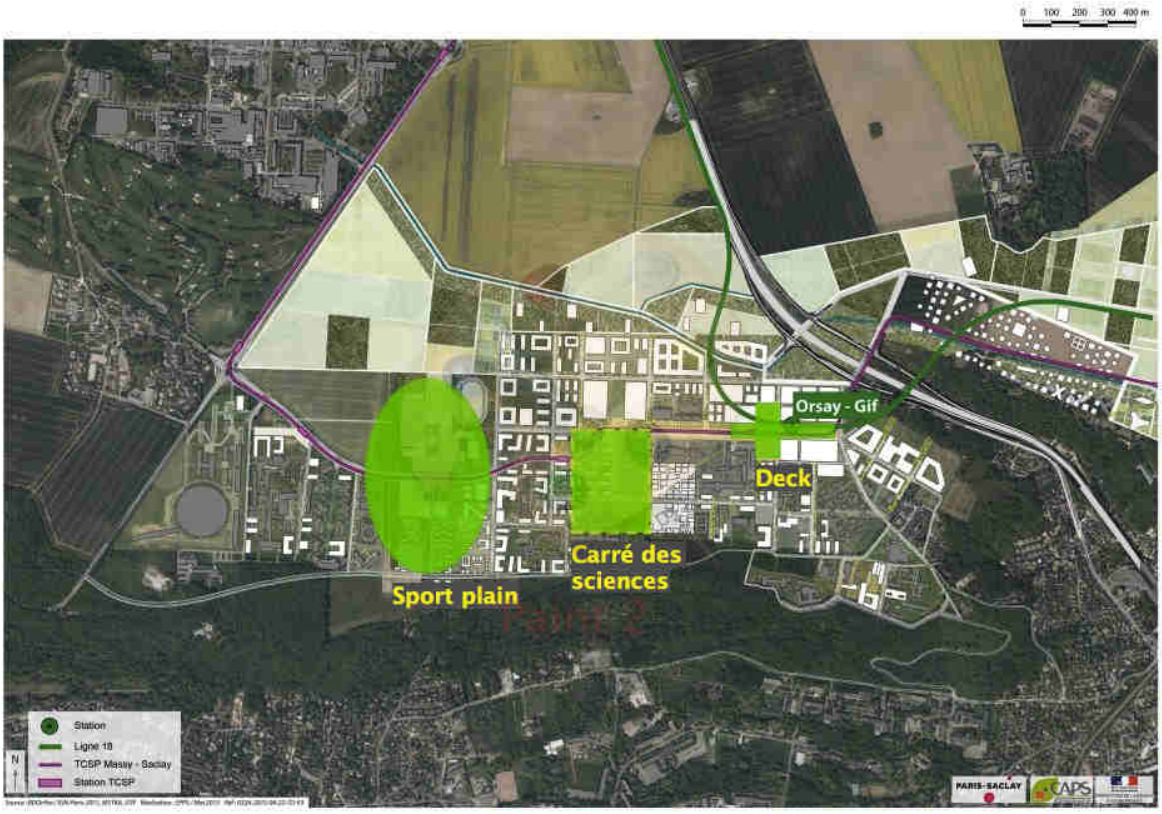

Figure 6.11 – Public space chain in the Moulon area.

The morphology of the future Moulon area is defined by its grid street plan, constituted of vehicle roads as well as pedways, as shown in Figure 6.12. This network structures spatially the campus and draws the future urban blocks, each of which provides a spatial unit for a specific program. Each urban block measures approximately 150 m × 150 m, and may be divided into subunits.

In a principle of mixture and compactness, the service and public equipments are to be constructed in proximity, e.g. at ground floors, extended by outdoor public spaces, in order to provide

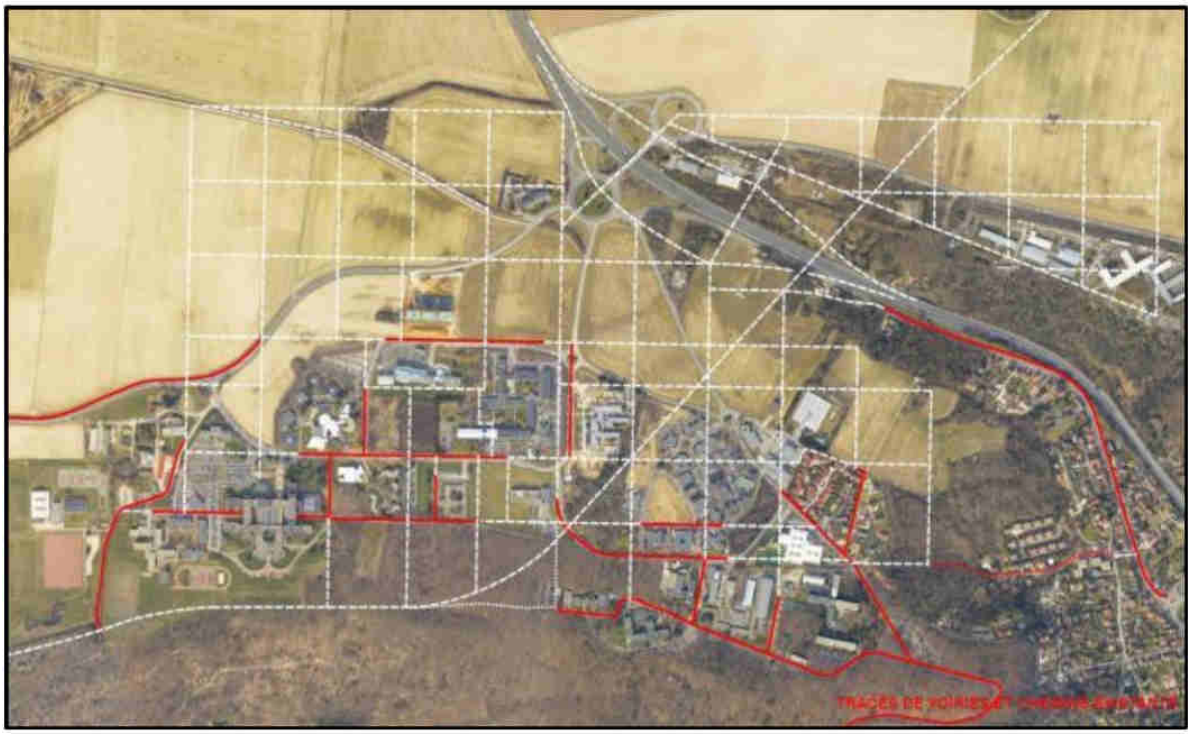

Figure 6.12 – Urban grid of the Moulon area.

an immediate and convenient service, which is believed the key for the success of the campus project.

6.6.3 Stormwater management at Moulon

6.6.3.1 Principles of water management on the plateau defined by EGGE

The Saclay plateau is located on the intersection of several catchments: Bièvre, Yvette and Mauldre. Each of the catchments has its own governing structures and regulation. The zone is set of a complex hydraulic system composed by channels and ponds. As a consequence, water management of the territory of Paris-Saclay is technically and administratively complex. It is thus essential to federate the territory with a common principle for water management. In this context, a specific study Étude Globale de Gestion des Eaux (general feasibility analysis of stormwater management), EGGE, was launched by region's prefect and led by EPPS from 2010 to 2012 in cooperation with water organizations. The study outlined current state of water management on the plateau, identified challenges with the arriving of the campus, and formulated guidelines for water managing at the territory scale.

Stormwater

The policy defined by EGGE is to maintain the at-source management for stormwater on the plateau in order to lower the risk of flooding in the densely-urbanized valleys. To meet this objective, a three-scale management approach has been adopted (Section 6.6.3.2).

Wastewater

Wastewater originating on the plateau is today conveyed by municipal collectors (of Orsay, Gif-sur-Yvette and Sain-Aubin) and treated in the WWTPs of Île-de-France. According to the EGGE, wastewater is to be treated on the plateau as far as technically possible and cost-effective. Besides the benefits regarding to the downstream area, tackling wastewater on the plateau can also provide an opportunity to exploit locally wastewater by innovative techniques (such as reuse or energy recovery). The possibility of constructing a WWTP on the plateau or in the valley is being studied.

Water supply

Drinking water on the plateau is today supplied by water treatment plants of the Seine and managed by local water syndicates[8]. The need on drinking water is going to rise as the campus develops. The syndicates have already planned works aiming to strengthen the capacity of their supply network. The strategy of water supply for future campus defined by EGGE is to create a network based on existing supply lines. Fire water is provided by the water supply system. New constructions are asked to limit and reduce their request on water. Landholders and constructors must take appropriate measures to this purpose such as installing facilities for rain water reuse.

Natural and historical heritage

The surface water quality on the plateau is currently classified as fair or poor. The water bodies generally suffer from hypertrophication. The problem becomes even severer if we takes into account the fact that three large-scale ponds (Étang de Saint-Quentin-en-Yveline, Étang vieux, Étang neuf) and numerous wetlands are existing on the territory, which have high biological and environmental importances.

Improving the quality of these water bodies is one of the objectives of the EGGE. To achieve this goal, natural water assimilation must be systematically considered in all new projects, and quality measuring for rain water is required. Maintenance of public spaces have to be done without any phytosanitary product.

The conservation and protection of natural, agricultural and forest zones on the Saclay plateau is written in the Law of Grand Paris. EPPS is actively working on an action plan pursuing a

[8]In France, a water syndicate is a local water authority.

ecologically friendly governing on the plateau and to incite environment-respecting agricultural practices.

6.6.3.2 Three-scale stormwater management in the Moulon area

In terms of stormwater management, the Moulon area covers the responsible perimeters of SIAVB[9] (north) and SIAHVY[10] (south), two inter-communal water syndicates. Each of them has its own rules on stormwater discharge based on different reference rainfall events.

A flood prevention plan was established in 2006 for the catchment of Yvette. Areas under flood risk are located in the valley and the Moulon zone is not concerned directly. However, the plateau has a major role in preventing flood risk in the valley areas because its discharge is ultimately conveyed into the Yvette River. In addition, the soil of the plateau is not much permeable and the hillside is abrupt, which intensifies surface flow during rainfall events.

In order to control efficiently discharge from the plateau, the EGGE gives recommendations for storm anticipation and defines a strategy of three-scale management that adapts to different rainfall events.

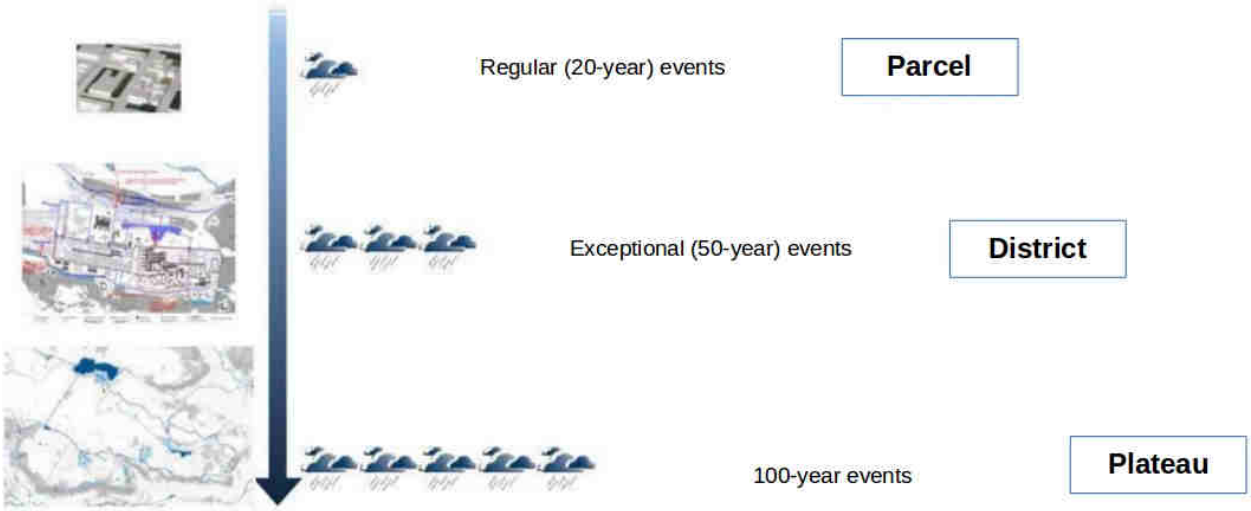

Figure 6.13 – Principles of stormwater management at three scales.

As illustrated in Figure 6.13, discharge due to regular rainfall events is managed within parcels. “Regular” corresponds to an indicative 20-year storm event with a 2-hour duration and 37 mm cumulative height. This referential event was selected from a panel of recorded events at weather stations of Météo France. For all event below this reference, landholders are requested to propose water-retaining solutions to achieve the objective of zero flow out of the parcel, in favoring surface detention facilities to underground basin. They are also encouraged to install purification systems for rain water. For events that exceed the reference, the parcels are authorized to release excess

[9]SIAVB: Syndicat Intercommunal pour l’Assainissement de la Vallé de la Bièvre
[10]SIAHVY: Syndicat Intercommunal pour l’Aménagement Hydraulique de la Vallée de l’Yvette

water to public management systems. In the center of Moulon where it is technically difficult to separate the rain water collection between existing and new buildings, storage facilities will be designed in taking into consideration of the discharge from existing roofs. For the areas which are already urbanized and have their own systems for stormwater drainage, the area of Orme in particular, the current drainage mode will be retained.

Public spaces of the campus are dedicated to manage events below an indicative "exceptional" events: 50-year storm event with a 2-hour duration and 60 mm cumulative height. Storage basins, wetlands and swales are existing or will be newly designed for storing water temporally during the storm and releasing it later in a regulated way, to Rigole de Corbeville. Accidental pollution is taken into account in the design of the drainage systems. Extreme events which exceed the 50-year event are managed on the plateau scale, by plains and parks that are designed for flooding purpose.

In terms of regulation on discharge rate (to the channel or to municipal sewer systems), a threshold value of 0.7 liter per second per hectare (l/s/ha) has been defined. This value is actually executed by SIAVB and is the most demanding regulation existing on the plateau.

For meeting and sustaining these objectives, the envisaged measures are:

- Favoring moderate (non-forced) infiltration. Permeable or semi-permeable materials should be chosen for ground covers.
- LID facilities are to be installed: swales, storage structures under green spaces, streets and parkings, specifically designed depressions that can be landscape amenity and have supplementary functions to hydraulic ones (park, parking, sports equipment).
- Setting up natural purification solutions: settling, filtration, phytoremediation.
- Reducing flow concentrations by privileging diffused flow in order to diminish pollution.
- Encouraging rain water reuse.

The drainage system of stormwater in future Moulon area is thus composed of two types of systems:

- classic underground pipes based mainly on the existing network
- A network of storage and infiltration swales in the direction north-south, connected to storage basins or to the Rigole de Corbeville, as illustrated in Figure 6.14.

It is forbidden to use existing channels for storage purpose (according to the SYB). But the edge zones of the Rigole de Corbeville could be used to create an expanding flood zone for the extreme case of 100-year storm. This expanding zone is projected to have a size of 4 ha, with a preserved perimeter of 9 ha.

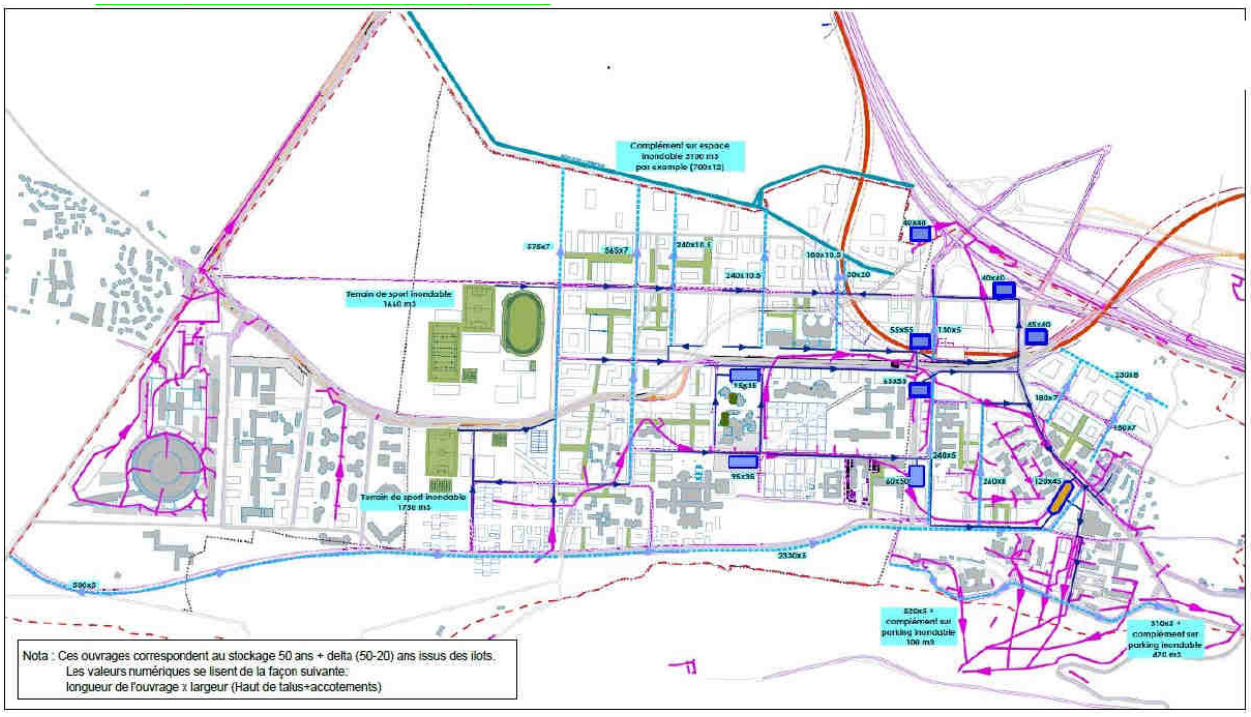

Figure 6.14 – Planned facilities for 50-year stormwater management in Moulon. In red, the existing underground pipelines; in blue, the projected stormwater network composed of underground pipelines, swales and basins.

Conclusion

Paris-Saclay is a national-wide urban-campus project that has profound educational, economic and social influences at regional scale as well as at national scale. As the home to the project, the morphology and landscape of the Saclay plateau will be radically updated in the coming years. The EPPS, as the leading actor in this project, is engaged in sustainable development of the plateau in supervising the setting up of innovative technology and facilities for a eco-friendly campus.

Face the great challenge of flooding risk in the valley areas, a low-impact management system for stormwater management is of central consideration of the EPPS and the water partners. A large variety of LID facilities will be adopted in the campus in order to balance the hydrological impacts of the urban development. It makes sens to draw an estimation of these possible impacts before suitable planning could be made. On the other hand, the hydrogeological condition of the subsurface does not favor surface infiltration. Therefore, the efficiency of the devices needs to be preliminarily evaluated. The next two chapters address these two issues: what is the current hydrological regime of the site and how it will be affected by the land use change and the stormwater management devices. The study focuses on the Moulon area, one of the two main ZAC to be developed in the coming years.

Chapter 7

Modeling of Moulon under pre-development (current) conditions

Contents

Introduction

As one of the core components of the future campus Paris-Saclay, Moulon is going to host dense development programs during the coming fifteen years. These programs will have inevitable impacts on local hydrology:

- Morphology and land use change. While some zones will be sealed for installations and traffic roads, others will be transformed to gardens or rain-storage terrains.
- Underground cellars are programmed for some installations, interacting with the superficial aquifer.
- Stormwater sewer network, as well as wastewater sewer network, is going to be radically changed. A part of existing underground pipes are to be removed, while a system of swales will be set up. Discharge out of Moulon will be regulated to meet the discharge threshold defined by the EGGE study (0.7 l/s/ha).
- Other LID infrastructures will also be constructed, impacting both quantitatively and qualitatively storm runoff.

The overall effect of the urban development and LID devices need to be preliminarily evaluated to help urban planners (EPPS and partners) in their decisions. Our modeling tool URBS-WTI, which is capable of modeling the water cycle in an integrated way in considering both surface flow and groundwater flow, offers a possibility to achieve this purpose.

In order to evaluate the impacts, it is necessary to know the hydrology of the area under its pre-development conditions. This is why a modeling study has been taken out for the pre-development (current) state of Moulon. This study is presented in this chapter. Section 7.1 and 7.2 outline the hydro-climatic and geographical datasets, and the geodata pre-processing for Moulon. As a newly created area for urban development, geodata of Moulon was cluttered and incomplete. The geodata pre-processing is not only necessary for the present work but also beneficial to future studies. Section 7.3 states the modeling framework. The physical parameters are difficult to estimate due to limited understanding on hydrology of the study area. A model base-run has been

done with a raw parameter estimation. The results of the Moulon base-run are given in Section 7.4, followed by a sensitivity analysis and calibration based on the same procedure as for the Pin Sec catchment (Chapter 3). The originality of the sensitivity analysis is the fact that only piezometric levels were available in this catchment for evaluating the relevance of the simulation. The results of calibrated run are shown in Section 7.6, followed by a discussion (Section 7.6.4). These results, although not totally validated due to few observation data, serve as a reference for evaluating the impacts of urbanization in Chapter 8.

7.1 Hydro-climatic and geodata

7.1.1 Rainfall and potential evapotranspiration

Measured rainfall intensity and potential evapotranspiration (PET) rates for the period of 2011-2013 are provided by the weather station of Météo France in the town Trappes. The rainfall intensity is at 6-min time step. PET is at daily time step and estimated by Penman-Monteith method (Choisnel, 1988).

Figure 7.1 plots the monthly rainfall and PET for the three-year period. Cumulative rainfall of the hydrological year 2011-2012 and 2012-2013 (Oct. - Sep.) is respectively 605 mm, lower than average (650 mm) and 710 mm, higher than the average. Abundant precipitation has been recorded during autumn-winter of 2012-2013, with 108.9 mm recorded in October 2012, the most rainy month of the entire period, and 95.0 mm in December 2012, which makes the winter 2013 relatively wet. At the same time, the lowest monthly PET (8.4 mm) has been recorded in January 2013.

7.1.2 Groundwater monitoring and piezometric data

In partnership with EPPS, the public research institution CEREMA - Direction territoriale Île-de-France (CEREMA hereinafter)[1] carried out a hydrogeological study in the Moulon area since 2012 (Dumont et al., 2013). This study was part of the research project Mystic funded by the region of Île-de-France, and aimed at constructing a hydrogeological model for Moulon and to enhance knowledge of the superficial aquifer. A literature review was put through in the first phase of the study. The second phase consisted of a geological investigation by borehole drilling and groundwater monitoring. Ten survey points has been defined for the borehole drilling (PzA - PzJ, Figure 7.2). Auger drilling was conducted continuously with portable trailer mounted rigs of 150 mm in diameter. The soil samples were than studied for precise descriptions for the superficial layers (cf. Chapter 6, Section 6.6.1). More detailed survey results are given in Appendix D.

During the borehole drilling (March - June 2012), water has been found in seven of the ten boreholes, in which were installed standpipe piezometers. The piezometer are of PVC type and 50

[1] http://www.cerema.fr/

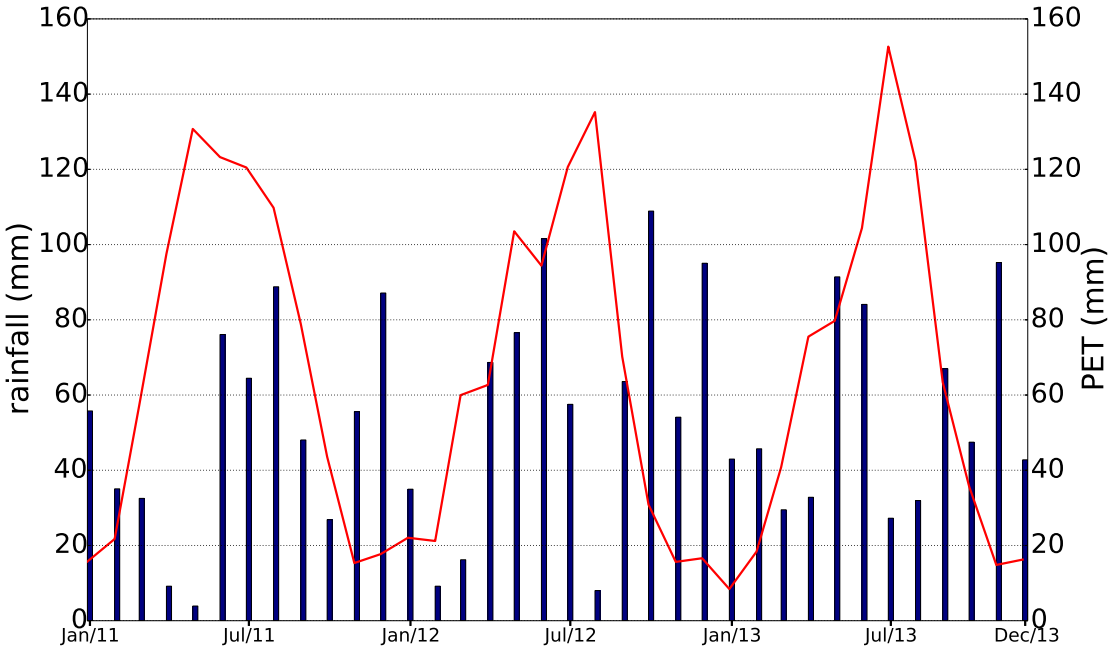

Figure 7.1 – Monthly rainfall amount (in blue) and potential evapotranspiration (in red) rate of 01/01/2011-31/12/2013 recorded by the weather station of Météo France (in Trappes).

mm in diameter, sealed by bentonite grout to prevent surface water infiltration. Characteristics of the installations are listed in Table 7.1. Groundwater monitoring started in June 2012, with water pressure and temperature records. The sensors were provided by two manufacturers and have similar functioning:

Table 7.1 – Description of the piezometers installed in Moulon by CEREMA.

piezometer	PzA	PzB	PzC	PzD	PzE	PzG	PzI
borehole depth (m)	-10.3	-9.0	-8.6	-6.0	-7.4	-10.5	-9.0
perforation upper (m)	-4.3	-3.0	-2.6	-0.0	-1.4	-2.0	-1.7

- PzA, PzB and PzI are equipped with "Mini-Diver" sensor of Schlumberger Water Services[2]. These sensors offer a pressure precision of ±0.5 cmH_2O and a temperature precision of ±0.1°C.
- PzC, PzD, PzE and PzG are equipped with "Levelogger Edge" sensor of Solinst[3]. These sensors offer a pressure precision of ±0.5 cmH_2O and a temperature precision of ±0.05°C.

Manual measurement was conducted during every maintenance of the instrument, and little difference has been found between the piezometric records and the manual measurement (< ±0.02 m).

[2]http://www.slb.com/services/additional/water.aspx
[3]http://www.solinst.com/

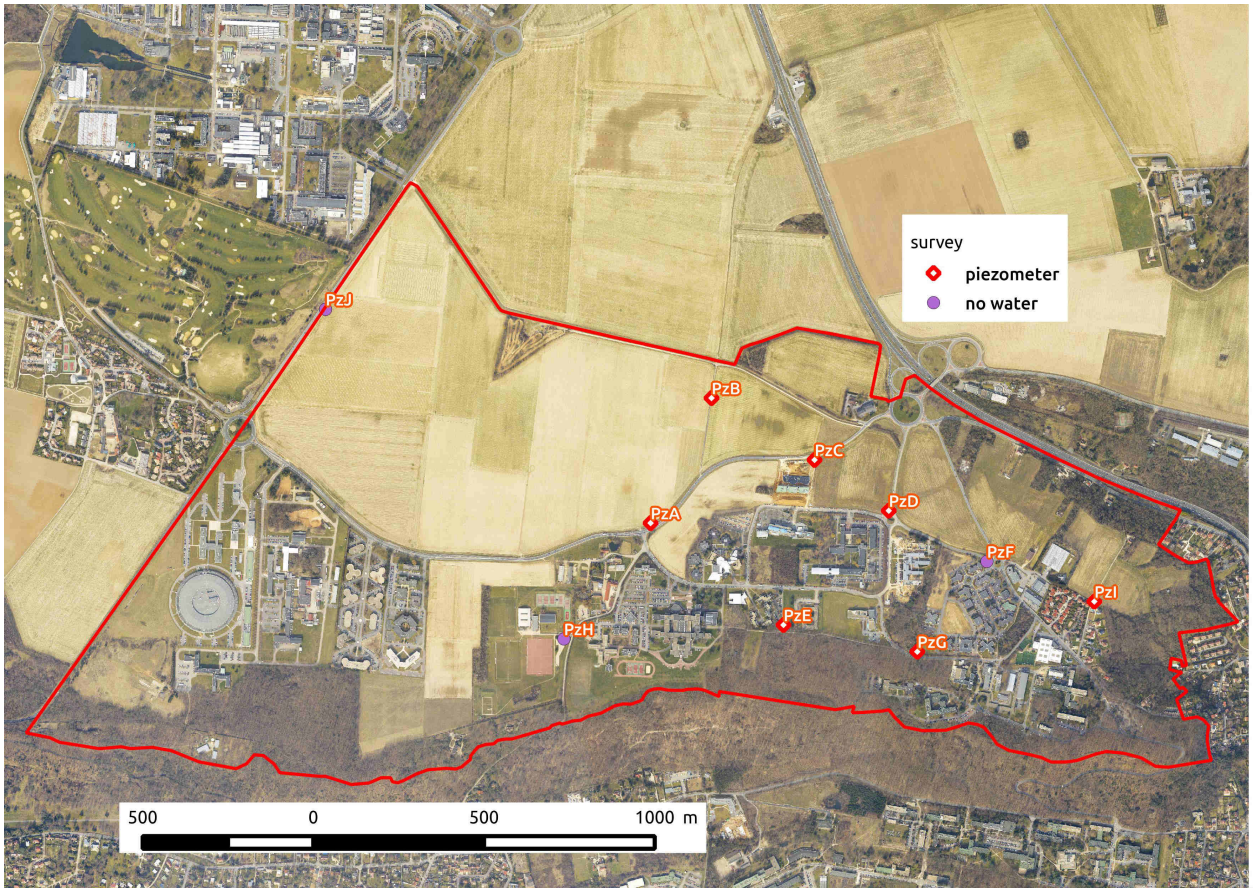

Figure 7.2 – Location of geological survey points and piezometers at Moulon area lead by CEREMA.

Existing piezometers installed earlier in the area (not monitored by CEREMA) were also measured at intervals for being compared with the continuous records.

The piezometric records of the period 06/06/2012 - 17/12/2013 are shown in Figure 7.3. We can identify three categories of curve patterns:

- PzA, PzB, PzC, PzD and PzI show a "typical" pattern: high level during winter and low level during summer, in a range of -3 m to -0.5 m.
- PzE starts with a low level (-4 m) and keeps decreasing up to December 2012, then jumps to -2 m (but still lower than the average). After a stagnant period of about one month, it joins the other piezometers during Spring 2013. From July 2013, the level begins to decrease rapidly and finally meets the initial low level at -4 m.
- PzG has a complete "atypical" pattern. The abrupt limbs observed in this curve can not be a priori explained by climate forcings, and suggests there may be anthropogenic activities impacting the aquifer, such as pumping. But further information is not available.

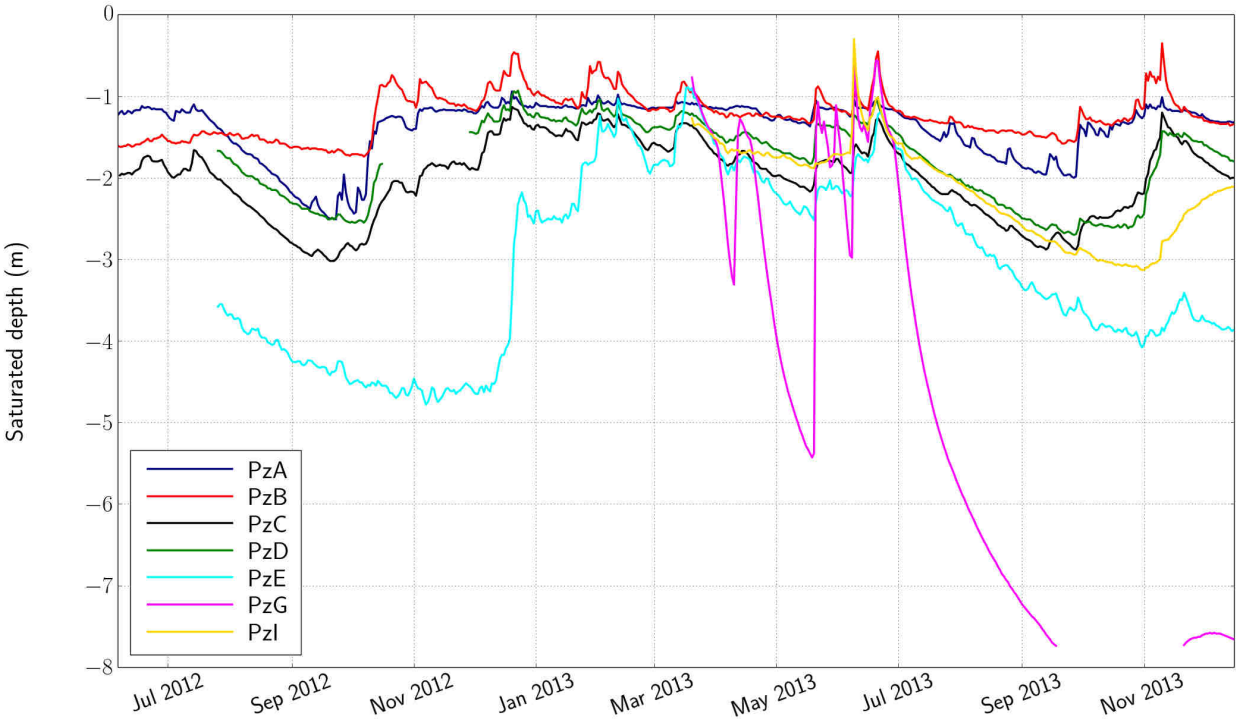

Figure 7.3 – Variation of groundwater level observed in the piezometers of Moulon for the period 06/06/2012 - 17/12/2013.

7.1.3 Geodata

Geospatial data of the Moulon area that are available for the present study include (Figure 7.4):

- vector maps of:
  - parcels (polygons), provided by DGFIP[4]
  - existing installations (buildings) (polygons), provided by DGFIP
  - streets (lines), provided by IGN[5]
  - vegetation covers (polygons), provided by IGN
- master plan of the site (land uses, installations, etc.) in the form of CAD file (.dwg), made by AutoCAD®
- an elevation file at 10m resolution, provided by IGN
- aerial photographs taken in 2012 at 5m resolution, provided by EPPS

[4]DGFIP: Direction Générale des Finances Publiques de France
[5]IGN: Institut national de l'information géographique et forestière de France

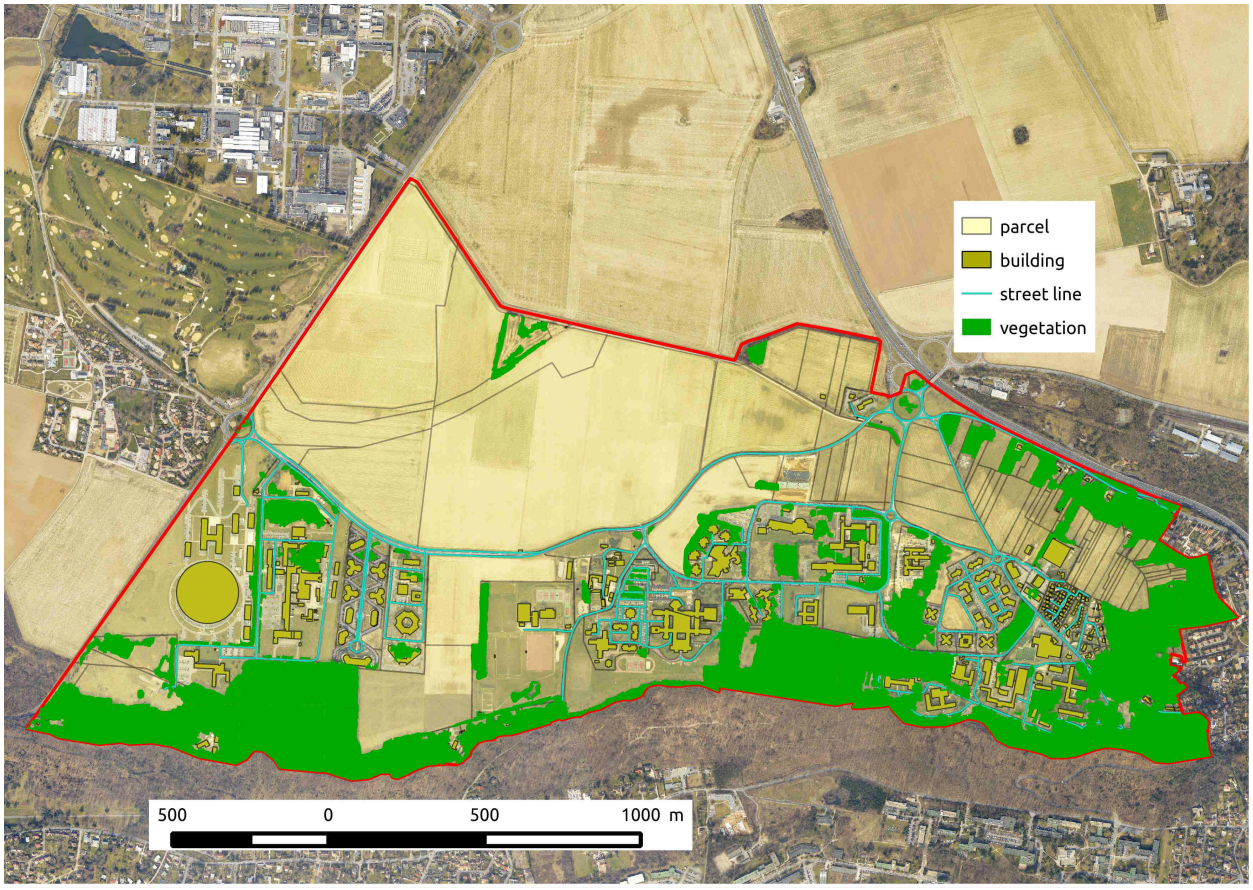

Figure 7.4 – Initial GIS datasets for the Moulon area

7.2 Geodata pre-processing

Departure from the datasets listed above, a pre-processing was conducted in order to prepare three geodata input files needed by our model: (1) UHEs, (2) Interfaces and (3) Flow routing map. This work was fulfilled by Zhou (2013) during his master's thesis supervised by both E. Berthier (of CEREMA) and me.

Topological and value errors were examined and corrected throughout the pre-processing. The work method and technique used are similar with that employed for the Pin Sec catchment (Chapter 4).

7.2.1 Parcels and buildings

The datasets of parcels and buildings are organized by towns. The Moulon area covers one part of each of three towns: Saint-Aubin, Gif-sur-Yvette and Orsay. The fragmented polygons are unified with the *Union* tool of QGIS.

7.2.2 Streets

The dataset of street lines has a satisfactory quality. Still some corrections and completing have been made based on the aerial photographs. The street polygons needed for constructing UHEs were constructed during this work. The technique consists in making a geometry difference between the whole Moulon area and the polygons of parcels, in such a way that no gap lefts between parcels and the generated street surfaces (Figure 7.5). With this procedure, we consider that the street covers the whole "public" area not included in the parcels.

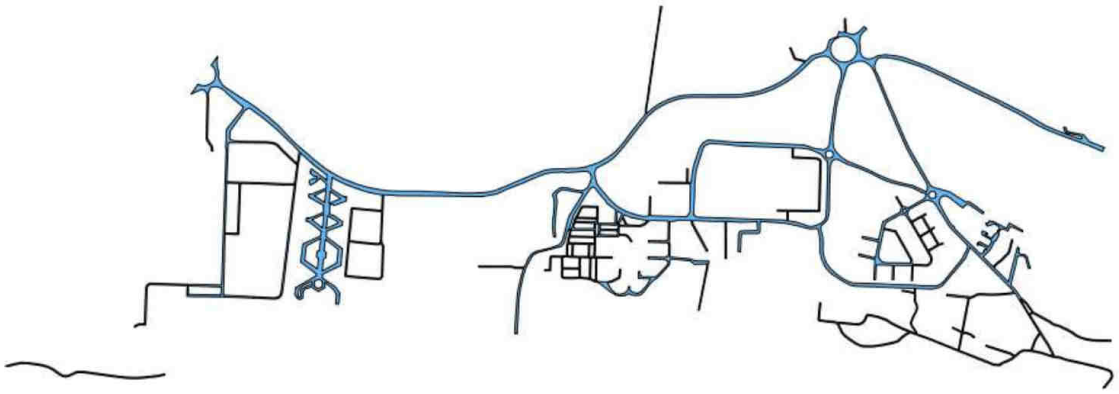

Figure 7.5 – Rendering of street surface construction (Zhou, 2013).

7.2.3 UHEs and Interfaces

The objects (polygons) of UHEs and Interfaces are constructed with the technique presented in Chapter 4, Sections 4.4 and 4.5. The processing is fulfilled with the SQL shell OrbisGIS. The entire SQL scripts are given in Appendix A.5. 379 UHEs are finally obtained, with 1092 Interfaces, as illustrated in Figure 7.6.

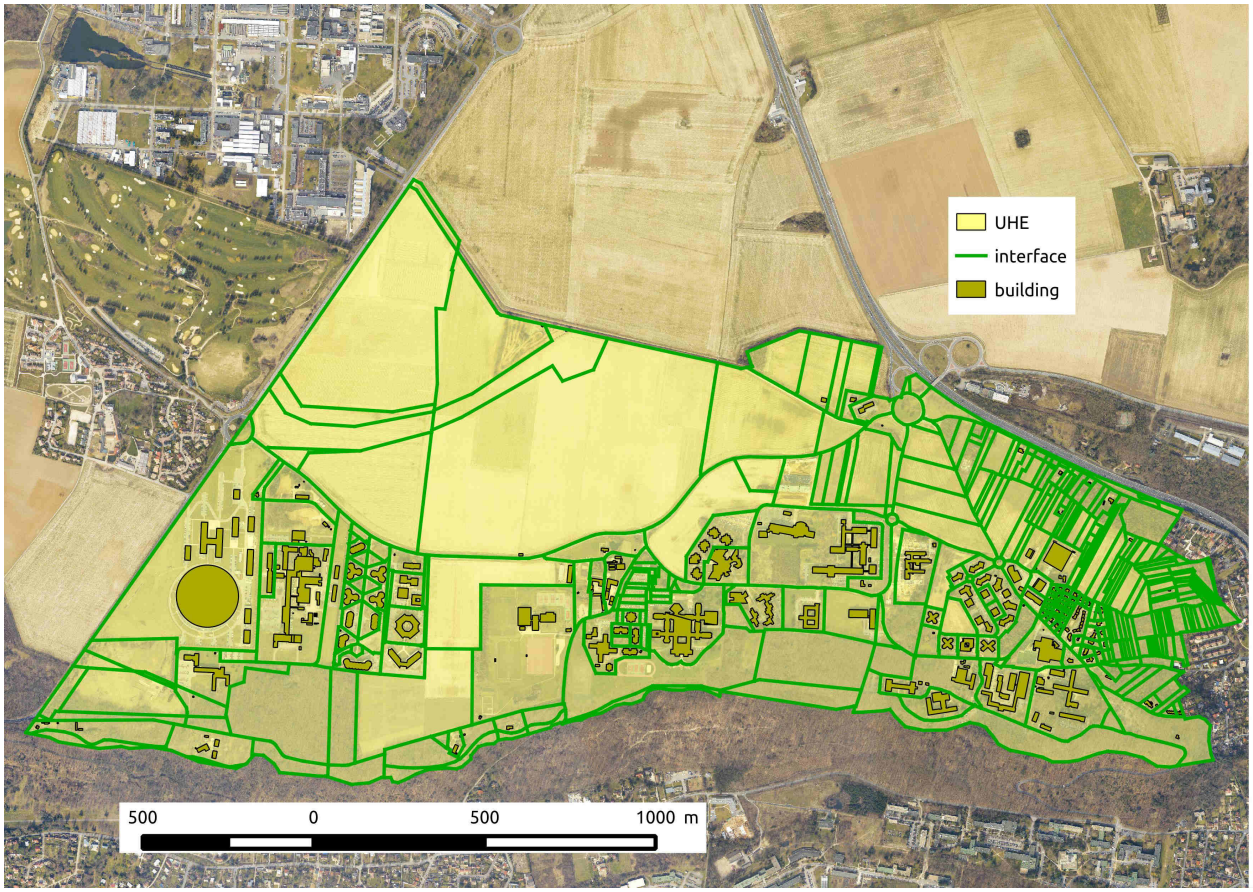

Figure 7.6 – UHEs and Interfaces of current Moulon obtained by geodata pre-processing.

7.2.4 Definition of geometrical parameter values

Geometrical parameters of UHEs, Interfaces and flow routing segments are in Table 2.1, 4.1 and 2.2 respectively. Some parameters are existing in the datasets of parcels, buildings and street lines, such as surface areas or street segment lengths. Others need to be calculated, such as coordinates and elevation of feature points, area of tree-cover, etc. This work is fulfilled with SQL shell of OrbisGIS, coupling with tools provided by QGIS and GRASS. The detailed SQL script is given in Appendix A.6.

7.2.5 Land use of current Moulon assessed by geodata pre-processing

Table 7.2 shows the surface areas of the land cover assessed by the geodata pre-processing. The total area A^{tot} of 338 hectares is composed by 291 hectares of natural land surface A^{nat} and 47 hectares of impervious land surface A^{imp}, which is divided into 20 hectares of buildings A^{hou} and 27 hectares of streets A^{str}. This land use type includes the impervious surfaces within the parcels, which have been estimated, for each parcel, based on the aerial photographies. The impervious surface ratio is 0.14. Tree-cover on natural lands (A^{nat}_{tree}) is 80 hectares, about 27%, and 2 hectares

on streets (A_{tree}^{imp}). Tree-cover represents overall 24% of the total catchment of Moulon (A_{tree}^{tot}).

The hydraulic conductivities and storage capacities of the land covers are derived from previous studies (Rodriguez et al., 2008), except the hydraulic conductivity of natural surface K_s^{nat}, which is estimated based on the hydrogeological study (Dumont et al., 2013) and on the literature (Section 7.3). Noted that a storage capacity of 0.5 mm for a roof corresponds to a slopping roof or to a flat roof having quick downspouts drainage (Azzout et al., 1994). The connection coefficients of the land uses to sewer networks are supposed to be the same as in Pin Sec (Chapter 5), as precise information is not available.

Table 7.2 – Land cover of Moulon at its pre-development conditions assessed by geodata pre-processing, and parameters of the different land use in URBS – hydraulic conductivity at saturation K_s^{nat}, storage capacity (S) and coefficient of connection to sewer networks.

symbol	area (ha)	signification	K_s^{nat} (m/s)	S (mm)	connection coef.
A^{nat}	291	natural surface area	1×10^{-6}	5	0.2
A^{hou}	20	roof surface area	0	0.5	1
A^{str}	27	street surface area	7.5×10^{-8}	3.5	1
A^{imp}	47	total impervious surface area	-	-	
A_{tree}^{nat}	80	tree cover on natural surface	-	-	
A_{tree}^{imp}	2	tree cover on streets	-	-	
A_{tree}^{tot}	82	total area of tree cover	-	-	
A^{tot}	338	total surface area of the catchment	-	-	

7.2.6 Construction of flow routing map

Flow routing network of URBS is composed of buried stormwater drainage network and streets (cf. Chapter 2). The construction of flow routing map consists in aggregating these two layers by establishing the connections between the segments (street to street, street to sewer, sewer to sewer), as explained in Chapter 2, Section 2.3. However, GIS layer of the stormwater networks is not available for the Moulon area. Data of the storm- and wastewater sewer networks is included in two types of files: (i) maps of drainage networks provided by the municipalities, in .pdf format; (ii) geotechnical survey reports by engineering consultancies missioned by EPPS, in .dwg (AutoCAD) format, as illustrated in Figure 7.7.

The flow routing map is thus constructed based on these two data sources. This work is composed of two main parts: (i) convert the objects in the .dwg files into GIS format (shape file); (ii) build geographical parameters for the drainage segments. The softwares (both AutoCAD and GIS softwares we use) have poor capabilities for layer conversion (from .dwg to .shp). Consequently,

the objects conversion is realized by a succession of steps in combining the functions of all the softwares. This work will not be detailed here.

A second difficulty is always related to the data quality: missing information and conflicting feature values are recurrent in the datasets, as illustrated in Figure 7.7. No process has thus been able to be deployed for automatically assigning geometrical parameter values. The work is done manually (segment by segment). The obtained layer of drainage network is shown in Figure 7.8.

The layers of streets and stormwater network are then merged to form the flow routing network. Connections of street segments to sewer segments are established according to the approach proposed by Rodriguez et al. (2003): if a sewer segment exists at a street intersection, the downstream of a street is a sewer segment, otherwise it is another street.

According to the current hydrological functioning of the area (cf. Chapter 6, Section 6.6.1), the stormwater outlets of Moulon are resumed by four points (Figure 7.8):

- outlet1 is the channel Rigole de Corbeville
- outlet2 and outlet3 correspond to the connections to downstream municipal sewer networks
- outlet4 is the connection to the stormwater system of the road N118

7.3 Modeling framework

7.3.1 Simulation period

There is no flow rate measurement for the Moulon area. Piezometric measurement is the only observation data with which we can compare the simulation results. The piezometric data covers the period of 06/06/2012 - 17/12/2013. The modeling is undertaken through the period of 01/01/2011 - 31/12/2013, period for which data of rainfall and potential evapotranspiration is available.

7.3.2 Boundary and initial conditions

Flow rates of the shallow groundwater is not clearly known (Chapter 6, Section 6.6.1), but the hydrogeological study driven by CEREMA (Section 7.1.2) shows that underground inflow and outflow of Moulon should not be significant. During the present study, a zero-flow boundary condition is defined at the lateral of the soil. No boundary condition is assigned on the bottom.

There is not information on the shallow groundwater level at the beginning of the modeling period (01/01/2011), as there was not groundwater monitoring before the piezometers of CEREMA were installed on the area. The average saturation depth on 01/01/2013 of the piezometers was -1.2 m. This value is applied as a uniform initial condition for saturation depth z_s^0.

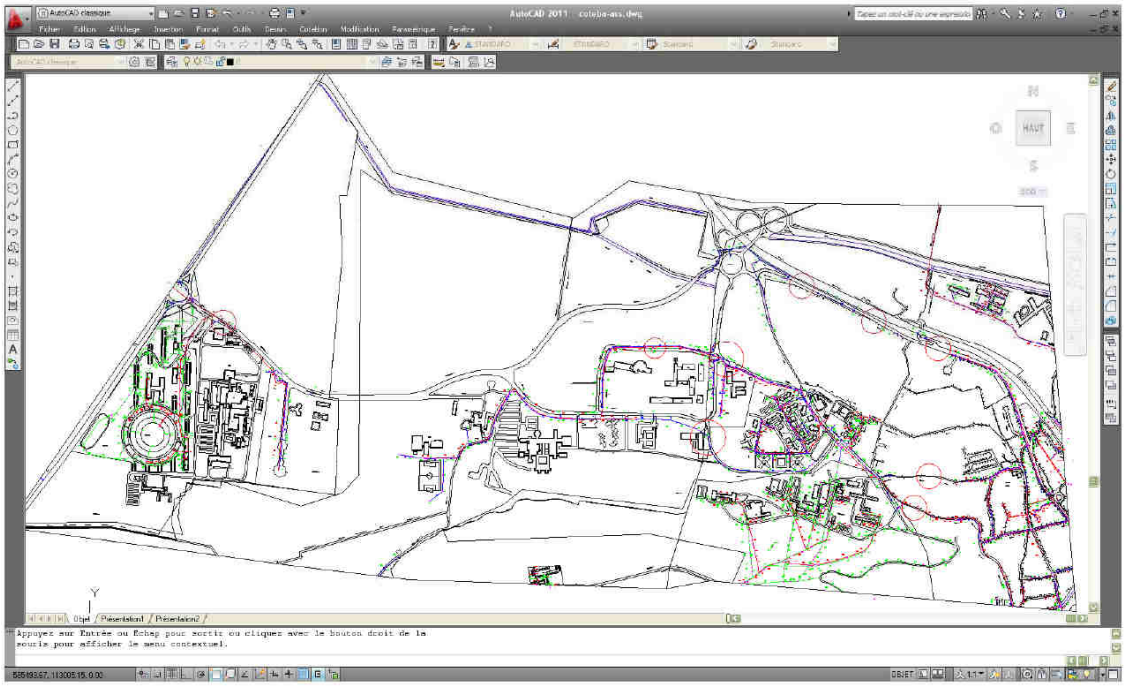

(a) Map of the stormwater drainage network in .dwg format. Red circles mark missing information on geometrical feature (elevation).

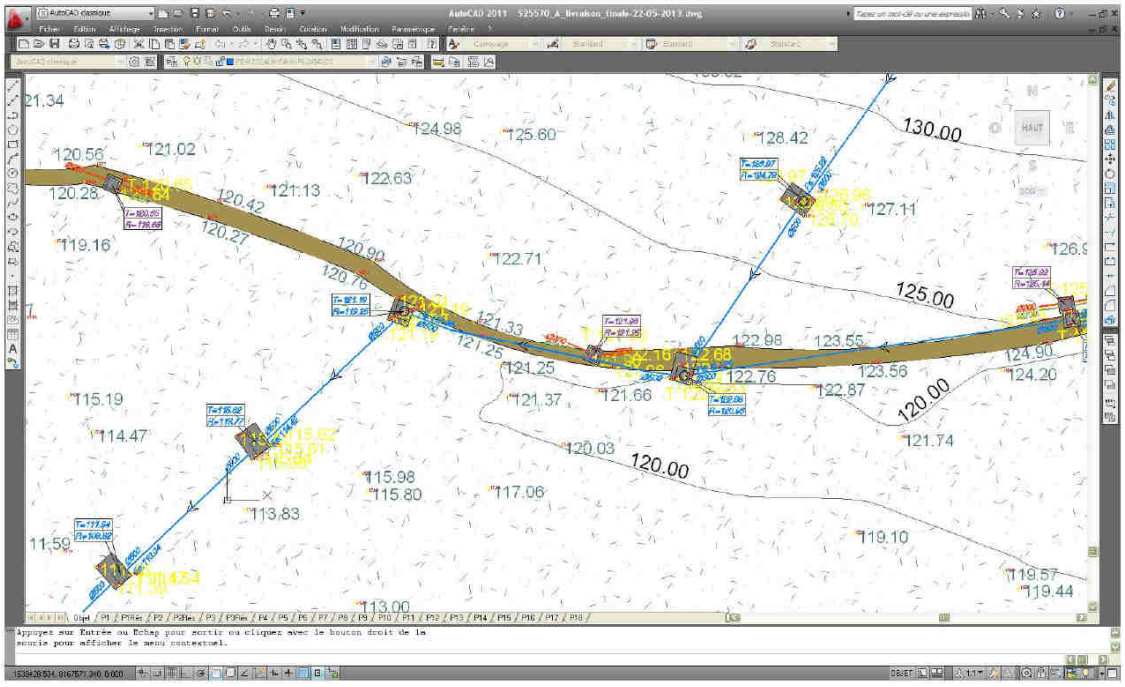

(b) A zoom: geometrical features of drainage network segments.

Figure 7.7 – Illustration of initial data of stormwater drainage network.

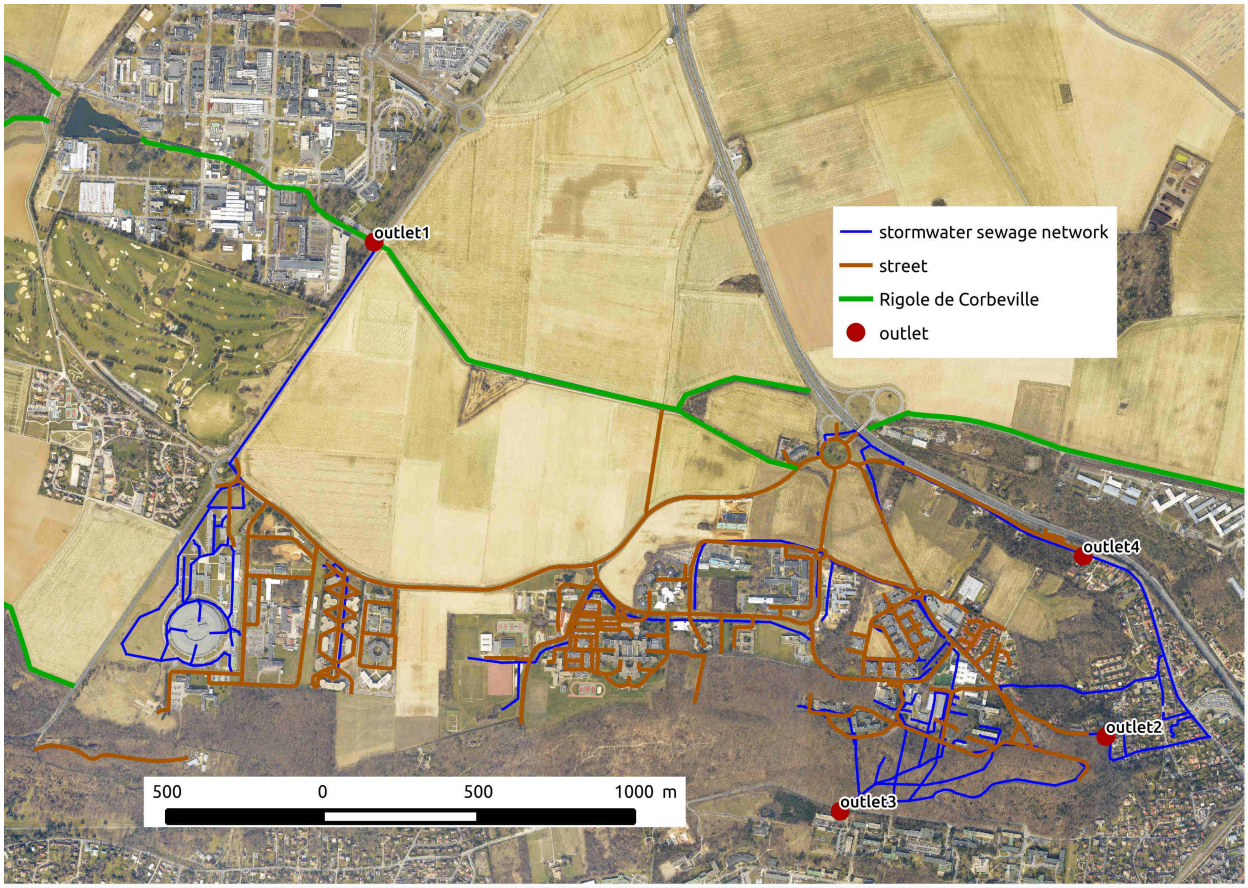

Figure 7.8 – Flow routing network of current Moulon constructed by geodata pre-processing.

7.3.3 Groundwater drainage by sewer networks

In the model, the groundwater infiltration flux of an UHE to its contiguous storm- and wastewater network segments are calculated with Equation 2.12. As explained in Chapter 2, Section 2.5, only the stormwater sewer networks are included in the model input, not the wastewater sewer networks. The fraction of groundwater drainage between the two networks are estimated approximately by their linear ratio. This ratio has been estimated as 1:2 for the Pin Sec catchment (Chapter 5). For the Moulon catchment, we do not have exploitable information on the linear ratio between the storm- and wastewater sewer networks. We remain to use the same ratio (1:2) as for the Pin Sec catchment.

7.3.4 Physical parameters

Due to the geological heterogeneity of the subsurface, it is very difficult to define the hydraulic conductivity of the superficial aquifer (Dumont et al., 2013). The fluctuations of this aquifer seems to be strongly controlled by rainfall. An area with dry subsoil at the end of summer can become completely saturated in winter. The agricultural drainage system over the northern part

is connected to Rigole de Corbeville and complicates the hydrogeological situation.

The permeability of the superficial soil layers estimated by historical pumping tests is between 6×10^{-5} and 7×10^{-6} m/s (BRGM, 1999). In the present study, the initial hydraulic conductivity at saturation K_s is defined at 1×10^{-6} m/s.

The value of the scaling parameter M has been calibrated at the Pin Sec catchment to 2. This parameter characterizes how K_s is reduced by the soil compacting in depth. Assigned on Moulon, M is a simplified parameterization of the soil condition which is composed of multiple layers. It is thus difficult to estimate the value of M, and $M = 2$ has been kept. A sensitivity study (Section 7.5) will allow to calibrate its value for this catchment.

The groundwater drainage coefficient λ has been calibrated to 30 during the study at the Pin Sec catchment. But a high λ value signifies a high leak rate by the sewer networks. Not having information about the conditions of the sewer networks at Moulon, we selected $\lambda = 4$.

The physical parameters and initial saturation depth discussed above are summarized in Table 7.3. The other physical parameters are derived of previous model development (Morena, 2004; Rodriguez et al., 2008). With such estimated parameters, a first modeling is carried out on Moulon, labeled as "Moulon base-run", which is the reference for the sensitivity analysis later.

Table 7.3 – Values of physical parameters applied for the Moulon base-run.

	signification	unit	initial Value	variation range
K_s	hydraulic conductivity at saturation	m/s	1×10^{-6}	$[1 \times 10^{-8}, 1 \times 10^{-5}]$
M	scaling parameter of the hydraulic conductivity	-	2	[0.1, 25]
λ	groundwater drainage coefficient	-	4	[0, 100]
z_s^0	initial saturation depth of the catchment	m	1.2	[0.2, 3]

7.3.5 Modeling results evaluation

Three categories of modeling outputs are examined for evaluating the Moulon base-run:

- Water balance
- Discharge at the outlets of the catchment
- Saturation depth

7.4 Results of Moulon base-run

Water balance

Table 7.4 shows the water balance simulated by the Moulon base-run. A total rainfall of 1962 mm has been recorded during the entire simulation period. 2% is intercepted by tree covers and 98% is non-intercepted rainfall P. The low interception rate is correlated with the low level of tree coverage on this catchment (8% over street surfaces and 27% over natural soil). Evapotranspiration (E + TR) accounts for more than 70% of P. Runoff generated on impervious surfaces (Q^{hou} + Q^{str}) equals to 8.2% of P. Considering the weak impervious surface ratio (0.14), this result is not surprising. However, natural surface produces a relatively high quantity of runoff Q^{nat}, equaling to 11.0% of P. At the same time, groundwater drainage by sewer networks Q^{drain} represents only 1.2% of P. The high contribution of natural surface and low contribution of groundwater drainage are similar to what was found in the base-run on Pin Sec (Chapter 5, Section 5.5). Apart from the fact that the natural surface ratio is high on Moulon (86% of total surface area), the parameter values, such as the groundwater drainage λ, should be partially the reason and should be reviewed. The overall recharge to groundwater is positive (Δstorage) and equivalent to 4.7% of P.

Table 7.4 – Simulated water balance of current Moulon by the base-run of URBS-WTI. All the flow and storage components are expressed in percentage of total rainfall.

Q^{hou}	Q^{str}	Q^{nat}	Q^{drain}	E	TR	Δstorage	P
5.0	3.2	11.0	1.2	11.9	63.3	4.7	100

Discharge at catchment outlets

The discharge volumes at the outlets simulated by Moulon base-run are shown in Table 7.5. A total volume of 1,353 10^3m^3 (Q^{tot}) is discharged from the catchment during the simulation period, equivalent to 400 mm in water depth. 41.2%, about 557 10^3m^3 (165 mm) is discharged to the Rigole de Corbeville (Q^{out1}). 28.5%, about 386 10^3m^3 (114 mm) is discharged to downstream municipal sewer networks ($Q^{out2+out3}$). Another 30.3%, about 410 10^3m^3 (121 mm) is released to the road ditch of N118 (Q^{out3}).

Table 7.5 – Simulated discharge of current Moulon by Moulon base-run – volumes (10^3m^3), fraction (%) and equivalent water depth (mm).

	Q^{out1}	$Q^{out2+out3}$	Q^{out4}	Q^{tot}
volume	557(41.2%)	386(28.5%)	410(30.3%)	1353
height (mm)	165	114	121	400

Saturation depth

Comparisons between observed and simulated saturation depths at the seven piezometers are shown in Figure 7.9. The simulated saturation depth at each piezometer has been calculated by the average of the simulated saturation depths of the UHEs near (< 50 m) the piezometer. And the comparison criteria are in Table 7.6. The groundwater levels are overestimated for all the piezometers, the same as the base-run on Pin Sec (Chapter 5). For several piezometers (PzA, PzB, PzC and PzD), the simulated soil is totally saturated during spring 2013. The overestimation leads to poor values of C_{nash}.

For the piezometers PzA, PzC and PzD, which have "typical" patterns with high level in winter and low level in summer, the simulated curves are comparable with the observed ones, with good R^2. For the other piezometers, it is expected that the model can not reproduce their "atypical" patterns.

Table 7.6 – Comparison criteria (C_{nash} and R^2) for groundwater levels by Moulon base-run. The criteria are computed for 06/06/2012-17/12/2013, period for which piezometric data is available.

Criteria	PzA	PzB	PzC	PzD	PzE	PzG	PzI
R^2	0.748	0.428	0.825	0.840	0.762	0.510	0.163
C_{nash}	-2.7	-3.4	-3.8	-2.6	-2.3	-1.9	-2.3

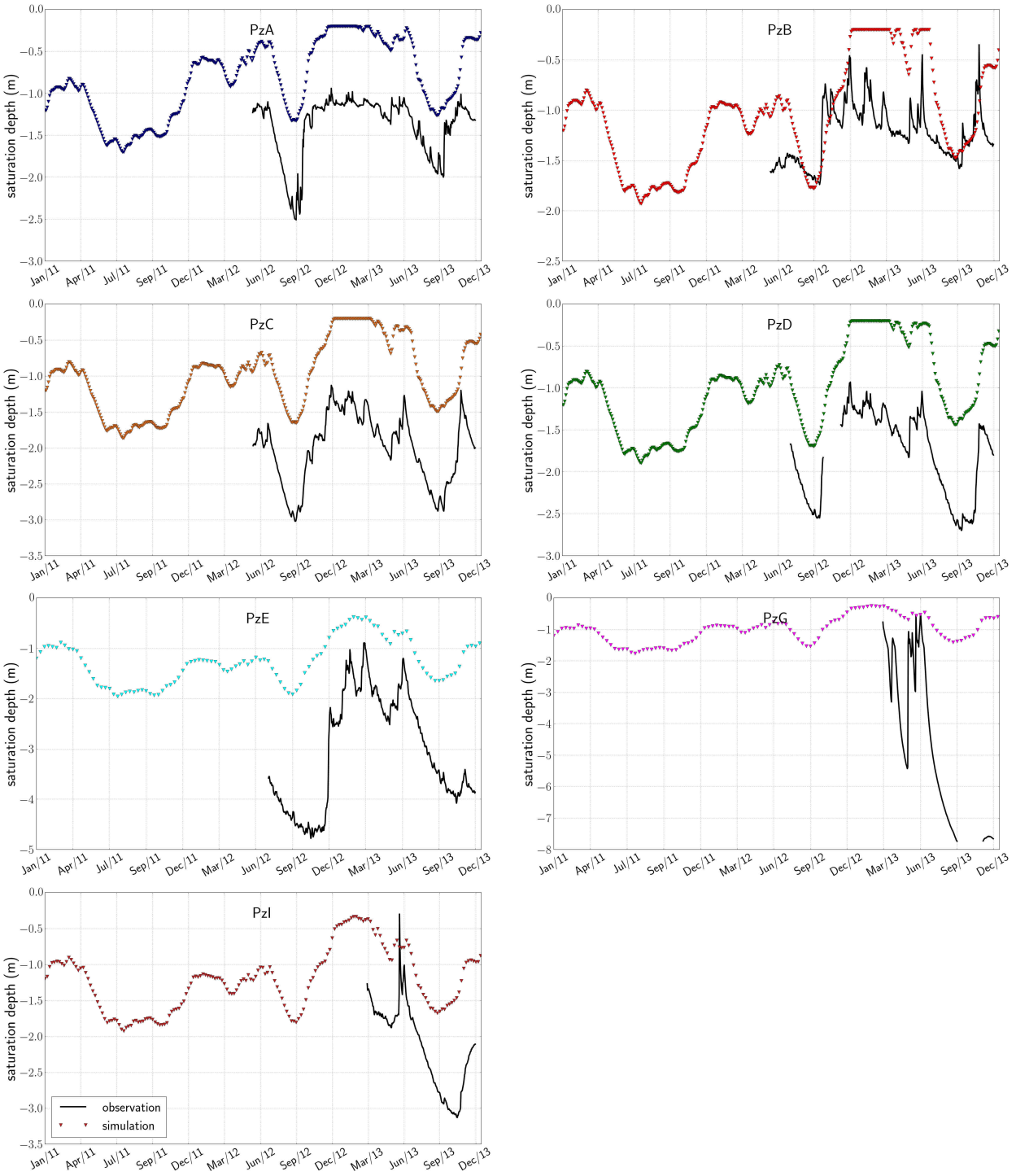

Figure 7.9 – Time series of simulated groundwater level at the seven piezometers by Moulon base-run, compared with measured series.

7.5 Sensitivity analysis and manual parameter calibration based on groundwater level simulation

The results of Moulon base-run suggest that we might face to a similar case as for the Pin Sec catchment (cf. Chapter 5): overestimation of the groundwater levels caused by weak dynamics of the flows, especially infiltration flow of groundwater to sewer networks. In the case of Pin Sec, raising the value of the parameters M and λ has been able to solve to some extent this problem. Nevertheless, given the fact that the multi-layer subsurface at Moulon is not analogous to that of Pin Sec, it is not rigorous to assign the same methodology as for on Pin Sec. In this section, a sensitivity study is conducted, with a manual parameter calibration based on groundwater level simulation.

The same parameters as for Pin Sec are chosen to be tested (Table 7.3): (i) hydraulic conductivity at saturation K_s (ii) scaling parameter M and (iii) groundwater drainage coefficient λ. The initial condition of saturation depth z_s^0 was also selected given that the groundwater levels are overestimated by the base-run.

The sensitivity analysis is undertaken with one-parameter-at-time method, i.e. a new simulation for every change of each parameter. As groundwater level is the only observation data series we have, the sensitivity analysis is based on the modeling results of groundwater level. The modeling quality is evaluated with the comparison criteria C_{nash} and R^2, calculated on the simulation/observation of groundwater levels, accompanied by visual examination of the curves when necessary. Due to the fact that the recorded groundwater level series are highly heterogeneous, investigating the piezometers one by one can be confusing and not lead to tangible conclusions. We have chosen to study the sensitivity from a general view on the piezometers: the criteria are calculated for each piezometer, and we examine the average of the criteria values.

Initial saturation depth

As the Moulon base-run overestimated the groundwater level, which questioned the initial condition on saturation depth z_s^0, this initial condition is firstly examined. As shown in Figure 7.10a, the criteria C_{nash} and R^2 display reverse trends: while C_{nash} increases with deeper initial z_s^0, expressing better fitting of simulated levels with to observed ones and corrected overestimation to some extent, R^2 decreases, signifying that the level dynamics has been damaged. The model sensitivity to z_s^0 is notable, announced by the relative large variation range of C_{nash} and R^2.

Hydraulic conductivity at saturation

As shown in Figure 7.10b, C_{nash} and R^2 show non-monotone patterns for K_s. Especially C_{nash}, which can be improved both by stronger and weaker values of K_s, with a "worst" value at 5×10^{-7} m/s. Noted that the plot criteria is the average of the piezometers and that the piezometers can

have different sensitivity to a same parameter, this non-monotone trend is not so surprising, which confirms furthermore the heterogeneity existed in the observed series. Small values of K_s reduce the dynamics of groundwater level, expressed by R^2. For values beyond 5×10^{-7} m/s, R^2 tends to be stable. As for z_s^0, the model is significantly sensible to K_s.

Scaling parameter

The model is not very sensitive to the scaling parameter M of hydraulic conductivity for values larger than 1, as illustrated in Figure 7.10c. But below this value the modeling quality can be dramatically damaged. C_{nash} trends slightly to be improved by large values of M.

Groundwater drainage coefficient

The criterion C_{nash} is sensitively variable with λ, with a variation range of -6 to -1. But it is not the case for R^2, as shown in Figure 7.10d. Stronger values of λ can improve the modeling quality of groundwater level for values between 0 and around 50. Beyond 50 the improvement is limited.

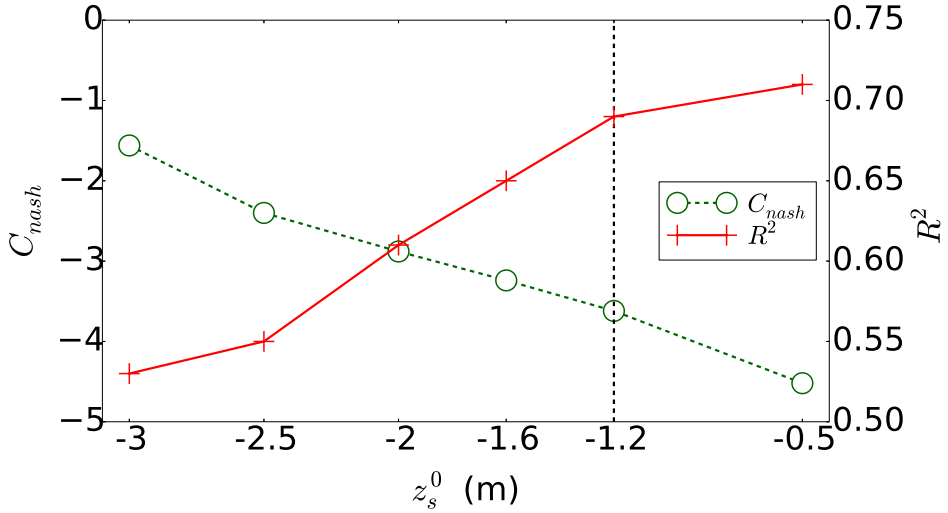

(a) z_s^0

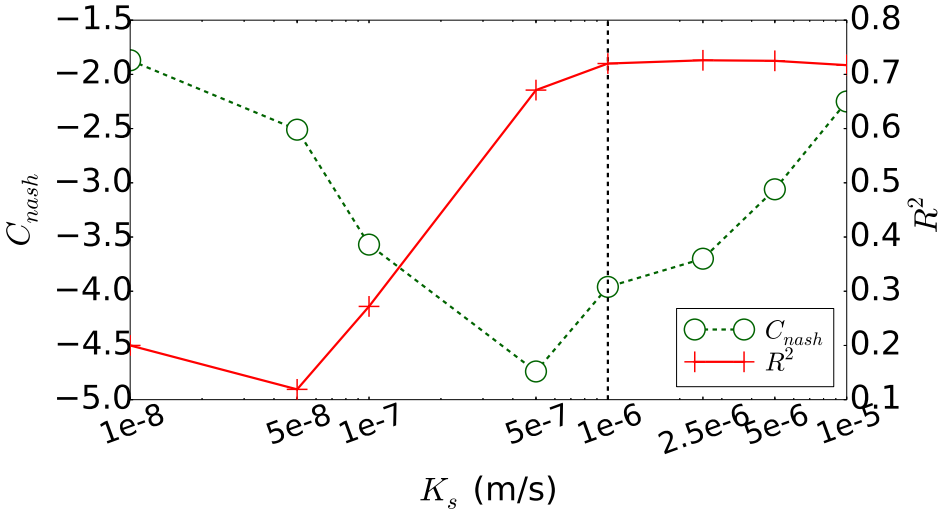

(b) K_s

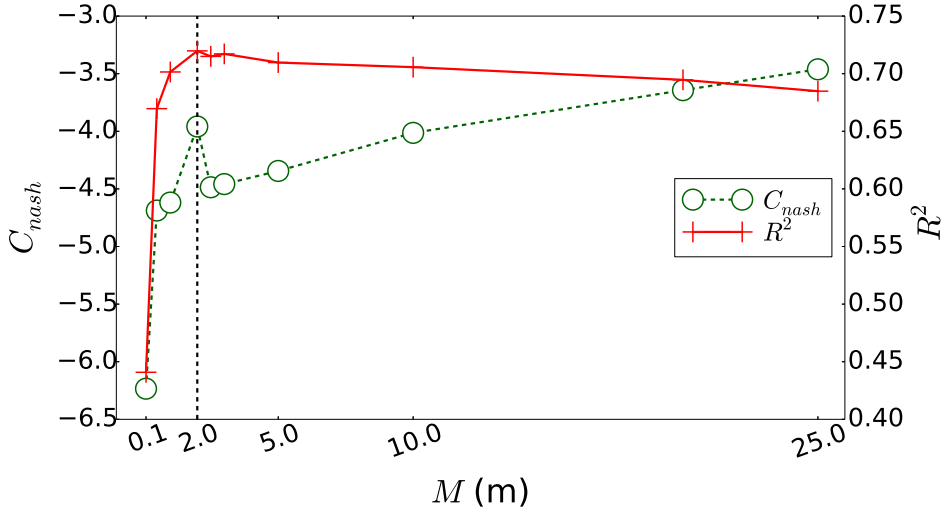

(c) M

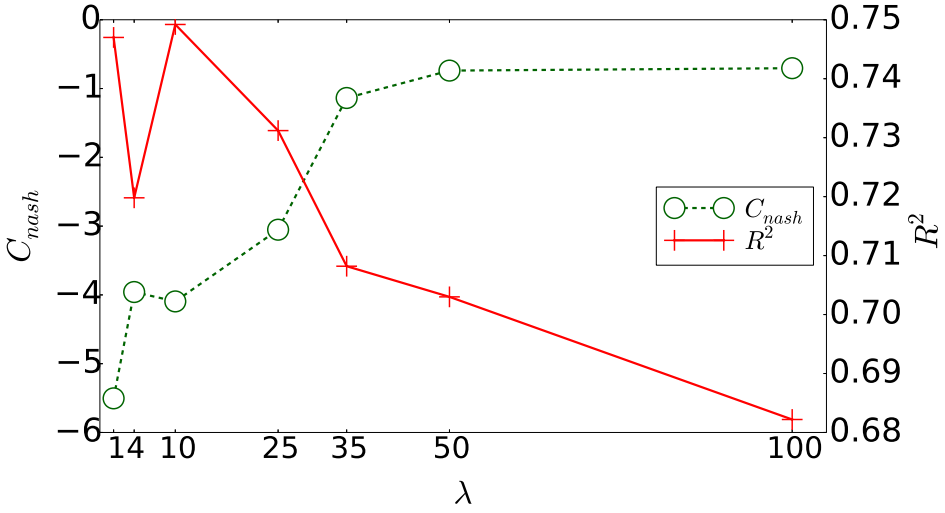

(d) λ

Figure 7.10 – Sensitivity to physical parameters of groundwater modeling at Moulon.

Selection of "best" parameter values

The model sensitivity in terms of groundwater level modeling measured by the criteria C_{nash} and R^2 presented above provides useful information on the model behaviour. However, how to define the "best" set of values for the tested parameters is a more complicated task that can not be based uniquely on the sensitivity analysis. First, the criteria values examined above are average values of the seven piezometers, which do not necessarily have a trend of evolution with a parameter. Second, for three parameters in four, C_{nash} and R^2 exhibit totally a reverse trend, i.e. while some parameter values permit a better fitting between the simulated and observed groundwater levels (correcting the initial overestimation among others), they deteriorate also the model capacity to well reproduce the dynamics observed in the groundwater level variation. Third, we must take in consideration of the physical meaning for the parameters in such a physically-based model.

Strong hydraulic conductivity K_s lead better values both for C_{nash} and R^2. Meanwhile, a too large K_s, e.g. 1×10^{-5} m/s, is not consistent with the results given in geological survey reports. We selected ultimately 2.5×10^{-6} m/s for K_s. Same as for K_s, large scaling parameter M seems to improve the modeling quality, at least seen from the C_{nash} curve. But a too large M is conflict with the conception for soil in the model, i.e. hydraulic conductivity decrease in depth due to soil compacting. Furthermore, the trends of the criteria are not significant for $M > 2$. We chose $M = 3$. Strong values for the groundwater drainage coefficient λ can notably improve C_{nash} (even if it is always negative) without too much impacting R^2. But a too large λ, 100 for example, suggests that the sewer networks have a very high level of leaking, which seems to be unrealistic, even we do not have further information on the real condition of the sewer networks. We selected 35 for λ. The selection of the initial saturation depth z_s^0 has proved to be troublesome. Deeper z_s^0 can reduce the bias error of simulated groundwater level with observed one, but the expense is highly reduced dynamics, e.g. for $z_s^0 = 3$ m, we have obtained totally flat groundwater level curves (not shown here), although the overestimation has been corrected. Ultimately we chose a small value for z_s^0, 0.5 m, aiming to keep the dynamics in the simulated groundwater level.

The calibrated parameter values are listed in Table 7.7. With such selected values for the parameters, a calibrated modeling has been carried out. The results are shown in the next section.

Table 7.7 – Calibrated parameter values for the Moulon catchment.

Parameter	Unit	Initial value	Calibrated value
K_s	m/s	1×10^{-6}	2.5×10^{-6}
M	-	2	3
λ	–	4	35
z_s^0	m	1.2	0.5

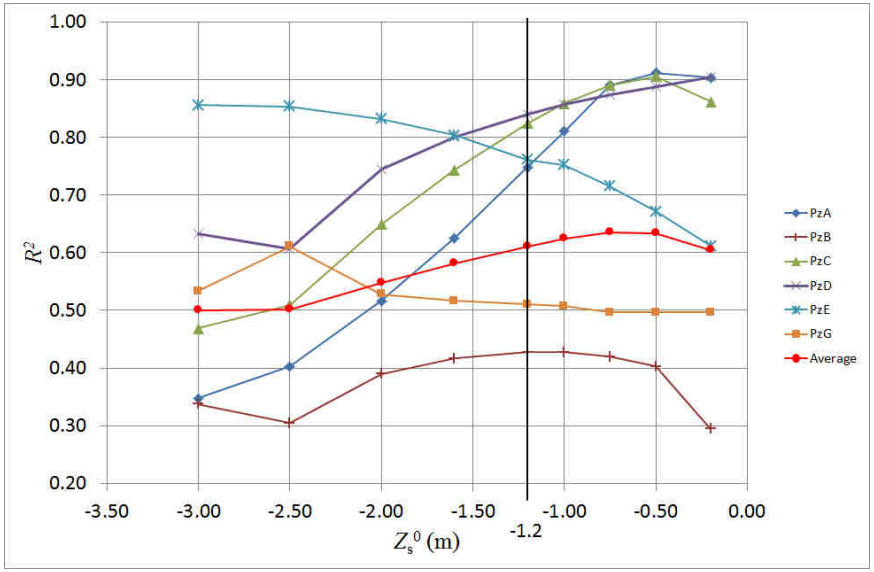

(a) z_s^0

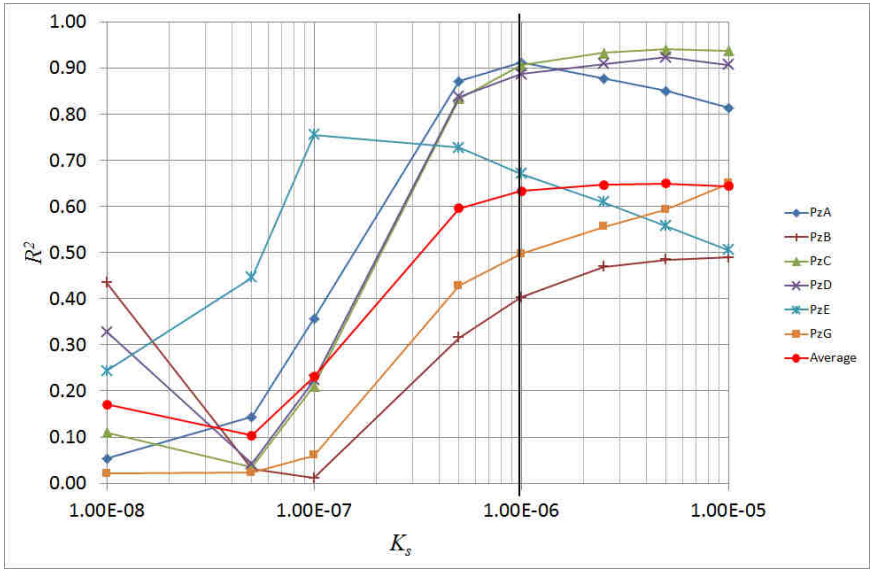

(b) K_s

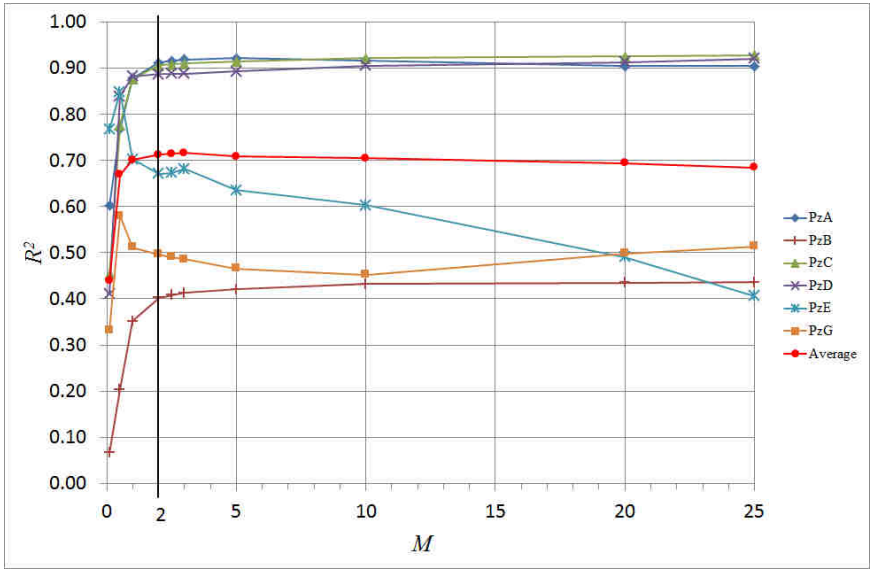

(c) M

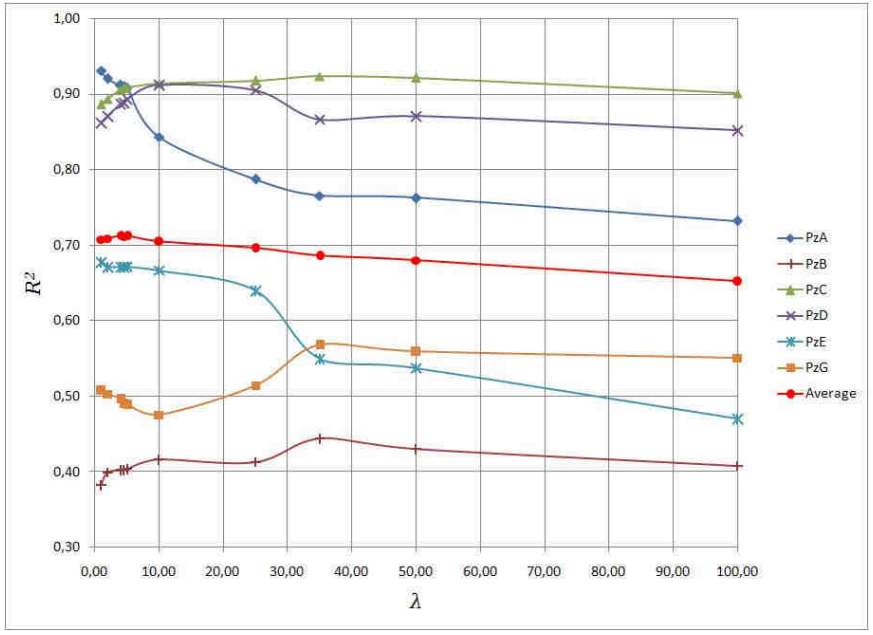

(d) λ

Figure 7.11 – Evolution of R^2 of the seven piezometers with the parameters.

7.6 Final modeling with calibrated parameters

7.6.1 Saturation depth

Figure 7.12 plots the simulated series of saturation depths at the piezometers by the calibrated modeling, against the observed series. Table 7.8 gives the values of comparison criteria C_{nash} and R^2.

For PzA, PzC and PzD, the simulation quality of groundwater levels is largely improved. The levels as well as their temporal variations are close to the observations, especially for PzC and PzD. Only the lowest levels in September have not been reproduced and overestimated about 0.5 m. For PzB, the temporal variation is relatively well reproduced, but not the abrupt fluctuations in the observed curve. The fluctuations are a priori generated by other factors than climate forcings, such as agriculture drainage, but the model does not represent these processes. For PzE, PzG and PzI, which have "atypical" observation patterns, the agreement between simulation and observation remains poor.

Table 7.8 – Comparison criteria (C_{nash} and R^2) for groundwater levels by Moulon calibrated run. The criteria are computed for 06/06/2012-17/12/2013, period for which groundwater observation data is available.

Criteria	PzA	PzB	PzC	PzD	PzE	PzG	PzI
R^2 base-run	0.748	0.379	0.845	0.849	0.654	0.546	0.714
R^2 calibrated	0.689	0.443	0.899	0.886	0.389	0.503	0.684
C_{nash} base-run	-2.7	-3.4	-3.8	-2.6	-2.3	-1.9	-2.3
C_{nash} calibrated	0.57	-0.36	0.80	0.83	-0.16	-1.16	0.40

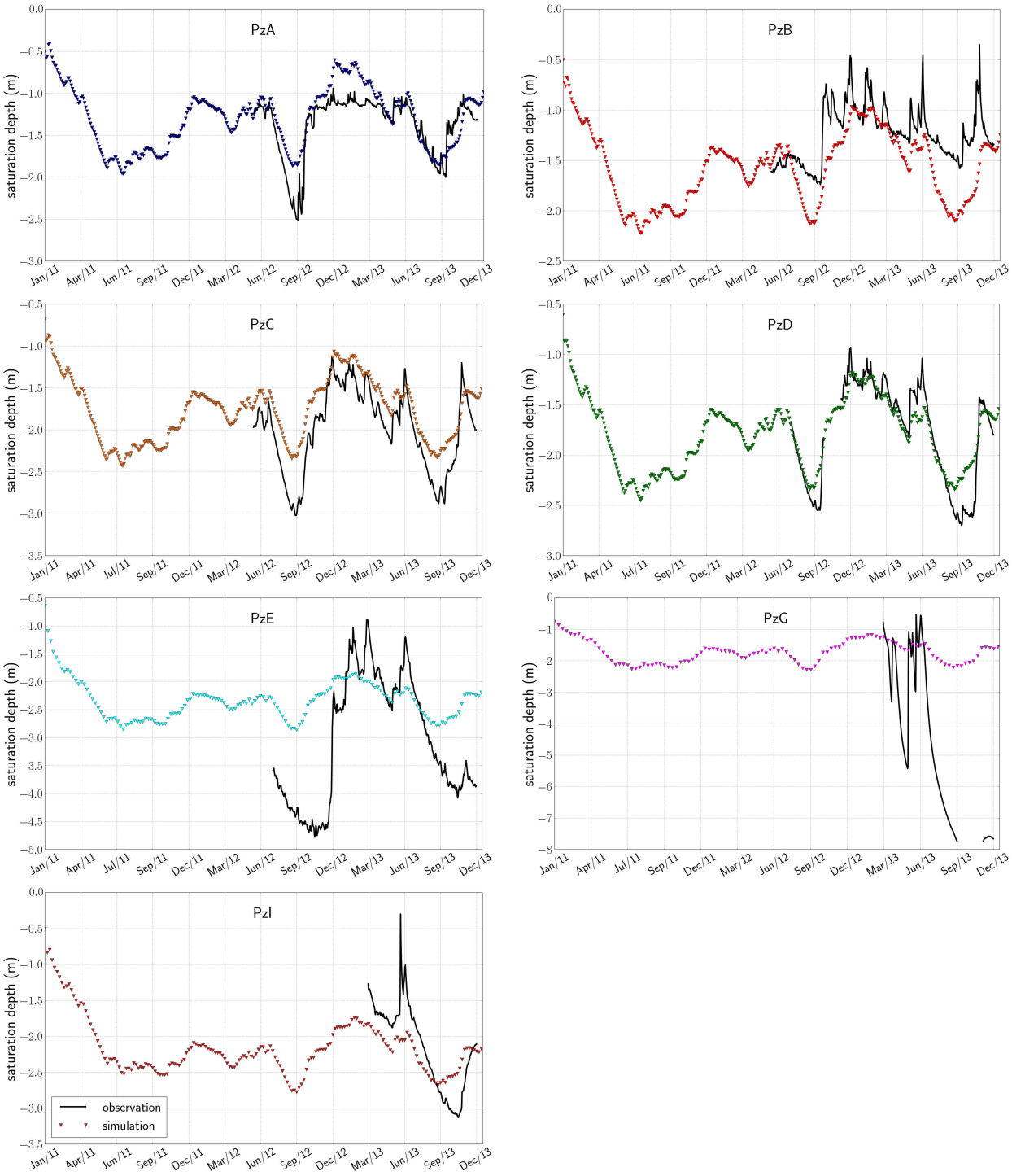

Figure 7.12 – Time series of simulated groundwater level of current Moulon at the seven piezometers by model calibrated run, compared with measured series.

7.6.2 Water balance

We examined then the catchment-wide water balance and discharge volumes assessed by the model calibrated run. Table 7.9 shows the simulated water balance, with flow and storage components expressed as percentage of the total rainfall.

Total rainfall P during the three-year simulation is 1962 mm. Evapotranspiration ($E + TR$) remains high and equals to to 69.1% of the total rainfall (75.2% by base-run), composed of 7.0% of evaporation and 62.1% of transpiration. E is reduced compared to the Moulon base-run (7.0% vs. 11.9%), implying that storage on the surface is reduced and that the soil saturation occurs less often than the base-run.

Table 7.9 – Estimated water balance of current Moulon by the calibrated run of URBS-WTI, compared with the water balance assessed by the model base-run.

	Q^{hou}	Q^{str}	Q^{nat}	Q^{drain}	E	TR	Δstorage	P
base-run	5.0	3.2	11.0	1.2	11.9	63.3	4.7	100
calibrated	5.0	2.6	2.2	30.3	7.0	62.1	-9.4	100

Surface runoff ($Q^{hou} + Q^{str} + Q^{nat}$) is reduced to 9.9% of the total rainfall, with 5.0% from building roof, 2.6% from streets, and 2.2% from natural surfaces. Compared to the base-run, runoff on natural surface is largely cut. Groundwater drainage Q^{drain} is raised to 30.3% of the total rainfall, split into 10.1% in stormwater network and 20.2% in wastewater network. Linked to the enforced Q^{drain}, the groundwater level is lowered (Δstorage).

Figure 7.13 shows, in a detailed manner, the catchment water balance estimated by the calibrated modeling.

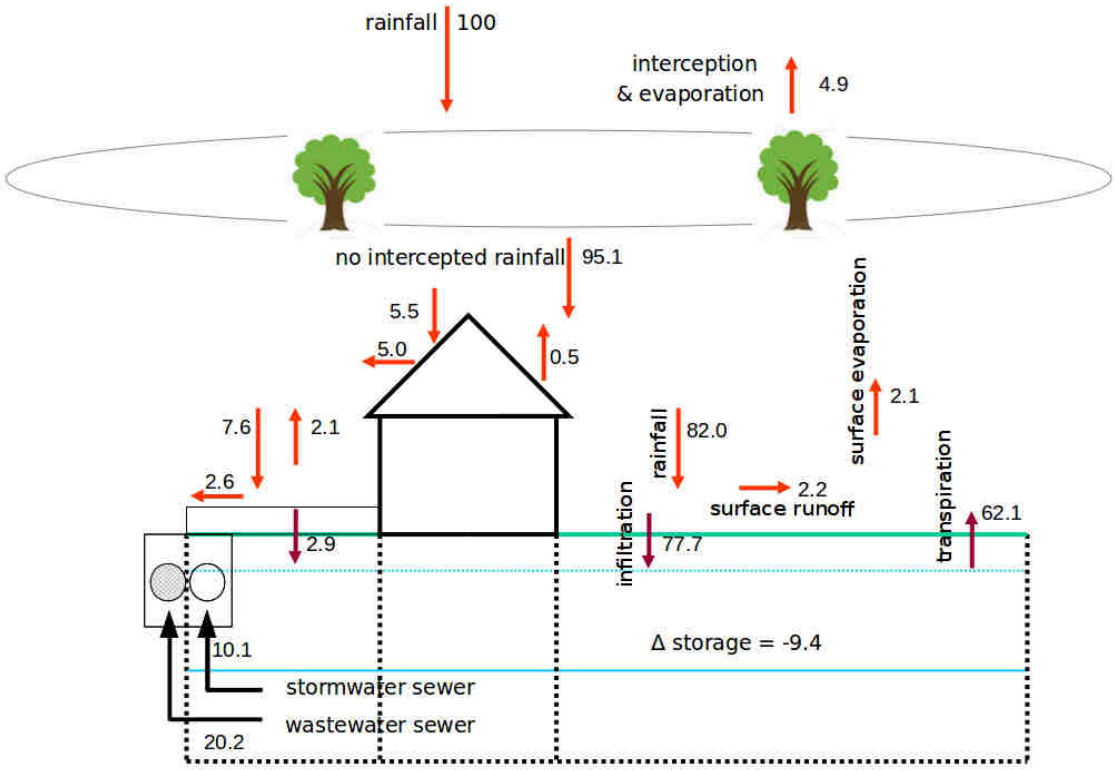

Figure 7.13 – Simulated water balance of the Moulon catchment at its pre-development (current) state, by the calibrated run of URBS-WTI. All variables are expressed in percentage of the gross rainfall. For a sake of convenience, fluxes are detailed for natural soil and are omitted for street and roof.

7.6.3 Discharge

Flow volumes at the outlets of the catchment simulated by the model calibrated run are shown in Table 7.10, in comparison with Moulon base-run. A total discharge of 1323 10^3m^3 is discharged from the catchment during the simulation period, equivalent to 391 mm in water depth, 9 mm less than Moulon base-run. 487 10^3m^3, about 36.8% is released into the Rigole de Corbeville (Q^{out1}). 406 10^3m^3, about 30.7% is released into municipal sewer networks ($Q^{out2+out3}$). The left 32.5%, 430 10^3m^3 is discharged to the road ditch of N118 (Q^{out4}).

Table 7.10 – Simulated discharge of current Moulon by calibrated run – volumes ($10^3 m^3$), fraction (%) and equivalent water depth (mm), compared with Moulon base-run.

		Q^{out1}	$Q^{out2+out3}$	Q^{out4}	Q^{tot}
base-run	volume	557(41.2%)	386(28.5%)	410(30.3%)	1353
	height	165	114	121	400
calibrated run	volume	487(36.8%)	406(30.7%)	430(32.5%)	1323
	height	144	120	127	391

7.6.4 Spatially distributed simulation of groundwater level

One leading feature of the URBS model is its capability to simulate spatial distribution of hydrological variables (Rodriguez et al., 2008). Figure 7.14 illustrates the seasonal cycle of the spatially distributed groundwater level simulated by URBS-WTI. The illustration period is from 01/09/2012 to 01/10/2013, covering a whole hydrological year.

After its seasonal descent during summer 2012 (Figure 7.12), the groundwater attains low levels in many of the parcels (01/09/2012), before rising again during winter 2012 (01/12/2012 and 01/03/2012). Then, by high evapotranspiration rates in summer 2013, the groundwater level goes down to attain, on 01/10/2013, a level similar to that on 01/09/2012. The east and south parts are highly covered by vegetations, thus show higher seasonal contrasts, while in the urbanized center zone, the variation of groundwater level is less pronounced. These results affirm the high importance of the evapotranspiration process in the evolution of groundwater level.

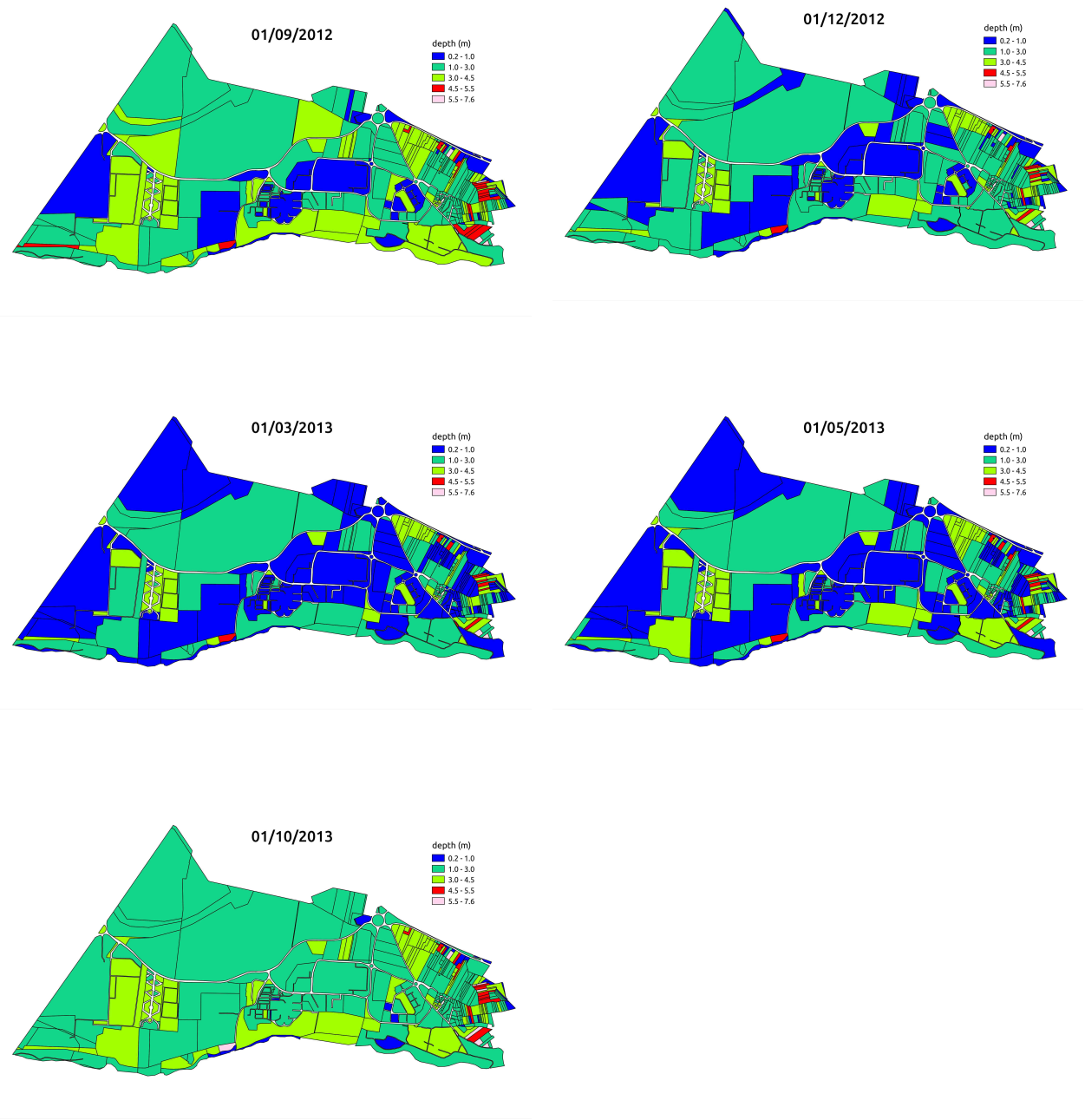

Figure 7.14 – Spatially distributed groundwater level simulated by URBS-WTI.

Discussion and conclusion

In this chapter we described the modeling study for the Moulon area at its pre-development (current) state. Coarse datasets have been treated and new data layers created with GIS-based tools in order to prepare the geodata input of Moulon for the model.

Initial parameter values applied in the base-run have been estimated in coarse way, in a context that information of the studied area is limited and that the formulations for subsurface flow is a conceptual parameterization of the soil. These estimated parameters have lead to mediocre modeling quality with high overestimation on groundwater level. Following the first results, a sensitivity analysis has been undertaken for several physical parameters for the subsurface. The modeling quality has been fully evaluated on groundwater level simulation, which is relatively original in urban hydrology, but which has ultimately conducted to plausible results.

Here again, the parameter calibration has been delicate due to both the heterogeneity shown by the piezometric observation series and physical meanings exhibited by the parameters. But the ultimately selected parameter values have permitted to relatively satisfying results.

Due to limited time, the integrated model URBS-WTI, validated at Pin Sec, has been directly applied on the Moulon catchment, and we did not test simulations without WTI. But the spatially distributed patterns of groundwater level on the several selected date seem to be sound.

The parameter set obtained with this “calibrated” simulation has been finally kept, and the modeling results with these calibrated parameters are considered to be “real” and reflective of the hydrological functioning of the Moulon area. This result series will be the reference for the study for post-development of the area described in the next chapter.

Chapter 8

Evaluation of hydrological impacts of the urban development of Moulon and of LID devices by scenario study under post-development (future) conditions

Contents

Introduction

Pre-development hydrological regime of the Moulon catchment was studied through a modeling approach by the URBS-WTI model, and presented in the last chapter. This regime will be altered by the urban development in the coming decades. Meanwhile, devices for low-impact stormwater management are planned to be implemented to minimize the impacts of the urbanization and control the flooding risk in the valley areas of Yvette and Bièvre.

In order to investigate urbanization effect on the hydrological response, as well as the efficiency of the LID devices, a scenario study has been conducted for the post-development state of the Moulon area.

For the sake of simplicity, the post-development state Moulon is described as "future Moulon", and scenarios of urban development are described as "scenarios of urbanization". This chapter is composed of five sections. Section 8.1 outlines the preparation work of geodata input files based on future geomorphological features of the site, considered to be the referential land use configuration of future Moulon. A referential modeling based on the referential land use is detailed in Section 8.2. An analysis on this result is presented in Section 8.3. After outlining the methodology for the scenario study in Section 8.4, the modeling results at catchment scale and urban block scale are presented in the last two sections.

8.1 Preparation of geodata input for future Moulon

This work has been realized by (Farias, 2013) during his master's thesis supervised by me.

8.1.1 Construction of flow routing map

The flow routing map of future Moulon is composed of two types of objects (cf. Chapter 2, Section 2.3): (i) street network, (ii) stormwater management and drainage network. The last refers to three types of devices (Chapter 6):

- buried sewer pipes
- storage basins
- swales and filter drains

Most of existing sewer pipes will be kept, a small part of them are to be withdrawn. Since precise information on the sewer pipe withdrawing is not available, we suppose that the entire existing sewers used for the current state modeling is kept. Existing and projected storage basins play a major role to runoff control of the future campus. But for instance the model URBS-WTI does not include any suitable module of storage basins. In the present modeling, the storage basins are replaced by swales. The layers of storage basins, swales and filter drains are drawn manually in QGIS preceded by an overall exploration of planning documents of every district of the campus provided by EPPS. Figure 8.1 shows an example of the reference document serving for the construction of these layers.

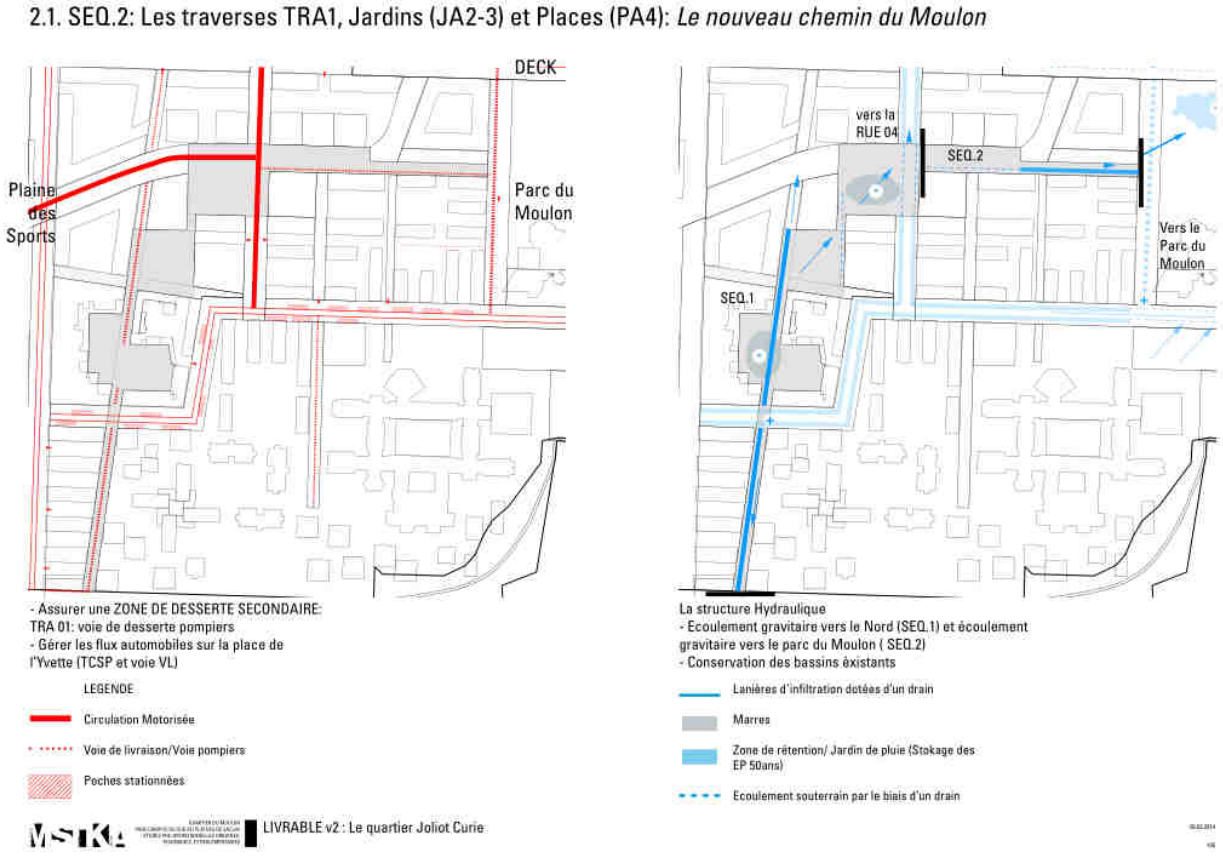

Figure 8.1 – An example of the documents referred to which the GIS layers of stormwater management devices (swales, filter drains and storage basins) are constructed: feasibility analysis of *Joliot Curie* district.

As well as the map of stormwater management devices, the street map of the future Moulon is not available, and is constructed during the present work based on information included in miscellaneous planning documents of EPPS. This map includes two types of objects: polygons of street surfaces serving for constructing UHEs, and lines of street segments.

Once all the GIS layers (sewer pipes, swales, filter drains, streets) are ready, the hydrological flow routing map of stormwater is built by linking all the objects with the same methods as before (Pin Sec and current Moulon):

- The upward/downward connection between two objects of the same layer is established by MNT[1].
- A street segment is connected downwardly either to an underground sewer pipe, a filter drain, a swale, if any of them exists, or to another street segment if not.
- If such established connection is in conflict with logical flow direction (towards storage basins or swales), it is corrected manually.

The outlets of the future Moulon are defined in the master plan of the Paris-Saclay project (Figure 8.2):

outlet 1 : the channel *Rigole de Corbeville*

outlet 2 : the channel along the road RN118

outlet 3 : a eastern connection to the sewer systems of the city of Orsay

outlet 4 : a southern connection to the sewer systems of the city of Orsay

In this way, stormwater originating in Moulon is conveyed finally into the Bièvre River (outlet 1 via the channel network of the plateau) in the north and Yvette River (outlet 2, 3 and 4) in the south .

8.1.2 Urban blocks and UHEs

The parcels of the future campus of Moulon are not yet defined today. Only urban blocks are outlined by the street network. An urban block may in reality contain more than one parcel. However, as our model does not have any constraint on the size of an UHE, an urban block can act as a parcel. The spatial discretization of the future Moulon is based on the urban blocks, and an UHE is consequently composed of an urban block and its adjacent street surface.

The UHEs are drawn based on the network of streets. The geometrical parameters of the UHEs are assessed with the same methods as Pin Sec and current Moulon (Chapter 4, Section 4.6.1 and Chapter 7, Section 7.2.3). 87 UHEs are finally obtained (Figure 8.2). Buildings within the UHEs are obtained by combining the existing buildings and available data for new buildings.

8.1.3 Interfaces

Interfaces are drawn from the UHEs with the method presented in Chapter 4, Section 4.5.

[1]The future topography of the site is considered to be little modified. The current MNT is thus used.

8.1.4 Assumptions on pavements within UHEs and on tree covers

No information is available on the allocation of impervious surfaces and tree covers within the urban blocks. Assumptions have been made on these surfaces:

- In addition to buildings, 15% of surface within urban blocks is supposed to be impervious.
- 5% of the natural surface as well as impervious surfaces are supposed to be covered by trees.
- These ratios are uniformly applied to all the UHEs.

The spatial pattern of land use of the future Moulon such obtained is shown in the map of Figure 8.2, with a land cover summary in Table 8.1. Compared to the current Moulon, natural surface area is reduced from 86% to 66% of total catchment's surface, and impervious surfaces (buildings + streets) are extended from 14% to 34% of the catchment's surface, an expansion of 1.5 times. Tree covers on natural surfaces are largely reduced from 80 ha to 11.1 ha. This questions the realness of the assumptions. Tree covers on streets are increased from 2 ha to 3.2 ha, which should favor the transpiration flow on the street land use. The physical parameters of the land uses as well as their connection coefficient are the same as for the current Moulon (Table 7.2).

Table 8.1 – Land cover of future Moulon, compared with current Moulon – land cover fractions and deviation.

	current (ha)	future (ha)	Δ (ha)	Δ(%)	connection coef.
A^{nat}	291 (86%)	223 (66%)	-68	-23	0.2
A^{hou}	20 (6%)	51 (15%)	31	155	1
A^{str}	27 (8%)	64 (19%)	37	135	1
A^{imp}	47 (14%)	115 (34%)	68	146	-
A^{nat}_{tree}	80 (24%)	11.1 (3%)	-69	-86	-
A^{str}_{tree}	2 (0.6%)	3.2 (1%)	1.2	60	-
A^{tot}_{tree}	82 (24.6%)	14.3 (4%)	-67.7	-83	-
					$A^{tot} = 338$ ha

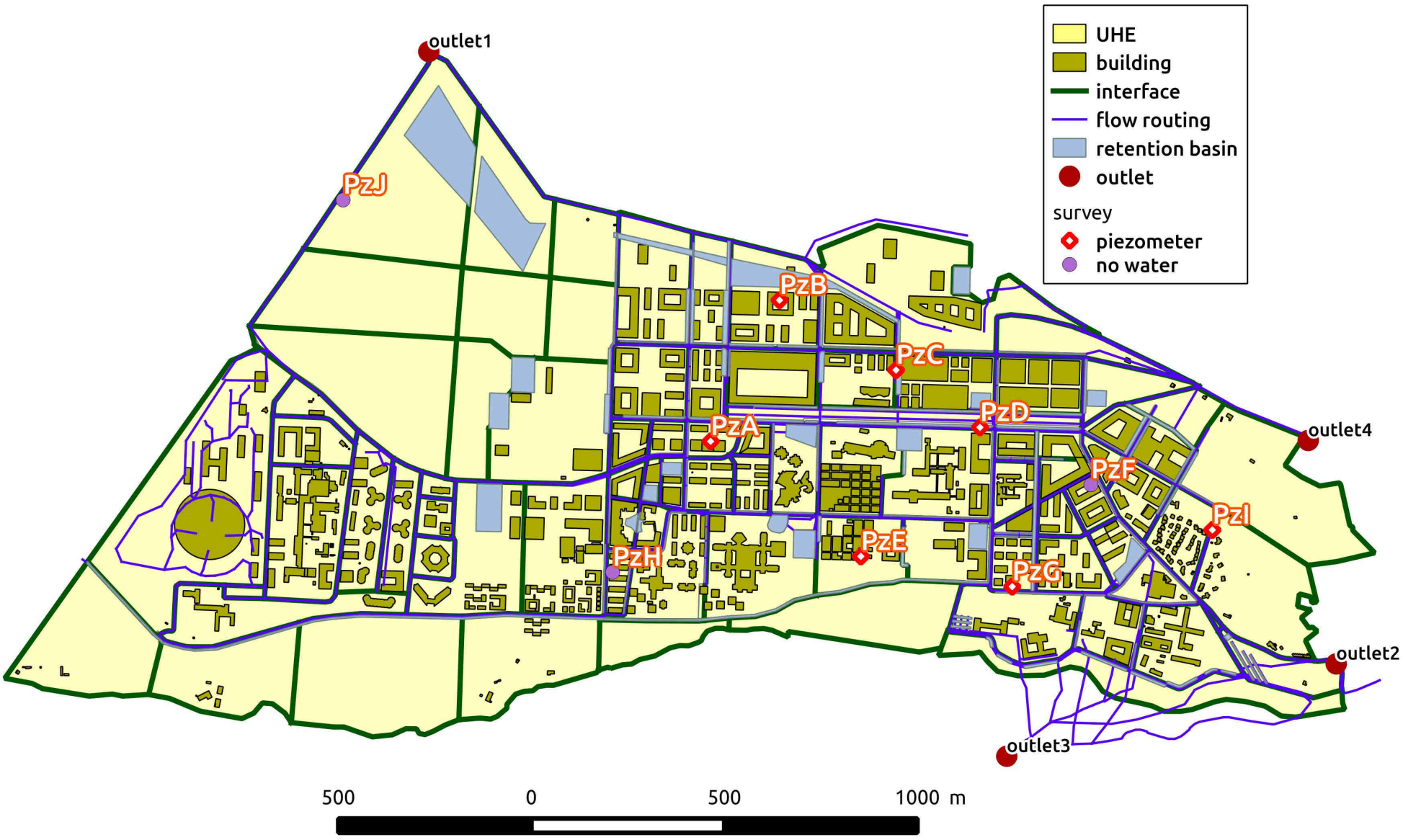

Figure 8.2 – Vector map of future Moulon by geodata pre-processing.

8.2 Referential modeling of future Moulon

A first modeling for the future Moulon is taken on with the morphological configuration obtained above. This first modeling is the reference of comparison for the following scenario study. Parameter values calibrated during the study for current Moulon (Table 7.7) are applied. Climatic inputs used are the same as that used in the modeling for current Moulon: rainfall intensity of the 3-year period of 01/01/2011 - 31/12/2013 with 6-minute time step and potential evapotranspiration for the same period with 1-hour time step.

Swales is a default option for stormwater management in the district level that will be constructed in Moulon (cf. Chapter 6). This device is thus not subjected to the scenario tests, but applied by default in the modeling. The swale module in URBS has been outlined in Chapter 2, Section 2.7.4. A swale is integrated in the flow routing network for which the model can assess the flow rate of any segment at any time. In addition to its water routing function, a swale also allows water to infiltrate within the surrounding soil. The infiltrated water is added into the vadose zone of adjacent UHEs.

A preliminary test has been carried out in order to see the impact of the infiltration function of the swales. The results show that with or without the infiltration function of the swales, the modeled results (water balance, groundwater levels and discharge) are not much different, as shown in the following. This could be related to: (i) the small density and linear of the swale grid (swales will only be set up in the northern part of Moulon); (ii) the swale module itself (performance and realness of the module), in particular the process of infiltration below the swales. This issue will be subjected to future work and is not included in the present study. In all the modeling of future Moulon (reference modeling and scenario modeling), the infiltration function of the swales is systematically implemented.

8.2.1 Water balance

Table 8.2 shows the simulated water balance of future Moulon, compared with current Moulon. Total rainfall P during the three-year simulation is 1,962 mm. Runoff of rooftops Q^{hou} and streets Q^{str} represents 13.4% and 6.3% of P, respectively, compared with 5.0% and 2.6% in current state, associated with the expansion of buildings (by 155%) and streets (by 135%). Runoff produced on natural surface Q^{nat} is also multiplied by three, equaling to 7.1% of P. This increase is caused by the increased groundwater level: the decrease in water storage in the soil between the end and the beginning of the simulation period Δstorage is equivalent to 2.5% of P, while in current state it was 9.4%. The total surface discharge is thus estimated as 25.4% of P, more than two times of the discharge at current state. The increased groundwater level is directly linked with the decrease almost by half of groundwater drainage by sewer networks Q^{drain} (see Section 8.3). Evaporation loss E is thus increased due to more available water on surface. At the same time, transpiration

loss TR is significantly reduced, from 62.1% of P in current state to 51.7% in future state. This reduction is caused by two factors: i) increase in impervious surface area ii) high retention of water on surface, which deactivates the transpiration processes, assumed by the model.

Compared to the case where the infiltration function is modeled (with swale), the "no swale" case only assesses slightly differences (in Q^{nat}, E and TR).

Table 8.2 – Simulated water balance of future Moulon, compared with current water balance. All the flow and storage components are expressed in percentage of total rainfall. In the "no swale" condition, only the convey function (in the flow routing network) of the swales are modeled, while in the "with swale" condition the infiltration function is also modeled.

State	Q^{hou}	Q^{str}	Q^{nat}	Q^{drain}	E	TR	Δstorage	P
current	5.0	2.6	2.2	30.3	7.0	62.1	-9.4	100
future (no swale)	13.4	6.2	5.8	18.0	7.3	53.4	-2.6	100
future (with swale)	13.4	6.3	7.1	18.3	8.1	51.7	-2.5	100

8.2.2 Saturation depth

The simulated groundwater level (Figure 8.3) confirms the Δstorage component in the water balance. Compared with the current state, the mean groundwater level is about 1 m higher during the simulation period, both for the simulations "no swale" and "with swale". This difference is generated at the beginning of the simulation period and lasts during the rest of the time. While surface sealing reduces surface infiltration, it reduces also losses by evapotranspiration, which is one of the reasons of the groundwater level arise. Another reason is groundwater drainage by sewer networks Q^{drain}. A deeper analysis on this issue is given in Section 8.3.

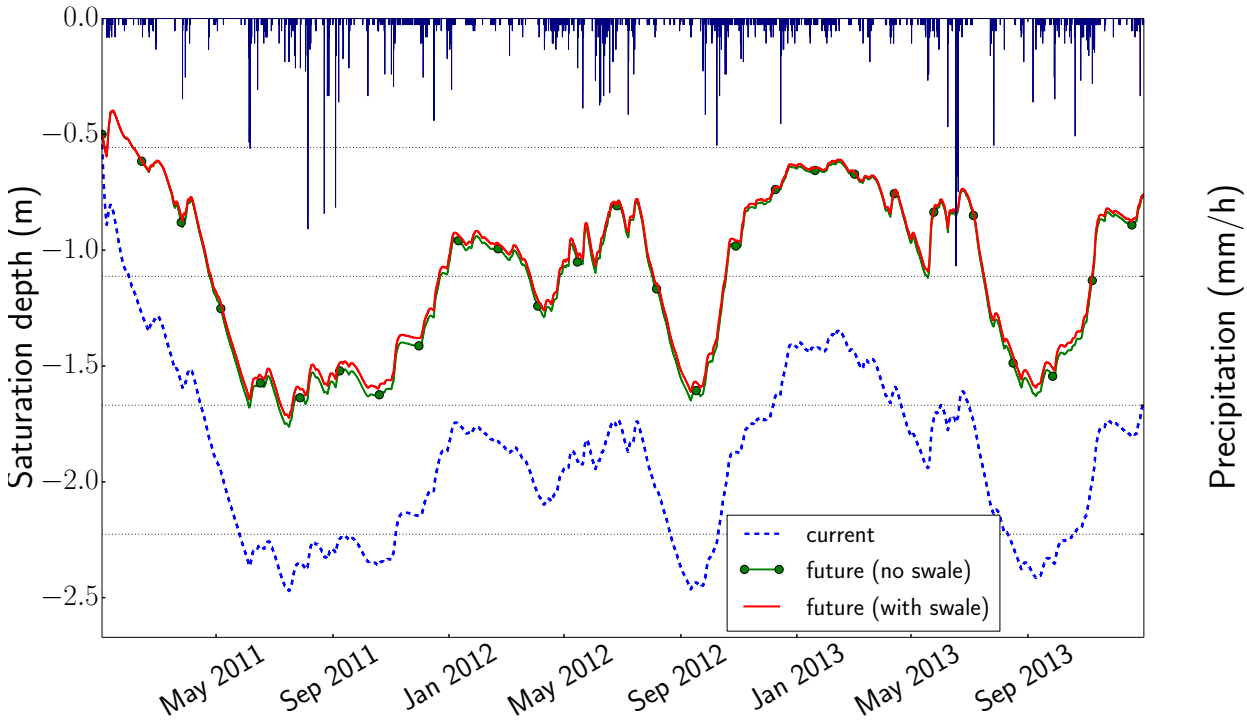

Figure 8.3 – Simulated average groundwater level of Moulon under its future state (solid line), with (no marker) or without (circle marker) the infiltration function of the swales, compared with current state (dashed line).

8.2.3 Discharge

Table 8.3 shows the estimated discharge volumes at each of the catchment outlets at the post-development state. A total volume of 1902/2040 $10^3 m^3$ is generated throughout the catchment, depending on if there is infiltration below the swales. Compared with the current state (1,321 $10^3 m^3$), it is an increase of 44%/54%. The rainfall/runoff ratio is raised to 28.6%/30.7%, compared to 20% at current state. 904/983 $10^3 m^3$, 47.6%/48.2% of the total volume, is discharged into the Rigole de Corbeville (outlet1). Compared to the current state, it is a significant rise both in volume and in fraction. The discharge fractions of other outlets have all been reduced compared with current state, in spite of the increased volumes.

Swale is the only LID device that has been implemented in this modeling, with uniquely its conveyance function represented but not the infiltration function. Another major facilities for stormwater management that will be set up in the area, storage basin, has not been represented due to the model capacity. Therefore, it has been expected that the overall discharge volume at the catchment scale is increased under future conditions caused by higher surface imperviousness.

Compared to the case “non swale”, the swales with infiltration function permits to reduce both the discharge volume of the catchment (by 7%), and at each outlet.

Table 8.3 – Simulated discharge of future Moulon, in comparison with current Moulon – runoff volume ($10^3 m^3$) at the outlets, their fraction (%) and equivalent water depth (mm).

		Q^{out1}	$Q^{out2+out3}$	Q^{out4}	Q^{tot}
current	volume	487(36.8%)	406(30.7%)	430(32.5%)	1323
	height	144	120	127	391
future (no swale)	volume	983(48.2%)	438(21.5%)	619(30.3%)	2040
	height	290	130	183	603
future (with swale)	volume	904(47.6%)	431(22.6%)	567(29.8%)	1902
	height	267	127	168	562

8.3 An analysis on the groundwater level increase

According to the referential modeling for future Moulon, the mean level of the shallow groundwater is about 1 meter higher than the current state (Figure 8.3). At the annual scale, the part of rainfall contributing to groundwater recharge can be coarsely estimated basing on a mass balance of the soil surface :

$$R = P - (Q^{hou} + Q^{str} + Q^{nat} + E + TR)$$

In applying this equation with the flux complaisant in Table 8.2, we can see that R equals to 21.1 for the current Moulon, and around 13.5 for the future Moulon, i.e. the recharge quantity in the future state is less than that of the current state. Consequently, the groundwater level increase can not be explained by R. At the mean time, groundwater drainage by sewer networks Q^{drain} has been sharply reduced by half (18.0% vs. 30.3%). This reduction in Q^{drain} retro-acts on the groundwater level: less drainage, higher groundwater level.

In theory, higher groundwater level should result in stronger groundwater drainage. Apparently this is not the case here. Why is it? As the values of the physical parameter (K_s^{nat}, M, λ) are the same in the two modeling, the groundwater drainage decrease can only be caused by the geometrical features in the two states. In looking at Equation 2.12 (below) that computes the groundwater infiltration fluxes to the drainage network, two geometrical parameters of the drainage segments defines the groundwater drainage volume Q^{drain}: (i) their depths ($z_{soil} - z_{net} - \overline{z_s}$); and (ii) the parameter d_f^u which reflects the influence radius of the drainage segments. The mean depth of sewer network in current and future states are not much different: current -2.58 m and future -2.49 m. Thus the decrease in Q^{drain} is not, a priori, caused by the depth of the drainage network. The sum of d_f^u, however, are significantly different: current 158 m and future 265 m. In addition, d_f^u appears with the square form in the denominator, which must be the main reason of the reduction in Q^{drain}.

$$I_{drain}^u = K_s^{nat} e^{\overline{-z_s}/M} \frac{\lambda}{d_f^{u2}} (z_{soil} - z_{net} - \overline{z_s})^{\mu}$$

The parameter d_f^u is the distance of the deepest point of the parcel P1 to its point of projection on the drainage network, which is an approximative estimation of the flow distance of u. This feature is in fact highly dependent on the spatial discretization of the model. As illustrated in Figure 8.4, suppose a rectangular UHE perpendicular (the simplest configuration) of area $A1$, perpendicular to the drainage segment, with the point of projection C_p1. d_f1 equals to the length (or width) of the UHE. If we divide P1 evenly into two parcels P2 ($A2$) and P3 ($A3$), then P2 and P3 share the point of projection C_p1, and for the parameter d_f^u, we have:

$$d_f2 = \frac{1}{2}d_f1 \text{ and } d_f3 = d_f1 \tag{8.1}$$

which signifies that for the same drained surface area, we have increased the parameter d_f. Consequently, for the same catchment, the thiner its spatial discretization is, the larger the sum of d_f^u is. And this is the case for Moulon: number of discretization units has been reduced from 379 parcels in the current state to 87 urban blocks in the future state, which explains the drastic reduction in the sum of d_f^u.

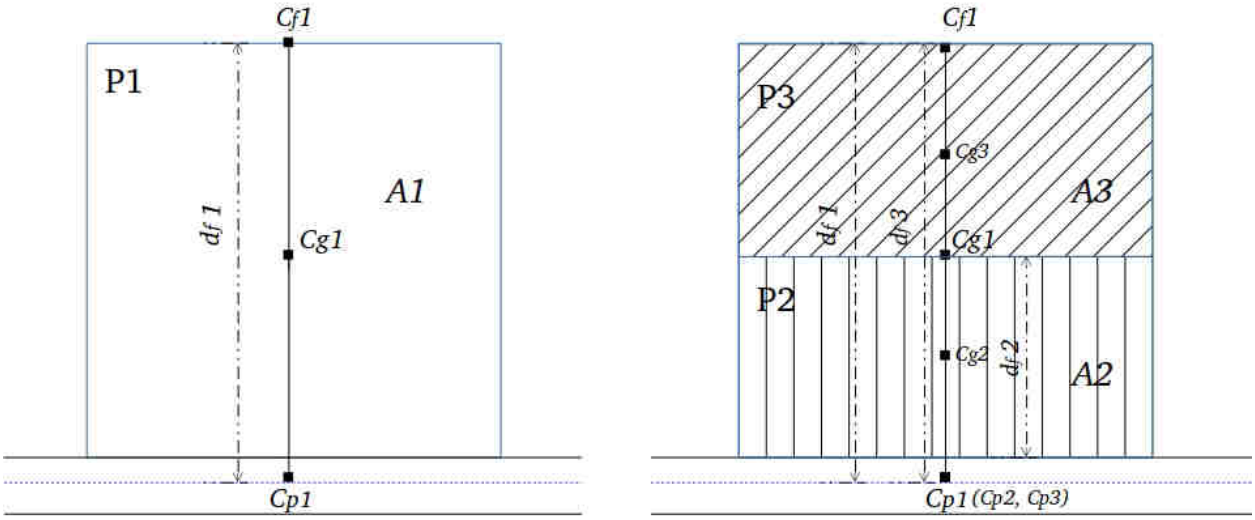

Figure 8.4 – An example of the impact of spatial discretization to the simulated drainage flow of groundwater by sewer network.

This analysis shows the high importance of spatial discretization on the modeling results in the model URBS, and questions consequently the reliability of the approximation made for calculating I_{drain}^u. This important issue should be paid full attention in future model development and application of URBS.

8.4 Methodology for scenario study

The valuation of hydrological impacts of the urban project of Moulon is done through a scenario study. Working with EPPS, we identified two types of scenarios that would be studied:

1. Urbanization. Scenarios for different land use and imperviousness density were generated as different possible future conditions of landscape surface. These scenarios are implemented by modifying directly the input table of the UHEs. The scenarios derived here consider uniform changes in the ensemble of UHEs:

   [pav+50%] increase by 50% of impervious pavements area within urban blocks (buildings not included)

   [pav+80%] increase by 80% of impervious pavements area within urban blocks (buildings not included)

   [hou+50%] increase by 50% of buildings area

   [hou−50%] decrease by 50% of buildings area

   Note that i) the total surface area of the catchment should be kept unvaried; ii) the three assumptions on the ratios of impervious pavements and tree covers (Section 8.2) remain valid for the scenarios hou+50% and hou−50%. Consequently a change in the area buildings brings also changes in streets. A summary of the land uses under these scenarios is in Table 8.5.

2. Low impact development (LID). Today, the model allows to introduce the following LID devices: flat roof, green roof, permeable pavement with storage structure and swale (Chapter 2, Section 2.7). Swales are implemented by default in the flow routing and is not tested in the scenario study. The modules of flat roof, green roof and permeable pavement with storage structure were reviewed in the present study and modified when necessary. The tested scenarios are termed:

   [flat roof 50%] 50% of sloping roofs converted to flat roofs, which are connected to stormwater drainage network

   [flat roof 100%] 100% of sloping roofs converted to flat roofs, which are connected to stormwater drainage network

   [flat roof - garden] 100% of sloping roofs converted to flat roofs, same as above, but with the roof downspouts directed into adjacent soil, thereby the shallow aquifer

   [green roof 50%] 50% of sloping roofs converted to green roofs , connected to stormwater drainage network

   [green roof 100%] 100% of sloping roofs converted to green roofs, connected to stormwater drainage network

Table 8.4 – Parameters of LID devices used in the scenario modeling.

Device	Parameter	Signification	Value
flat roof	$S_{max}^{f.r.}$	maximum storage	70 mm
	$S_{drain}^{f.r.}$	threshold for drainage	1.5 mm
	$a^{f.r.}$	coefficient of orifice drainage flow	10^{-4} $\sqrt{\text{mm}}$/s
green roof	$S_{max}^{g.r.}$	maximum storage	70 mm
	$z^{g.r.}$	thickness of substrate layer	0.15 m
	$S_{drain}^{g.r.}$	maximum storage in the drainage layer	40 mm
	$a^{g.r.}$	coefficient of orifice drainage flow	10^{-4} $\sqrt{\text{mm}}$/s
permeable pavements	$K_{sat}^{p.p.}$	hydraulic conductivity of reservoir	0.7 m/s
	$S_{max}^{p.p.}$	retention capacity	160 mm
	$S_{min}^{p.p.}$	threshold for drainage flow	80 mm
	K_{sat}^{voi}	hydraulic conductivity of pavement	10 mm/s

[permeable pav] permeable pavements with storage structure for all the streets

The structure and mechanism of these devices and how they are represented in the model have been described in Chapter 2, Section 2.7. The parameter values for the devices are listed in Table 8.4. The flat roofs are set to have a storage capacity of 70 mm with a drainage threshold at 0.5 mm. These values are representative of bared (without gravel) flat rooftops with drain inlets installed just above the roof surface (Coornaert, 2014). The orifice coefficient $a^{f.r.}$=10^{-4} $\sqrt{\text{mm}}$/s corresponds to a drainage flow of 0.4 mm/h under a storage height of 70 mm (Azzout et al., 1994). The green roofs are set to have a storage capacity of 70 mm. The thickness of the substrate layer ($z^{g.r.}$) is set to 15 cm. And the drainage layer is set to have a thickness of 4 cm ($S_{drain}^{g.r.}$). The hydraulic conductivity of the pavements are set as 10 mm/s (Azzout et al., 1994), and that of the underlying storage reservoir at 0.7 m/s. The retention capacity of the reservoir is fixed at 160 mm. Taking account of a porosity of 0.33, this corresponds to a layer height of 480 mm. The threshold for the activation of drainage flow $S_{min}^{p.p.}$ is set at mid-height 80 mm. The land cover configurations under these scenarios are given in Table 8.8.

The scenario study is carried out on two levels: catchment level and urban block level. The evaluation of each scenario is based on the three types of modeling output:

- Water balance. Flow and storage components in the water balance simulated for each scenario are compared to that of the referential modeling.
- Saturation depth. The focus is laid on the average groundwater level of the catchment.
- Discharge. Flow-duration curves (FDCs) are plotted for hourly discharge. An FDC describes

the percentage of time in which a given flow is equaled or exceeded over a period of time (Vogel and Fennessey, 1995).

8.5 Scenario study at catchment scale

8.5.1 Urbanization

Water balance

Table 8.6 shows the simulated catchment-wide water balance of future Moulon for the scenarios of urbanization. Table 8.5 summarizes the surface areas of the land uses under each scenario. With the assumptions made in Section 8.1.4, the street area is larger in [hou−50] than in [hou+50], which seems not realistic, and should be re-examined in future studies.

Table 8.5 – Land cover under scenarios of urbanization.

Area (ha)	A^{nat}	A^{str}	A^{hou}	A^{nat}_{tree}	A^{str}_{tree}	A^{tot}_{tree}
Reference	223	64	51	11.1	3.2	14.3
pav+50%	203	84	51	10.2	4.1	14.3
pav+80%	192	95	51	9.6	4.7	14.3
hou+50%	201	60	77	10.1	3.0	13.1
hou−50%	245	68	25	12.2	3.4	15.6
						$A^{tot} = 338$ ha

Table 8.6 – Simulated water balance of future Moulon for the scenarios of urbanization. The components are expressed in percentage of total rainfall.

Scenario	Q^{hou}	Q^{str}	Q^{nat}	Q^{drain}	E	TR	Δstorage	P
Reference	13.4	6.3	7.1	18.3	8.1	51.7	-2.5	100
pav+50%	13.4	8.8	7.8	19.5	9.4	46.1	-2.4	100
pav+80%	13.4	10.4	8.0	20.1	10.1	42.9	-2.3	100
hou+50%	20.1	5.9	6.3	17.7	8.5	46.7	-2.7	100
hou−50%	6.7	6.8	7.9	19.5	7.8	56.2	-2.6	100

Extension of impervious pavements leads to increase of surface runoff (Q^{str}). 50% or 80% of extension increases Q^{str} by 40% and 65% respectively. Surface evaporation is also slightly increased due to more available water on surface. Due to the shrink of natural surface (A^{nat}), transpiration TR is reduced by 11% and 17%, despite the large tree-covered area on street surface (A^{str}_{tree}). The balance effect of reduced surface infiltration and transpiration loss is an increase in soil storage, despite the enforced drainage by sewer networks Q^{drain}. This increase leads probably to more frequent soil saturation, seen from the increased natural surface runoff Q^{nat}.

An extension (or a shrink) by 50% of the building area results in 50% more (less) rooftop runoff Q^{hou}. The degree of influence of the building area is thus higher than that of the streets. This is explained by the hydraulic conductivity attributed to the two types of surface: $K_s^{hou} = 0$ while $K_s^{str} = 10^{-7}$ m/s. Runoff on natural land and streets are also modified, as a consequence of the changes in the two surface area (A^{nat} and A^{str}) along with the building area. Transpiration is reduced (enforced) correspondingly. In the case of [hou+50%], the balance effect of reduced surface infiltration and reduced transpiration loss is a decrease in soil storage, and in Q^{drain}. In the case of [hou−50%], the balance effect of enforced surface infiltration and enforced transpiration loss is an increase in groundwater level, and in Q^{drain}.

In summary, four points are revealed by the assessed water balance:

- The extension of impervious surfaces (streets or buildings) increases the runoff generated on these surfaces. Although the surface area of the streets are larger than that of the buildings, the latter have more impact (in terms of runoff volume) than than the first, related to their assumed permeability.

- Due to the dominance of natural surface area than streets (2-3 times larger), the transpiration flux is impacted mainly by the change in natural surface area, at the expense of tree-covers. It is to noted that the transpiration process occurs over all the natural surfaces, while on streets it occurs only on tree-covered parts.

- The transpiration is a key factor influencing the groundwater, in counter-balancing the reduction in infiltration due to surface sealing. The balance of the two processes is variable from one case to another.

- Groundwater drainage by sewer network is highly correlated with the groundwater level. But its role is dominated by the balance between transpiration and infiltration.

Saturation depth

Figure 8.5 plots the simulated groundwater level series for the scenarios of urbanization. During dry period (June-October), an extension/shrink of building area (brown/green lines) leads to higher/lower groundwater level compared to the reference, while the reverse trend is observed for wet period (November-May). This observation confirms the different recharge regimes at different seasons. In winter, the dominant process is precipitation and infiltration, as evapotranspiration rate is weak. The extension/shrink of building area reduces/enforce the infiltration, thus lowers/raises the groundwater level. In summer, the process of evapotranspiration has the predominant role. While an extension of building ([hou+50%]) area reduces infiltration, it also reduces the loss by evapotranspiration. If the reduction in evapotranspiration dominates the reduction in infiltration,

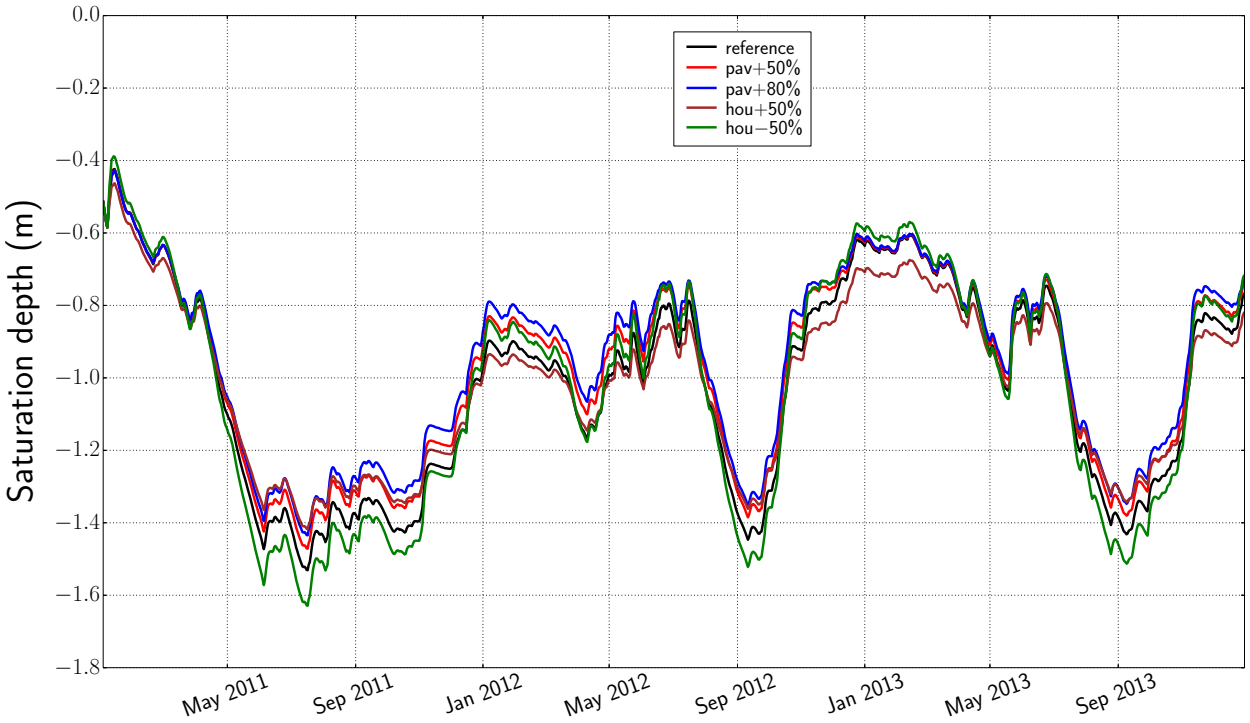

Figure 8.5 – Simulated catchment-wide mean groundwater level of Moulon under the scenarios of urbanization, compared with the reference modeling.

the resultant groundwater level will be raised (observed in the brown curve). The same reasoning can be given to [hou − 50%].

The patterns of impervious pavements are slightly different: their expansions conduct to higher groundwater level, during both dry and wet periods. And the larger the impervious surface is (blue line), the higher the groundwater level tends to be. This is probably the result of two mechanisms: i) the "impervious" pavements are in fact not absolutely impervious in the model, but have a weak permeability, so infiltration is not totally stopped, compared with the case [hou+50%]; ii) the reduction in evapotranspiration by extended impervious surfaces, which dominates the infiltration.

Discharge

Figure 8.6 shows the catchment-wide discharge FDCs for the urbanization scenarios, and Table 8.7 shows the corresponding discharge rates of the exceeding probability 0.1%, 1% and 10% (noted $Q_{0.1\%}$, $Q_{1\%}$ and $Q_{10\%}$). These percentages correspond to 9 hours, 3.6 days and 36.5 days at a duration of one year. The lowest discharge is around 10^{-3} m^3/s. This values corresponds to the groundwater drainage flux by sewer networks.

Figure 8.6 shows that both extension of pavements and built area can increase high flow rates, as could be expected. With 50% and 80% more impervious pavements on the catchment, the high flow $Q_{0.1\%}$ rises from 1.8 to 2.9 and 3.5 m^3/s respectively, and $Q_{1\%}$ from 0.5 to 0.8 and 0.95

m^3/s. The low flow $Q_{10\%}$ does not change with the impervious surface area. Changes in built area conduct to similar variations: an increase/decrease of 50% in building area will shift $Q_{0.1\%}$ from 1.8 to 2.6/1.6 m^3/s, and $Q_{1\%}$ from 0.5 to 0.7/0.4 m^3/s. The degrees of variation seem, however, slighter than for impervious pavements.

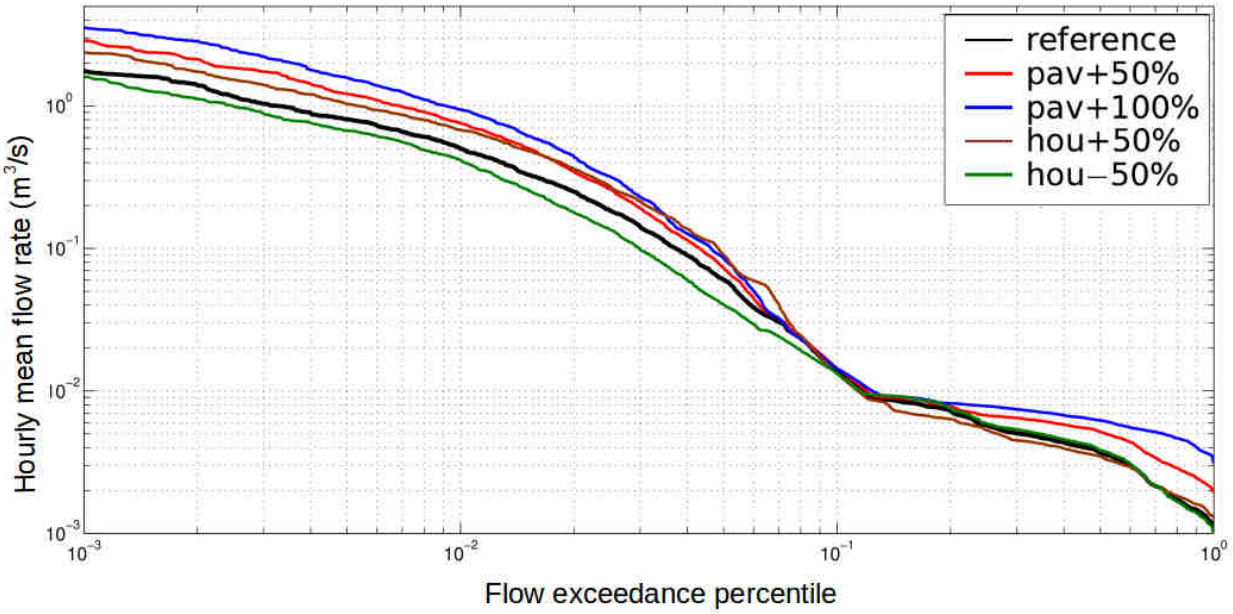

Figure 8.6 – Flow-duration curves determined from hourly mean discharge volume of Moulon, for the scenarios of urbanization.

Table 8.7 – Characteristic discharges of the scenarios of urbanization given by the flow-duration curves at catchment scale of Moulon.

Scenario	$Q_{0.1\%}$ (m^3/s)	$Q_{1\%}$ (m^3/s)	$Q_{10\%}$ (m^3/s)
Reference	1.8	0.5	0.013
pav+50%	2.9	0.8	0.013
pav+80%	3.5	0.95	0.013
bui+50%	2.6	0.7	0.013
bui−50%	1.6	0.4	0.013

8.5.2 LID

Water balance

Table 8.9 shows the simulated catchment-wide water balance of future Moulon for the scenarios of low impact development (LID). Table 8.8 summarizes the surface areas of the land uses under each scenario.

Table 8.8 – Land cover under LID scenarios. *f.r* is for *flat roof*, *g.r.* for *green roof*.

Area (ha)	A^{hou}	$A^{hou}_{f.r.}$	$A^{hou}_{g.r.}$	A^{str}	A^{str}_{perv}
Reference	51	-	-	64	-
flat roof 50%	51	25.5	-	64	-
flat roof 100%	51	51	-	64	-
flat roof - garden	51	51	-	64	-
green roof 50%	51	-	25.5	64	-
green roof 100%	51	-	51	64	-
permeable pav	51	-	-	64	64
					$A^{tot} = 338$ ha

Table 8.9 – Simulated water balance of future Moulon for LID scenarios. The components are expressed in percentage of total rainfall.

Scenario	Q^{hou}	Q^{str}	Q^{nat}	Q^{drain}	E	TR	Δstorage
Reference	13.4	6.3	7.1	18.3	8.1	51.7	-2.5
flat roof 50%	12.5	6.3	7.1	18.6	9.0	51.6	-2.5
flat roof 100%	11.5	6.3	7.1	18.6	10.0	51.6	-2.5
flat roof - garden	0	6.8	13.4	23.4	12.0	49.4	-2.0
green roof 50%	11.9	6.3	7.1	18.6	7.0	52.8	-2.5
green roof 100%	10.4	6.3	7.1	18.3	6.0	53.9	-2.5
permeable pav	13.4	1.8	11.1	21.3	9.3	47.9	-2.3

With the sloping roofs converted to flat roofs, the catchment-wide water balance does not change much. Rooftop runoff Q^{hou} is reduced, and surface evaporation E increased, both in slight manners. As explained in Section 8.4, the flat roofs tested here have the features of bared roofs which release water in regulated rate (orifice flow) once the storage exceeds 1.5 mm. The performance of the device is therefore more in the reduction of peak flow, and the no-significant effect on the flow volume could be expected.

In the case where all the flat roofs are disconnected from drainage systems and release water onto natural land ([flat roof - garden]), natural surface runoff is increased by two, causing consequently a higher groundwater level due to enforced surface infiltration, seen from Δstorage. But the total surface runoff (Q^{hou}+Q^{str}+Q^{nat}) is reduced to 20.9% of the total rainfall P. As a consequence of the raised groundwater level, drainage by sewer networks is enforced (from 18.3% of P to 23.4%). In taking account of this component, the total discharge (Q^{hou}+Q^{str}+Q^{nat}+Q^{drain}) is equivalent to 44.9% of P, almost the same as in the reference (45.1%). Besides, transpiration TR is slightly reduced, probably due to the soil surface saturation that occurs more often (transpiration process is stopped when there is stagnant water on surface, as explained above).

With 50% and 100% of roofs converted to green roofs, rooftop discharge is reduced respectively to 11.9% and 10.4% of P. Green roofs can evaporate 31% of the rainfall, which seems to be weaker than the values in the literature (VanWoert et al., 2005; Dietz, 2007; Hathaway et al., 2008; Carpenter and Kaluvakolanu, 2011; Razzaghmanesh et al., 2012).

When the altogether streets are converted to permeable pavements with storage structure, the total produced surface runoff are notably reduced from 6.3% of P to only 1.8%, a reduction of 71%. On the other hand, the permeable pavements lead to an increase of natural surface runoff Q^{nat} (11.1% vs. 7.1%). In fact, compared to conventional impervious asphalt, the permeable pavements absorb more surface water, which infiltrates to the subsoil after being temporarily stored. Consequently the overall quantity of water arriving into the soil is increased, which makes the soil saturation to be more recurrent. As shown by Δstorage in Table 8.9 and confirmed by the curve in Figure 8.7 below, the average groundwater level has been raised with the presence of permeable pavements. Due to more frequent saturated soil, transpiration loss TR has been reduced in the favor of surface evaporation E.

Saturation depth

The average groundwater level is affected for the scenarios [flat roof-garden] and [permeable pav], which conduct both to higher mean groundwater level, as shown in Figure 8.7. Both devices favor retention and infiltration for the purpose of runoff reduction, the rise in groundwater level in the two cases can thus be expected. Especially in the case [flat roof-garden], the maximum difference with the reference curve reaches to 0.3 m. And the impacts seem to be more pronounced during high-water period in winter than in summer.

Discharge volumes

Figure 8.8 shows the flow-duration curves of the produced discharge volume under the LID scenarios. All the LID systems have an effect of lowering the extreme discharge magnitude. Flat roofs (the red and blue lines) are more efficient in this than green roofs and permeable pavements, except when they are disconnected from sewer systems (the pink line). For the low magnitudes, all the scenarios increase their frequency, except the two green roof scenarios.

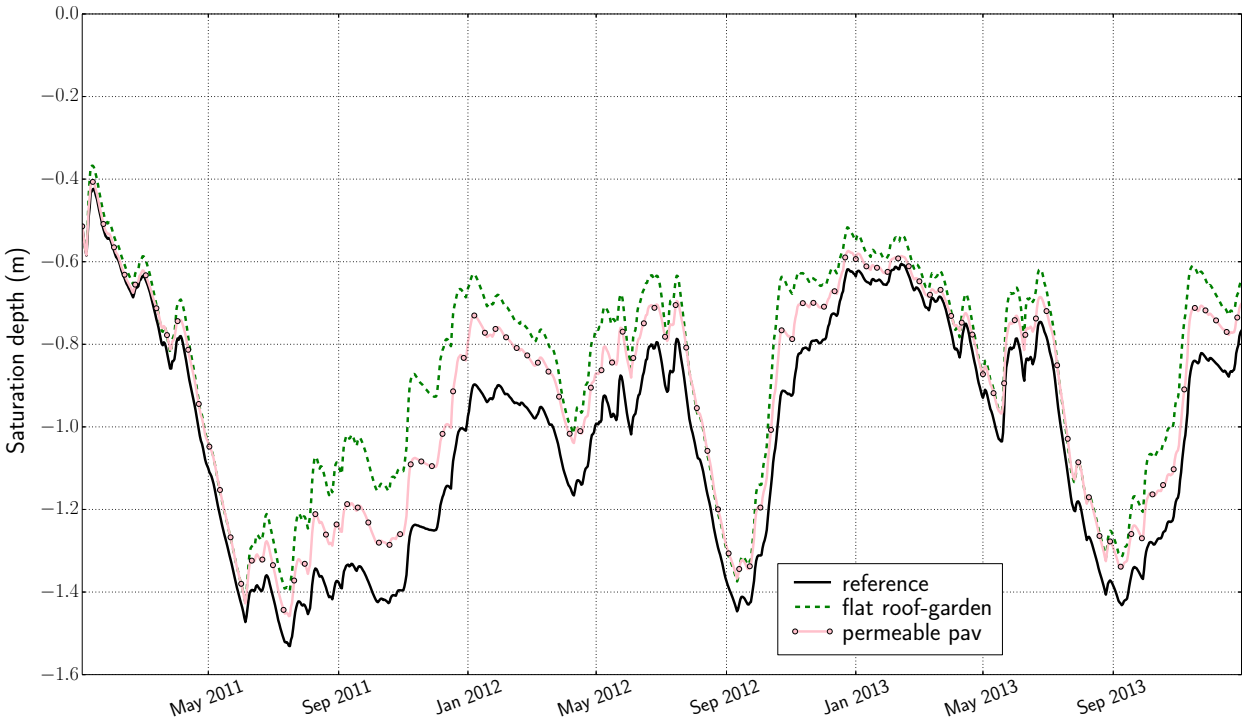

Figure 8.7 – Simulated catchment-wide mean groundwater level of Moulon under the scenarios of [flat roof-garden] and [permeable pav], compared with the reference modeling.

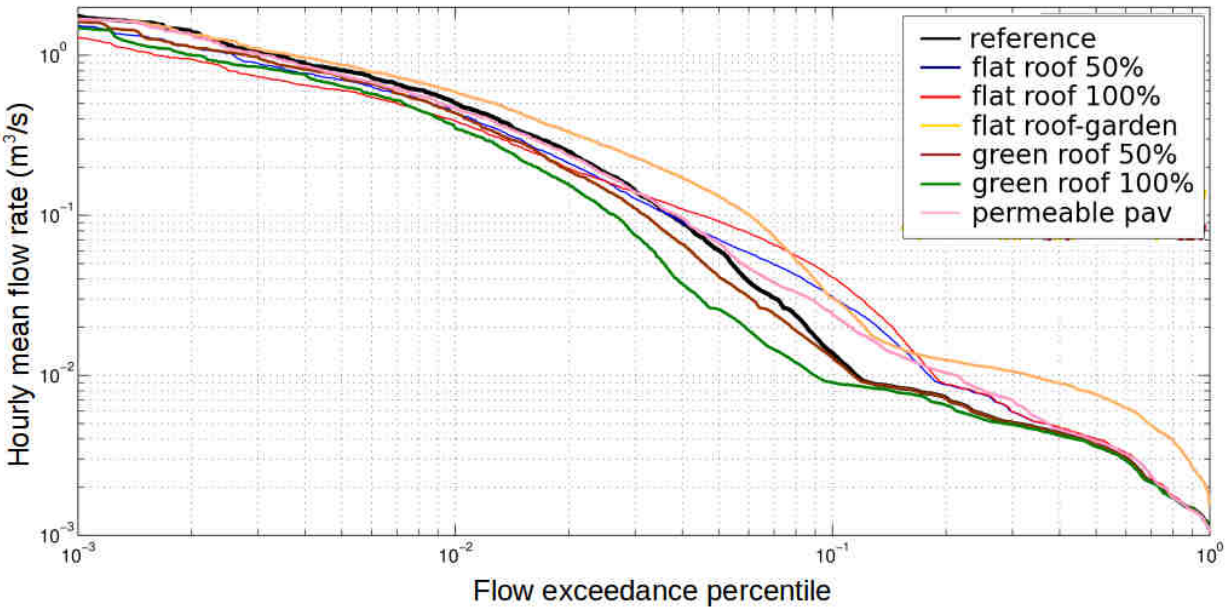

Figure 8.8 – Flow-duration curves determined from daily mean discharge volume of Moulon, for LID scenarios.

8.6 Scenario study at urban block scale

A block of the future campus of École Normale Supérieur has been chosen to be studied (UHE 5 in Figure 8.9). This block locates at the center-east of Moulon and has a surface area 3.78 hectares, with 37% of buildings, 16% of streets, which make an impervious ratio of 53%. The left 47% is considered to be natural land. The ratio of tree covers on the (natural and street) surfaces were the same as the whole catchment: 5% on natural land and 1.5% on street.

This morphological configuration is considered to be the reference for the study at this urban block. Tested scenarios are the same as for the study at catchment scale: four scenarios of urbanization and six scenarios of LID. The surface areas of the land covers under each scenario are shown in Table 8.10 and 8.11.

In terms of modeling domain, we have two options:

(a) Run the model at only UHE 5 by defining subsurface boundary conditions for it.

(b) Run the model at the entire catchment and analyze the results for the UHE.

Compared with Option (a), Option (b) can take into account the interactions of the studied UHE with adjacent UHEs and show if it has analogical behaviour with the entire catchment. It is thus this option that has been chosen.

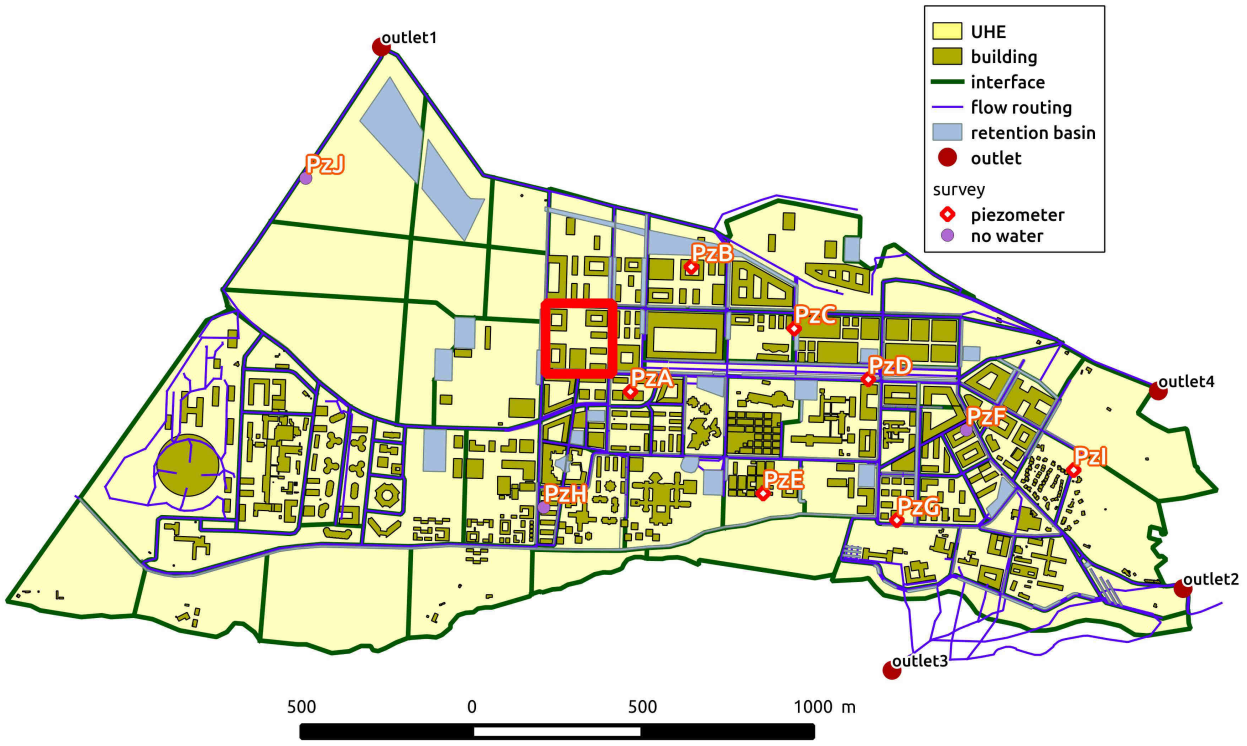

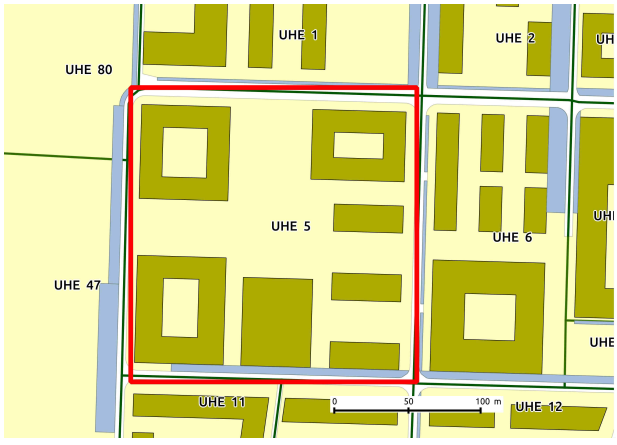

	Area (ha)	Percentage (%)
A^{tot}	3.78	100
A^{nat}	1.77	47
A^{hou}	1.39	37
A^{str}	0.62	16
A^{imp}	0.20	53
A^{nat}_{tree}	0.09	1.5
A^{str}_{tree}	0.03	5.0
A^{tot}_{tree}	0.12	3.2

Figure 8.9 – UHE 5 chosen for the scenario study at urban block scale. Land cover is summarized in the table. Underground stormwater network associated to this UHE (not shown in the figure) is situated at -0.5 m.

Table 8.10 – Land cover of UHE 5 under the scenarios of urbanization.

Area (ha)	A^{nat}	%	A^{hou}	%	A^{str}	%	A^{tot}_{tree}	%
Reference	1.77	47	1.39	37	0.62	16	0.12	3.2
pav+50%	1.61	43	1.39	37	0.78	20	0.12	3.2
pav+80%	1.52	40	1.39	37	0.87	23	0.12	3.2
hou+50%	1.18	31	2.09	55	0.51	14	0.08	2.2
hou−50%	2.36	62	0.70	19	0.72	19	0.15	4.1
							$A^{tot} = 3.78$ ha	

Table 8.11 – Land cover of UHE 5 under the scenarios of LID.

Area (ha)	A^{hou}	$A^{hou}_{f.r.}$	$A^{hou}_{g.r.}$	A^{str}	A^{str}_{perv}
Reference	1.39	-	-	0.62	-
flat roof 50%	1.39	0.70	-	0.62	-
flat roof 100%	1.39	1.39	-	0.62	-
flat roof - garden	1.39	1.39	-	0.62	-
green roof 50%	1.39	-	0.70	0.62	-
green roof 50%	1.39	-	1.39	0.62	-
permeable pav	1.39	-	-	0.62	0.62
				$A^{tot} = 3.78$ ha	

8.6.1 Water balance

Table 8.12 shows the simulated water balance of the UHE 5 by the reference modeling. Compared to the water balance at the catchment scale, slight differences are observed, including:

- Rooftop runoff is higher (31.9% vs. 13.4%), due to higher proportion of buildings (37%) in UHE 5 than the catchment average (15%).
- Runoff originated from streets and natural surface is 6.3% and 6.0% respectively, similar to the catchment-wide values.
- Groundwater drainage by sewer networks Q^{drain} is weaker, due to probably the depth of the sewer segment (-0.5 m vs. -2.49 m for the catchment).
- Surface evaporation loss is the same as that of the catchment (10%).
- Transpiration loss equals to 42.4% of P, weaker than catchment average (51.6%), due to the smaller ratio of natural surface (47% vs. 66%).

Table 8.12 – Simulated water balance of the UHE 5 by the reference modeling.

Q^{hou}	Q^{str}	Q^{nat}	Q^{drain}	E	TR
31.9	6.3	6.0	6.4	10.0	42.4

The simulated water balance under the scenarios of urbanization and LID devices are in general agreement with that of the catchment, thus not detailed here.

8.6.2 Saturation depth

The simulated groundwater level series under the scenarios of the block UHE 5 (Figure 8.10 and 8.11) have similar trends as that of the catchment (Figure 8.5 and 8.7).

Compared with the mean groundwater level of the catchment, the groundwater level of UHE 5 show that this block suffers from more recurrent overland flooding[2]. Especially during winter 2012-2013, the soil is under saturation during more than four months (10/11/2012 - 20/02/2013) under all scenario. Imperviousness expansion ([pav+50%], [pav+80%] and [hou+50%]) seem to have the trend to aggravate the situation: the soil is saturated during winter 2011-2012 under these scenarios, while this is not the case under reference condition. The phenomena of the enforced recurrence of soil saturation is even more visible in the two LID scenarios: while the soil is not at all saturated during the winter 2011-2012 under the reference condition, it is saturated early under the scenarios [flat roof-garden] and [permeable pav] and last for about four months. Especially in the first case, notable groundwater rise is observed short after the beginning of the simulation period. The issue of "overcompensation" in groundwater recharge in the stormwater management by infiltration devices has been addressed in certain studies (Morris et al., 1997; Göbel et al., 2004). Here, although we can not quantify the soil saturation and subsequent overland flooding by "overcompensation", as there is no reference for defining a "natural recharge regime", the results do question the possible side-effects of certain LID practices, in terms of impact on groundwater recharge.

[2]The phenomena of saturation in the modeling of URBS-WTI has been discussed in Chapter 3, Section 3.3.

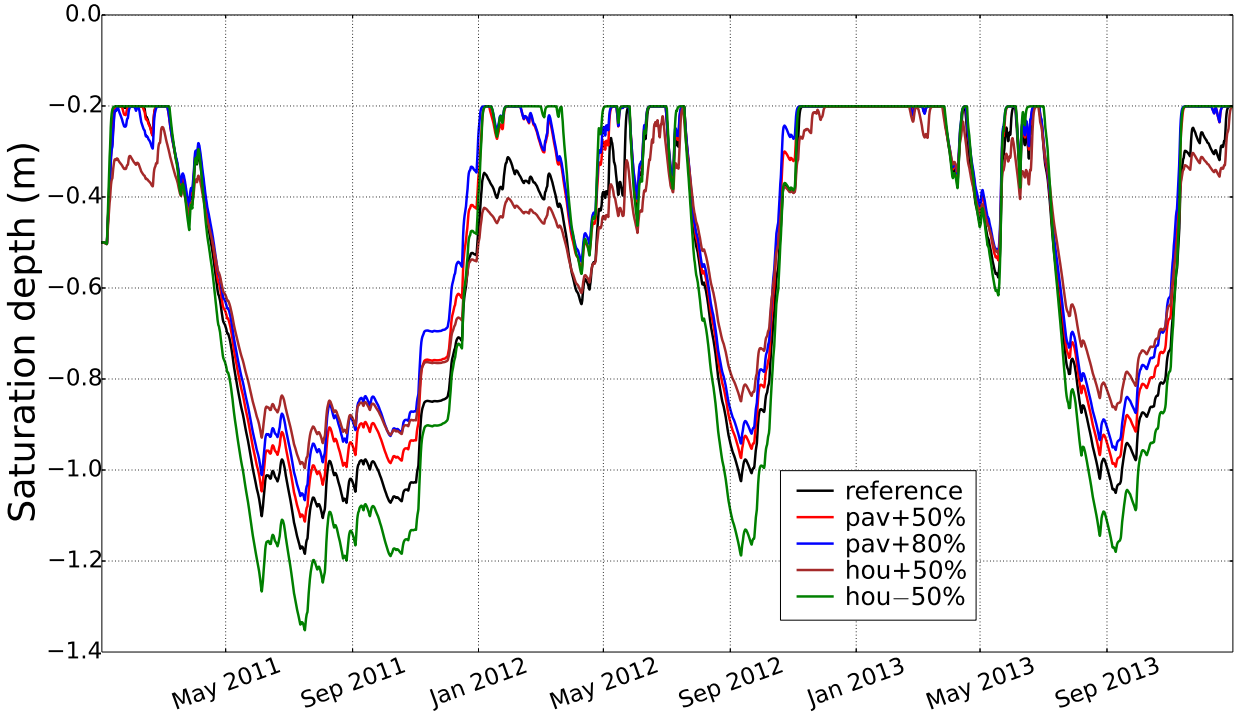

Figure 8.10 – Simulated mean groundwater level of UHE 5 under the scenarios of urbanization.

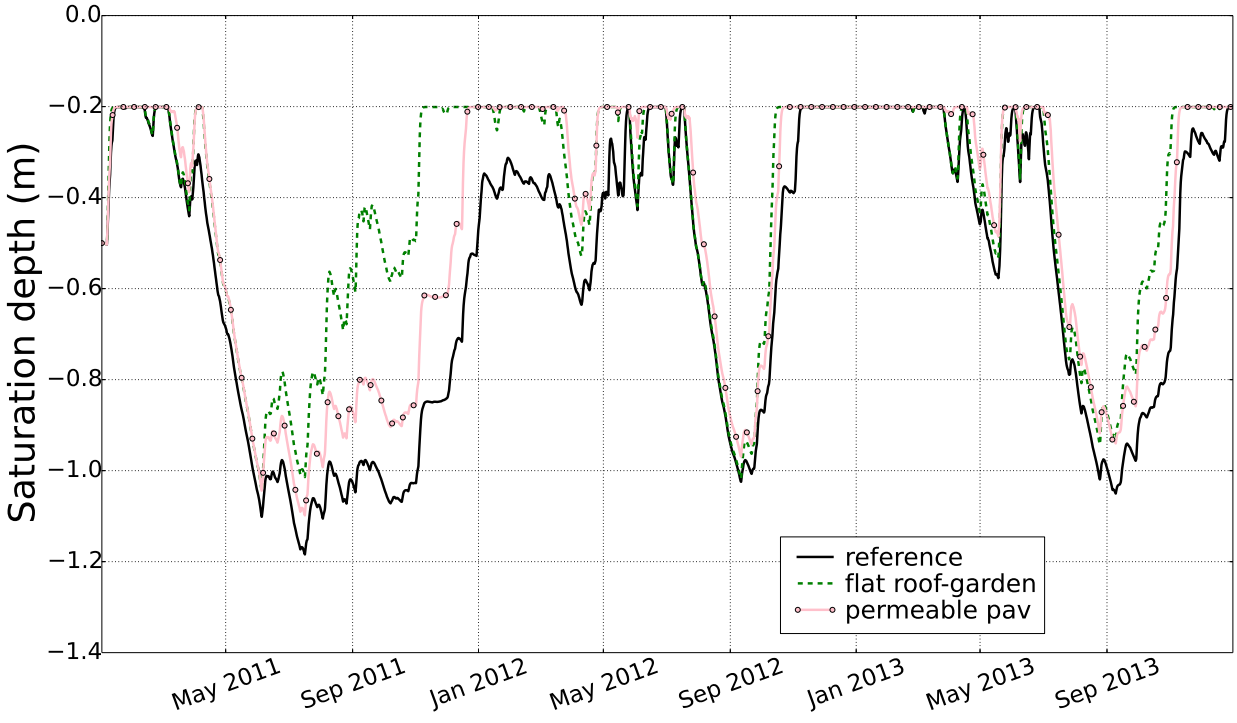

Figure 8.11 – Simulated mean groundwater level of UHE 5 under LID scenarios.

Discussion and conclusion

This chapter describes our study for the post-development state of the Moulon area. The study objective is to estimate both the hydrological impacts of urban development and the efficiency of certain LID devices. The study is conducted by scenario modelings with the model URBS-WTI. The reference modeling is the one with the land use derived from the programs defined in Paris-Saclay urban project. The associated information has been collected and analysed as objectively as we can, but assumptions are always necessary and the land cover defined in the study can be slightly different from the final layout of the area.

The results of the reference modeling show a change in the runoff fraction of the impervious surfaces, the natural surfaces and the groundwater drainage by sewer networks. The total produced runoff volume is only slightly increased compared with the pre-development state: while the expansion of impervious surfaces increases surface runoff to the detriment of evapotranspiration, groundwater drainage by sewer networks is cut by half. The spatial discretization in the model has an important role in this reduction (Section 8.3) and worths further examinations. The increase in groundwater level estimated by the model should be interpreted and used with caution. As a consequence of the increased groundwater level, which favors the drainage by sewer networks, the simulated entire discharge quantity at the outlets is increased by 50%. But it is important to note that the storage basins and discharge regulation devices planned in the project are not implemented in the model for instance, and all produced runoff volume is free to be conveyed till the outlets. The real future discharge volumes of the campus could be different with the estimation by modeling.

Four scenarios of urban development and six scenarios of LID have been evaluated and compared with the referential modeling results. Studies are carried out at two spatial scales: catchment scale and urban block scale. The outputs at the two scales are in general accordance. Impacts of urban expansion are clearly observed: enhanced runoff volumes on impervious surfaces and reduced evapotranspiration. The evapotranspiration, coupling with the surface infiltration, controls the variation of groundwater level. The two processes are counter-balanced, and the resultant groundwater level depends on the dominating one. Besides, the modeling result highlights the different recharge regime between summer and winter, related to different evapotranspiration rates. The impacts of surface sealing on groundwater level are conditioned by this seasonal difference. Groundwater drainage by sewer networks is highly correlated with the groundwater level: in all the tested scenarios the drainage flux varies along with the mean groundwater level. Contribution to urban runoff of the natural land is not neglected in any case. Especially with at-source stormwater management devices implemented, such as garden-directed rooftops, local excess infiltration can lead to frequent soil saturation and overland flooding, as shown by the results on the urban block scale. This phenomena is of course highly associated with the underlying hydrogeological setting. All the LID scenarios could reduce the magnitude of extreme discharge: some of them are also efficient in reducing the durations of low flow, especially the green roof structure.

This study for the pre-development state of Moulon through hypothetical scenarios shows the possibility for the model URBS-WTI to provide sound information for stormwater management, through its capability of simulating divers hydrological variables at scales ranging from parcel to catchment. However, for being a suitable and robust decision-making tool for urban projects, which is a long-term objective of the model development, several aspects of the model need to be reviewed and developed. The model is quite demanding in terms of geodata input: both land uses within urban parcels and geometrical features of sewer networks need to be well documented. These types of information are relatively easy to obtain for areas that are already urbanized, thanks to the developing urban databanks, but this is not the case for new developed areas. If the difficulty in achieving information on land uses can be overcome through hypothesis, which is the case in the present study, the lack of detailed information on sewer networks seem more problematic.

Part V

General conclusion

Main results and achievements

During this Ph.D work, two main objectives have been achieved: a scientific one, with the enhancement of an urban hydrological model, and a more operational one, with the application of the model to a real urban planing scenario. In a first step, the saturation flow module Water Transfer Interface (WTI) has been implemented into the distributed urban hydrological model URBS as an optional module that can be activated according to the modeling need. Both URBS and WTI have been adapted to the service of the module integration. This choice for the saturated flow module in URBS is a suitable approach, as it allows to build the saturation flow modeling in URBS based on physical formulation (Darcy law) without changing the feature soil configuration neither the spatial discretization in the initial model. The integrated model URBS-WTI has been evaluated on the well documented urban catchment of Pin Sec. Continuous modeling have been carried out for the 5-year period of 01/01/2006-31/12/2010 at 5-min time step. Different modeling outputs, including catchment water balance, stormwater discharge, and groundwater levels, have been examined. The module has proved to be able to improve significantly the model performance, in particular for the simulation of groundwater levels. The capacity of the model to consider the atmosphere-surface-groundwater interactions has been confirmed.

The model has been applied on a real urban development zone, the Moulon area on the Saclay plateau, in taking account of the shallow aquifer flow. The model evaluation on this case study has been undertaken based uniquely on groundwater observation data, which forms an originality of the study. Water balance of the site under its pre-development conditions has been estimated by the model. This is the first time that the water balance of the territory is estimated in a detailed manner (evapotranspiration, infiltration, runoff, recharge, etc.). Even if it concerns only a small part of the Saclay plateau, the results should be relevant for similar studies in the future.

The scenario study for the post-development Moulon area has allowed to give a first estimation of the impacts of the urban-campus development on local hydrology. Impacts have been assessed for different hypothesis of both urbanization density and stormwater management techniques. The reduction effect of sealed surfaces on the infiltration and evapotranspiration has been studied. Because of the complex interactions between the processes, the overall impact on the water balance can not be predicted easily. The seasonal differences in the regime of groundwater recharge has been illustrated. Several LID devices have been integrated in the modeling, and have shown their beneficial function to runoff control. Moreover, the infiltration-based devices influence the groundwater recharge regime. Excess recharge quantity can be the origin of local soil saturation flooding, which have been observed in the scenario modeling for an urban block. It is thus recommended to estimate the impact on groundwater recharge preliminarily to the setting up of infiltration-based LID devices. This study shows, to some extent, the feasibility, interests and limits of the application of URBS on a new developing area. The model calibration for Moulon has be carried out only on groundwater monitoring data, and the simulated discharge rates have not been validated because

of lack of measurement data. Flow regulation devices that are planned in the project Paris-Saclay have not been integrated in the model. The assessed results of discharge should thus be used with caution.

Analyzing the components of the water balance has proved to be essential for knowing the mechanism in the model and for understanding the other type of results. This is particularly true when the groundwater flow is represented in the model. It has been demonstrated that the overall water balance and groundwater recharge are conditioned by the balance effect of the different processes. The process of evapotranspiration has shown great importance in the water cycle, as well as groundwater drainage by sewer networks, which represents about 30% of the annual rainfall in both case studies, although this has not been validated for Moulon. The model has shown great sensibility to soil parameters; the sensibility depends on both the study case and the examined variable, which shows the necessity of doing sensibility analysis for future model applications of URBS. The complexity in fitting the observation and simulation groundwater curves due to different behaviors of these observation series implies the heterogeneity of soil properties in urban settings. The interest of the distributed model URBS for modeling hydrological variables in urban catchments has been confirmed.

Beyond the initial objective of study, a series of programs for geodata pre-processing via GIS softwares have been developed or adapted and ready-to-use for model application on other catchments. These established programs and their methodology should be beneficial to future studies.

Limits of the study

The integrated WTI module has been evaluated on a variety of modeling outputs. The relatively good quality of groundwater level modeling has allowed the module to be validated. The homogenization effect of the module has been evaluated by a simple criterion: the standard deviation of groundwater levels between the UHEs. The simulated WTI flux seems to be predominated by vertical fluxes by climate forcing : a manual forcing through a coefficient has been necessary for the simulated groundwater levels to fit the observations. It will be interesting to analyze the physical signification of this coefficient. The zero-flux boundary condition assigned on the soil flow may not to be totally adequate, especially at the downstream boundary of the system. The model probably needs to evacuate water out of the modeling domain in order to meet the piezometric observations.

Due to limited information of land use of the future Moulon, hypothesis have been made on the imperviousness of surface, as well as tree-covered areas. It is recognized that these hypothesis are not totally “reasonable”. Furthermore, assigning a uniform impervious ratio to all the urban blocks is obviously a simplified approach. With the progressing of the campus project, a re-examination of these hypothesis should help to assess more realistic results.

Comment on the model

As a distributed and physically-based urban hydrological model, URBS-WTI has shown its adaptability to the modeling of small urban catchments. It represents the urban stormwater cycle in an integrated way, in taking into account both the natural atmosphere - surface - groundwater interactions and the buried sewer networks. It is capable of carrying long-term continuous simulations at small time steps. The utilization of urban parcels as spatial units allows to simulates hydrological behavior at fine spatial level. It provides a variety of modeling outputs permitting to understand the catchment response to rainfall in a detailed manner. All these features make the model a convenient choice for developing physically-based modeling tool for decision making.

As a research model, URBS-WTI has also shown limits during the present work. The most evident one relies on its high exigence on geodata details (parcels, streets, sewer networks). The model application on the catchments of Pin Sec and Moulon has required great quantities of GIS pre-processing work that have been subject to two master thesis. In the case where the quality of initial GIS data is mediocre, the difficulties for generating the geodata files are significant. We believe that this can be a constrain for the model to be applied on large catchments. In the case of new urban projects, detailed descriptions for land use and sewer networks are probably not available at the first stages. The fact that the model requires these data as input seems to be contradictory with the its long term objective to be a decision-making tool. Another weak point of the model is related to the structural organization of the program. All the main simulated processes are currently organized in a unique file of 5000-6000 lines, which make the verification of problems quite tedious and error-prone. We believe that the program needs to be re-organized if we want to set ambitious objectives for the model development. But this may require important investigations in terms of programming.

Perspectives

It will be valuable to compare the results of Moulon (water balance and discharge) with other studies within the Saclay plateau. To the author's knowledge, this type of studies is currently rare, but things can change with the rising interests of researchers on the plateau, evoked by the Paris-Saclay University project.

The model URBS-WTI is now ready to be applied at other catchments, which may have more available observation data. This can help to further evaluate the performance of the saturation module. Some questions have been raised about the model during the thesis, such as its capacity to take into consideration of the spatial variability of soil properties and the influence of spatial discretization on modeling results. These questions deserve further examinations.

The cooperation between the EPPS, CEREMA and IFSTTAR has been renewed for three years. One of the defined program is to reinforce the hydrological modeling of Moulon, in order

to provide more tangible results that can be used in the urban planning. Following this objective, the development of URBS-WTI in the short term consists of the implementation of two elements in the model: (1) a module for taking account of basement drainage, and (2) representation of flow regulation devices in the drainage network, particularly at the outlets of the swales.

Appendix A

GIS processing on geodata

A.1 Difficulties encountered during the geodata error correction

The first difficulty in this procedure locates in the error messages that are not always meaningful to the user. Figure A.1 is a screen shot of the geometry validity verification for the *parcel* layer, the numbers of segments which have problem (e.g. 12 and 15 in the first line) are interior identities of the *Geometry validity* procedure itself and do not mean anything for the end user (maybe useful for software developers). Two lines below, it indicates that the geometry has eight errors nothing more precise. In fact, the error mentioned in this line is the same as that of the first line and the number "8" is absolutely meaningless. As to GRASS, it gives nothing but the quantity of errors. In summary, the only way to understand the real problem is to check by eyes every point at the problem location indicated by the table. Since the errors exposed in the table could be related and thus be corrected unconsciously, the *Geometry validity* function needs to be launched following every correction in order that the error list is renewed.

The second difficulty lies on the correction process itself. In fact, among the errors, many are situated in a infinitesimal spatial scales (on order of 1 meter or even smaller), with points that have been drawn inappropriately. To understand the error and correct it, it is compulsory to largely zoom in the map. Sometimes even with the maximum zoom possibility afforded by the software, hardly the problem could be seen clearly. In case the problem should be analyzed in association with surrounding features (e.g. in taking account of the entire polygon), it is obviously needed to zoom out, with the possibility to lose the error location...Nothing but this repetitive zoom manipulation for understanding the problem is quite time consuming.

This double-filter checking is carried on each of the three vector layers (*parcel, street surface* and *street line*). When no error is detected neither by QGIS nor by GRASS in any of the vectors, it is possible to launch the automation program for UHEs creation (presented below in section 4.4). And there, unfortunately, we have to deal with new problems that have not been detected by the

Figure A.1 – Error message given by *Geometry validity* of QGIS for *parcel* layer.

checking tools but appear with the automation program.

The "new" problems concern, in most of the time, relationships between the vectors. For example, a border line of a parcel (polygon) must have, in theory, the same points with the border line of the adjacent street surface (polygon). Another example is the incoherence between the segments of the *street surface* layer and that of the *street line* layer.

If they can not be characterized as an "error", the automation program can not run properly with them, which is normal. Given that the automation program covers multiple stages, this kind of problem can be detected at any stage. Once a problem is detected by the program, the vector concerned needs to be reviewed and corrected with the process presented above, after which used again for testing the automation program, until no error is felt.

A.2 Python program for *UHE* vector map

```
1  #!usr/bin/env python
2  '''
3  Created on mai 2010
4  @author: paille
5  Modified by yinghao Li for Pinsec application
6  '''
7  import grass.script as grass
8  '''Affiche le contenu du mapset'''
9  '''Display the mapset'''
10 env = grass.gisenv()
11 print env
```

```
vectors = grass.read_command("g.list", type='vect')
print vectors

'''1. Merge street surface sections'''
grass.run_command("v.dissolve", input='voirie', output='voirie_d', column='extraction', overwrite=True)

'''2. selecting street's parcels, masked parcels and all of entities that touch the street'''
grass.run_command("v.select", ainput='parcelles', binput='voirie', output='parcelles_viaires', overwrite=True)
grass.run_command("v.overlay", ainput='parcelles', binput='voirie', output='parcelles_masquees', operator='not', overwrite=True)
grass.run_command("v.select", ainput='parcelles', binput='voirie', output='elements_viaires', overwrite=True)

'''3. merging 'voirie_dissolve' with 'elements_viaires' to obtain, after,
   boundaries by neighbour analysis'''
grass.run_command("v.overlay", ainput='elements_viaires', binput='voirie_d', output='temp', operator='or', overwrite=True)
grass.run_command("v.build.polylines", input='temp', output='temp1', cats='multi', overwrite=True)

'''4. indentifying common boundaries and neighbour's categories'''
grass.run_command ("v.category", input='temp1', output='category', layer='2', type='boundary', option='add', overwrite=True)
grass.run_command ("v.db.addtable", map='category', layer='2', columns='left integer, right integer', overwrite=True)
grass.run_command("v.to.db", map='category', option='sides', col='left, right', layer='2', type='boundary', overwrite=True)

'''5. extracting boundaries of the adjacent parcel to the street'''
grass.run_command("v.edit", map='temp', tool='create', overwrite=True)
liste_col=grass.read_command("v.db.select", map='temp1', columns='cat', where="b_extracti = 'route'")
print liste_col
for i in liste_col.splitlines():
    grass.run_command("v.extract", input='category', output='temp2', layer='2', where="left ¡¿ -1 AND right = %s"%i ,overwrite=True)
    grass.run_command("v.extract", flags='t', input='category', output='temp3', layer='2', where="left = %s AND right =! -1"%i, overwrite=True)
    grass.run_command("v.patch", input='temp,temp2,temp3', output='temp4', overwrite=True)
    grass.run_command("g.remove", vect='temp,temp2,temp3', overwrite=True)
    grass.run_command("g.rename", vect='temp4,temp', overwrite=True)
grass.run_command("v.category", input='temp', output='extract', type='boundary', overwrite=True)
grass.run_command("v.db.addtable", map='extract', layer='1', overwrite=True)

'''6. extracting points situated between boundaries'''
grass.run_command("v.to.points", flags='nt', input='extract', output='temp2', type='line,boundary', overwrite=True)
grass.run_command("v.clean", input='temp2', output='temp3', type='point', tool='rmdupl', overwrite=True)
grass.run_command("v.category", input='temp3', output='temp4', option='del', type='point', overwrite=True)
grass.run_command("v.category", input='temp4', output='temp5', type='point', overwrite=True)
grass.run_command("v.db.addtable", map='temp5', overwrite=True)
grass.run_command("v.select", ainput='temp5', atype='point', binput='voirie_d', output='temp6', overwrite=True)

'''7. creating a line between extracted points and centerline'''
grass.run_command("v.distance", _from='temp6', from_type='point', to='filvoirie',
                  to_type='line', output='distance', upload='dist', column='cat', overwrite=True)
grass.run_command("v.edit", map='distance', type='point', tool='delete', ids='1-99999', overwrite=True)

'''8. merging the street, the centerline of the street and lines of v.distance to obtain the layer 'trottoir' '''
grass.run_command("v.category", input='voirie_d', output='temp1', type='boundary', option='add', overwrite=True)
grass.run_command("v.extract", input='temp1', output='temp2', type='boundary', overwrite=True)
grass.run_command("v.type", input='temp2', output='temp3', type='boundary,line', overwrite=True)
grass.run_command("v.patch", input='distance,temp3,filvoirie', output='temp4', overwrite=True)
grass.run_command("v.clean", input='temp4', output='temp5', type='line,point', tool='snap,break,rmdupl,rmline', thresh='0.1', overwrite=True)
```

```
grass.run˙command("v.type", input='temp5', output='temp6', type='line,boundary', overwrite=True)
grass.run˙command("v.centroids", input='temp6', output='temp7', overwrite=True)

'''8.1. extracting unwanted polygons from the layer 'trottoir' (the topology have maked polygons in gaps)'''
grass.run˙command("v.overlay", flags='t', ainput='temp7', binput='voirie˙d', output='temp8', operator='and', overwrite=True)
grass.run˙command("v.category", input='temp8', output='temp9', option='del', type='boundary', overwrite=True)
grass.run˙command("v.db.addtable", map='temp9', col='id˙uhe integer, area double precision', overwrite=True)
grass.run˙command("v.to.db", map='temp9', option='area', units='meters', columns='area', overwrite=True)
grass.run˙command("v.extract", flags='r', input='temp9', output='temp10', type='area', where="area = 0", overwrite=True)

'''8.2. updating neighborhood relation between street's polygons and street's parcels polygons to create UHE'''
grass.run˙command("v.distance", ˙from='temp10', from˙type='centroid', from˙layer='1', to='elements˙viaires',
        to˙type='area', to˙layer='1', upload='cat', column='id˙uhe', overwrite=True)

'''8.3. reclassing polygons and merging common boundaries + calculating total area of each street's polygons'''
grass.run˙command("v.dissolve", input='temp10', output='temp11', column='id˙uhe', overwrite=True)
grass.run˙command("v.db.addtable", map='temp11', col='id˙uhe integer, area double precision', overwrite=True)
grass.run˙command("v.db.update", map='temp11', layer='1', column='id˙uhe', qcolumn='cat', overwrite=True)
grass.run˙command("v.to.db", map='temp11', option='area', units='meters', columns='area', overwrite=True)
grass.run˙command("g.rename", vect='temp11,trottoir', overwrite=True)
grass.run˙command("g.remove", vect='category,extract,distance,temp,temp1,temp2,temp3,
        temp4,temp5,temp6,temp7,temp8,temp9,temp10', overwrite=True)
```

A.3 GRASS commande for *interface* vector map

```
v.category input=uhe_update2_tt_2 output=interfaces_uhe layer=2 type =boundary option=add --o
v.db.addtable map=interfaces_uhe layer=2 {columns=left integer,right integer} --o
v.to.db map=interfaces_uhe option=sides {col=left,right}  layer=2 --o
```

A.4 OrbisGIS SQL commande for generation of attribute table for the Interfaces

```
create table uhe_center_g as select ST_Centroid(uhe_finale.the_geom) as center, interfaces_fusion.
the_geom as geom_interfaces, interfaces_fusion.gauche as gauche,
interfaces_fusion.droite as droite from uhe_finale , interfaces_fusion
where uhe_finale.cat=interfaces_fusion.gauche;

// for computing the distances between UHE centroid and interfaces
create table uhe_center_g as select
ST_Centroid(uhe_finale.the_geom) as center, interfaces_fusion.the_geom
as geom_interfaces, interfaces_fusion.gauche as gauche,
interfaces_fusion.droite as droite from uhe_finale , interfaces_fusion
where uhe_finale.cat=interfaces_fusion.gauche;
alter table uhe_center_g add column distance double ;
update uhe_center_g set distance = ST_Distance(center,  geom_interfaces);
create table dist_temp_1 as select a.*,  b.distance as distanceA
from interfaces_fusion a, uhe_center_g b where a.gauche=b.gauche
```

```
and a.droite=b.droite;
create table temp2 as select * from interfaces_fusion where
interfaces_fusion.gauche=-1;
alter table dist_temp_2 add column distanceA double;
create table dist_temp_3 as select *
from dist_temp_1
UNION
select *
from dist_temp_2;
create table uhe_center_d as select ST_Centroid(uhe_finale.the_geom)
as center, interfaces_fusion.the_geom as geom_interfaces,
interfaces_fusion.gauche as gauche, interfaces_fusion.droite as droite
from uhe_finale , interfaces_fusion
where uhe_finale.cat=interfaces_fusion.droite;
alter table uhe_center_d add column distance double;
update uhe_center_d set distance = ST_Distance(center,  geom_interfaces) ;
create table dist_temp_d as select a.*,  b.distance as distanceB from
interfaces_fusion a, uhe_center_d b where a.gauche=b.gauche
and a.droite=b.droite;create table dist as select dist_temp_3.*,
dist_temp_d.distanceB as distanceB from dist_temp_3, dist_temp_d
where dist_temp_3.gauche=dist_temp_d.gauche and
dist_temp_3.droite=dist_temp_d.droite;
// for computing the elevations
create table alti as select * from
ST_Interpolate("mnt_grandpinsec_point",1, 'ALTI');
create table alt_temp1 as select a.*, b.center as ct_parA from dist a,
uhe_center_g b where a.gauche=b.gauche and a.droite=b.droite;
create table alt_temp2 as select * from dist where dist.gauche=-1;
alter table alt_temp2 add column ct_parA geometry;
create table alt_temp3 as select *
from alt_temp1
UNION
select *
from alt_temp2;
create table alt_temp2 as select * from dist where dist.gauche=-1;
alter table alt_temp2 add column ct_parA geometry;
create table alt_temp3 as select *
from alt_temp1
UNION
select *
from alt_temp2;
create table alt_temp4 as select a.*, b.center as ct_parB from dist a,
uhe_center_d b where a.gauche=b.gauche and a.droite=b.droite;
create table alt_temp5 as select a.*, b.ct_parB as ct_parB from alt_temp3 a,
alt_temp4 b where a.gauche=b.gauche and a.droite=b.droite;
create table alt_temp6 as select a.*, ST_AddZFromRaster(a.ct_parA, b.raster)
as ct_parA_raster, ST_AddZFromRaster(a.ct_parB, b.raster) as ct_parB_raster
from alt_temp5 a, alti b;
alter table alt_temp6 add column ct_parA_z double, add column ct_parB_z double;
update alt_temp6 set ct_parA_z=st_z(ct_parA_raster),
ct_parB_z=st_z(ct_parB_raster);
// for computing the length of the interfaces
create table altitude_length as select *, ST_Length(the_geom) as length
```

```
69 from alt_temp
```

A.5 OrbisGIS SQL commande for constructing polygons of UHEs and Interfaces of the Moulon catchment

```
1  SQL("create table parcel_fil as select a.IDOBJ, a.gravity_center, a.gravity_z, b.NUMOBJ
2  as NUMFIL, b.the_geom as fil_geom from parcel_caract_3 a, " +filvoie+ " b where
3  st_intersects(a.the_geom, st_buffer(b.the_geom,45)); ");
4  SQL("alter table parcel_fil add column projection geometry;");
5  SQL("update parcel_fil set projection=st_nearestpoints(gravity_center, fil_geom);");
6  SQL("create table parcel_fil_1 as select a.IDOBJ, a.gravity_center, a.gravity_z,
7  a.NUMFIL, a.fil_geom, ST_AddZFromRaster(a.projection, b.raster) as projection from
8  parcel_fil a, alti b;");
9  SQL("alter table parcel_fil_1 add column diff_z double;");
10 SQL("update parcel_fil_1 set diff_z=(gravity_z-st_z(projection));");
11 SQL("create table parcel_fil_2 as select IDOBJ, max(diff_z)as max from parcel_fil_1
12 group by IDOBJ;");
13 SQL("create table parcel_fil_3 as select a.* from parcel_fil_1 a, parcel_fil_2 b where
14 a.IDOBJ=b.IDOBJ and a.diff_z=b.max;");
15 SQL("alter table parcel_fil_3 add column length_fil double;");
16 SQL("update parcel_fil_3 set length_fil=st_length(fil_geom);");
17 SQL("create table parcel_fil_4 as select IDOBJ, max(length_fil)as max from parcel_fil_3
18 group by IDOBJ;");
19 SQL("create table parcel_fil_5 as select a.* from parcel_fil_3 a, parcel_fil_4 b where
20 a.IDOBJ=b.IDOBJ and a.length_fil=b.max;");
21
22 SQL("drop table parcel_fil, parcel_fil_1, parcel_fil_2, parcel_fil_3, parcel_fil_4;");
23 SQL("create table isol as select IDOBJ from parcel_fil_5;");
24 SQL("alter table isol add column code double;");
25 SQL("update isol set code=1;");
26 SQL("create table isol_1 as select IDOBJ from parcel_caract_3;");
27 SQL("alter table isol_1 add column code double;");
28 SQL("update isol_1 set code=0;");
29 SQL("create table isol_2 as select * from isol union select * from isol_1;");
30 SQL("create table isol_3 as select IDOBJ, sum(code) as code from isol_2 group by
31 IDOBJ;");
32 SQL("create table isol_4 as select a.IDOBJ, b.the_geom, b.gravity_z from isol_3 a,
33 parcel_caract_3 b where a.code=0 and a.IDOBJ=b.IDOBJ;");
34 SQL("create table isol_5 as select a.IDOBJ, b.the_geom, b.gravity_z from isol_3 a,
35 parcel_caract_3 b where a.code=1 and a.IDOBJ=b.IDOBJ;");
36 SQL("create table isol_6 as select a.IDOBJ as isol, b.IDOBJ as other_par, (a.gravity_z-
37 b.gravity_z) as diff_z from isol_4 a, isol_5 b where st_intersects(a.the_geom,
38 b.the_geom); ");
39 SQL("create table isol_7 as select isol, max(diff_z) as max from isol_6 group by isol;");
40 SQL("create table isol_8 as select a.* from isol_6 a, isol_7 b where a.isol=b.isol and
41 a.diff_z=b.max;");
42 SQL("create table isol_9 as select a.isol as IDOBJ, b.NUMFIL from isol_8 a,
43 parcel_fil_5 b where a.other_par=b.IDOBJ;");
44 SQL("drop table isol, isol_1, isol_2, isol_3, isol_4, isol_5, isol_6, isol_7, isol_8;");
45 SQL("create table isol_10 as select a.*, b.the_geom as fil_geom from isol_9 a, "
```

```
+filvoie+ " b where a.NUMFIL=b.NUMOBJ;");
SQL("create table isol_11 as select a.*, b.gravity_center from isol_10 a, parcel_caract_3
b where a.IDOBJ=b.IDOBJ;");
SQL("alter table isol_11 add column projection geometry;");
SQL("update isol_11 set projection=st_nearestpoints(gravity_center, fil_geom); ");
SQL("create table isol_12 as select a.IDOBJ, a.NUMFIL, a.fil_geom, a.gravity_center,
ST_AddZFromRaster(a.projection, b.raster) as projection from isol_11 a, alti b;");
SQL("create table parcel_fil_6 as select IDOBJ, NUMFIL, projection from parcel_fil_5
union select IDOBJ, NUMFIL, projection from isol_12;");
SQL("create table parcel_caract_4 as select a.*, b.NUMFIL, b.projection from
parcel_caract_3 a, parcel_fil_6 b where a.IDOBJ=b.IDOBJ;");
SQL("drop table isol_9, isol_10, isol_11, isol_12, parcel_caract_3, parcel_fil_5,
parcel_fil_6;");
SQL("alter table parcel_caract_4 add column proj_x double;");
SQL("alter table parcel_caract_4 add column proj_y double;");
SQL("alter table parcel_caract_4 add column proj_z double;");
SQL("update parcel_caract_4 set proj_x=st_x(projection);");
SQL("update parcel_caract_4 set proj_y=st_y(projection);");
SQL("update parcel_caract_4 set proj_z=st_z(projection);");
```

A.6 OrbisGIS SQL commande for defining geometrical parameters of UHEs and Interfaces of the Moulon catchment

```
// calculate the built area of the parcels
SQL("create table built_area as select a.IDOBJ, b.the_geom as built_geom,
st_area(b.the_geom)as built_area from " +parcelles+ " a," +batidur+ " b where
st_contains(a.the_geom, b.the_geom);" );
SQL( "create table built_area_1 as select IDOBJ, sum(built_area) from built_area group
by IDOBJ;");
SQL("create table built_area_2 as select IDOBJ from " + parcelles+";");
SQL("alter table built_area_2 add column built_area double;" );
SQL("update built_area_2 set built_area=0;");
SQL("create table built_area_3 as select * from built_area_2 union select * from
built_area_1;");
SQL("create table built_area_4 as select IDOBJ, sum(built_area) as built_area from
built_area_3 group by IDOBJ;");
SQL("drop table built_area_1, built_area_2, built_area_3;");

//compute the gravity of parcels. If there exist several building in one parcel, choose the
gravity of the biggest building
SQL("create table built_gravity as select IDOBJ, max(built_area) as max_area from
built_area group by IDOBJ;");
SQL("create table built_gravity_1 as select a.IDOBJ, a.built_geom from built_area a,
built_gravity b where a.IDOBJ=b.IDOBJ and a.built_area=max_area;");
SQL("create table built_gravity_2 as select IDOBJ, st_centroid(built_geom)as
gravity_center from built_gravity_1;");
SQL("create table parcel_gravity as select IDOBJ from " + parcelles+";");
SQL("alter table parcel_gravity add column gravity_center geometry;");
SQL("create table parcel_gravity_1 as select * from built_gravity_2 union select * from
parcel_gravity;");
```

```
28
29 SQL("create table parcel_gravity_2 as select IDOBJ, st_union(gravity_center)as
30 gravity_center from parcel_gravity_1 group by IDOBJ;");
31 SQL("drop table built_area, built_gravity, built_gravity_1, built_gravity_2,
32 parcel_gravity, parcel_gravity_1;");
33 //integrate the tables
34 SQL("create table parcel_caract as select a.*, st_area(a.the_geom) as surface, b.built_area
35 from "+ parcelles+" a, built_area_4 b where a.IDOBJ=b.IDOBJ;");
36 SQL("create table parcel_caract_1 as select a.*, b.gravity_center from parcel_caract a,
37 parcel_gravity_2 b where a.IDOBJ=b.IDOBJ;");
38 SQL("update parcel_caract_1 set gravity_center=st_centroid(the_geom) where
39 built_area=0;");
40 SQL("create table parcel_voie as select a.IDOBJ as IDPAR, st_area(a.the_geom) as
41 parcel_area, b.NUMOBJ as IDVOIE, ST_Area(b.the_geom)as voie_area from "
42 +parcelles+ " a, " +surfvoie+ " b where ST_Intersects(st_buffer(a.the_geom,0),
43 st_buffer(b.the_geom,0));");
44 SQL("create table voie_parcel as select a.NUMOBJ as IDVOIE, b.IDOBJ as IDPAR,
45 ST_Area(b.the_geom)as parcel_area from " +surfvoie+ " a, " +parcelles+ " b where
46 ST_Intersects(st_buffer(a.the_geom,0), st_buffer(b.the_geom,0));");
47 SQL("create table voie_parcel_1 as select IDVOIE, sum(parcel_area) as
48 total_parcel_area from voie_parcel group by IDVOIE;");
49 SQL("create table parcel_voie_1 as select a.*, b.total_parcel_area from parcel_voie a,
50 voie_parcel_1 b where a.IDVOIE=b.IDVOIE;");
51 SQL("alter table parcel_voie_1 add column street_adj double;");
52 SQL("update parcel_voie_1 set street_adj=voie_area*parcel_area/total_parcel_area;");
53 SQL("create table parcel_voie_2 as select IDPAR, sum(street_adj)as street_adj from
54 parcel_voie_1 group by IDPAR;");
55 SQL("create table parcel_voie_3 as select IDOBJ as IDPAR from "+parcelles+";");
56 SQL("alter table parcel_voie_3 add column street_adj double;");
57 SQL("create table parcel_voie_4 as select * from parcel_voie_2 union select * from
58 parcel_voie_3 ;");
59 SQL("create table parcel_voie_5 as select IDPAR, sum(street_adj) as street_adj from
60 parcel_voie_4 group by IDPAR;");
61 SQL("drop table parcel_voie, parcel_voie_1, parcel_voie_2, parcel_voie_3,parcel_voie_4,
62 voie_parcel, voie_parcel_1;");
63 SQL("create table parcel_caract_2 as select a.*, b.street_adj from parcel_caract_1 a,
64 parcel_voie_5 b where a.IDOBJ=b.IDPAR;");
65 SQL("alter table parcel_caract_2 add column gravity_x double;");
66 SQL("alter table parcel_caract_2 add column gravity_y double;");
67 SQL("update parcel_caract_2 set gravity_x=st_x(gravity_center);");
68 SQL("update parcel_caract_2 set gravity_y=st_y(gravity_center);");
69 SQL("drop table parcel_caract, parcel_caract_1, built_area_4, parcel_voie_5,
70 parcel_gravity_2;");
71 //generate the layer of altitude raster
72 SQL("create table alti as select * from ST_Interpolate("+mnt+",1, 'ALTI');");
73 SQL("create table parcel_caract_3 as select a.the_geom, a.IDOBJ, a.surface, a.built_area,
74 a.street_adj, ST_AddZFromRaster(a.gravity_center, b.raster) as gravity_center,
75 a.gravity_x, a.gravity_y from parcel_caract_2 a, alti b; ");
76 SQL("alter table parcel_caract_3 add column gravity_z double;");
77 SQL("update parcel_caract_3 set gravity_z=st_z(gravity_center);");
78 SQL("drop table parcel_caract_2;");
79 //SQL("alter table parcel_caract_3 drop gravity_center;");
80 //connection between parcel and street
```

```
81  SQL("create table parcel_fil as select a.IDOBJ, a.gravity_center, a.gravity_z, b.NUMOBJ
82  as NUMFIL, b.the_geom as fil_geom from parcel_caract_3 a, " +filvoie+ " b where
83  st_intersects(a.the_geom, st_buffer(b.the_geom,45)); ");
84  SQL("alter table parcel_fil add column projection geometry;");
85  SQL("update parcel_fil set projection=st_nearestpoints(gravity_center, fil_geom);");
86  SQL("create table parcel_fil_1 as select a.IDOBJ, a.gravity_center, a.gravity_z,
87  a.NUMFIL, a.fil_geom, ST_AddZFromRaster(a.projection, b.raster) as projection from
88  parcel_fil a, alti b;");
89  SQL("alter table parcel_fil_1 add column diff_z double;");
90  SQL("update parcel_fil_1 set diff_z=(gravity_z-st_z(projection));");
91  SQL("create table parcel_fil_2 as select IDOBJ, max(diff_z)as max from parcel_fil_1
92  group by IDOBJ;");
93  SQL("create table parcel_fil_3 as select a.* from parcel_fil_1 a, parcel_fil_2 b where
94  a.IDOBJ=b.IDOBJ and a.diff_z=b.max;");
95  SQL("alter table parcel_fil_3 add column length_fil double;");
96  SQL("update parcel_fil_3 set length_fil=st_length(fil_geom);");
97  SQL("create table parcel_fil_4 as select IDOBJ, max(length_fil)as max from parcel_fil_3
98  group by IDOBJ;");
99  SQL("create table parcel_fil_5 as select a.* from parcel_fil_3 a, parcel_fil_4 b where
100 a.IDOBJ=b.IDOBJ and a.length_fil=b.max;");
101
102 SQL("drop table parcel_fil, parcel_fil_1, parcel_fil_2, parcel_fil_3, parcel_fil_4;");
103 SQL("create table isol as select IDOBJ from parcel_fil_5;");
104 SQL("alter table isol add column code double;");
105 SQL("update isol set code=1;");
106 SQL("create table isol_1 as select IDOBJ from parcel_caract_3;");
107 SQL("alter table isol_1 add column code double;");
108 SQL("update isol_1 set code=0;");
109 SQL("create table isol_2 as select * from isol union select * from isol_1;");
110 SQL("create table isol_3 as select IDOBJ, sum(code) as code from isol_2 group by
111 IDOBJ;");
112 SQL("create table isol_4 as select a.IDOBJ, b.the_geom, b.gravity_z from isol_3 a,
113 parcel_caract_3 b where a.code=0 and a.IDOBJ=b.IDOBJ;");
114 SQL("create table isol_5 as select a.IDOBJ, b.the_geom, b.gravity_z from isol_3 a,
115 parcel_caract_3 b where a.code=1 and a.IDOBJ=b.IDOBJ;");
116 SQL("create table isol_6 as select a.IDOBJ as isol, b.IDOBJ as other_par, (a.gravity_z-
117 b.gravity_z) as diff_z from isol_4 a, isol_5 b where st_intersects(a.the_geom,
118 b.the_geom); ");
119 SQL("create table isol_7 as select isol, max(diff_z) as max from isol_6 group by isol;");
120 SQL("create table isol_8 as select a.* from isol_6 a, isol_7 b where a.isol=b.isol and
121 a.diff_z=b.max;");
122 SQL("create table isol_9 as select a.isol as IDOBJ, b.NUMFIL from isol_8 a,
123 parcel_fil_5 b where a.other_par=b.IDOBJ;");
124 SQL("drop table isol, isol_1, isol_2, isol_3, isol_4, isol_5, isol_6, isol_7, isol_8;");
125
126 SQL("create table isol_10 as select a.*, b.the_geom as fil_geom from isol_9 a, "
127 +filvoie+ " b where a.NUMFIL=b.NUMOBJ;");
128 SQL("create table isol_11 as select a.*, b.gravity_center from isol_10 a, parcel_caract_3
129 b where a.IDOBJ=b.IDOBJ;");
130 SQL("alter table isol_11 add column projection geometry;");
131 SQL("update isol_11 set projection=st_nearestpoints(gravity_center, fil_geom); ");
132 SQL("create table isol_12 as select a.IDOBJ, a.NUMFIL, a.fil_geom, a.gravity_center,
133 ST_AddZFromRaster(a.projection, b.raster) as projection from isol_11 a, alti b;");
```

```
SQL("create table parcel_fil_6 as select IDOBJ, NUMFIL, projection from parcel_fil_5
union select IDOBJ, NUMFIL, projection from isol_12;");
SQL("create table parcel_caract_4 as select a.*, b.NUMFIL, b.projection from
parcel_caract_3 a, parcel_fil_6 b where a.IDOBJ=b.IDOBJ;");
SQL("drop table isol_9, isol_10, isol_11, isol_12, parcel_caract_3, parcel_fil_5,
parcel_fil_6;");
SQL("alter table parcel_caract_4 add column proj_x double;");
SQL("alter table parcel_caract_4 add column proj_y double;");
SQL("alter table parcel_caract_4 add column proj_z double;");
SQL("update parcel_caract_4 set proj_x=st_x(projection);");
SQL("update parcel_caract_4 set proj_y=st_y(projection);");
SQL("update parcel_caract_4 set proj_z=st_z(projection);");
//furthest
SQL("alter table parcel_caract_4 add column furthest geometry;");
SQL("update parcel_caract_4 set furthest=ST_FurthestPoint(projection, the_geom);");
SQL("create table parcel_caract_5 as select a.the_geom, a.IDOBJ, a.surface, a.built_area,
a.street_adj, a.gravity_x, a.gravity_y, a.gravity_z, a.NUMFIL, a.proj_x, a.proj_y, a.proj_z,
ST_AddZFromRaster(a.furthest, b.raster) as furthest from parcel_caract_4 a, alti b;");
SQL("alter table parcel_caract_5 add column fur_x double;");
SQL("alter table parcel_caract_5 add column fur_y double;");
SQL("alter table parcel_caract_5 add column fur_z double;");
SQL("update parcel_caract_5 set fur_x=st_x(furthest);");
SQL("update parcel_caract_5 set fur_y=st_y(furthest);");
SQL("update parcel_caract_5 set fur_z=st_z(furthest);");
SQL("alter table parcel_caract_5 drop furthest;");
SQL("drop table parcel_caract_4, alti;");

--generate the new layer of th UHE
--create table trottoir_UHE as select ST_Union(the_geom) as the_geom, cat from trottoir
group by cat;
--create table par_UHE as select the_geom, cat from parcelles;
--create table par_trottoir as select * from par_UHE union select * from trottoir_UHE;
--create table UHE as select ST_UNION(the_geom) as the_geom, cat from par_trottoir
group by cat;
--EXECUTE Export(UHE, 'D:\Documents and Settings\qingxiao\result\UHE.shp');
--create table inter_par as select a.*, b.ID AS NUMPAR, b.centroid, b.Zcenter as
ct_par_z from UHE a, parcelles_58 b where a.cat=b.cat;
--create table inter_par_2 as select * from inter_par;
--create table interface as select st_intersection(a.the_geom, b.the_geom) as the_geom,
AUTONUMERIC() as ID, a.NUMPAR as NUMPAR_A, b.NUMPAR as NUMPAR_B,
a.ct_par_z as ct_parA_z, b.ct_par_z as ct_parB_z, a.centroid as a_cent, b.centroid as
b_cent, a.cat as gauche, b.cat as driote from inter_par a, inter_par_2 b where
st_intersects(a.the_geom, b.the_geom) and a.cat!=b.cat;
--create table interface_1 as select ID, NUMPAR_A, NUMPAR_B, st_distance(a_cent,
the_geom) as distanceA, st_distance(b_cent, the_geom) as distanceB, ct_parA_z,
ct_parB_z, ST_Length(the_geom) as length, gauche, driote as droite from interface;
--select ID from interface where st_dimension(the_geom)=2;
--create table test as select the_geom, ID, gauche, driote as droite from interface;
--create
 table
 interface_2
 as
 select
```

```
 ID,
 NUMPAR_A,
 NUMPAR_B,
(distanceA*ct_parB_z+distanceB*ct_parA_z)/(distanceA+distanceB) as altInterface,
distanceA, distanceB, ct_parA_z, ct_parB_z, length, gauche, droite from interface_1
where length>0;
--create table interface_3 as select length, min(gauche) as gauche from interface_2 group
by length;
--create table interface_4 as select a.* from interface_2 a, interface_3 b where
a.length=b.length and a.gauche=b.gauche;
--select distinct gauche from interface_2;
--update interface set length=st_length(the_geom);
--create table orbis_func as select * from FunctionHelp();
--create table interface_q as select the_geom, ID from interface;
--alter table interface_5 add column bed_interfac double;
--alter table interface_5 add column bed_parA double;
--alter table interface_5 add column bed_parB double;
--update interface_5 set bed_interfac=-99;
--update interface_5 set bed_parA=-99;
--update interface_5 set bed_parB=-99;
--create table interface_6 as select ID, NUMPAR_A, NUMPAR_B, altInterface,
bed_interfac, distanceA, distanceB, ct_parA_z, ct_parB_z, bed_parA, bed_parB, length,
gauche, droite from interface_5;
--create table interface_7 as select a.the_geom, AUTONUMERIC() as ID,
b.NUMPAR_A, b.NUMPAR_B, b.altInterface, b.bed_interfac, b.distanceA, b.distanceB,
b.ct_parA_z, b.ct_parB_z, b.bed_parA, b.bed_parB, b.length, b.gauche, b.droite from
interface_4 a, interface_6 b where a.ID=b.ID;
--create table boundary as select ST_Boundary(st_union(the_geom)) as the_geom from
UHE;
--create table boundary_1 as select ST_INTERSECTION(a.the_geom, b.the_geom) as
the_geom, b.cat as droite from boundary a, UHE b where ST_INTERSECTS(a.the_geom,
b.the_geom);
--alter table boundary_1 add column distanceA double;
--alter table boundary_1 add column distanceB double;
--update boundary_1 set distanceA=0;
--create table boundary_2 as select a.centroid, a.Zcenter as ct_parB_z, b.* from
parcelles_58 a, boundary_1 b where a.cat=b.droite;
--update boundary_2 set distanceB=st_distance(centroid, the_geom);
--alter table boundary_2 add column ct_parA_z double;
--update boundary_2 set ct_parA_z=ct_parB_z;
--alter table boundary_2 add column length double;
--update boundary_2 set length= st_length(the_geom);
--alter table boundary_2 add column gauche double;
--update boundary_2 set gauche=-1;
--alter table boundary_2 add column NUMPAR_A text;
--alter table boundary_2 add column NUMPAR_B text;
--alter table boundary_2 drop column NUMPAR_B;
--create table boundary_3 as select a.*, b.ID as NUMPAR_B from boundary_2 a,
parcelles_58 b where a.droite=b.cat;
--alter table boundary_3 add column altInterface double;
--update boundary_3 set altInterface=ct_parA_z;
/*alter table boundary_3 add column bed_interfac double;
alter table boundary_3 add column bed_parA double;
```

```
240 alter table boundary_3 add column bed_parB double;
241 update boundary_3 set bed_interfac=-99;
242 update boundary_3 set bed_parA=-99;
243 update boundary_3 set bed_parB=-99;
244 create table interface_8 as select the_geom, NUMPAR_A, NUMPAR_B, altInterface,
245 bed_interfac, distanceA, distanceB, ct_parA_z, ct_parB_z, bed_parA, bed_parB, length,
246 gauche, droite from interface_7 union select the_geom, NUMPAR_A, NUMPAR_B,
247 altInterface, bed_interfac, distanceA, distanceB, ct_parA_z, ct_parB_z, bed_parA,
248 bed_parB, length, gauche, droite from boundary_3;*/
249 --create table interface_9 as select the_geom, AUTONUMERIC() as ID,NUMPAR_A,
250 NUMPAR_B, altInterface, bed_interfac, distanceA, distanceB, ct_parA_z, ct_parB_z,
251 bed_parA, bed_parB, length, gauche, droite from interface_8;
```

Appendix B

Theory of water flow in the soil

B.1 General three-dimensional saturated-unsaturated groundwater flow equation

The general three-dimensional saturated-unsaturated flow equation is written as:

$$\frac{\partial}{\partial x}(K_x(h)\frac{\partial h}{\partial x}) + \frac{\partial}{\partial y}(K_y(h)\frac{\partial h}{\partial y}) + \frac{\partial}{\partial z}(K_z(h)(\frac{\partial h}{\partial z} + 1)) + Q = [C(h) + S_w S_s]\frac{\partial h}{\partial t} \tag{B.1}$$

where K_i is the component on the direction i of the hydraulic conductivity tensor, h the hydraulic head, $C(h) = \frac{\partial \theta}{\partial h}$ the specific moisture capacity (the slope of the moisture retention curve), S_w the saturated fraction of the porous medium ($S_w = \frac{\theta}{\eta}$ with η the porosity), S_s the specific storage representing the volume of water released per unit volume of aquifer per unit decline in pressure head, Q a volumetric source or sink term. Equation B.1 is called the "modified Richards equation" and obtained by combining the continuity equation and the Darcy equation, under several assumptions:

- The aquifer and water are slightly compressible in the saturated confined zone but incompressible in the unsaturated zone and in the unconfined saturated zone;
- The principle axis of anisotropy is aligned with the principle axis of flow;
- Water density does not vary spatially.

In the saturated zone, we have:

$$C(h) = \frac{\partial \theta}{\partial h} = 0$$
$$K(h) = K_s = \text{constant}$$
$$S_w = \frac{\theta}{\eta} = 1$$

and

$$h \geq h_{air\ entry}$$

Therefore, in the saturated zone, equation B.1 becomes

$$\frac{\partial}{\partial x}(K_s(h)\frac{\partial h}{\partial x}) + \frac{\partial}{\partial y}(K_s(h)\frac{\partial h}{\partial y}) + \frac{\partial}{\partial z}(K_s(h)(\frac{\partial h}{\partial z} + 1)) + Q = S_s\frac{\partial h}{\partial t} \tag{B.2}$$

In the unsaturated zone, we have:

$$C(h) \neq 0 \quad \text{and} \quad C(h) \gg S_w S_s$$
$$S_w = \frac{\theta}{\eta} < 1$$
$$h < h_{air\ entry}$$
and
$$K(h) = \text{function of h}$$

Therefore, in the unsaturated zone, equation B.1 becomes

$$\frac{\partial}{\partial x}(K_x(h)\frac{\partial h}{\partial x}) + \frac{\partial}{\partial y}(K_y(h)\frac{\partial h}{\partial y}) + \frac{\partial}{\partial z}(K_z(h)(\frac{\partial h}{\partial z} + 1)) + Q = C(h)\frac{\partial h}{\partial t} \tag{B.3}$$

$$\frac{\partial}{\partial x}(K_x(h)\frac{\partial h}{\partial x}) + \frac{\partial}{\partial y}(K_y(h)\frac{\partial h}{\partial y}) + \frac{\partial}{\partial z}(K_z(h)(\frac{\partial h}{\partial z} + 1)) + Q = \frac{\partial \theta}{\partial t} \tag{B.4}$$

Using the term $\partial\theta/\partial t$ converts the pressured-based modified Richards equation into a mixed form of the modified Richards equation. Celia et al. (1990) showed that the modified Pcard iterative procedure for the mixed form of the Richards equation is fully mass conserving in the unsaturated zone.

The hydraulic conductivity K is constant with respect to time and equal to the saturated hydraulic conductivity K_s in the saturated zone. The hydraulic conductivity in the unsaturated zone is defined as a function of the pressure head, which can be derived from moisture-retention curves, h versus θ. Various references exist about the relationships $K(h)$ and $\theta(h)$, among which we can cite the Brooks and Corey (1964) equations and the van Genuchten and Nielsen (1985) relations.

Appendix C

Modifications to the initial model of URBS during the WTI module implementation

The modifications brought to the program during the work of introducing the WTI module are listed below. Classification of the modifications are based on their purposes, as described in Chapter 3, Section 3.3. Every modification requires naturally to add, delete, or change in more than one code in the program in order to keep the coherence (in equations, variables and so on). So the list given above is by no means exhaustive. The line numbers are also indicative.

C.1 Type 1: For the introduction of the WTI module

- Add an option of activation or deactivation of the WTI module, 1 for activation and 0 for deactivation.
- Add the computing of σGWL and write it in the output file "production" (line 1527).

C.2 Type 2: Modifications related to the problem of capillarity fringe

- Check if deficit $< \Delta z_{cf}$ (thickness of the capillarity fringe), instead of deficit < 0 (ground) (line 3204).
- The storage of the capillarity fringe is considered in the balance of the vadose zone. The modified code include:
  - Initialization of S_{vad} (line 426 - 428).

  - Check the excess of water in the vadose zone in taking into consideration of the capillarity fringe (line 3214).
  - Take into consideration of the capillarity fringe in the computing of the infiltration flux I (line 3287) and the flux between the vadose zone and the saturated zone F (line 3398).

C.3 Type 3: For computing water balance and error-check

- Compute water balance in the end of each time step (line 1275).
- Supplementary variables necessary to the computing of water balance: PertePar[p], ET[p], Sspar[0][p], Sspar[1][p].
- Add an output file "test_deficit" for verifying if "deficit" could be negative (between line 771 and 772).

C.4 Type 4: For the purpose of rigour

- In the computing in surface reservoirs, add a check condition for the case where no building exists in the parcel (line 2771).
- Resolve the problem of warning message by correcting the output format of "springf" (in each output file creation).

C.5 Type 5: Error correction in the initial model

- The total transpiration volume of a UHE should take into account of the transpiration flux on street surface (line 896).
- Take into account of the tree-covered pavement area (par[3][p]) in the computing of tree evaporation, which was initially missing (line 986).
- Δz_{cf} of Equation (18) in Rodriguez et al. (2008) was missing (line 3373).

C.6 Type 6: Introduction of anisotropy to the model

- Introduce the variable K_s^{lat}.
- Replace K_s^{nat} by K_s^{lat} in the equation of Q^{drain}.
- Set the option for activating/deactivating the anisotropy.

Appendix D

Hydrogeological survey at Moulon lead by the CEREMA

Table D.1 – Superficial geological formations in the Moulon sector investigated by the CEREMA.

Formations géologiques		PzA (z)	PzB (z)	PzC (z)	PzD (z)	PzE (z)	PzF (z)	PzG (z)	PzH (z)	PzI (z)	PzJ (z)	PzJ refus (z)	Épaisseur moyenne (m)
Limon des plateaux	toit	158.3	154.7	154.8	153.2	158.7	154.5	155.8	161.9	152.5	155.4	155.8	1,0
	mur	156.9	153.7	154.2	152.0	157.7	152.8	155.3	160.3	152.2	154.2	154.9	
Formation de Lozère	toit	156.9	153.7	154.2	152.0	157.7	152.8	155.3			154.2	154.9	1,7
	mur	152.1	152.0	152.8	151.6	156.0	152.5	153.4			152.5	153.4	
AM de Beauce (calcaire à blocs)	toit	152.1	152.0	152.8	151.6	156.0	152.5	153.4	160.3		152.5	153.4	2,8
	mur	149.7	147.2			153.7	146.7	151.9	159.0		150.7		
AM de Beauce (argileux compact)	toit	149.7	147.2			153.7	146.7	151.9	159.0	152.2	150.7		5,3
	mur							147,5		145.2	148.2		

Besides the piezometers by CEREMA (PzA - PzG), all other piezometers in the sector of Moulon were subjected to occasional measurements. The data were compared with the continuous observed series of the piezometers by CEREMA. Figure D.1 shows the location of all existing piezometers in the sector in December 2013.

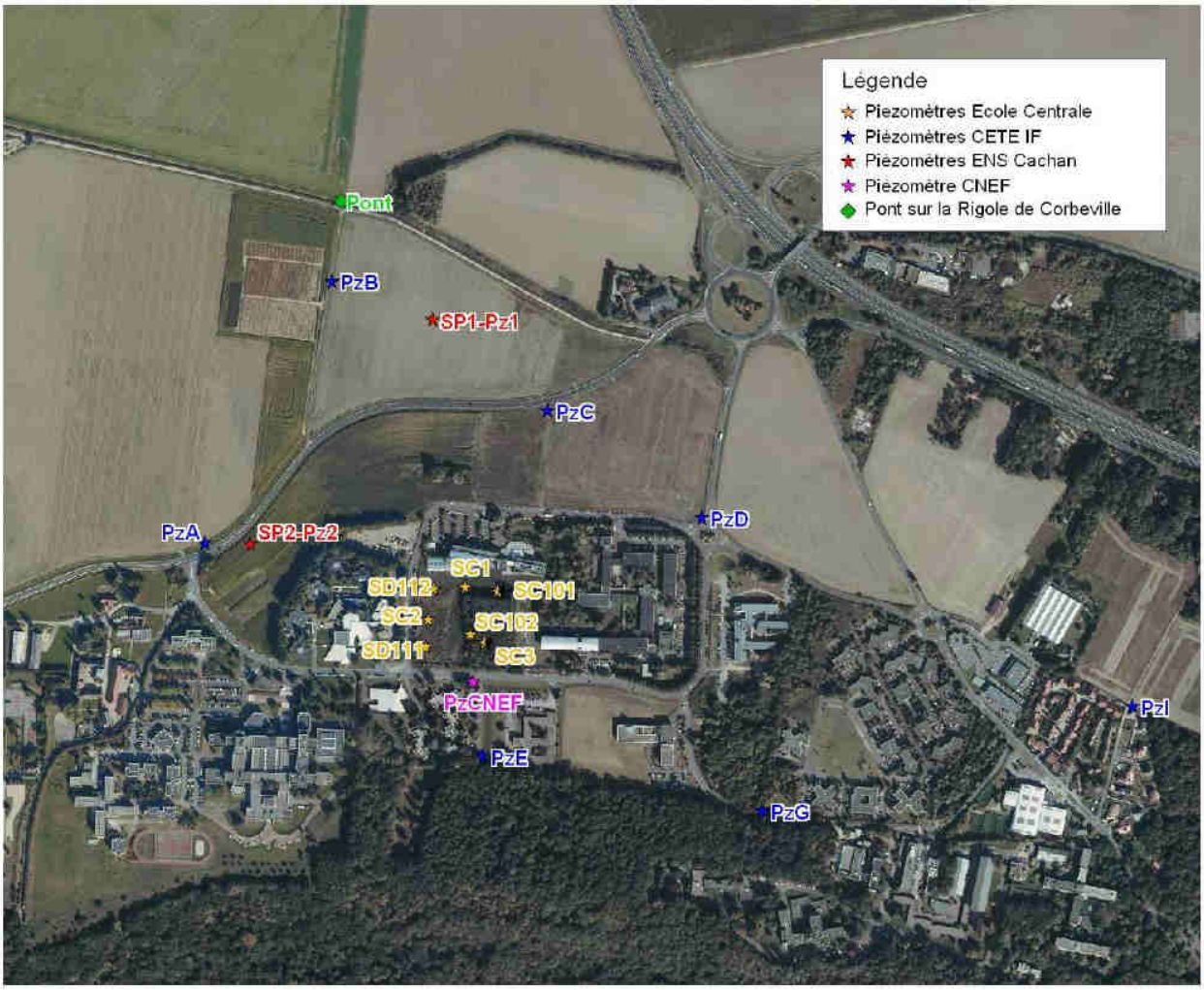

Figure D.1 – Piezometers installed and monitored by CEREMA and all other existing piezometers in the sector of Moulon in December 2013.

Appendix E

Information about Paris-Saclay

E.1 List of partners of Paris-Saclay project

The list below, no exhaustive, gives the mains partners in the project Paris-Saclay.

Université Paris-Sud 11	Agro ParisTech
École Centrale Paris	ENSAE ParisTech
ENSTA ParisTech	École Polytechnique
HEC Paris	IOGS
Supélec	École Normale Supérieure de Cachan
École Supérieur d'Optique	Institut Télécom
CEA	Université Versailles-Saint-Quentin
CNRS	INRA
INRIA	ONERA
IHES	Fondation de Coopération Scientifique
Digitéo-Triangle de la physique	Pôle de compétitivité System@tic
Synchrotron Soleil	

E.2 Transport

The transport issue is one of the major challenges in the project Paris-Saclay. Backed up on the general transport network of the future Grand Paris, in particular the Grand Paris Express which go through the Saclay plateau, the campus Paris-Saclay will be equipped by a level-classified transport network both for motorized transportation and soft mobility. Below are several illustrations of the

future transport network of Paris-Saclay.

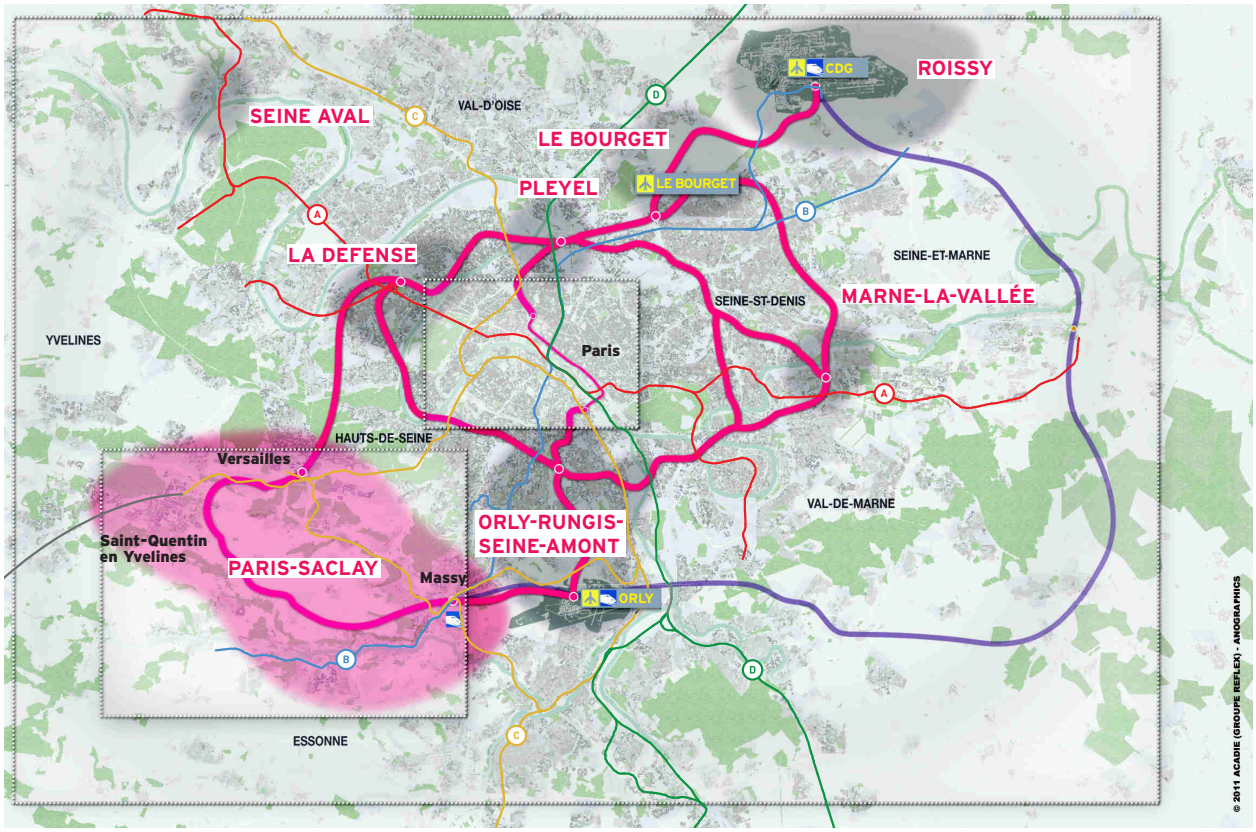

Figure E.1 – Paris-Saclay in the future Grand Paris, with: current commuter train network RER (line A-D), the Parisian airports Roissy-CDG and ORLY, major economic and educational districts of the Paris region (red bold label), and the enlarged transport network of Grand Paris (red bold loop).

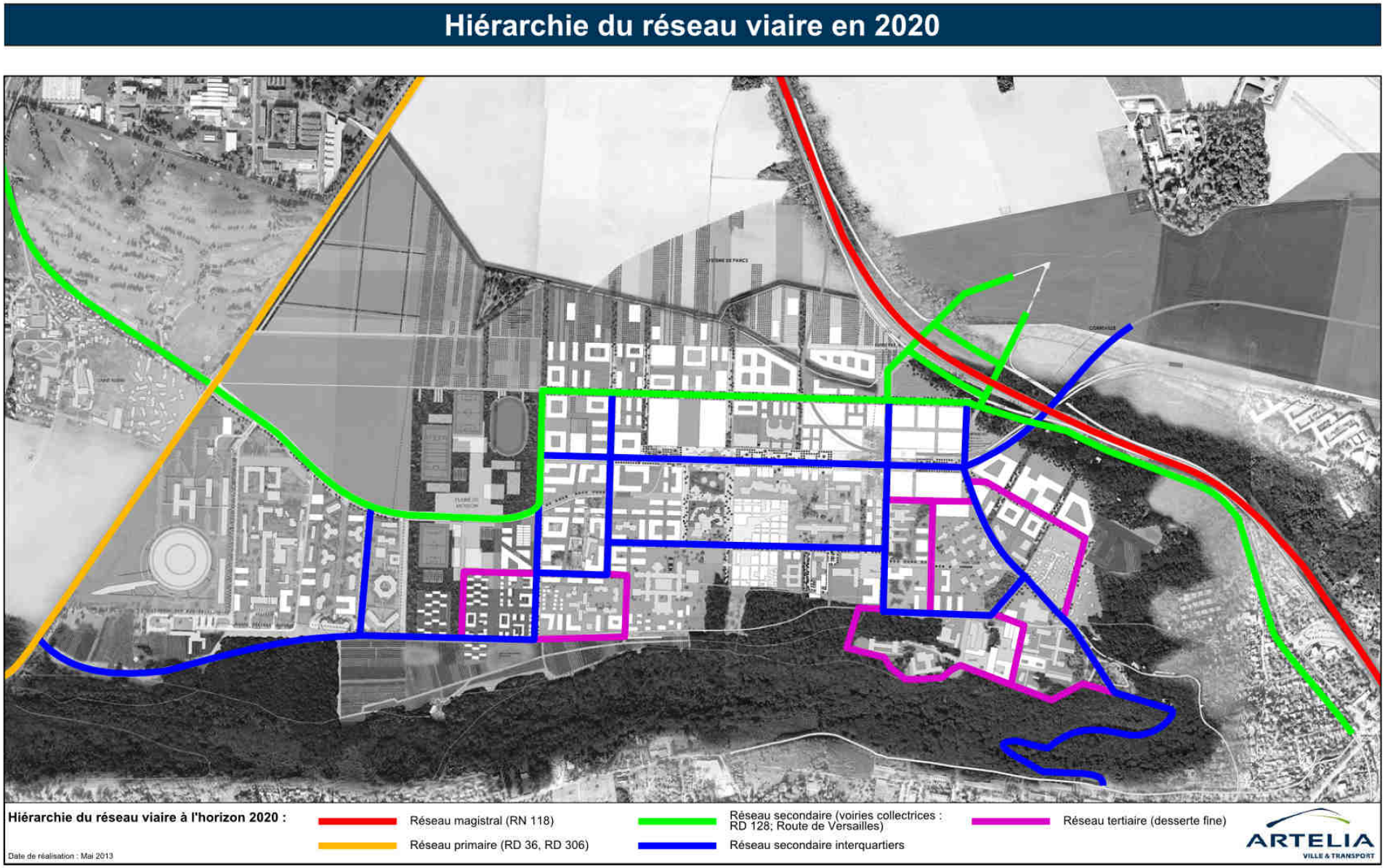

Figure E.2 – Illustration of the level-classified mobility network in the Moulon area in 2020, with: highway N118 (in red), primary roads (in orange), secondary roads (in green), local roads (in blue) and shared space (in violet).

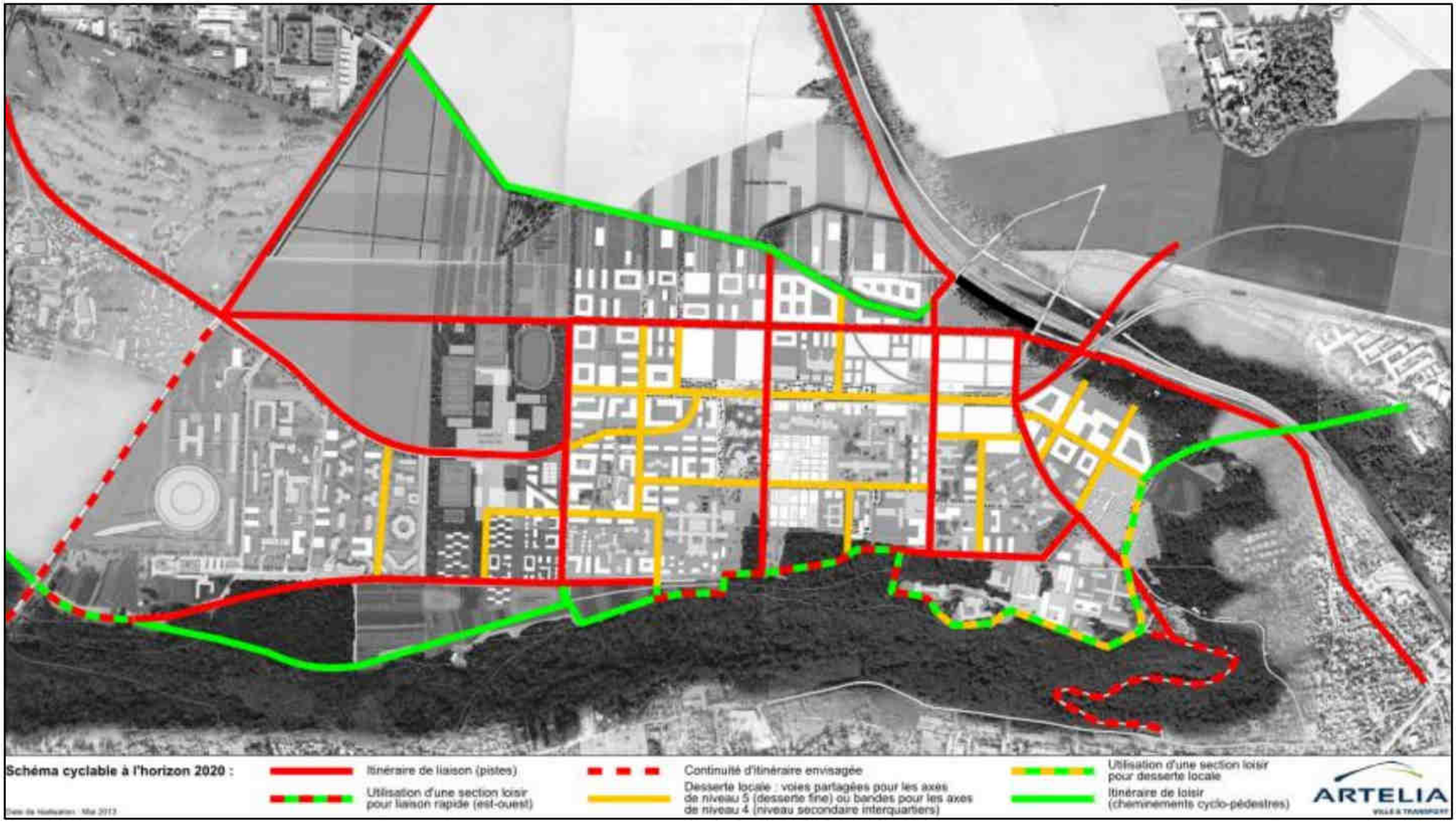

Figure E.3 – Network of cycling and pedestrian paths in the Moulon area in 2020.

E.3 Construction program in Moulon

Existing installations in the Moulon area are as the following:

- housing: 1500 students housings and 200 family housings
- business district: about 60,000 m^2 spreading over three business parks
- university and research: 240,000 m^2 including Synchrotron Soleil, Orme area of CEA, Supélec, a part of Université Paris-Sud 11, CNRS, Digiteo Labs, INRA, and LGEP

The education and research feature of the territory will be kept for the future campus, but will be converted to a campus more open and more mutualising. 870,000 m^2 of construction program is planned in the ZAC:

Table E.2 – Construction program in the Moulon area.

Programme	M² SPC
Enseignement supérieur et recherche et équipements liés	350 000 m²
Développement économique	200 000 m²
Logements étudiants	90 000 m²
Logements familiaux	180 000 m²
Services commerces, équipements	50 000 m²
TOTAL	870 000 m²

Figure E.4 – Spatial organization (indicative) of the construction program in the Moulon area.

Bibliography

Abbott, M. B., Bathurst, J. C., Cunge, J. A., O'Connell, P. E., and Rasmussen, J. (1986). An introduction to the European Hydrological System Systeme Hydrologique Europeen, SHE, 1 History and philosophy of a physically based, distributed modelling system. *Journal of Hydrology*, 87(1-2):45–59.

Ackerman, D. and Stein, E. (2008). Evaluating the effectiveness of best management practices using dynamic modeling. *Journal of Environmental Engineering*, 134.

Ahiablame, L., Engel, B., and Chaubey, I. (2012). Effectiveness of Low Impact Development Practices: Literature Review and Suggestions for Future Research. *Water, Air & Soil Pollution*, 223:4253–4273.

Allen, R. B. and Bridgeman, S. G. (1986). Dynamic programming in hydrop-power scheduling. *Journal of Water Resources Planning and Management*.

Alley, W. and Veenhuis, J. (1983). Effective impervious area in urban runoff modeling. *Journal of Hydrologic Engineering*, 109(2):313–319.

Alley, W. M. and Smith, P. E. (1982a). Distributed Routing Rainfall-Runoff Model: Version II. Geological Survey Open File Report 82-344. Technical report, US Geological Survey.

Alley, W. M. and Smith, P. E. (1982b). Multi-Event Urban Runoff Quality Model. Geological Survey Open File Report 82-764. Technical report, US Geological Survey.

Ando, Y., Musiake, K., and Takahasi, Y. (1984). Modelling of hydrologic processes in a small urbanized hillslope basin with comments on the effects of urbanization. *Journal of Hydrology*, 68:61–83.

Andrieu, H. and Chocat, B. (2004). Introduction to the special issue on urban hydrology. *Journal of Hydrology*, 299(3-4):163–165.

Azzout, Y., Barraud, S., Cres, F., and Alfakih, E. (1994). *Techniques Alternatives En Assainissement Pluvial - Choix, Conception, Réalisation et Entretien.* Lavoisier, Tec & Doc. Insa Lyon.

Barron, O., Barr, A., and Donn, M. (2013). Effect of urbanisation on the water balance of a catchment with shallow groundwater. *Journal of Hydrology*, 485:162–176.

Beasley, D., Huggins, L., and E.J., M. (1980). ANSWERS: A Model for Watershed Planning. In *Transactions of the ASABE. 23 (4)*, pages 938–944.

Beecham, S., Pezzaniti, D., and Kandasamy, J. (2012). Stormwater treatment using permeable pavements. In *Proceedings of the Institution of Civil Engineers - Water Management*, volume 165(3), pages 161–170.

Behera, P. K., Papa, F., and Adams, B. J. (1999). Optimisation of regional storm-water management systems. *Journal of Water Resources Planning and Management*, 3:339–353.

Berthier, E. (1999). *Contribution à une modélisation hydrologique à base physique en milieu urbain - Elaboration du modèle et première évaluation*. PhD thesis, L'institut National Polytechnique de Grenoble, Grenoble, France. (in French).

Berthier, E., Andrieu, H., and Creutin, J. D. (2004). The role of soil in the generation of urban runoff: development and evaluation of a 2D model. *Journal of Hydrology*, 299:252–266.

Berthier, E., Dupont, S., Mestayer, P. G., and Andrieu, H. (2006). Comparison of two evapotranspiration schemes on a sub-urban site. *Journal of Hydrology*, 328:635–646.

Bettess, R., Pitfield, R. A., and Price, R. K. (1978). A surcharging model for storm sewer systems. In Halliwell, P R, editor, *Urban Storm Drainage*, pages 306–316. Pentech Press, London.

Beven, K. and Kirkby, M. (1979). A physically based, variable contributing area model of basin hydrology. *Hydrologiques, Hydrological Sciences-bulletin-des Sciences*, 24(1):43–69.

Bhatt, G., Kumar, M., and Duffy, C. J. (2008). Bridging the gap between geohydrologic data and distributed hydrologic modeling. In Sànchez-Marrè, J., Béjar, J., Comas, A., Rizzoli, and Guariso, G., editors, *Proceedings iEMSs 2008: International Congress on Environmental Modelling and Software: Integrating Sciences and Information Technology for Environmental Assessment and Decision*.

Bian, L., Sun, H., Blodgett, C. F., Egbert, S. L., Li, W., Ran, L., and Koussis, A. D. (1996). Integration architecture and internal database for coupling a hydrological model and ARC/INFO. In *HydroGIS 96: Application of Geographic Information Systems in Hydrology and Water Resources Management*. IAHS.

Bocher, E., Petit, G., Fortin, N., Gouge, A., Lecoeuvre, M., and Martin, J. (2014). Orbisgis. `http://www.orbisgis.org/`.

Booth, D. B., Hartley, D., and Jackson, R. (2002). Forest cover, impervious-surface area, and the mitigation of stormwater impacts1. *JAWRA Journal of the American Water Resources Association*, 38(3):835–845.

Booth, D. B. and Jackson, C. R. (1997). Urbanization of aquatic systems: Degradation thresholds, stormwater detection, and the limits of mitigation1. *JAWRA Journal of the American Water Resources Association*, 33(5):1077–1090.

Boyd, M. J., Bufill, M. C., and Knee, R. M. (1994). Predicting pervious and impervious storm runoff from urban drainage basins. *Hydrological Sciences - Journal des Sciences Hydrologiques*, 39(4):321–332.

Brandes, D., Cavallo, G. J., and Nilson, M. L. (2005). Base flow trends in urbanizing watersheds of the Delaware River basin. *Journal of the American Water Resources Association*, 41(6):1377–1391.

Brandt, A., Bresler, E., Diner, N., Ben-Asher, L., Heller, J., and Goldman, D. (1971). Infiltration from a trickle source: 1. mathematical models. *Soil Science Society of America Proceedings*, 35:675–689.

Branger, F. (2007). *Utilisation d'une plate-forme de modélisation environnementale pour représenter le rôle d'aménagements hydro-agricoles sur les flux d'eau et de pesticides: application au bassin de la Fontaine du Theil (Ille-et-Vilaine).* PhD thesis, INP Grenoble. (in French).

Branger, F., Braud, I., Viallet, P., and Debionne, S. (2008). Modeling the influence of landscape management practices on the hydrology of a small agricultural catchment. In Wang,S.S.Y and Kawahara,M and Holtz,K.P. and Tsujimoto,T and Toda,Y, editor, *Proceedings of the 8th International Conference on HydroScience and Engineering*, pages 586–594, Nagoya, Japan.

Braud, I., Breil, P., Thollet, F., Lagouy, M., Branger, F., Jacqueminet, C., Kermadi, S., and Michel, K. (2013). Evidence of the impact of urbanization on the hydrological regime of a medium-sized periurban catchment in france. *Journal of Hydrology*, 485(0):5 – 23. Hydrology of peri-urban catchments: processes and modelling.

Breil, P. (1990). *Drainage des eaux claires parasites par les réseaux sanitaires. Mécanismes et approche quantitative.* PhD thesis, Université des sciences et techniques du Languedoc (in French).

Brett, M., Mueller, S., and Arhonditsis, G. (2005). A daily time series analysis of stream water phosphorus concentrations along an urban to forest gradient. *Environmental Management*, 35(1):56–71.

BRGM (1999). Étude hydrogéologique du plateau de Saclay, rapport 40840. Technical report, BRGM (in French).

Brooks, R. and Corey, A. (1964). Hydraulic properties of porous media. *Colorado State University Hydrology Paper*, 3.

Brunner, G. W. (2010). *HEC-RAS River Analysis System, User's Manual Version 4.1.*

Burns, D., Vitvar, T., McDonnell, J., Hassett, J., Duncan, J., and Kendall, C. (2005). Effects of suburban development on runoff generation in the Croton River basin, New York, USA. *Journal of Hydrology*, 311:266–281.

Cap, P. A. (1961). *Oeuvres complétes de Bernard Palissy - des eaux et fontaines.* Albert Blanchards, Paris.

Carpenter, D. and Kaluvakolanu, P. (2011). Effect of roof surface type on storm-water runoff from full-scale roofs in a temperate climate. *Journal of irrigation and Drainange Engineering*, 137:161–169.

Carrera-Hernández, J. and Gaskin, S. (2006). The groundwater modeling tool for GRASS (GMTG): Open source groundwater flow modeling. *Computers & Geosciences*, 32:339–351.

Carter, T. and Rasmussen, T. (2005). Vegetated roofs as a stormwater best management practice in an ultra-urban watershed. In Hatcher,K.J, editor, *Proceedings of the 2005 Georgia Water Resources Conference*. University of Georgia, Athens, GA.

Cassan, M. (1986). *Aide-mémoire d'hydraulique souterraine.* Presses de l'Ecole Nationale des Ponts et Chaussées.

Celia, M. A., Bouloutas, E. T., and Zarba, R. L. (1990). A general mass-conservative numerical solution for the unsaturated flow equation. *Water Resources Research*, 26(7):1483–1496.

Choisnel, E. (1988). Estimation de l'évapotranspiration potentielle à partir de données météorologiques. *La météorologie*, 7(23):19–27.

Chu, C. S. and Bowers, C. E. (1977). Computer programs in water resources. *WRRC Bulletin 97*.

CIRIA (2013). Demonstrating the multiple benefits of suds a business case (phase 2). Technical report, Construction Industry Research and Information Association.

Cojean, R. (1975). *Contribution à une cartographie géotechnique pour l'aménagement régional et urbain. Plateaux de Trappes-Saclay, Vallées de la Bièvre et de l'Yvette*. PhD thesis, MINES ParisTech (in French).

Collins, K., Hunt, W., and Hathaway, J. (2008). Hydrologic comparison of four types of permeamble pavement and Standard Asphalt in Eastern North Carolina. *Journal of Hydrologic Engineering*, 13:1146–1157.

Coornaert, M. (2014). Mise en oeuvre d'un outil d'aide à la conception des toitures vgtalises pour la gestion des eaux pluviales urbaines. Master's thesis, University Pierre et Marie Curie, Paris.

Cunge, J. (1969). Au sujet d'une méthode de calcul de propagation de crues (méthode muskingum). *Journal of Hydraulic research*, 7(2):205–230.

Danish Hydraulic Institute (1998). *MOUSE version 4.01, User Manuel and Tutorial*. Danish Hydraulic Institute, Hoersholm, Denmark.

Darcy, H. (1856). Détermination des lois d'écoulement de l'eau à travers le sable. Les fontaines publiques de la ville de Dijon. *Dalmont, Paris*, 70.

Davies, H. (1981). Measurements of rainfall-runoff volume relationships and water balance for roofs and roads. In *Second International Conference on Urban Storm Drainage*, pages 434–443, Illinois.

De Wiest, R. J. M. (1965). *Geohydrology*. John Wiley & Sons Inc, New York.

Deal, B. and Daniel, S. (2004). Spatial dynamic modelling and urban land use transformation: a simulation approach to assessing the costs of urban sprawl. *Ecological Economics*, 51:79–95.

DeKeyser, W., Gevaert, V., Verdonck, F., Nopens, I., De Baets, B., and Vanrolleghem, P. (2010). Combining multimedia models with integrated urban water system models for micropollutants. *Water Science and Technology*, 62:1614–1622.

Desbordes, M. (1987). *Contribution à l'analyse et à la modélisation des mécanismes hydrologiques en milieu urbain*. PhD thesis, University of Montpellier 2, Montpellier, France. (in French).

Dietz, M. (2007). Low impact development practices: a review of current research and recommendations for future directions. *Water, Air & Soil Pollution*, 186:351–363.

Dietz, M. and Clausen, J. (2007). Stormwater runoff and export changes with development in a traditional and low impact subdivision. *Journal of Environmental Management*, 87:560–566.

Dogan, A. (1999). *Variably saturated three-dimensional rainfall driven groundwater pumping model*. PhD thesis, University of Florida.

Dumont, E., Kreziac, C., Diome, C., and Bogaert, M. (2013). Projet scientifique SACLAY - Synthèse géologique et hydrogéologique. Technical report, CEREMA - Direction territoriale Île-de-France.

Dupasquier, B. (1999). *Modélisation hydrologique et hydraulique des infiltrations d'eaux parasites dans les réseaux séparatifs d'eaux usées*. PhD thesis, Ecole Nationale du Génie Rural, des Eaux et Forts (in French).

Dupont, S., Mestayer, P. G., Guilloteau, E., Berthier, E., and Andrieu, H. (2006). Parameterization of the Urban Water Budget with the Submesoscale Soil Model. *Journal of Applied Meteorology and Climatology*, 45(4):624–648.

Dupuit, J. (1863). *Études théoriques et pratiques sur le mouvement des eaux dans les canaux découverts et à travers les terrains perméabls: avec des considérations relatives au régime des grandes eaux, au débouché à leur donner, et à la marche des alluvions dans les rivières à fond mobile*. Dunod.

Elliott, A. and Trowsdale, S. (2007). A review of models for low impact urban stormwater drainage. *Environmental Modelling & Software*, 22:394–405.

Endreny, T. (2005). Land use and land cover effects on runoff processes: urban and suburban development. In Anders,M.G, editor, *Encyclopedia of Hydrological Sciences*, pages 1775–1804, Chichester, UK. John Wiley & Sons Ltd.

ESRI (2014). Geodatabase topology rules and topology error fixes. `http://help.arcgis.com/en/arcgisdesktop/10.0/help/index.html#//001t000000sp000000.htm`.

Evans, B. M., Grimm, J., Thornton, L., and Sanders, P. (1992). Linking GIS with Hydrologic Modeling. In Engman, T., editor, *Irrigation and Drainage: Saving a Threatened ResourceIn Search of Solutions. 19th ASCE National Conference on Irrigation and Drainage*, pages 499–504. American Society of Civil Engineers.

eWater CRC (2009). Model for urban stormwater improvement conceptualisation (MUSIC). 4.0 ed. Canberra: eWater Cooperative Research Center.

eWater CRC (2014). Urban developer website. eWater Cooperative Research Center. `http://www.ewater.com.au/products/music/related-tools/urban-developer/`.

Fach, S., Engelhard, C., Wittke, N., and Rauch, W. (2011). Performance infiltration swales with regard to operation in winter times in alpine region. *Water Science and Technology*, 51:37–45.

Farias, K. (2013). Moélisation hydrologique urbaine intégrée sur un réel projet d'aménagement d'envergure. Master's thesis, École National des Ponts et Chaussées, Marne-le-Vallée, France. (in French).

Fassman, E. and Blackbourn, S. (2010). Urban runoff mitigation by a permeable pavement system over impermeable soils. *Journal of Hydrologic Engineering*, 15:475–485.

Fassman-Beck, E. A. and Simcock, R. (2013). Living roof review and design recommendations for stormwater management. Technical report, Auckland UniServices for Auckland Council.

Fatta, D., Naoum, D., and Loizidou, M. (2002). Integrated environmental monitoring and simulation system for use as a management decision support tool in urban areas. *Journal of Environmental Management*, 64:333–343.

Favreau, G. and Leduc, C. (1998). Fluctuations à long terme de la nappe phratique du Continental Terminal près de Niamey (Niger). In *Water Resources Variability in Africa during the XXth Century (Proceedings of the Abidjan '98 Conference*, volume 252, Abidjan, Côte d'Ivoire.

Feddes, R. A., Hoff, H., Bruen, M., Dawson, T., de Rosnay, P., Dirmeyer, P., Jackson, R. B., Kabat, P., Kleidon, A., Lilly, A., and Pitman, A. J. (2001). Modeling Root Water Uptake in Hydrological and Climate Models. *Bulletin of the American Meteorological Society*, 82(12):2797–2809.

Feldman, A. D. and DeVantier, B. A. (1993). Review of GIS applications in hydrologic modeling. Technical report, US Army Corps of Engineers, Hydrologic Engineering Center.

Fénié, B. and Benie, J. (2000). *Dictionnaire des payes et provinces de France*. Sud-Ouest.

Fletcher, T., Andrieu, H., and Hamel, P. (2013). Understanding, management and modelling of urban hydrology and its consequences for receiving waters: A state of the art. *Advances in Water Resources*, 51(0):261 – 279. 35th Year Anniversary Issue.

Fletcher, T., Deletic, A., and Hatt, B. (2004a). A Review of Stormwater Sensitive Urban Design in Australia. Technical report, Department of Civil Engineering & Institute for Sustainable Water Resources, Monash University.

Fletcher, T., Wong, T., Duncan, H., Deletic, A., Coleman, J., and Jenkins, G. (2004b). Recent advances in decision-support for stormwater management: the music approach. Novatech 2004.

Fletcher, T. D., Shuster, W., Hunt, W. F., Ashley, R., Butler, D., Arthur, S., Trowsdale, S., Barraud, S., Semadeni-Davies, A., Bertrand-Krajewski, J.-L., Mikkelsen, P. S., Rivard, G., Uhl, M., Dagenais, D., and Viklander, M. (2014). SUDS, LID, BMPs, WSUD and more The evolution and application of terminology surrounding urban drainage. *Urban Water Journal*, pages 1–18.

Forchheimer, D. H. (1898). Grundwasserspiegel bei brunnenanlagen. *Zeitschrift Öestterr. Ingenieur - und Architekten-Vereines*, 44:629–635.

Foster, S., Hirata, R., and Garduno, H. (2010). Urban Groundwater Use Policy - Balancing the Benefits and Risks in Developing Nations. GW-MATE Strategic Overview Series 3. World Bank, Washington, DC, USA. Available at www.worldbank.orggwmate.

Foster, S. and Vairavamoorthy, K. (2013). Urban Groundwater - Policies and institutions for integrated management. Global Water Partenership.

Furusho, C., Andrieu, H., and Chancibault, K. (2014). Analysis of the hydrological behaviour of an urbanizing basin. *Hydrological Processes*, 28(4):1809–1819.

Garcia-Fresca, B. and Sharp, J. M. (2005). Hydrogeologic considerations of urban development: Urban-induced recharge. *Reviews in Engineering Geology*, 16:123–136.

GDAL (2013). GDAL - Geospatial Data Abstraction Library .

GEOS (n.d). GEOS - Geometry Engine, Open Source. `http://trac.osgeo.org/geos/`.

GEOTHER (2014). École Centrale PARIS - Rue Joliot Curie à Gif-sur-Yvette (91). Technical report, GEOTHER. (in French).

Giangola-Murzyn, A., Gires, A., Richard, A., Tchiguirinskaia, I., and Schertzer, D. (2012). Multi-Hydro: a multi module physically based model to evaluate effect of implementation of the flood resilience measure. *Geophysical Research Abstracts*, 14.

Gilli, E., Mangan, C., and Maudry, J. (2004). *Hydrogéologie*. Sciences Sup, Dunod edition.

Gires, A., Giangola-Murzyn, A., Abbes, J., Tchiguirinskaia, I., Schertzer, D., and Lovejoy, S. (2014). Impacts of small scale rainfall variability in urban areas: a case study with 1D and 1D/2D hydrological models in a multifractal framework. *Urban Water Journal*.

Göbel, P., Stubbe, H., Weinert, M., Zimmermann, J., Fach, S., Dierkes, C., Kories, H., Messer, J., Mertsch, V., Geiger, W. F., and Coldewey, W. G. (2004). Near-natural stormwater management and its effects on the water budget and groundwater surface in urban areas taking account of the hydrogeological conditions. *Journal of Hydrology*, 299(3-4):267–283.

Golroo, A. and Tighe, S. (2011). Alternative modeling framework for pervious concrete pavement condition analysis. *Construction and Building Materials*, 25:4043–4051.

Goodchild, M. F., Steyaert, L. T., Parks, B. O., Johnston, G., Maidment, D., Crane, M., and Glendinning, S. (1996). *GIS and Environmental Modeling: Progress and Research Issues*. WILEY.

GRASS GIS (2014). GRASS GIS - the world's leading free GIS software. `http://grass.osgeo.org/`.

Gregoire, B. and Clausen, J. (2011). Effect of a modular extensive green roof on stormwater runoff and water quality. *Ecological Engineering*, 37:963–969.

Greswell, R., Lloyd, J., Lerner, D., and Knipe, C. (1993). Rising groundwater in the Birmingham area. In Wilkinson, W., editor, *Groundwater pollution in urban areas. Proceedings of Conference of the Institution of Civil Engineers*, pages 64–75.

Grimmond, C. S. B., Blackett, M., Best, M. J., Barlow, J., Baik, J.-J., Belcher, S. E., Bohnenstengel, S. I., Calmet, I., Chen, F., Dandou, A., Fortuniak, K., Gouvea, M. L., Hamdi, R., Hendry, M., Kawai, T., Kawamoto, Y., Kondo, H., Krayenhoff, E. S., Lee, S.-H., Loridan, T., Martilli, A., Masson, V., Miao, S., Oleson, K., Pigeon, G., Porson, A., Ryu, Y.-H., Salamanca, F., Shashua-Bar, L., Steeneveld, G.-J., Tombrou, M., Voogt, J., Young, D., and Zhang, N. (2010). The International Urban Energy Balance Models Comparison Project: First Results from Phase 1. *Journal of Applied Meteorology and Climatology*, 49:1268–1292.

Grimmond, C. S. B. and Oke, T. R. (1991). An evapotranspiration-interception model for urban areas. *Water Resources Research*, 27(7):1739–1755.

Gromaire, M.-C., Ramier, D., Seidl, M., Berthier, E., Saad, M., and de Gouvello, B. (2013). Impact of extensive green roofs on the quantity and the quality of runoff - first results of a test bench in the Paris region. Novatech 2013, Lyon.

Gustafsson, L. (2000). Alternative Drainage Schemes for Reduction of Inflow/Infiltration - Prediction and Follow-Up of Effects with the Aid of an Integrated Sewer/Aquifer Model. In *1st International Conference on Urban Drainage via Internet*, pages 21–37.

Gustafsson, L., Winberg, S., and Refsgaard, A. (1996). Towards a distributed physically based model description of the urban aquatic environment. *Water Science and Technology*, pages 89–93.

Haase, D. (2009). Effects of urbanisation on the water balance A long-term trajectory. *Environmental Impact Assessment Review*, 29(4):211–219.

Hardy, M. J., Kuczera, G., and Coombes, P. J. (2005). Integrated urban water cycle management: the UrbanCycle model. *Water Science and Technology*, 52:1–9.

Harris, E. and Rantz, S. (1964). Effect of Urban Growth on Streamflow Regime of Permanente Creek, Santa Clara County, California. *U.S. Geological Survey Water Supply Paper*. 1591-B,18p.

Hathaway, A., Hunt, W., and Jennings, G. (2008). A field study of green roof hydrologic and water quality performance. *Transactions of ASABE*, 51(1):37–44. American Society of Agricultural Engineers.

Haverkamp, R., Vauclin, M., Touma, J., Wierenga, P. J., and Vachaud, G. (1977). A comparaison of numerical simulation models for one-dimensional infiltration. *Journal of Soil Science Society of America*, 41:285–295.

Hawley, R. J. and Bledsoe, B. P. (2011). How do flow peaks and durations change in suburbanizing semi-arid watersheds? A southern California case study. *Journal of Hydrology*, 405:69–82.

Hollis, G. E. and Ovenden, J. C. (1988). The quantity of stormwater runoff from ten stretches of road, a car park and eight roofs in Hertfordshire, England during 1983. *Hydrological Processes*, 2(3):227–243.

Hood, M. J., Clausen, J. C., and Warner, G. S. (2007). Comparison of stormwater lag times for low impact and traditional residential development. *Journal of the American Water Resources Association*, 43(4):1036–1046.

Huang, H.-j., Cheng, S.-j., Wen, J.-c., and Lee, J.-h. (2008). Effect of growing watershed imperviousness on hydrograph parameters and peak discharge. *Hydrological Processes*, 22(13):2075–2085.

Huber, W. and Dickinson, R. (1988). *Storm water management model. Version 4. User's Mannual. Report No EPA/600/3-88/001a*. US Environmental Protection Agency, Athens, Georgia, USA.

Hunt, W. and Lord, W. (2006). Evaluating bioretention hydrology and nutrient removal at three field sites in North Carolina. *Journal of Irrigation and Drainage Engineering*, 132(6):600–608.

Hunt, W., Traver, R., Davis, A., Emerson, C., Collins, K., and Stagge, J. (2010). Low Impact Development Practices: Designing to Infiltrate in Urban Environments. In Chang, N., editor, *Effects of Urbanization on Groundwater*, pages 308–343. American Society of Civil Engineers.

Hutchinson, D., Abrams, P., Retzlaff, R., and Liptan, T. (2003). Stormwater monitoring two ecoroofs in Portland, Oregon, USA. *Greening Rooftops for Sustainable Communities*.

Hydrologic Engineering Center (1977). *Storage, Treatment, Overflow, Runoff Model, STORM, User's Manual*. US Army Corps of Engineers, Hydrologic Engineering Center, Davis, California, USA.

Jankowfsky, S. (2011). *Understanding and modelling of hydrological processes in small peri-urban catchments using an object-oriented and modular distributed approach - Application to the Chaudanne and Mercier sub-catchments (Yzeron catchment, France).* PhD thesis, Université de Grenoble.

Jankowfsky, S., Branger, F., Braud, I., Rodriguez, F., Debionne, S., and Viallet, P. (2014). Assessing anthropogenic influence on the hydrology of small peri-urban catchments: Development of the object-oriented PUMMA model by integrating urban and rural hydrological models. *Journal of Hydrology*, 517(0):1056 – 1071.

Jeppesen, J., Christensen, S., and Ladekarl, U. L. (2011). Modelling the historical water cycle of the Copenhagen area 1850–2003. *Journal of Hydrology*, 404(34):117 – 129.

Jia, Y., Ni, G., Kawahara, Y., and Suetsugi, T. (2001). Development of WEP model and its application to an urban watershed. *Hydrological Processes*, 15(11):2175–2194.

JTS (2013). JTS Topology Suite. `http://www.vividsolutions.com/jts/JTSHome.htm`.

Karpf, C., Hoeft, S., Scheffer, C., Fuchs, L., and Krebs, P. (2011). Groundwater infiltration,surface water inflow and sewerage exfiltration considering hydrodynamic conditions in sewer systems. *Water Science and Technology*, 9:1277–1290.

Karpf, C. and Krebs, P. (2011a). A new sewage exfiltration model - parameters and calibration. *Water Science and Technology*, 63:2294–2299.

Karpf, C. and Krebs, P. (2011b). Quantification of groundwater infiltration and surface water inflows in urban sewer networks based on a multiple model approach. *Water Research*, 45:3129–3136.

Kashef, A. I. (1986). *Groundwater Engineering.* McGraw-Hill Book Company, New York.

Kauffman, G. J., Belden, A. C., Vonck, K. J., and Homsey, A. R. (2009). Link between Impervious Cover and Base Flow in the White Clay Creek Wild and Scenic Watershed in Delaware.

Kirby, J., Durrans, S., Pitt, R., and Johnson, P. (2005). Hydraulic resistance in grass swales designed for small flow conveyance. *Journal of Hydraulic Engineering*, 131(1):65–68.

Konrad, C. and Booth, D. (2005). Hydrologic changes in urban streams and their ecological significance. *American Fisheries Society Symposium*, pages 157–177.

Krause, S., Jacobs, J., and Bronstert, A. (2007). Modelling the impacts of land-use and drainage density on the water balance of a lowland-floodplain landscape in northeast Germany. *Ecological Modelling*, 200:475–492.

Ku, H., Nathan, W., and Herbert, T. (1992). Effects of Urban Storm-Runoff Control on Ground-Water Recharge in Nassau County,New York. *Ground Water*, 30(4).

Lagacherie, P., Rabotin, M., Colin, F., Moussa, R., and Voltz, M. (2010). Geo-MHYDAS : a landscape discretization tool for distributed hydrological modeling of cultivated areas. *Computers and Geosciences*, 36:1021–1032.

Lasserre, F., Razack, M., and Banton, O. (1999). A GIS-linked model for the assessment of nitrate contamination in groundwater. *Journal of Hydrology*, 224:81–90.

Last, E. and Mackay, R. (2010). City Water Balance: A new tool for scoping integrated urban water management options.

Laurini, R. (2001). *Information systems for urban planning*. Taylor & Francis.

Le Delliou, A. L. (2009). *Rôle des intéractions entre les réseaux d'assainissement et les eaux souterraines dans le fonctionnement hydrologique d'un bassin versant en milieu urbanisé - Approches expérimentales et modélisations*. PhD thesis, École Centrale de Nantes, Nantes, France. (in French).

Lee, J.-Y., Choi, M.-J., Kim, Y.-Y., and Lee, K.-K. (2005). Evaluation of hydrologic data obtained from a local groundwater monitoring network in a metropolitan city, Korea. *Hydrological Processes*, 19(13):2525–2537.

Lemonsu, A., Masson, V., and Berthier, E. (2007). Improvement of the hydrological component of an urban soilvegetationatmospheretransfer model. *Hydrological Processes*, 21(16):2100–2111.

Leopold, L. (1968). Hydrology for Urban Land Planning- A Guidebook on the Hydrologic Effects of Urban Land Use. *Geological Survey Circular*, 554:1–21.

Lerner, D. (2002). Identifying and quantifying urban recharge: a review. *Hydrogeology Journal*, 10(1):143–152.

Lerner, D., Halliday, D., and Hoffman, J. (1994). The impact of sewers on groundwater quality. In Wilkinson WB, editor, *Groundwater problems in urban areas*, pages 64–75,93–104. Thomas,Telford, London.

Lerner, D. and Tellam, J. (1997). The protection of urban ground-water from pollution. *Journal of the Institution of Water and Environmental Management*, 6(2):28–37.

Lhomme, J., Bouvier, C., and Perrin, J. L. (2004). Applying a GIS-based geomorphological routing model in urban catchments. *Journal of Hydrology*, 299:203–216.

Lynch, K. (1960). *The Image of the City*. MIT Press.

Maidment, D. (1993). Developing a spatially distributed unit hydrograph by using GIS. In *Proceedings HydroGIS'93*, volume 211, pages 181–192, Vienna, Austria.

Maidment, D. R. (1991). GIS and Hydrologic Modeling - an Assessment of Progress. In *1st International Conference on GIS and Environmental Modeling*. National Center for Geographic Information and Analysis.

Masson, V., Grimmond, C., and Oke, T. (2002). Evaluation of the Town Energy Balance (TEB) Scheme with Direct Measurements from Dry Districts in Two Cities. *Journal of Applied Meteorology*, 41:1011–1026.

Mcdonald, M. G. and Harbaugh, A. W. (1988). A modular three-dimensional finite-difference groundwater flow model. *U.S. Geological Survey Techniques of Water-Resources Investigations*, Book 6, chap. A1.

Mestayer, P., J-M, R., F, R., and J-M, R. (2011). The experimental campaign fluxsap 2010: Climatological measurements over a heterogeneous urban area. *Urban Climate News*, 40:22–30.

Meyer, S. C. (2002). INVESTIGATION OF IMPACTS OF URBANIZATION ON BASE FLOW AND. In *Proceedings, 12th Annual Illinois Groundwater Consortium Symposium*. Illinois Groundwater Consortium.

Michel Devisgne Paysagiste (2013). Schéma directeur du Sud du plateau.

Misstear, B., White, M., Bishop, P., and Anderson, G. (1995). Reliability of sewers in environmentally sensitive areas . Funders report IP/14, CIRIA, London.

Mistasova, H. and Mitas (1993). Interpolation by regularized spline with tension: I. Theory and implementation. *Mathematical Geology*, 25:641–655.

Mitchell, V., Duncan, H., Inman, M., Rahilly, M., Stewart, J., and Vieritz, A. e. a. (2007). Integrated urban water modelling past, present and future. *Rainwater 2007*.

Mitchell, V. G., Cleugh, H. A., Grimmond, C. S. B., and Xu, J. (2008). Linking urban water balance and energy balance models to analyse urban design options. *Hydrological Processes*, 22(16):2891–2900.

Moniod, F. (1983). Deux paramètres pour caractériser le réseau hydrographique. *Cahiers de l'Orstom, série Hydrologie*, 20:191–204. (in French).

Monteith, J. (1981). Evaporation and surface temperature. *Quarterly Journal of the Royal Meteorological Society*, 107:1–27.

Morena, F. (2004). *Modélisation hydrologique distribuée en milieu urbanisé* . PhD thesis, Institut National Polytechnique de Grenoble (in French).

Morris, B., Lawrence, A., and Foster, S. (1997). Sustainable groundwater management for fast-growing cities: mission achievable or mission impossible? In Chilton,J, editor, *Groundwater in the Urban Environment-Problems, Processes and Management, Proceedings of the 27. IAH-Congress on Groundwater in the Urban Environment, 21-27*, pages 55–66, Nottigham,UK.

Morris, M. (1991). Factorial sampling plans for preliminary computational experiments. *Technometrics*, 33(2):161–174.

Mougin, B. and Conil, P. (2005). Profondeur des eaux souterraines sur le périmètre intérieur au périphérique nantais. Technical report, BRGM.

Musolff, A., Leschik, S., Reinstorf, F., Strauch, G., and Schirmer, M. (2010). Micropollutant loads in the urban water cycle. *Environmental Science & Technology*, 44:4877–4883.

Nash, J. and Sutcliffe, J. (1970). River flow forecasting through conceptual models part IA discussion of principles. *Journal of hydrology*, 10:282–290.

Neuman, S. P. (1973). Saturated-unsaturated seepage by finite elements. *ASCE Journal of the Hydraulics Division*, 99:2233–2250.

Noilhan, J. and Planton, S. (1989). A Simple Parameterization of Land Surface Processes for Meteorological Models. *Monthly Weather Review*, 117(3):536–549.

Ogden, F. L., Debarry, P. A., Johnson, L. E., and Johnson, L. E. (2001). GIS and Distributed Watershed Models II. *USDA Agricultural Research Service/UNL Faculty*, pages 515–523.

OSGEO (2014). OSGeo - Your Open Source Compass. http://www.osgeo.org/home.

Paille, Y. (2010). Automatisation du pré-traitement des données spatiales pour la modélisation hydrologique distribuée en zone périurbaine à l'aide du logiciel libre GRASS. Master's thesis, Université de Nantes (in French), Nantes, France.

Pitt, P. (1999). Small storm hydrology and why it is important for the design of stormwater control practices. In James, W., editor, *Advances in Modeling the Management of Stormwater Impacts*, volume 7. Computational Hydraulics International, Guelph, Ontario and Lewis Publishiers/CRC Press.

Pitt, R., Clark, S., and Field, R. (1999). Groundwater contamination potential from stormwater infiltration practices. *Urban Water*, 1:217–236.

Price, K., C.R., J., and J., P. A. (2010). Variation of surfacial soil hydraulic properties across land uses in the southern blue ridge mountains. north carolina, usa. *Journal of Hydrology*, 383:256–268.

Prigiobbe, V. and Giulianelli, M. (2009). Quantification of sewer system infiltration using δ^{18}O hydrograph separation. *Water Science and Technology*, 60:727–735.

Prince George's County (1999). Low-impact development hydrologic analysis. Department of Environmental Resources, Prince George's County, Maryland.

PSC (2014). GRASS Project Steering Committee (PSC). http://trac.osgeo.org/grass/wiki/PSC.

Python (2014). Python 2.7.8 documentation. Available at https://docs.python.org/2/.

QGIS (2014). Topology checker plugin, documentation qgis 2.0. http://docs.qgis.org/2.0/en/docs/user_manual/plugins/plugins_topology_checker.html.

Ramier, D., Berthier, E., and Andrieu, H. (2011). The hydrological behaviour of urban streets: Long-term observations and modelling of runoff losses and rainfall-runoff transformation. *Hydrological Processes*, 25:2161–2178.

Rauch, W., Bertrand-Krajewski, J., Krebs, P., Mark, O., Schilling, W., Schutze, M., Vanrolleghem, P. A., and PA, V. (2002). Deterministic modelling of integrated urban drainage systems. *Water Science and Technology*, 45(3):81–94.

Razzaghmanesh, M., Beecham, S., and Kazemi, F. (2012). The role of green roofs in WaterSensitive Urban Design in South Australia. In *7th international conference on Water Sensitive Urban Design, Melbourne, Australia*.

Rodriguez, F. (1999). *Intérêt des banques de données urbaines pour l'hydrologie-Détermination des fonctions de transfert de bassins versants urbains*. PhD thesis, LCPC.

Rodriguez, F., Andrieu, H., and Creutin, J.-D. (2003). Surface runoff in urban catchments: morphological identification of unit hydrographs from urban databanks. *Journal of Hydrology*, 283(1-4):146–168.

Rodriguez, F., Andrieu, H., and Morena, F. (2008). A distributed hydrological model for urbanized areas model development and application to case studies. *Journal of Hydrology*, 351(34):268 – 287.

Rodriguez, F., Andrieu, H., and Zech, Y. (2000). Evaluation of a distributed model for urban catchments using a 7-year continuous data series. *Hydrological Processes*, 14(5):899–914.

Rodriguez, F., Augris, P., Flahaut, B., Jankowfsky, S., Lebouc, L., Mosini, M.-L., Mosset, A., Pineau, L., Rouaud, J., and Yilmaz, D. (2013). Apport des observations hydrologiques à différentes échelles en milieu urbain. In *Quelles innovations pour la gestion durable des eaux pluviales en milieu urbain? Projet INOGEV & GEDEP*.

Rose, S. and Peters, N. (2001). Effects of urbanization on streamflow in the Atlanta area (Georgia, USA): a comparative hydrological approach. *Hydrological Processes*, 15:1441–1457.

Rossman, L. A. (2004). *Storm water management model user manual. Version 5*.

Rowe, D. (2011). Green roofs as a means of pollution abatement. *Environmental Pollution*, 159:2100–2110.

Ruban, V., Rodriguez, F., Rosant, J. M., Larrarte, F., Joannis, C., Mestayer, P., and Andrieu, H. (2007). Hydrologic and energetic experimental survey of a small urban watershed. *Novatech 2007*.

SAGA (2014a). Bassins d'expansion cinquantennales et centennales - ZAC du Moulon - Gif sur Yveztte (91). Rapport 04543 V1. Technical report, SAGA Ingénierie. (in French).

SAGA (2014b). Projet d'aménagement de la ZAC de MOULON, Orsay (91) - Étude Géotechnique Prémiminaire - Mission G5 + G12. 04261-Version 01. Technical report, SAGA Ingénierie. (in French).

Salavati, B., Oudin, L., Furusho, C., and Ribstein, P. (2014). A method for reducing climate variation influence on the study of the urbanization impact assessment over 200 watersheds stream flow in usa. In *European Geosciences Union General Assembly 2014*.

Schirmer, M., Leschik, S., and Musolff, A. (2013). Current research in urban hydrogeology - A review. *Advances in Water Resources*, 51:280–291.

Schirmer, M., Strauch, G., Schirmer, K., and Reinstorf, F. (2007). Urban hydrogeology - challenges in research and practice. *Grundwasser*, 12:178–188.

Schoonover, J., Lockaby, B., and Helms, B. (2006). Impacts of land cover on stream hydrology in the west Georgia piedmont, USA. *Journal of Environmental Quality*, 35(6):2123–2131.

Selbig, W. and Bannerman, R. (2008). A comparison of runoff quantity and quality from two small basins undergoing implementation of conventional- and low-impact-development (LID) strategies: Cross Plains, Wisconsin, water years 19992005. Geological Survey Scientific Investigations Report, 2008-5008, p.57.

Sheeder, S. A., Ross, J. D., and Carlson, T. N. (2002). Dual urban and rural hydrograph signals in three small watersheds. *Journal of the American Water Resources Association*, 38(4):1027–1040.

Shepherd, K. A., Ellis, P. A., and Rivett, M. O. (2006). Integrated understanding of urban land, groundwater, baseflow and surface-water quality - The city of Birmingham, UK. *Society Total Environment*, 49:180–195.

Shuster, W. D., Bonta, J., Thurston, H., Warnemuende, E., and Smith, D. R. (2005). Impacts of impervious surface on watershed hydrology: A review. *Urban Water Journal*, 2(4):263–275.

Simmons, D. L. and Reynolds, R. J. (1982). Effects of urbanization on base flow of selected south-shore streams, long island, new york1. *Journal of the American Water Resources Association*, 18(5):797–805.

Smith, M. B. and Brilly, M. (1992). Automated grid element ordering for GIS-based overland flow modeling. *Photogrammetric Engineering and Remote Sensing 58*, 5:579–585.

Sogreah and Insavalor (2005). *Manuel d'utilisation de CANOE* . Sogreah and Insavalor (in French).

Sommer, T., Karpf, C., Ettrich, N., Haase, D., Weichel, T., Peetz, J.-V., Steckel, B., Eulitz, K., and Ullrich, K. (2009). Coupled modelling of subsurface water flux for an integrated flood risk management. *Natural Hazards and Earth System Science*, 9(4):1277–1290.

Spieksma, J. and Schouwenaars, J. (1997). A simple procedure to model water level fluctuations in partially inundated wetlands. *Journaly of Hydrology*, 196:324–335.

Srinivasan, R. and Arnold, J. G. (1994). Integration of a basin-scale water-quality model with GIS. *Water Resources Bulletin*, 30(3):453–462.

Stovin, V., Vesuviano, G., and Kasmin, H. (2012). The hydrological performance of a green roof test bed under UK climatic conditions. *Journal of Hydrology*, 414:148–161.

Sudicky, E., Jones, J., Brunner, D., McLaren, R., and VanderKwaak, J. (2000). A fully-coupled model of surface and subsurface water flow: model overview and application to the Laurel Creek watershed. In Bentley,L and Sykes,J and Brebbia,C and Gray,W and Pinder,G, editor, *Proceedings of the XIII International Conference on Computational Methods in Water Resources*, pages 1093–1099, Calgary, Alberta, Canada.

Sui, D. Z. and Maggio, R. C. (1999). Integrating GIS with hydrological modeling: practices, problems, and prospects. *Computers, Environment and Urban Systems*, 23:33–51.

Tait, N., Davison, R., Whittaker, J., Leharne, S., and Lerner, D. (2004). Borehole Optimisation System (BOS)A GIS based risk analysis tool for optimising the use of urban groundwater. *Environmental Modelling & Software*, 19:1111–1124.

Thiem, G. (1906). *Hydrologische Methoden*. Gebhardt, Leipzig.

Thomas, A. (2006). Modelling of recharge and pollutant fluxes to urban groundwaters. *Science of The Total Environment*, 360:158–179.

United Nations (2014). World urbanization prospects: the 2014 Revision, Highlights (ST/E-SA/SER.A/352). Technical report, United Nations, Department of Economic and Social Affairs, Population Division.

USEPA (1999). Stormwater technology fact sheet. Porous pavement. Office of Water, US Environmental Protection Agency, Washington, D.C. EPA 832-F-99-023.

USEPA (2000). Low impact development (LID). A literature review. Office of Water, US Environmental Protection Agency, Washington, D.C. EPA 841-B-00-005.

van Genuchten, M. T. and Nielsen, D. R. (1985). On describing and predicting the hydraulic properties of unsaturated soils. *Annales Geophysicae*, 3:615–628.

VanderKwaak, J. (1999). *Numerical simulation of flow and chemical transport in integrated surface-subsurface hydrologic systems*. PhD thesis, University of Waterloo, Waterloo, Ontario, Canada.

VanWoert, N., Rowe, D., Andresen, J., Rugh, C., Fernandez, R., and Xiao, L. (2005). Green roof stormwater retention: effects of roof surface, slope and media depth. *Journal of Environmental Engineering*, 34:1036–1044.

Vázquez-Suñé, E., Carrera, J., Tubau, I., Sánchez-Vila, X., and Soler, A. (2010). An approach to identify urban groundwater recharge. *Hydrology and Earth System Sciences*, 14(10):2085–2097.

Vogel, R. and Fennessey, N. (1995). Flow duration curves II: a review of applications in water resources planning. *Water Resources Bulletin*, 31(6):1029–1039.

Walsh, C. J. and Kunapo, J. (2009). The importance of upland flow paths in determining urban effects on stream ecosystems. *Journal of the North American Benthological Society*, 28:977–990.

Wang, J., Endreny, T. A., and Nowak, D. J. (2008). Mechanistic simulation of tree effects in an urban water balance model1. *Journal of the American Water Resources Association*, 44(1):75–85.

Wang, X., Shuster, W., Pal, C., Buchberger, S., Bonta, J., and Avadhanula, K. (2010). Low impact development design-integrating suitability analysis and site planning for reduction of post-development stormwater quantity. *Sustainability*, 2(8):2467–2482.

Weng, P., Giraud, F., Fleury, P., and Chevallier, C. (2003). Characterising and modeling groundwater discharge in an agricultural wetland on the French Atlantic coast. *Hydrology and Earth System Sciences*, 7(1):33–42.

Wild, T. and Davis, A. (2009). Simulation of the performance of a storm-water BMP. *Journal of Environmental Engineering*, 135(12):1257–1267.

Wolf, L., Eiswirth, M., and Hötzl, H. (2006). Assessing sewer-groundwater interaction at the city scaled based on individual sewer defects and marker species distributions. *Environmental Geology*, 49:849–857.

Wyns, R. O., Baltassat, J. E. A. N. I., Lachassagne, P. A., and Legchenko, A. N. (2004). Application of proton magnetic resonance soundings to groundwater reserve mapping in weathered basement rocks (Brittany, France). *Bulletin de la Société Géologique de France*, 175(1):21–34.

Yang, Y., Lerner, D. N., Barrett, M. H., and Tellam, J. H. (1999). Quantification of groundwater recharge in the city of Nottingham, UK. *Environmental Geology*, 38(3):183–198.

Yao, X., Wang, T., Chen, H., Gao, W., Fowler, A., and Raussendorf, R. (2012). Experimental demonstration of topological error correction. *Nature*, 482:489–494.

Yeh, G. T., Cheng, J. R., Cheng, H. P., Lin, H. J., Richards, D. R., and Jones, N. L. (1996). FEMWATER: A three-dimensional finite-element computer model for simulating density dependent flow and transport. Technical Report HL-96, GMS, The Department of Defense, Washington, DC.

Young, F. A., Onstad, C. A., Bosch, D. D., and Anderson, W. P. (1989). AGNPS: A nonpoint-source pollution model for evaluating agricultural watersheds. *Journal of Soil and Water Conservation*, 44(2):168–173.

Zech, Y., Sillen, X., Debources, C., and Van Hauwaert, A. (1994). Rainfall-Runoff Modelling of Partly Urbanized Watersheds: Comparison Between a Distributed Model Using GIS and Other Models Sensitivity Analysis. *Water Science and Technology*, 29(1-2):163–170.

Zhang, L., Dawes, W. R., and Walker, G. R. (2001). Response of mean annual evapotranspiration to vegetation changes at catchment scale. *Water Resources Research*, 37:701–708.

Zhou, Q. (2013). Development of toos of GIS pre-treatment for hydrological modeling of urban watersheds. Master's thesis, École Centrale de Nantes, Nantes, France.

Zoppou, C. (2001). Review of urban storm water models. *Environmental Modelling & Software*, 16:195–231.

l'université nantes angers le mans
PÔLE DE RECHERCHE ET D'ENSEIGNEMENT SUPÉRIEUR

Centrale Nantes

Thèse de Doctorat

Yinghao LI

Modélisation des processus hydrologiques au sein d'un bassin versant urbain -- Étude d'un module d'écoulement dans la zone saturée et application au projet

Modeling of hydrological processes of an urban catchment - Study of a saturated soil flow module and application to an urban development zone of the future Paris-Saclay University

Résumé

La gestion des eaux pluviales urbaine se développe vers des contrôles « at source » via la mise en place de techniques alternatives (TA). La modélisation hydrologique en milieu urbain tend vers des approches distribuées, intégrées, et à base physique. Ce travail de thèse consiste à contribuer au développement du modèle distribué URBS. La contribution scientifique s'articule sur l'intégration du module de la zone saturée WTI. Le modèle URBS-WTI est évalué sur un bassin versant expérimental à Nantes. La qualité de simulation est satisfaite pour les niveaux de nappe et les débits de sortie. L'effet antagoniste entre certains processus explique la complexité dans l'estimation du bilan hydrologique et de la recharge de nappe en milieu urbanisé. La difficulté rencontrée lors de la calibration du modèle est liée à variabilité spatiale des propriétés du sol urbain. Une fois validé, le modèle URBS-WTI est appliqué sur un réel projet d'aménagement. Des simulations continues sont menées à des pas de temps fins sur un quartier du futur campus Paris-Saclay. Le régime hydrologique actuel du site avant aménagement est estimé, ce qui met en avant l'importance des processus de l'évapotranspiration et du drainage d'eau du sol par les réseaux d'assainissement et leurs tranchées de pose. Puis une étude de scénarios est menée pour l'état futur du site après aménagement. L'étude montre que l'imperméabilisation des surfaces peut conduire à l'augmentation de ruissellement de surface et la réduction d'évapotranspiration. Tous les scénarios de TA testés ont montré leurs capacité d'atténuer les débits de pointe. L'inondation locale causée par la saturation des surfaces du sol est observée. De manière générale, l'introduction du module WTI a permis d'améliorer la robustesse du modèle URBS, en particulier pour la simulation des écoulements dans la zone saturée.

Mots clés
Hydrologie urbaine, gestion des eaux pluviales, techniques alternatives, modèle distribué, modèle de zone saturée, réseaux d'assainissement

Abstract

Urban stormwater management is developed towards to at-source controls through low impact development (LID) practices. Urban hydrological modeling turns towards to distributed, physically-based, integrated approaches. This Ph.D consists of contributing to the development of the distributed model URBS. The scientific contribution focuses on the implementation of the saturated flow module WTI, and the model URBS-WTI is evaluated at an experimental catchment. The simulation of both groundwater levels and discharge rate with the calibrated model is satisfying. The contradictory effect of some processes explains the complexity in estimating water balance and groundwater recharge in urban areas. The difficulty in model calibration shows the spatial variability of soil properties. Once validated, the model URBS-WTI is applied on an urban development area of the future Paris-Saclay University. Continuous simulations are carried out with small time steps. The pre-development hydrological regime of the site is estimated, emphasizing the great importance of both the evapotranspiration and groundwater drainage by sewer networks. Then a scenario study for the post-development hydrology is undertaken at both the catchment and urban block scales. This study shows that surface sealing can increase runoff volume and reduce the evapotranspiration loss. All tested LID practices can reduce peak discharge. Overland flow caused by soil saturation is observed locally. Generally speaking, the WTI module has improved the model robustness of URBS, in particular in the modeling of groundwater flow.

Key Words
Urban hydrology, stormwater management, low impact development, distributed model, groundwater modeling, sewer network